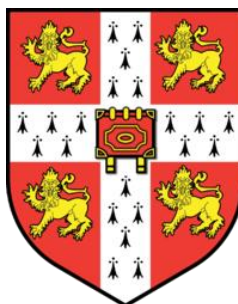# A role for microRNA-155 in the control of infection

By
Victoria Francis John

2010

This dissertation is submitted for the degree of Doctor of Philosophy

Trinity Hall
University of Cambridge

Abstract

MicroRNAs (miRNAs) are small (~22 nucleotide) non-coding regulatory RNA molecules which influence the expression of genes within eukaryotic cells. miRNAs function through targeted binding to the 3' un-translated region (UTR) of messenger RNAs (mRNAs) in a sequence specific manner. Recent studies have implicated microRNA-155 (miR-155) as an important player in the development and function of a number of immune cells including B and T cells, macrophages and dendritic cells. The aim of this study was to investigate the role of miR-155 in controlling either a mucosal *Citrobacter rodentium* or a systemic *Salmonella enterica* serovar Typhimurium infection in the context of the overall immune response. Here we present evidence that miR-155-deficient mice are less competent in their ability to eradicate a mucosal *C. rodentium* infection compared with wild type control C57BL/6 mice. We show that miR-155-deficient mice have a higher *C. rodentium* burden in gastrointestinal tissue and also exhibit spread into systemic tissues. Additionally, we demonstrate that germinal centre formation and humoral immune responses are impaired in the absence of miR-155. In view of the fact that this phenotype is largely reproduced in μMT (B cell-deficient) mice reconstituted with miR-155-deficient B cells we conclude that miR-155 is required to control *C. rodentium* infection. Further, miR-155-deficient mice were able to clear a primary infection with an attenuated strain of *S.* Typhimurium but were defective in their immune response to *Salmonella*.

Acknowledgements

First and foremost, I would like to say a massive THANKS to my family, especially Mum, Dad, Russ and Aled, for endlessly listening to me, encouraging me and for not letting me give up. Without their eternal support I definitely would not have made it this far.

I would like to thank Professor Gordon Dougan for allowing me to complete my PhD in his laboratory and for all his expert help and guidance.

Thank you to members of Team 15 and ex-Team 100, particularly Sally, Fernanda, Dave and Del for cheering me up every day.

A special thanks to Cordy for all her amazing help and the many stress-relieving shopping trips and also thanks to Amy and Zahra for all the tea, chats and cupcakes.

Finally I'd like to say a huge thanks to Gemma Langridge with whom I started my PhD. She has helped me enormously throughout the last four years and has been a truly fabulous friend.

Declaration

I hereby declare that this dissertation is the result of my own work and contains no material written by any other person. It includes nothing that is the outcome of work done in collaboration except where specifically indicated here or in the Materials and Methods section. I was fully involved in all aspects of the design and the experimental work presented.

Dr S Clare (Wellcome Trust Sanger Institute, Hinxton, Cambridge), assisted the author in performing tissue collection from experimental animals and performed immunisations and animal procedures during the studies.

David Goulding (Wellcome Trust Sanger Institute, Hinxton, Cambridge) performed the Scanning Electron and Transmission Electron Microscopy in assistance with the author.

Following RNA extraction, transcript analysis was performed by the Microarray Facility at the Wellcome Trust Sanger Institute, Cambridge. In addition, microarray data analysis was conducted by Cei Abreu-Goodger (European Bioinformatics Institute, Hinxton, Cambridge).

Dr Elena Vigorito (Babraham Institute, Cambridge) created all chimeric mice used throughout this study.

None of the material presented herein has been submitted previously for the purpose of obtaining another degree. I confirm that this thesis does not exceed 300 single-sided pages of double spaced text, or 60,000 words.

Victoria F. John

October, 2010

Contents

List of Figures

List of Tables

List of Printed Supplementary Figures and Tables

Abbreviations

ADCC   Antibody-dependent cell-mediated cytotoxicity

A/E lesion   Attaching and effacing lesion

AICDA   Activation-induced cytidine deaminase

ALV   Avian leukosis virus

AP   Activator protein

APCs   Antigen presenting cells

BALT   Bronchus-associated lymphoid tissue

BCR   B-cell receptor

Bfp   Bundle forming pili

BIC   B-cell integration cluster

BL   Burkitt lymphoma

BSA   Bovine serum albumin

CFU   Colony forming units

CGG   Chicken gamma globulin

CSR   Class switch recombination

CTLs   Cytotoxic T-lymphocytes

CXCR   Chemokine, CXC Motif, Receptor

DC   Dendritic cell

D-PBS   Dulbecco's phosphate buffered saline

DNP   Dinitrophenylated

EHEC   Enterohaemorrhagic *Escherichia Coli*

ELISA   Enzyme-linked immunosorbant assay

EPEC   Enteropathogenic *Escherichia Coli*

ESP   Expressed surface protein

EST   Expressed sequence tag

FAE   Follicle associated epithelium

FasL   Fas Ligand

FDC   Follicular dendritic cell

GA   Glutaraldehyde

GALT   Gastric-associated lymphoid tissue

GAPDH   Glyceraldehyde 3-phosphate dehydrogenase

GC   Germinal centre

gDNA   Genomic DNA

GO   Gene ontology

HEV   High endothelial venule

HL   Hodgkin lymphoma

HRP   Horse radish peroxidase

HUL   Haemolytic uraemic syndrome

IBD   Inflammatory bowel disease

ICAM	Intracellular adhesion molecule
IFN	Interferon
Ig	Immunoglobulin
IHC	Immunohistochemistry
IL	Interleukin
ILF	Isolated lymphoid follicle
INOS	Inducible nitric oxide synthase
ITAM	Immunoreceptor tyrosine activation motif
i.v.	Intravenous
KEGG	Kyoto Encyclopedia of Genes and Genomes
KDa	Kilo Dalton
KLH	Keyhole limpet hemocyanin
LB	Luria Bertani
LEE	Locus of enterocyte effacement
LPS	Lipopolysaccharide
LT	Lymphotoxin
MALT	Mucosal-associated lymphoid tissue
M cell	Microfold cell
MHC	Major histocompatability complex
miRNA	microRNA

mLN	Mesenteric lymph node
MMP	Matrix metalloproteinase
MMR	Mismatch repair
MPEC	Murine-pathogenic *Escherichia Coli*
mRNA	messenger RNA
Myd88	Myeloid differentiation factor 88
Mø	Macrophage
µMT mice	B cell-deficient mice
NALT	Nasal-associated lymphoid tissue
NEO	Neomycin
NF	Nuclear factor
NFAT	Nuclear factor of activated cells
NHL	Non-Hodgkin lymphoma
NK	Natural Killer cell
NP	3-hydroxy-4-nitro-phenylacetyl
OPD	O-Phenylenediamine dihyrochloride
ORF	Open reading frame
PAMPs	Pathogen associated molecular patterns
PBS	Phosphate buffered saline
PFA	Paraformaldehyde

pi	Post-inoculation
pIgR	Polymeric immunoglobulin receptor
PNA	Peanut agglutinin
PO	Propylene oxide
Pol	Polymerase
PP	Peyer's patch
RAG	Recombination activating gene
RISC	RNA-induced silencing complex
PKC	Protein kinase C
rpm	Revolutions per minute
PRRs	Pattern recognition receptors
RSS	Recombination signal sequences
RT	Room temperature
RNIs	Reactive nitrogen intermediates
RT-PCR	Reverse transcription-polymerase chain reaction
SCs	Stromal cells
SEM	Standard error mean
SHM	Somatic hypermutation
STAT	Signalling transducer and activator of transcription
TBMs	Tingible body macrophages

TCR   T-cell receptor

TdT   Terminal deoxynucleotidyl transferase

TetC   Tetanus toxin fragment C

T_H T helper

TIR   Translocated intimin receptor

TLR   Toll-like receptor

TMCH   Transmissible murine colonic hyperplasia

TNF   Tumour necrosis factor

Tween   Polyoxyethylene-sorbitan monolaurate

T3SS   Type 3 Secretion System

UTR   Untranslated region

1 Introduction

1.1 MicroRNAs

1.1.1 Discovery

Viktor Ambros and colleagues discovered miRNAs whilst conducting a study of genes involved in the development of the nematode worm, *Caenorhabditis elegans* (*C. elegans*)[1-3]. They identified that the gene *lin-4* was essential for post-embryonic developmental stages in *C. elegans* and functioned by negatively regulating the level of LIN-14 protein[4]. Surprisingly, when the genomic sequence of the *lin-4* gene was analysed for potential open reading frames it was shown not to encode any functional proteins[5]. Further analysis of the transcripts of *lin-4* led to the discovery that they contained complementary sequences to a repeated sequence in the 3' untranslated region (UTR) of the lin-14 mRNA and thus they speculated that lin-4 may function via an antisense RNA-RNA mechanism[5]. Initially, miRNAs were believed to be unique to *C. elegans*, however, it is now known that they are not just an oddity of this worm species. Indeed, miRNAs have now been documented in an incredibly diverse range of organisms from plants and animals to bacteria and viruses.

1.1.2 MicroRNAs post-transcriptionally regulate gene expression

During the preliminary studies looking at how *lin-4* was able to exert an inhibitory effect on the translation of the LIN-14 protein, it was shown that transcripts of the lin-4 gene were able to bind directly to the lin-14 mRNA. Thus, it was hypothesised that it functioned through an antisense RNA-RNA mechanism[5]. The exact action of miRNAs is now commonly known to involve bases within the 5' end of the miRNA, which mediate complementary base pairing to the 3' un-translated region (UTR) of target mRNAs[6-8]. The degree of complementarity between the sequences is thought to determine

whether the mRNA is degraded directly by RNA- induced silencing complex (RISC) or not[9-11]. If the sequences are a perfect or very close to perfect match, the mRNA is cleaved directly by Argonaute2 (AGO2) protein within the RISC (Figure 1)[9-11]. However, perfect complementarity is rare in animals; it is thought to occur mainly in plants. Incomplete or imperfect base pairing leads to accumulation of target mRNAs within discrete cytoplasmic foci called GW bodies (or Processing (P)-bodies) where they are inaccessible to the translational machinery (Figure 1)[12, 13]. The translationally repressed mRNA is then either destroyed by RNA-degrading enzymes or stored[8, 12-14].
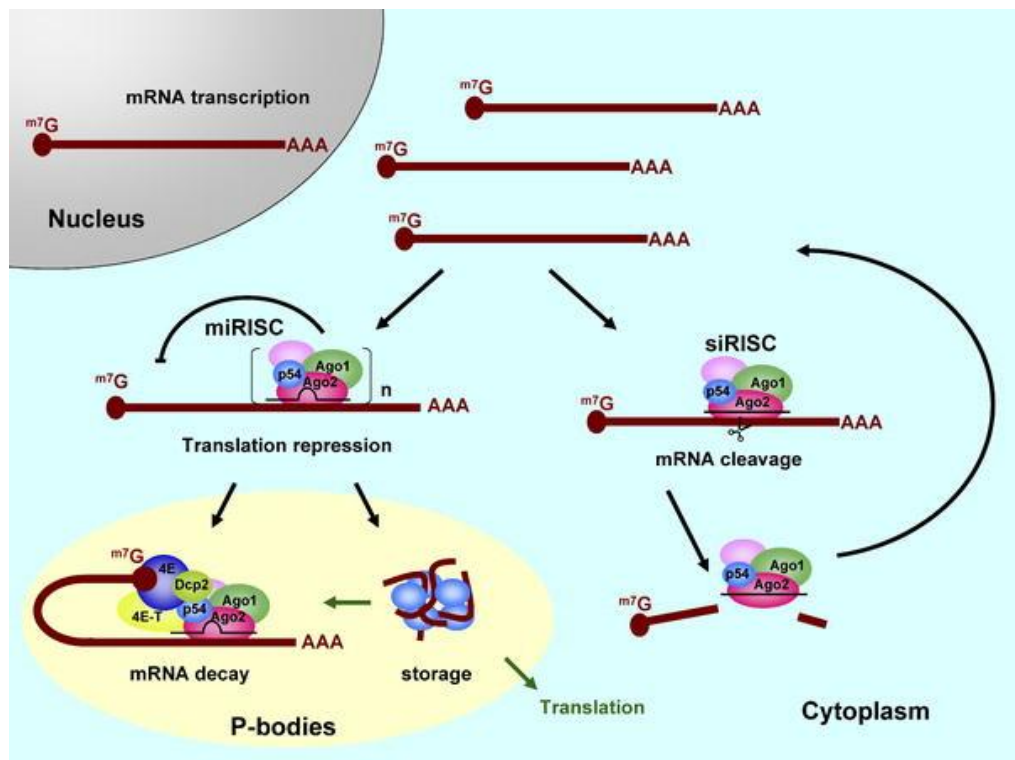
Figure 1. A Model for Human RISC Function Involving miRNA and siRNA

RISC contains Ago2 (red), Ago1 (green), RCK/p54 (blue, labelled p54), and other known (e.g., Dicer and TRBP) and unidentified proteins (pink) and is distributed throughout the cytoplasm. RISC binds to its target mRNA by perfectly matching base pairs, cleaves the target mRNA for degradation, recycles the complex, and does not require P-body structures for its function. Multiple numbers *(n)* of miRISC bind to target mRNA by forming a bulge sequence in the middle that is not suitable for RNA cleavage, accumulate in P-bodies, and repress translation by exploiting global translational suppressors such as RCK/p54. The

translationally repressed mRNA is either stored in P-bodies or enters the mRNA decay pathway for destruction. Depending upon cellular conditions and stimuli, stored mRNA can either re-enter the translation or mRNA decay pathways.

1.2 miR-155/ B cell integration cluster (BIC)

One particular miRNA, miR-155, has received a great deal of interest over recent years because it has been implicated as an important player in the development and/or function of a number of different immune cells and has also been shown to be involved in the generation and control of cancer.

1.2.1 Identification of miR-155

The loci encoding miR-155 was indirectly identified by Clurman and Hayward, during a study of the common oncogenes activated during avian leukosis virus (ALV)-induced B-cell lymphoma development[15]. They showed that in the majority of ALV induced lymphomas, dysregulation of *c-myc* expression occurred as a result of proviral integration within or near the *c-myc* gene. However, although disruption of *c-myc* expression occurred early in lymphomagenesis they determined that additional proto-oncogene activations were required for the induction of later stages of the disease. Using an experimental strategy to identify proto-oncogenes they found that ALV commonly integrated into three loci within the chicken genome; *c-myb*, *c-myc* and the newly identified locus which they called *c-bic* (B-cell integration cluster). Comparative sequence analysis of the *c-bic* locus with sequences held within the then GenBank data base revealed that *c-bic* was an unidentified locus. Furthermore, analysis of the genomic sequence for potential reading frames revealed that the locus did not encode any obvious proteins.

Amid a myriad of papers describing how mRNA-like non-coding RNAs can act as 'riboregulators' Tam *et al* pioneered the suggestion that *BIC* may function as a non-coding RNA[16-18]. Unfortunately, none who tried were able to provide a definitive mechanism by which *BIC* worked until in 2002, Lagos-

Quintana *et al* conclusively showed that the *c-bic* locus encoded a microRNA, which later became known as miR-155[19].

1.2.2 miR-155 as an oncogenic microRNA

Several different studies have described the accumulation of miR-155 transcripts in human lymphomas[20-26]. Van den Berg *et al* were first to demonstrate the high expression of miR-155 in the Hodgkin lymphoma (HL)-derived cell line, DEV and other HL derived cell lines[23]. They noted that miR-155 was not detectably expressed in non-Hodgkin lymphoma (NHL)-derived cell lines or normal tissue controls. However, analysis of normal human lymph node and tonsil tissues revealed the presence of miR-155 transcripts in a small number of germinal centre CD20^{+} B cells. Using the Burkitt lymphoma (BL)-derived cell line Ramos they later demonstrated that the expression of miR-155 could be up-regulated by B-cell receptor (BCR) triggering and consequently hypothesised that miR-155 may play a role in B cell selection and/or function. The BCR-induced expression of miR-155 in Ramos was found to involve protein kinase C (PKC) and the downstream transcription factor nuclear factor-κB (NF-κB)[24]. Metzler *et al* supported Van den Berg hypothesis and further showed that miR-155 was highly expressed in tissues from children with BL[22]. Costinean *et al* generated the first transgenic mice carrying a miR-155 transgene, the expression of which was targeted and overexpressed in B cells (Eμ-mmu-miR155)[27]. The transgenic mice in the study developed preleukemic pre-B cell proliferation in the spleen and bone marrow resulting in B cell malignancy[27].

1.2.3 miR-155 is important for normal immune function

1.2.3.1 The role of miR-155 in innate immunity

Two recent studies looking at miRNA expression in stimulated macrophages have shown that miR-155 may play a significant role in the innate immune response[28, 29]. In the first study, microarray technology was used to probe which miRNAs were induced in primary murine macrophages stimulated with

the virally relevant stimuli polyriboinosinic:polyribocytidylic acid [poly(I:C)] or interferon beta (IFN-β). miR-155 was identified as the only assayed microRNA that was substantially induced upon stimulation. Additionally, when macrophages were stimulated with bacterially relevant Toll-like receptor (TLR) ligands; such as lipopolysaccharide (LPS), hypomethylated DNA (CpG) or a synthetic lipoprotein, Pam3CSK4, miR-155 expression was once again found to be upregulated in response to all TLR ligands. Using myeloid differentiation factor 88 (MyD88)- or TRIF-deficient macrophages lacking the TLR signalling adaptor proteins it was demonstrated that signalling through either of these pathways is sufficient to induce miR-155 expression[29]. During a second study, mir-155 transcript levels were measured in Raw 264.7 macrophages stimulated with LPS. Analogous with the previous analysis, miR-155 was shown to be up-regulated in cells after six hours of stimulation. Further, when splenocytes were extracted from wild-type C57BL/6 mice inoculated intraperitoneally with *S. enteritidis*-derived LPS the levels of miR-155 were not only found to be increased but this up-regulation was shown to enhance the production of tumour necrosis factor-alpha (TNF-α), an important cytokine produced by macrophages in response to LPS. In unstimulated Raw 264.7 macrophages, TNF-α transcripts are known to be expressed but not translated. Translational repression is due to a self-inhibitory element in the 3' UTR of *TNF-α* mRNAs, miR-155 is thought to eliminate this inhibition but as yet the mechanism has not been elucidated.

1.2.3.2 miR-155 function in T cells

Haasch *et al* discovered that miR-155 is rapidly expressed in normal human T cells after activation[30]. Using expressed sequence tag (EST) technology they identified a number of ESTs that were more abundantly expressed in normal CD4+ T lymphocytes activated with anti-CD3 and -CD28 antibodies. One EST was of particular interest because it was copiously expressed in other EST libraries produced from arthritic joint synovial fluids, colon samples from patients with ulcerative colitis as well as lymphoma and thymus samples. The EST identified contained no open reading frames (ORFs) and

was thus deemed to be non-protein coding. Sequence comparison analysis revealed that the EST was miR-155. Subsequently, they were able to show that the expression of miR-155 in activated T cells could be repressed by the administration of immunosuppressive drugs that affect either calcineurin-dependent NFAT activation or AP-1 and NF-κB activation[30]. Thus, it was concluded that miR-155 might play an important role in T cell function.

1.2.3.3 The miR-155-deficient mouse

To further elucidate the role of miR-155 *in vivo*, Antony Rodriguez and colleagues used a gene targeting strategy to create a miR-155-deficient mouse (Figure 2)[31].
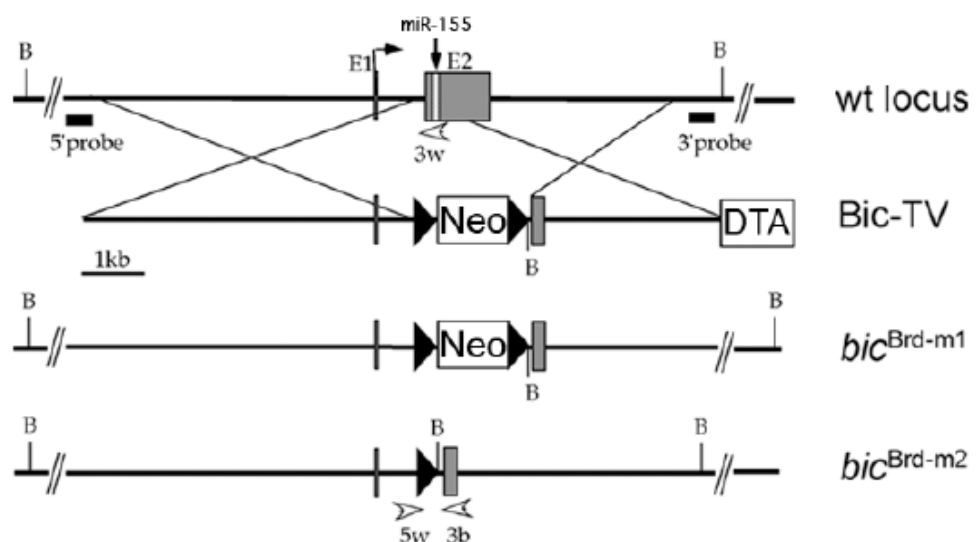
Figure 2. Gene targeting strategy to generate bic/miR-155-deficient mice

Schematic illustration of bic/miR-155 genomic locus and the targeting vector used to generate bic/miR-155 null alleles (bic[brd-m1] & bic[brd-m2]). The two alleles are null for miR-155 stemming from its physical deletion by the PGK-*Neo* (NEO) cassette flanked by *lox*P sites (black triangles).

Whilst the miR-155-deficient mice generated were viable and fertile, at age 320-350 days old approximately half the mice exhibited enhanced remodelling of the lung airway, characterised by a significant increase in bronchiolar subepithelial collagen deposition and in the numbers of

leukocytes in bronchoalveolar lavage fluids. In addition, miR-155-deficient mice were prone to enteric inflammation (symptoms typically seen when the immune response is skewed toward T_h2 differentiation) reminiscent of inflammatory bowel disease (IBD) thus, suggesting that miR-155 may be involved in regulating the homeostasis of the immune system. When miR-155-deficint mice were intravenously (i.v.) immunized with live attenuated *Salmonella enterica* subspecies *enterica* serovar Typhimurium[32] (*S.* Typhimurium) and later challenged orally with virulent *S.* Typhimurium to assess their degree of immunity, miR-155-deficient mice were less readily protected after vaccination compared with wild-type C57BL/6 mice, with approximately 80% of mice succumbing to infection. Furthermore, following immunisation with tetanus toxin fragment C protein (TetC), a T cell-dependent antigen, miR-155-deficient mice produced significantly less antigen-specific antibodies and splenocytes retrieved from immunised mice and restimulated *in vitro* with TetC produced significantly less interleukin (IL)-2 and interferon (IFN)-γ. Similarly, uncommitted naive miR-155-deficient CD4$^+$ T cells cultured with anti-CD3 and-CD28 antibodies were also less able to produce IFN-γ and miR-155-deficient B cells stimulated *in vitro* with LPS or IL-4 proliferated normally but were unable to yield significant levels of IgG1. Dendritic cells (DCs) from miR-155-deficient mice were also tested for their ability to activate T cells in culture and despite their normal expression of major histocompatability complex (MHC)-II and co-stimulatory molecule CD86, miR-155-deficient DCs failed to activate cognate T cells. Thus, it appears that miR-155 is required for the function of a number of different cells of the immune system, including T cells, B cells and DCs.

1.2.3.4 miR-155 is required for normal B cell function and germinal centre formation

T cell-dependent antibody affinity maturation and memory B cell generation occurs within germinal centres (GCs), this is discussed in more detail in chapter 1.3.2.2. miR-155-deficient mice immunized with alum-precipitated 3-hydroxy-4-nitro-phenylacetyl (NP) coupled to chicken gamma globulin

(CGG) produced significantly less and smaller splenic GCs and NP-CGG-specific antibodies than wild-type control mice (Figure 3)[33]. However, sequencing of the antibody $V_H186.2$ gene segments showed that the absence of miR-155 had no effect on somatic hypermutation rate. Considered together these results suggest that miR-155 may be involved in GC formation. Thai *et al* showed using reverse transcription-polymerase chain reaction (RT-PCR) that miR-155 may partially control the GC response by regulating cytokine production. B cells stimulated in vitro with a BCR cross-linking agent produced significantly less TNF-α and lymphotoxin (LT)-α transcripts.
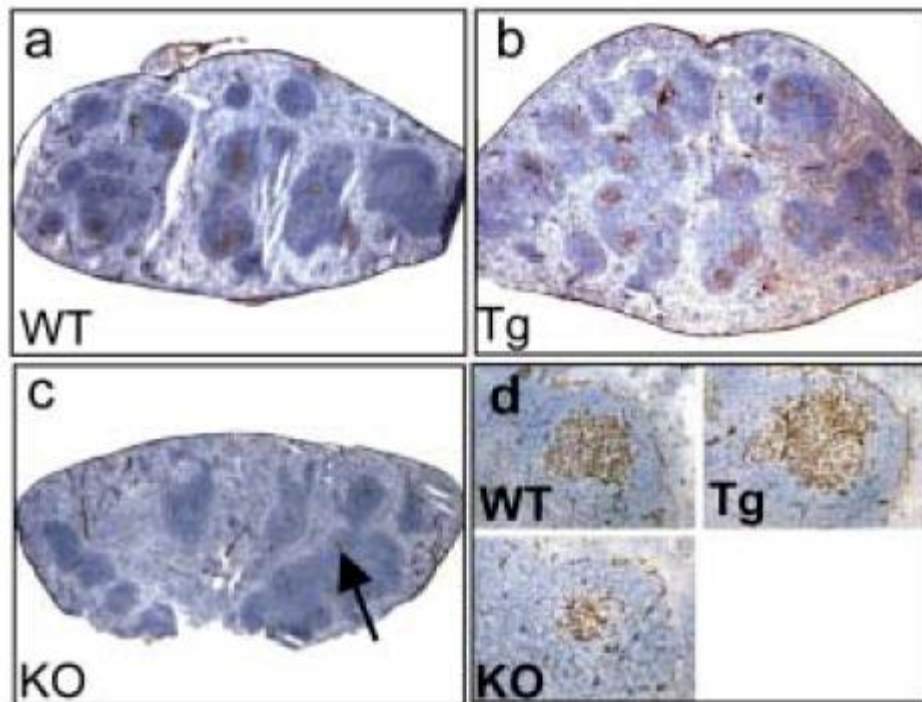
Figure 3. miR-155-/- mice show impaired T cell-dependent antibody responses

Immunohistochemistry performed on day 14 NP-immunized spleen sections from wild-type (a), B cell^miR-155 (b), and knockout mice (c) to detect GCs (brown, PNA+; blue, haematoxylin). High-magnification image is shown in (d). Images are representative of three mice per group[33].

Vigorito *et al* have further shown that B cells lacking miR-155 generated reduced extrafollicular and germinal centre responses when mice were immunised with a T cell-independent antigen, dinitrophenylated

lipopolysaccharide (DNP-LPS) and a T cell-dependent antigen, 4-hydroxy-3-nitrophenylacetyl conjugated to keyhole limpet hemocyanin (NP-KLH). Immunised miR-155 deficient B cells produced significantly less antigen specific antibodies and exhibited defective antibody class switching[34]. They too showed that miR-155 was not required for somatic hypermutation and that it was dispensable for class switch recombination (CSR)[33, 34]. Furthermore, expression of the enzyme activation-induced cytidine deaminase (*Aicda*) which controls CSR was found to be normal in activated miR-155-deficient B cells. Most recently however, miR-155 has been identified as a direct negative regulator of Aicda[35-37]. The 3' UTR of Aicda mRNA possesses a miR-155 target site, disruption of which results in deregulation of Aicda expression, increased CSR and impaired affinity maturation[35, 37].

What is apparent is that miR-155 affects the function and development of a number of different cells of the immune system.

1.3 **The immune system and infection control**

Humans and vertebrates constantly come into contact with a variety of microbial organisms, many of which have the potential to cause disease, thus they have evolved an array of protective mechanisms to help combat these challenges. Firstly, they possess a number of anatomical barriers such as the outer layer of skin which is rich in keratin, a very tough and insoluble protein which physically prevents infection. Glands within the skin secrete lysozyme and oleic acid, antimicrobial compounds which kill bacteria. Gastrointestinal, genitourinary and respiratory tracts however prove problematic because they provide a means of access into the body which must also be protected. Accordingly these surfaces are covered in a layer of mucus which traps microorganisms, largely preventing them from adhering to the epithelium. Mucus also contains a number of important antimicrobial peptides such as defensins which play a major role in resistance against pathogens. In addition, microbiota in the gastrointestinal and genitourinary tracts limit the outgrowth of pathogenic bacteria by competing with them for vital nutrients and space[38].

Occasionally microorganisms are able to penetrate these anatomical barriers and for this reason many organisms have evolved an immune system. The immune system of mammals can be further divided into two components; the innate and the adaptive immune system.

1.3.1 The innate immune system

The innate immune system provides an immediate and largely non-specific response against any microorganism that is able to breach the physical, chemical and biological barriers[39, 40]. Cells and molecules of the innate immune system recognise small molecular motifs that are conserved between groups of organisms called pathogen associated molecular patterns (PAMPs). PAMPs include microbial DNA, lipids, polysaccharides and flagella proteins. Pattern recognition receptors (PRRs) allow the recognition of PAMPs and once activated the innate immune system responds in two main ways; inflammation and phagocytosis[41-58]. Cells that become infected or damaged release inflammatory mediators such as cytokines and eicosanoids, which

promote increased blood flow, and the chemotaxis of immune cells, leukocytes (white blood cells), into infected tissues. However, after an infection has resolved the innate immune system provides no long-term memory against a specific pathogen. Upon subsequent challenges with the same pathogen the innate immune system responds in the same generic way as it did previously. It is however worth noting that although the innate immune system is non-specific and possesses no immunological memory it is critically important for activating and directing the adaptive immune response.

1.3.2 The adaptive immune system

Vertebrates have evolved an adaptive in addition to an innate immune system which, enables the generation of specific and long-lasting protection against a particular pathogen, so that a stronger and faster attack can be mounted each time the pathogen is encountered. The adaptive immune system is centred upon highly specialised cells called lymphocytes. The two main types of lymphocytes are T cells which are involved in cell-mediated and B cells which are involved in antibody-mediated responses.

1.3.2.1 T lymphocytes

T cells can be distinguished from other lymphocytes because they express T cell antigen receptors (TCR) on their cell surface. TCRs are critical for recognition of foreign antigen associated with major histocompatability complexes (MHC) on the surface of antigen presenting cells. Additionally, T cells express one of two key surface co-receptors, CD8 or CD4 glycoproteins.

CD8$^+$ T cells are able to recognise antigen when it is complexed with MHC class I molecules. They are often referred to as Cytotoxic T lymphocytes (CTLs) because they are capable of destroying cells infected with protozoa, viruses and intracellular bacteria as well as cancer cells via the release of cytotoxins, perforin, granulysin and granzymes. Furthermore, upon activation, CTLs up-regulate expression of Fas Ligand (FasL), a surface transmembrane protein which aids in the recognition of Fas molecules expressed on target

cells. Binding of FasL to Fas initiates a caspase signalling cascade which ultimately results in apoptosis of target cells.

The CD4 surface glycoprotein is expressed on the surface of all T helper cells (T_h cells), so called because they provide 'help' to effector cells such as B cells, macrophages and CTLs. Thus despite having no cytotoxic or phagocytic capabilities T_h cells play an essential role in activating, regulating and directing other immune cells. Unlike CD8$^+$ T cells, CD4$^+$ T cells are capable of recognising antigen complexed with MHC class II molecules expressed on the surface of specialised innate immune cells called professional antigen presenting cells (APCs). Macrophages, B cells and dendritic cells are all examples of professional APCs, although dendritic cells are considered to be the most efficient at presenting antigen, particularly to naïve cells. During an infection, activated APCs positioned within infected tissues phagocytose foreign antigen and up-regulate co-stimulatory molecules including CD40, CD80 (B7.1) and CD86 (B7.2) and chemokine receptors such as CCR7 which, allow them to traffic into the lymph nodes. Once within the lymph nodes, APCs process the phagocytosed material and present derivative peptides complexed with MHC class II to naive CD4$^+$ T cells.

In order to become fully activated CD4$^+$ T cells require two independent signals; the first signal comes as a result of TCR recognition and binding of cognate peptide-MHC II expressed on the APC surface while the second signal is provided by the interaction of CD28 on the CD4$^+$ T cell surface with the APC co-stimulatory molecules, CD80 or CDCD86 (Figure 4). Once both signals have been received, the naive CD4$^+$ T cell is licensed to begin proliferating.
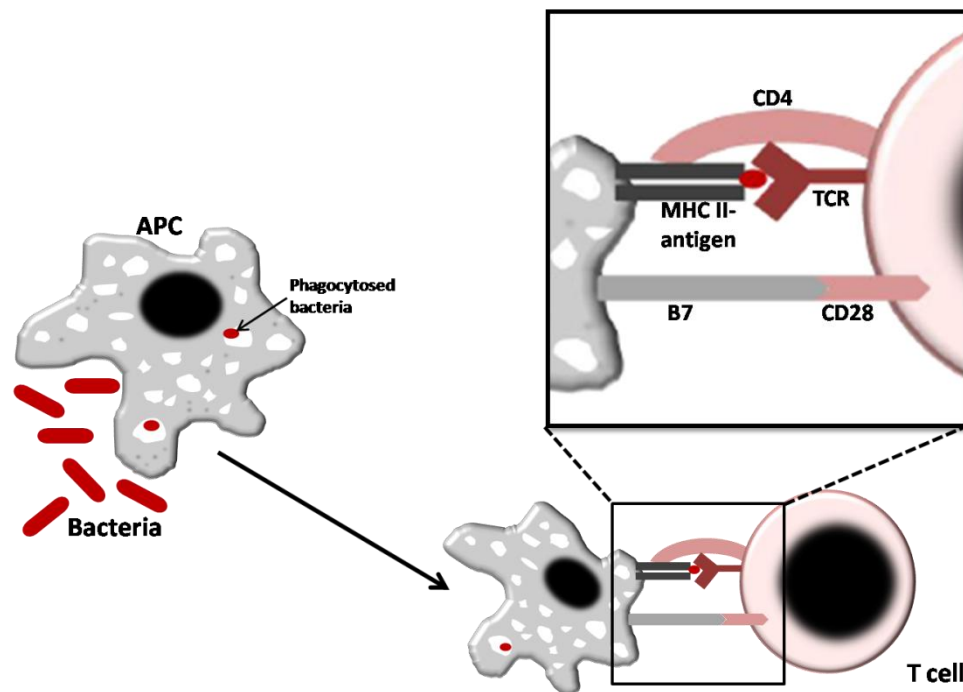
Figure 4. Antigen presentation between a professional APC and naive CD4$^+$ T cell

Professional APCs within infected tissues phagocytose and process foreign material e.g. bacteria and then traffic to the lymph nodes. Within the lymph nodes APCs present pathogenic peptides complexed with MHC class II to naive CD4 T cells. Naive CD4 T cells can only become activated after recognition and binding of cognate TCR to peptide/MHC complex as well as CD28-B7 co-receptor signalling.

After activation, CD4$^+$ helper T cells initially differentiate into T$_h$0 cells capable of secreting IL-2, IL-4 and interferon-γ (IFN-γ). The decision to further develop along the T$_h$1- or T$_h$2- differentiation pathways into either T helper 1 (T$_h$1) or T helper 2 (T$_h$2) cells respectively then depends on the milieu of cytokines elicited from pathogen-activated innate immune cells (Figure 5). Both T helper cell subtypes possess specific effector functions appropriate for dealing with different classes of pathogens. For example, T$_h$1 cells are characterised by their production of IFN-γ, lymphotoxin α (LTα) and IL-2, while T$_h$2 cells by their production of interleukin-4 (IL-4), interleukin-5 (IL-5), interleukin-6 (IL-6), inteleukin-10 (IL-10) and interleukin-13 (IL-13).

T_h1 cells have specifically evolved to aid the clearance of viral and intracellular pathogens, their differentiation is dependent upon the co-operative actions of IFN-γ and IL-12 (Figure 5)[59, 60]. Upon infection, IFN-γ is rapidly produced by natural killer (NK) cells and cytotoxic $CD8^+$ T cells while activated dendritic cells (DCs) and macrophages are the major producers of IL-12. All naive T cell precursors express functional receptors for type I and type II interferons, IFN-γ and IFN-α, respectively. Signalling through these cytokine receptors activates signalling transducer and activator of transcription 1 (STAT1) which, in turn up-regulates T-bet, a T_h1-specific transcription factor[61]. Expression of T-bet simultaneously inhibits T_h2 differentiation whilst inducing T_h1 differentiation. T-bet functions by increasing both the production of IFN-γ and the expression of the IL-12 receptor (IL-12R) signalling subunit, IL-12Rβ2. Consequently, IL-12 signalling through IL-12Rβ2 activates STAT4 and induces IL-18Rα expression. Mature T_h1 cells that express both IL-12Rβ2 and IL-18Rα are able to produce IFN-γ through TCR-dependent and independent pathways, in response to IL-12 plus IL-18[60]. T_h1 cells have been shown to play a vitally important role in macrophage-mediated inflammatory responses[62-64]. The IFN-γ produced by T_h1 cells has two key functions; firstly it enhances the microbial actions of macrophages and is therefore critical for enhancing macrophage killing efficacy. Secondly, it stimulates B cells to produce IgG antibodies which, bind and opsonise microbes thus promoting phagocytosis. IgG2a and IgG3 are the main IFN-γ-dependent antibody isotypes produced in mice[64, 65]. In addition, IFN-γ together with the T_h1 cytokine, IL-2 promote the differentiation of $CD8^+$ T cells into active CTLs[64].

Conversely, T_h2 cells have developed specifically to enhance the clearance of parasites. It is known that signalling through the Interleukin-4 receptor (IL-4R) and subsequent activation of Stat-6 in conjunction with TCR signalling is sufficient to promote T_h2 cell differentiation (Figure 5)[66, 67]. Simultaneous Stat-6 activation and TCR signalling results in the up-regulation of GATA-3, a transcription factor responsible for the transcription of all T_h2 cytokine genes[67]. T_h2 cells are involved in stimulating B cells to proliferate and for

inducing antibody class-switching (Figure 5). For instance, IL-4 a key T_h2 cytokine induces B cells to switch to the production of IgE which, in turn activates mast cells and basophils. T_h2 cells also stimulate B cells to produce high levels of IgM and non-complement-fixing IgG isotypes, such as IgG1 in mice[65].
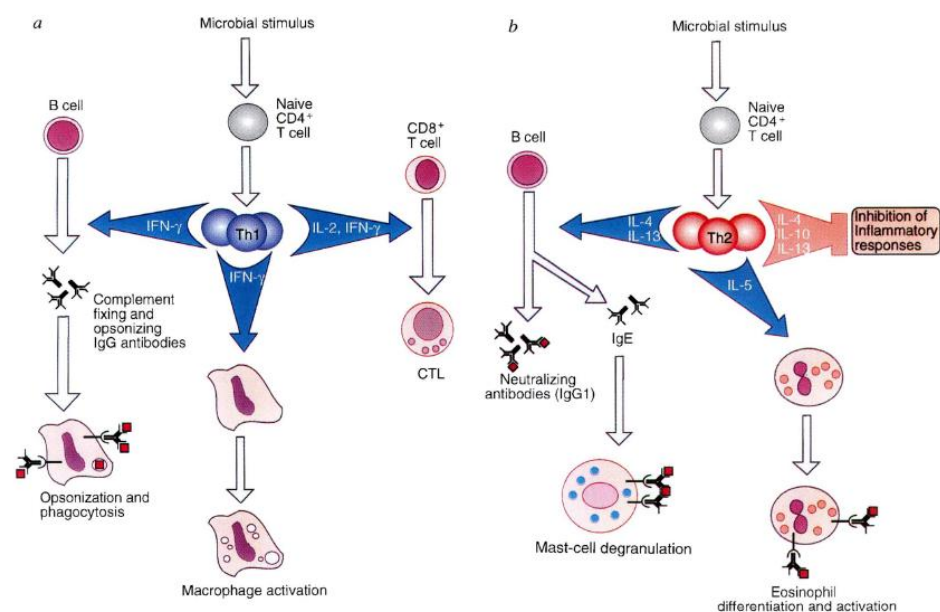
Figure 5. Effector functions of Th1 and Th2 subsets of CD4 helper T lymphocytes.

Th1 cells (a) induce phagocyte and T-cell mediated defence reactions against microbes; Th2 cells (b) induce IgE-dependent mast-cell degranulation and eosinophil activation, two components of the immediate hypersensitivity response[64].

1.3.2.2 B lymphocytes

B cells are the component of the adaptive immune system responsible for the production of antibodies (or immunoglobulins) during humoral immune responses. Antibodies are heavy (~150 KDa) globular plasma proteins consisting of four polypeptide chains; two identical heavy chains and two identical light chains linked by disulphide bonds (Figure 6). Antibodies can be either membrane-bound, as part of the B cell receptor (BCR) or secreted by B cells in a soluble form.

There are five different types of heavy chain; Alpha (α), Delta (δ), Epsilon (ε), Gamma (γ) and Mu (μ) which, determine the antibody isotype IgA, IgD,

IgE, IgG and IgM respectively. Different antibody isotypes occupy distinct functional locations within the body and possess unique effector properties. Each heavy chain has two regions; a constant region which is identical between antibodies of the same isotype and a variable region which is unique to each B cell. In mammals, there are two different immunoglobulin light chains, Kappa (κ) and Lambda (λ) and each antibody will possess two identical light chains of either type. Analogous to the heavy chain, each light chain has both a constant and variable region.
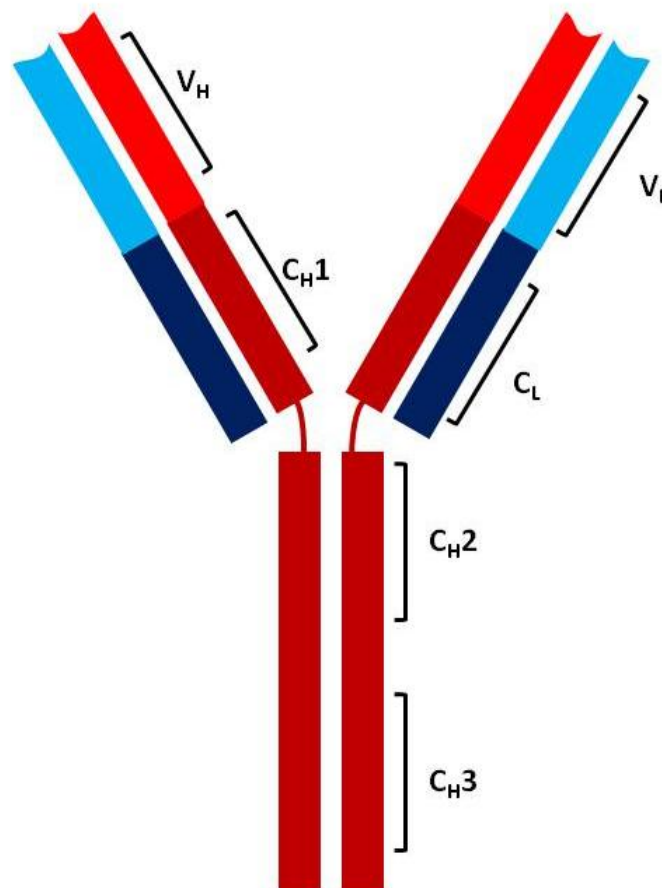
Figure 6. General structure of an antibody molecule

Antibodies consist of four polypeptide chains; two identical heavy chains and two identical light chains connected by disulphide bonds. Each heavy chain has a constant (C_H1, C_H2 and C_H3) and a variable (V_H) region. Each Light chain has a constant domain (C_L) and a variable domain (V_L)

The variable regions of the heavy and light immunoglobulin chains are encoded by multiple genes organised into distinct segments (Figure 7). The genes encoding the heavy chain variable region are segregated into variable (V) genes, Diversity (D) genes and Joining (J) genes whilst the genes encoding the light chain variable region are organised into V and J genes (Figure 7). The process by which recombination of V, D and J gene segments occurs during lymphocyte development is called somatic recombination and it enables the production of a considerable lymphocyte repertoire from a limited number of genes[68]. For example, there is estimated to be approximately 10^{12} unique B cells in the human body, each capable of binding a distinct epitope of an antigen[69].
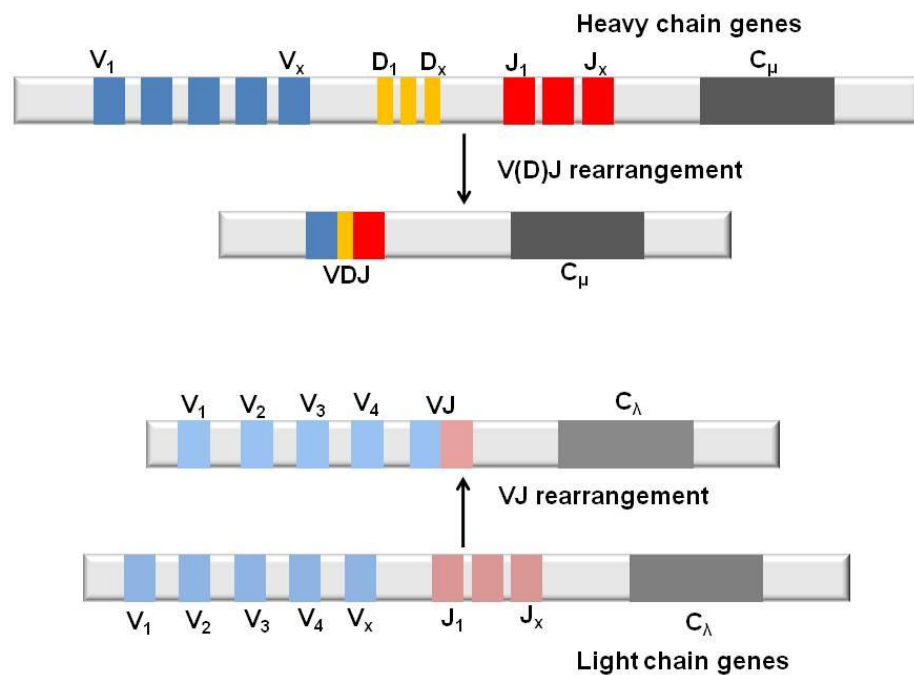
Figure 7. Immunoglobulin Somatic Recombination

The variable regions of immunoglobulin heavy and light chains are encoded by multiple genes arranged into segments. The heavy chain genes are organised into Variable (V), Diversity (D) and Joining (J) genes whilst the light chain genes are arranged into V and J genes.

B cell development is a highly regulated process that occurs in the liver during mid-to-late foetal development and within the bone marrow after birth. B cells are generated from a common lymphoid progenitor that also give rise to T cells, NK cells and lymphoid dendritic cells[70]. Lymphoid progenitor cells can only begin development upon receiving specific developmental signals from stromal cells within the bone marrow. Interactions between the stromal cell transmembrane protein, stem cell factor (SCF) and CD117 (c-Kit receptor) expressed on lymphoid progenitor cells are known to be important signals for initiating the development of both B and T cells, as is the binding of cytokine IL-7 (secreted from stromal cells) to the IL-7 receptor (IL-7R) on developing lymphoid progenitor cells. Co-ordinated signalling through these receptors induces the expression of recombination-activating genes (RAG-1 and RAG-2) and terminal deoxynucleotidyl transferase (TdT) in lymphoid progenitor cells. RAG-1 and RAG-2 are crucial for somatic recombination as mice with disruptions of either gene are completely defective in V(D)J recombination[68]. During recombination, RAG protein complexes bind to recombination signal sequences (RSSs), consisting of a conserved nonamer and heptamer element, separated by a spacer of 12 or 23 nucleotides, proceeding two immunoglobulin gene segments to be joined together[68]. As a consequence of binding between the RAG protein complexes, the two RSSs are brought into close proximity. RAGs then cleave the DNA at the heptamer/coding borders creating hairpin structures at the ends of the segments to be joined. The hairpin structures are subsequently opened, processed and ligated to form an imprecise coding joint. The processing and ligation stages are mediated by terminal deoxynucleotidyl transferases (TdT) and non-homologous end-joining factors which are responsible for the addition and subtraction of nucleotides from the segment ends, thus leading to greater antibody diversity.

The first stages in B cell development involve the joining of the D and J gene segments on the Heavy (H) chain chromosome to form early pro-B cells (Figure 8). At this stage, the cells also begin expressing CD45 (B220) and MHC class II. In the late pro-B cell, the V segment is joined to the already

combined D-J$_H$ genes and if V(D)J rearrangement is successful, cells begin expressing membrane μ chains together with surrogate light chains (which are the same on every pre-B cell) and the signal transduction molecule, CD79 (formerly known as IgαIgβ) in a complex known as the pre-B receptor (pre-BCR), this represents the large pre-B cell stage (Figure 8). At this juncture, if the pre-BCR binds antigen, phosphorylation of the Immunoreceptor Tyrosine Activation Motifs (ITAMs) within the cytoplasmic tails of CD79 results, subsequently initiating a cytoplasmic signalling cascade that immediately halts recombination of the H chain and activates B cells to proliferate into a clone of cells all expressing the same μ chain (Figure 8). Following proliferation, the small pre-B cells formed begin combining their V and J segments on one Light (L) chain chromosome until the L chain is successfully rearranged and expressed on the cell surface with the μ chain (Figure 8). Next immature B cells undergo a process known as negative selection whereby cells that recognise self-antigen within the bone marrow die via apoptosis, this eliminates potentially harmful self-reactive B cells. B cells that do not recognise self-antigens are licensed to exit the bone marrow and become mature naive B cells expressing both membrane IgM and IgD (Figure 8).
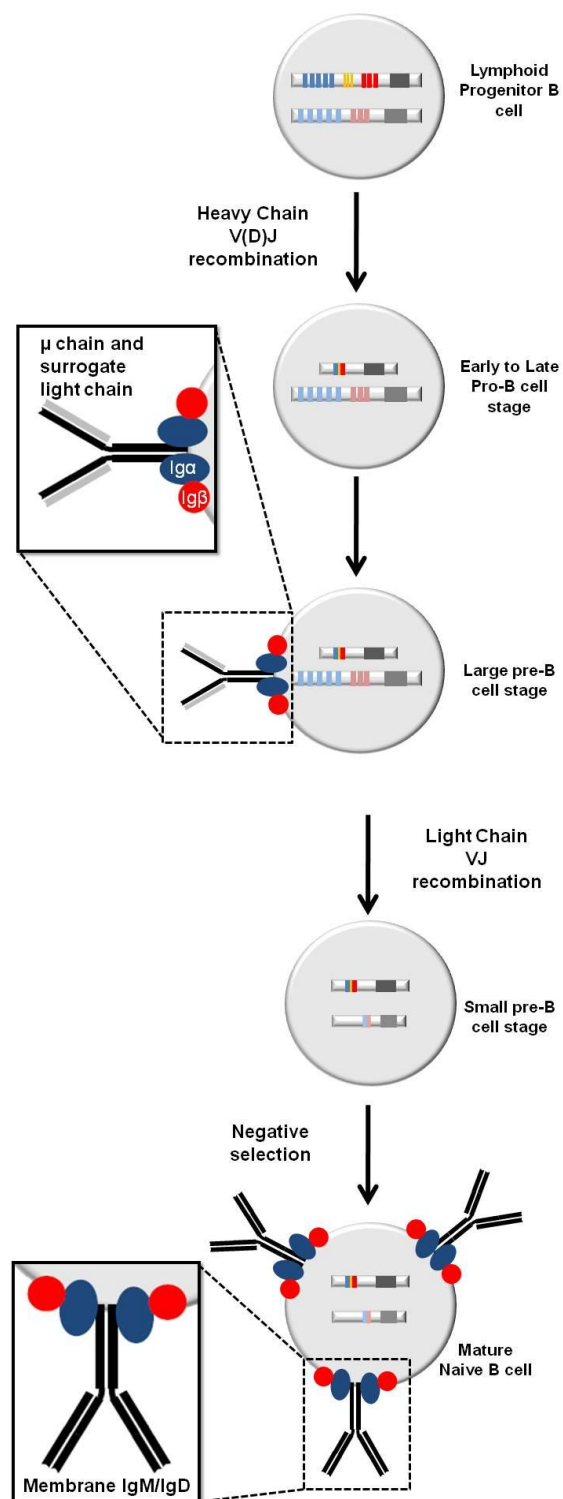
Figure 8. Stages in B cell development

With appropriate signals lymphoid progenitor B cells are stimulated to begin V(D)J

recombination. In the first stage, D and J gene segments on the Heavy (H) chain chromosome

are recombined, the resulting cells are known as early pro-B cells. In late pro-B cell stage, cells begin expressing CD45 (B220) and MHCII and complete V(D)J rearrangement with the V segment joining to the combined D-J_H genes. After successful V(D)J recombination, cells begin to express pre-B receptor which, consists of membrane μ chains together with surrogate light chains and signal transduction molecules, IgαIgβ, this represents the large pre-B cell stage. Intracellular signalling resulting from binding of the pre-B receptor to antigen halts recombination of the H chain gene segments and stimulates cells to proliferate. Following clonal expansion, small pre-B cells begin combining their V and J segments on one Light (L) chain chromosome. If the L chain is successfully rearranged it will subsequently be expressed on the cell surface with the μ chain, this represents the immature B cell. Before exiting the bone marrow, immature B cells are negatively selected for their ability to bind self-antigen. B cells that do not recognise self-antigen are licensed to exit the bone marrow and are now referred to as mature naive B cells.

1.3.2.2.1 B cell activation

Mature naive B cells that have exited the bone marrow circulate continuously in the blood and lymph until they encounter antigen specific to their BCR. Antigen cross-linking of the BCR results in the recruitment and formation of multi-protein signalling complexes and consequently triggers a number of important signalling cascades (Figure 9)[71]. The culmination of the signalling cascades is the activation of a number of transcription factors and the transcription of various genes, including miR-155, responsible for B cell activation and enhanced expression of cell surface antigen presentation molecules[72].
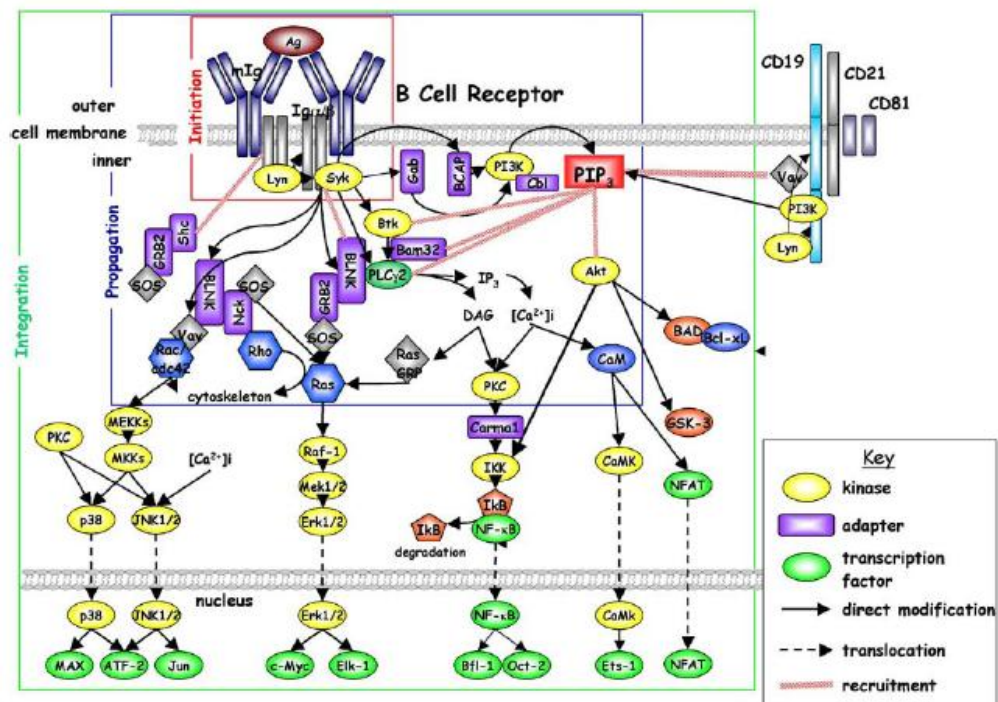
Figure 9. B cell antigen receptor signal transduction cascade

Signal transduction initiates at the cell membrane following ligand-induced aggregation of the membrane immunoglobulin (mIg) and associated signal transducing elements Igα and Igβ. Signals are then propagated by means of protein phosphorylation, modification, and interaction. The culmination of the signalling cascade is the regulation of transcription factor activation and gene expression. While not shown, accessory receptor molecules, such as CD19 or CD22, can influence BCR signalling at various levels in the signalling pathway[71].

During a T cell-dependent antibody response effector T_h cells recognise and bind antigen-MHCII on cognate B cells (Figure 10). Signals delivered through direct TCR-MHCII interaction greatly enhances B cell activation but also and more importantly stimulates B cells to traffic into the extrafollicular T cell rich regions of secondary lymphoid organs to begin differentiation into plasmablasts and plasma cells capable of secreting low affinity antibodies (Figure 10). Alternatively, several B cells relocate to primary follicles within the B cell zone and undergo exponential growth amongst a network of follicular dendritic cells (FDCs), this is known as the germinal centre reaction (Figure 10)[73-77].
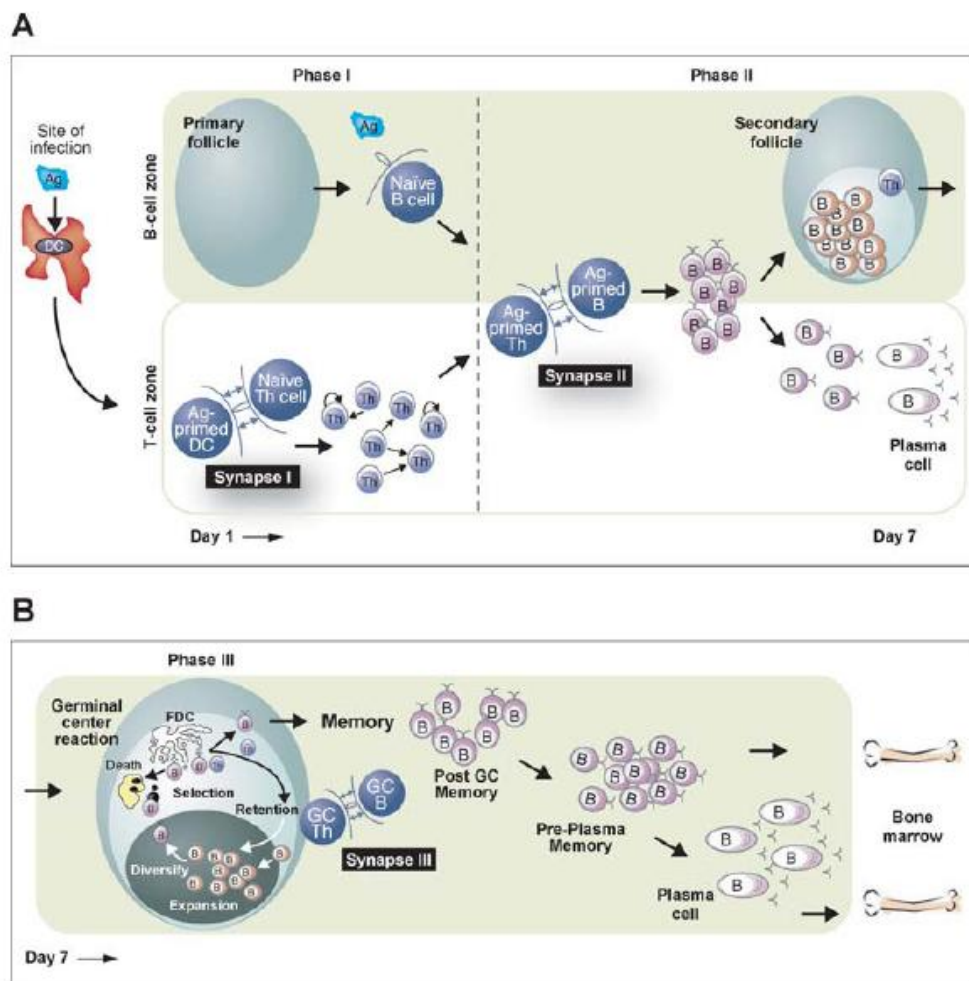
Figure 10. Th cell-regulated B cell memory development

(A) Schematic of the cellular interactions that proceed in the secondary lymphoid organs toward development of antigen-specific effector Th cells (Phase I) and effector B cells (Phase II). (B) A schematic of cellular activity in the GC cycle (Phase III) that leads to the development of antigen-specific memory B cell subsets. The three main cellular products of the GC are depicted[78].

Besides the MHCII-TCR interaction, several other receptor-ligand interactions are known to play an important role in T cell-dependent B cell activation (Figure 11)[72, 78]. CD40, an integral membrane protein constitutively expressed by B cells is known to play a pivotal role in governing humoral and cell-mediated immunity. Engagement of CD40 with CD40L (CD154) up-regulated on activated T_h cells can lead to B cell clonal expansion, germinal centre formation, isotype switching, affinity maturation and generation of

long-lived plasma cells[72, 78-80]. Furthermore, engagement of CD72, CD134 Ligand (CD134L), B cell activating factor (BAFF) and a proliferation-induced ligand (APRIL) as well as CD27 with their corresponding T cell ligands are all thought to be potentially important during humoral immune responses[72, 81]. Cell adhesion molecules, ICAM-1 (CD54) and LFA-1 (CD11a-CD18), have additionally been shown not only to enhance adhesiveness between B and T cells but directly transmit activation signals to B cells themselves,

B cell receptor	T cell ligand	B cell effector functions
Class II MHC	TCR; CD4	Cooperates with other activation signals to stimulate proliferation, differentiation and enhanced antigen presentation
CD11a–CD18/CD54	CD54/CD11a–CD18	Cell adhesion, enhanced antigen presentation and enhanced activation
CD72	CD100	Development of B-1 B cells, production of high-affinity IgG response and enhanced antigen presentation
CD40	CD154	Proliferation, differentiation, isotype switching, cytokine production, protection from apoptosis, and germinal center and memory response development
CD134L/OX40L	CD134/OX40	Stimulation and enhancement of IgG response
CD137L/4-1BBL	CD137/4-1BB	Stimulation of T cells through CD137
CD27	CD70	Differentiation into plasma cells
CD30/CD153	CD153/CD30	Inhibition of B cell responses, such as isotype switching and plasma cell differentiation
CD95/Fas	CD95L/FasL	Induction of programmed cell death (apoptosis)

Figure 11. B cell transmembrane receptors and T cell ligands involved in contact-dependent regulation of B cell activation[72].

contributing to enhanced B cell antigen-presentation and activation[72]. Furthermore, in addition to cell surface molecules which promote B cell activation there are a number of molecules which negatively regulate humoral immune responses. For example, CD30- CD153 interactions appear to inhibit isotype switching while B cells expressing CD95/Fas are more susceptible to CD95L-induced apoptosis in the absence of additional survival signals.

1.3.2.2.2 Germinal centres

Germinal centres (GCs) are regions within primary lymphoid follicles which support the generation of memory B cells and plasma cells capable of producing high affinity antibodies for a particular antigen[74, 82-98]. GCs only develop in response to immunogenic stimuli, this is highlighted in the fact that GCs are completely absent in germ-free animals[97]. In a T cell-dependent B cell response, GCs develop and persist during the first 3 weeks following immunization or exposure to antigen[77]. Naive B cells are activated within T cell-rich extrafollicular areas of secondary lymphoid organs before migrating to primary follicles to form germinal centres (Figure 10)[77]. However, before primary follicles are involved in antigenic responses they consist mainly of B cells re-circulating through a follicular dendritic cell (FDC) network. It has previously been shown that each follicle is colonized by an average of three B cell blasts, thus the resulting germinal centres are oligoclonal. Once within the follicle the aforementioned B blasts begin undergoing massive clonal expansion and somatic hypermutation (SHM) of their antibody variable region genes. Substantial clonal expansion of blasts displaces the small re-circulating follicular B cells to the outer edge of the FDC network where they form the follicular mantle (Figure 12). After approximately 3 days of rapid division, the B blasts are induced to move to one pole of the FDC network and differentiate into centroblasts ultimately forming the dark zone of the mature germinal centre (Figure 12)[76, 77]. It is known that the CXC chemokine receptor, CXCR4, which is highly expressed on centroblasts and, its ligand SDF-1 are required for repositioning of centroblasts to the dark zone[99, 100]. Proliferating centroblasts give rise to centrocytes which, are no longer in cell cycle and relocate to the light zone of the GC to interact with the network of FDCs (Figure 12)[101].
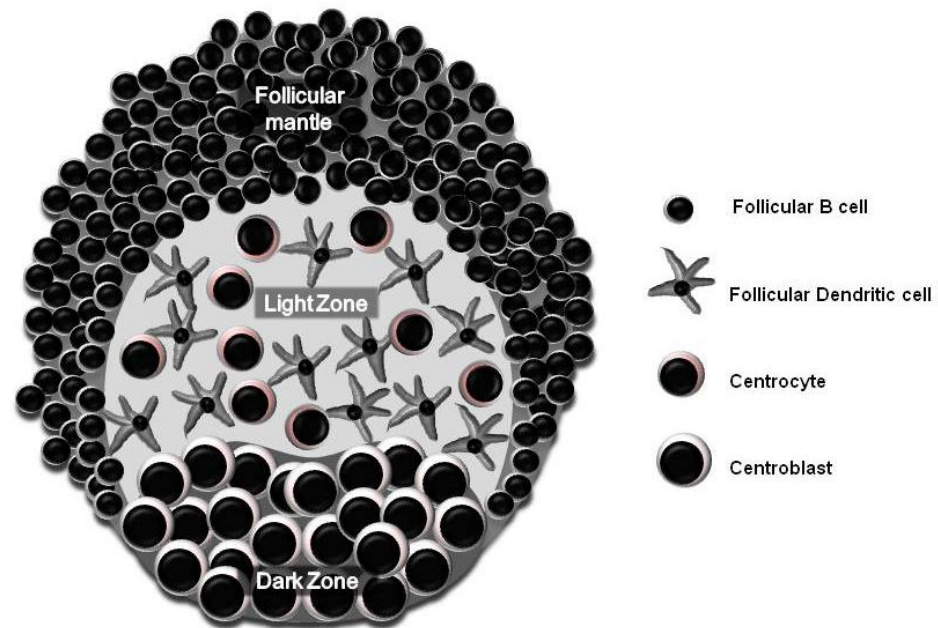
Figure 12. Schematic representation of germinal centre compartments

Small re-circulating follicular B cells displaced to the outer edge of the FDC network form the follicular mantle. The dark zone contains densely packed centroblasts, many of which are undergoing proliferation. The dark zone is adjacent to the T cell zone in the spleen and lymph nodes and the serosa in Peyer's patches. The light zone contains both non-dividing centrocytes and FDCs. In the spleen, the light zone is proximal to the marginal sinus while in the lymph nodes it is positioned close to the subcapsular sinus. Additionally, in the Peyer's patches, tonsils and appendix, the light zone is orientated toward the mucosal surface[101].

The FDCs in the light zone have the unique ability to capture and display large amounts of antigen in the form of immune complexes on their cell surface for periods of over a year[77, 101]. Centrocytes that have undergone successful SHM are selected on the basis of their affinity to bind such immune complexes. Based on the presence of tingible body macrophages within GCs it has been suggested that most B cells die during this selection process[101, 102]. Two possible models for GC B cell selection have been suggested; the first hypothesises that selection is based solely on adequate BCR signalling (Figure 13). B cells with no or very low affinity for antigen receive inadequate BCR signalling and rapidly die by apoptosis while those that express immunoglobulin (Ig) with increased affinity are able to survive and proliferate

with T cell help. In the second model, robust BCR signalling is necessary but, additional T cell help is required (Figure 13)[101]. Engagement of the BCR, ligation of CD40 and/or expression of *bcl-XL* or *bcl-2* inhibits apoptosis and promotes survival. It is important to note that in both models there is a strong positive selection for B cells that produce high affinity antibodies for the stimulating antigen.
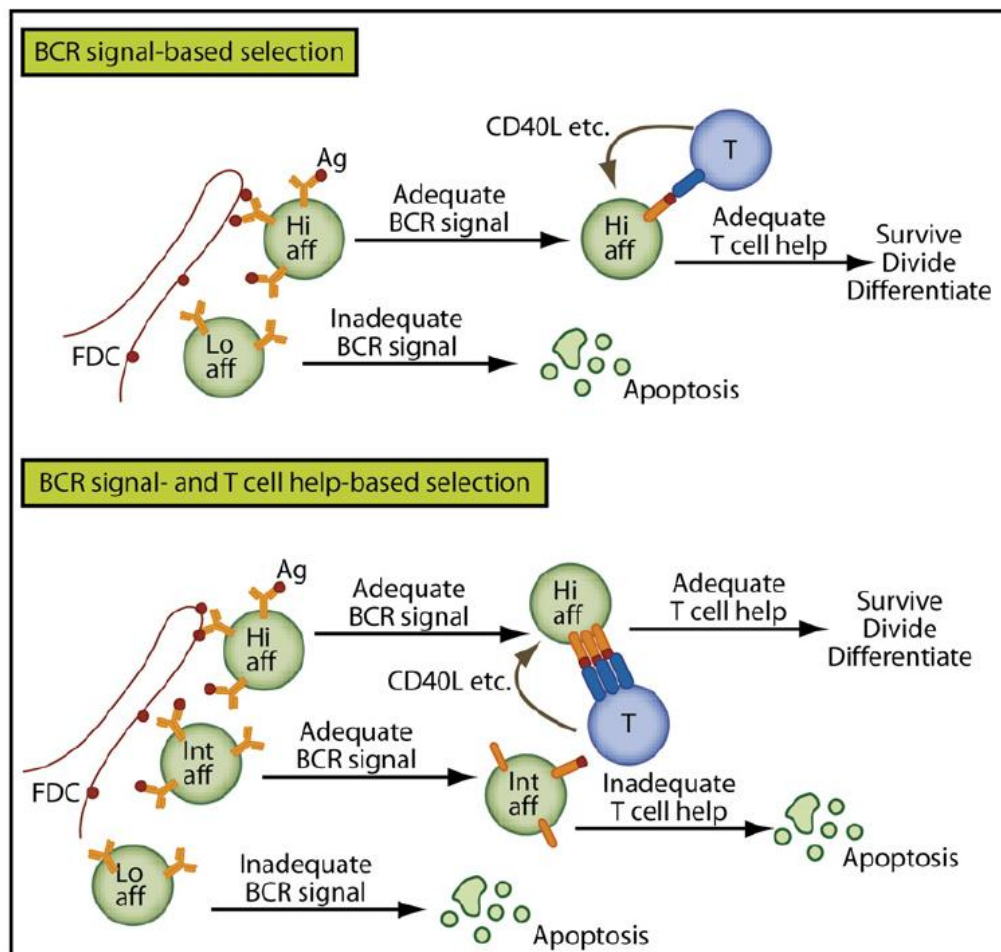
Figure 13. Two models of GC B cell Selection within the GC

In the first model, discrimination between cells of different affinity for the foreign antigen occurs solely at the level of different strengths of BCR signalling. In the second model, sufficient BCR engagement is still necessary, but further selection occurs because of competition for T cell help. B cells that have captured, processed, and presented more antigen as MHC-peptide complexes go on to receive T cell help at the expense of cells that have captured less antigen. "Hi Aff," "Int Aff," and "Lo Aff" refer to B cells with high-, intermediate-, and low-affinity BCRs, respectively[101].

1.3.2.2.3 Antibody Affinity maturation

During infection the average affinity of serum antibody to stimulating antigen has been shown to increase over time and has thus been termed affinity maturation. Affinity maturation is known to occur within germinal centres and involves both somatic hypermutation (SHM) and class switch recombination (CSR) (Figure 14). SHM involves the addition of point mutations into the variable- regions of heavy and light chain coding sequences. The mutation rate during SHM is extremely high, occurring approximately one million times faster than spontaneous mutations in other genes and as a result one mutation occurs per V-region coding sequence per cell generation. During CSR the default Ig constant region (Cμ) is exchanged with different constant regions such as Cγ, Cα, Cδ and Cε[83]. The RNA-editing deaminase, activation-induced cytidine deaminase (Aicda or AID) is both required and sufficient to induce SHM and CSR[103]. During SHM, aicda deaminates cytosine residues on the single stranded DNA (ssDNA) exposed in the non-transcribed strand of double stranded DNA (dsDNA) during transcription (Figure 14)[103-110]. Uracil·guanine (U·G) mismatches are recognised by the mismatch repair (MMR) complex and processed in a number of ways. Replication over the lesion by high fidelity polymerases results in a C→T transition on the newly synthesised strand (Figure 14). Alternatively U residues might be excised leading to the production of abasic sites that are unfaithfully repaired (Figure 14). For CSR to occur, aicda must generate double-stranded breaks within the donor switch constant μ region and the recipient donor switch region of another downstream constant exon (Figure 14). The donor switch regions are then joined together via non-homologous end joining creating a different antibody isotype and the constant exons between the two breaks are deleted (Figure 14)[103].
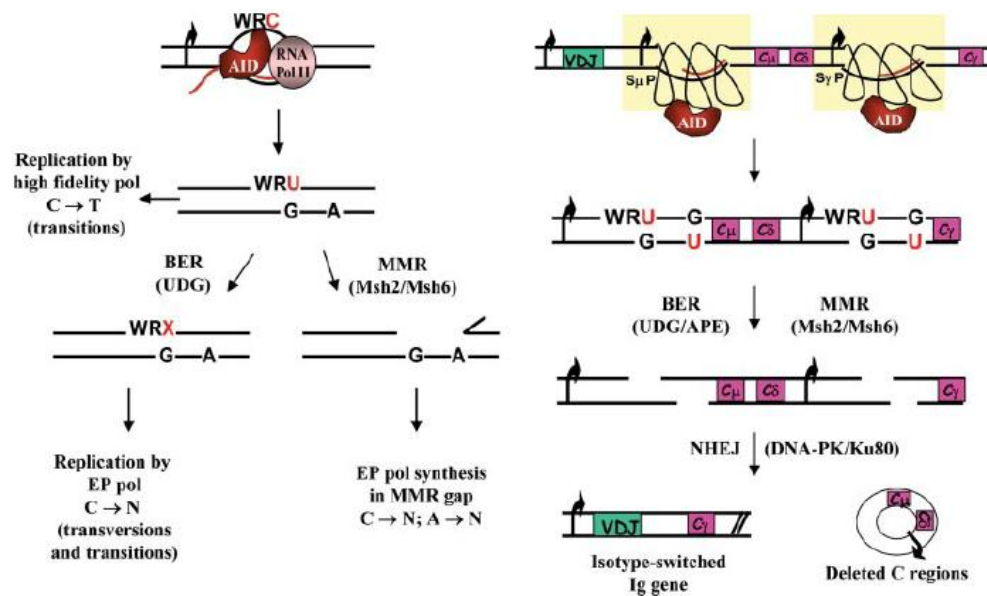
Figure 14. Processing the AID-induced U•G mismatches during SHM (left) and CSR (right)

AID deaminates C on ssDNA exposed during transcription in V and S regions. In the V region, U may be copied with high fidelity polymerases (*Pols*) giving rise to C→T transitions. Alternatively, uracil glycosylase (UDG) may remove U to create an abasic site, and if replicated over with error prone (EP) *Pols*, C→N transitions and transversions could be created. Mismatch repair (MMR) proteins could recognise the U·G mismatch and creates a large repair gap. If the gap is filled in by EP *pols*, C→N and A→N mutations could arise. AID-generated U in the donor switch (S) regions may be processed by basic excision repair (BER) or MMR enzymes to generate dsDNA breaks. The breaks are then repaired by non-homologous end-joining proteins giving rise to an isotype-switched Ig gene[103].

1.3.3 Lymphoid tissue and the Mucosal immune system

In vertebrates, the lymphatic system consists of a network of vessels transporting lymph fluid, circulating lymphocytes, leukocytes and APCs around the body. Most importantly, lymphatic vessels pass through lymphoid tissue whose main function is in the generation of immunity. Lymphoid tissue is rich in B and T lymphocytes as well as accessory cells such as macrophages and reticular cells. It is commonly classified according to the stage of lymphocyte development and maturation it participates in; for example, primary (central) lymphoid tissue such as the thymus and bone marrow are involved in the generation and early selection of lymphocytes, whilst the lymph nodes and lymphoid follicles within the tonsils, Peyer's patches, spleen, adenoids and skin constitute the secondary (peripheral) lymphoid tissues and are involved in the generation of immune responses.

Because secretory epithelia such as the gastrointestinal and respiratory tracts provide a portal into the body for pathogenic organisms, a large amount of lymphoid tissue is associated with mucosal surfaces[111]. The mucosa-associated lymphoid tissue (MALT) consists of organised lymphoid aggregates dispersed along the surfaces of all mucosal tissues. MALT is organized similarly to lymph nodes, with B cell follicles surrounded by interfollicular T cell areas and an efferent lymphatic system however, a striking difference is that there is no afferent lymph supply[112-114]. MALT is often subdivided depending upon the mucosal surface in which it resides; gut-associated lymphoid tissue (GALT), nasal-associated lymphoid tissue (NALT) and bronchus-associated lymphoid tissue (BALT).

GALT is comprised of patches of lymphoid tissue within the gastric mucosa of the small and large intestine, termed Peyer's patches (Figure 15)[115-119]. Peyer's patches are found in greatest density in the jejunum and are considered to be the main site for the development of IgA$^+$ B cells. In mice, there is a further collection of lymphoid tissue located near the blind end of

the caecum, called the caecal patch. Additionally, multiple small isolated lymphoid follicles (ILFs) have recently been identified on the anti-mesenteric wall of the mouse small intestine[120, 121]. ILFs are similar in structure and function to Peyer's patches with a follicle associated epithelium (FAE) over-laying aggregates of lymphocytes but distinctly lack T-cell rich interfollicular regions (Figure 15)[121-123]. It has been suggested that, in addition to the Peyer's patches, the ILFs may represent an important source of IgA$^+$ B cells.
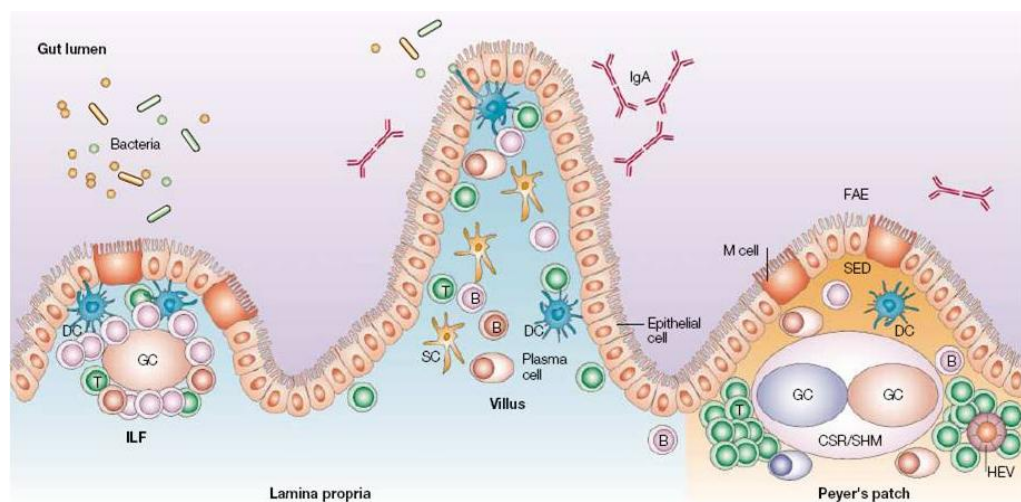
Figure 15. Gastric-associated lymphoid tissue (GALT)

Schematic representation of the gastric-associated lymphoid tissue (GALT), with organised lymphoid structures; Peyer's patches and isolated lymphoid follicles (ILFs) — and diffuse tissue of the epithelium and the lamina propria. Peyer's patches and ILFs are composed of a specialized follicle-associated epithelium (FAE) containing M cells, a subepithelial dome (SED) rich in dendritic cells (DCs), and B-cell follicle(s) that contain germinal centers (GCs), where follicular B cells efficiently undergo class-switch recombination (CSR) and somatic hypermutation (SHM). Migration of B cells into the mucosa takes place through high endothelial venules (HEVs), located in the interfollicular regions of Peyer's patches, which contain mostly T cells. The diffuse tissues of the lamina propria contain a large number of immunoglobulin A (IgA)$^+$ plasma cells, T and B cells, macrophages, dendritic cells (DCs) and stromal cells (SCs). IgA$^+$ B cells and plasma cells are shown in red, IgG$^+$ cells in blue and IgM$^+$ cells in pink[124].

1.3.3.1 Follicle-associated epithelium (FAE)

Simple columnar epithelial cells lining the small and large intestine are joined together by tight junctions which, render the epithelium impermeable to molecules and ions as well as pathogenic organisms and pathogen-derived antigens[125]. Yet in order to generate protective immune responses it is critical that cells of the immune system sample antigens from the gut lumen. To overcome this challenge the GALT is enclosed by a specialized epithelium dedicated to antigen sampling, termed the follicle-associated epithelium (FAE) (Figure 15 and 16)[126-146]. Interspersed within the FAE are unique, antigen sampling microfold (M) cells (Figure 16). M cells have several distinctive characteristics that allow them to be easily identified. These cells differ from normal enterocytes because they lack the typical enterocyte apical brush border. In its place they possess irregular, short, broad and poorly organised microfolds. M cells do not secrete mucus or digestive enzymes and the filamentous brush border glycocalyx (an extracellular polysaccharide layer found throughout the intestine adjacent to enterocytes) is either much thinner or completely absent, allowing them to readily sample antigen from the gut lumen. Notably, M cells have an extremely high capacity for transporting antigens through the epithelium, it has been documented that M-cell mediated endocytosis, translocation and exocytosis can take as little as 10 minutes[145, 146, 147]. Another unique feature of M cells is their intraepithelial 'pocket' formed by a large invagination of the basolateral membrane. Harboured within these 'pockets' are lymphoid cells and APCs such as macrophages which, phagocytose transcytosed antigen (Figure 16)[132]. Some bacteria however have adapted to exploit the use of M cells for invasion of the body. M cells, especially those clustered in the FAE of Peyer's patches are believed to be a major portal of entry for *Yersinia* and *Salmonella*[148].

It is also worth noting that antigen sampling in the mucosal epithelium of the oral cavity, pharynx, oesophagus, urethra and vagina can be carried out by lamina propria DCs directly projecting dendrites into the lumen[132, 149-151].
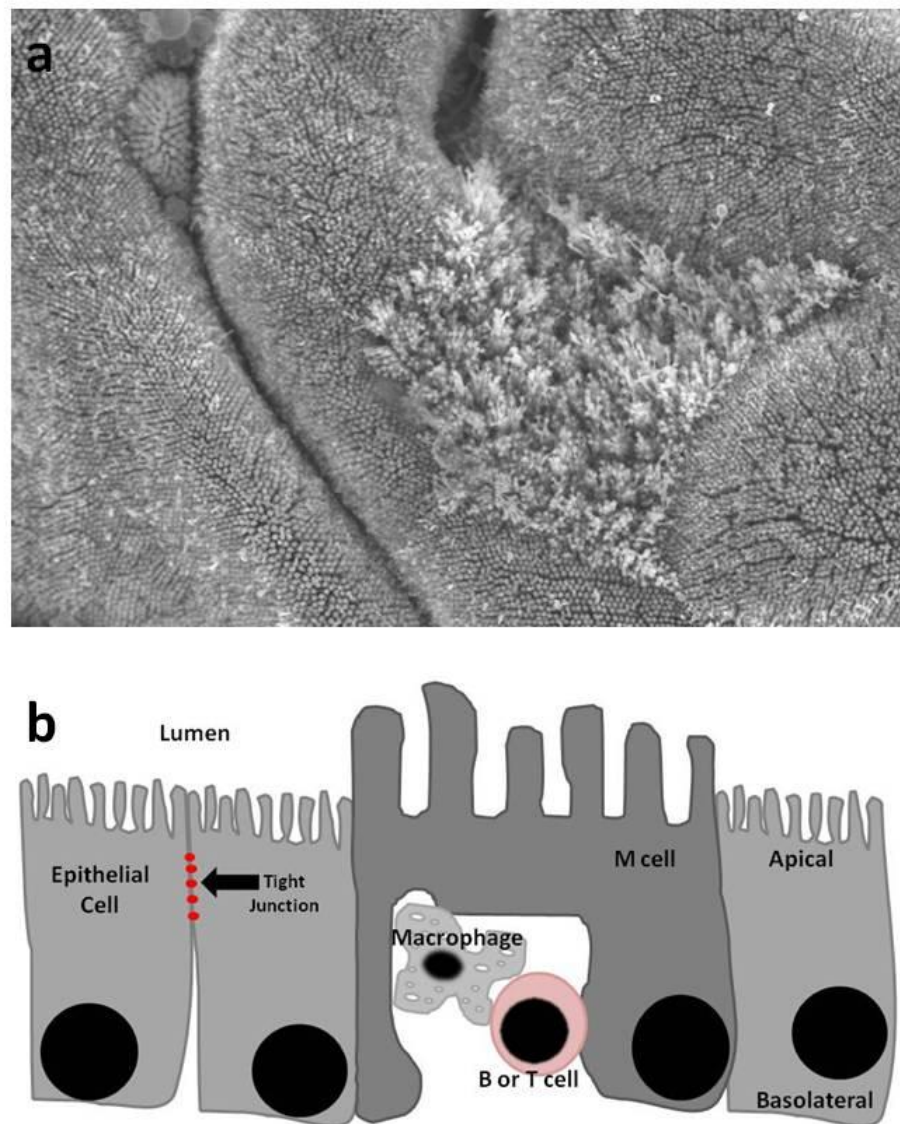
Figure 16. M cell

M cells are specialised residents of the FAE that mediate uptake and transcytosis of antigen from the intestinal lumen to APCs in the underlaying sub-epithelial dome (SED). (a) SEM of an Intestinal M cell, positioned within the FAE surrounded by enterocytes possessing uniform apical brush borders. The apical membrane of M cells is specially arranged into irregular, short and poorly organised microfolds instead of microvilli. Furthermore, M cells do not secrete mucus or digestive enzymes and the filamentous brush border glycocalyx (an extracellular polysaccharide layer found throughout the intestine attached to enterocytes) is much thinner or absent. (b) Schematic representation of an M cell within the FAE. Intestinal simple columnar epithelial cells (enterocytes) are joined together by tight junctions which prevent the passage of molecules, ions and pathogens through the spaces between cells. M

cells endocytose, translocate and exocytose antigen from the gut lumen to lymphoid cells and APCs positioned within an intraepithelial 'pocket'.

1.3.3.2 Mucosal immune system

There are two functional compartments associated with the GALT; inductive sites, where the immune response is initiated, and effector sites, where the immune response exerts its effects (Figure 17)[124]. At mucosal inductive sites, APCs phagocytose transcytosed pathogen-derived antigen and become activated, up-regulating their expression of MHCII and co-stimulatory molecule B7 (Figure 17). In addition they begin secreting cytokines such as IL-1, 6, 8, 12 and TNF-α which help to activate and recruit other cells of the immune system. Upon activation, APCs begin trafficking to secondary lymphoid tissues such as the Peyer's patches/ILFs, spleen and mesenteric lymph nodes where they initiate a GC response and the development of committed antigen-specific B cells (Figure 17).
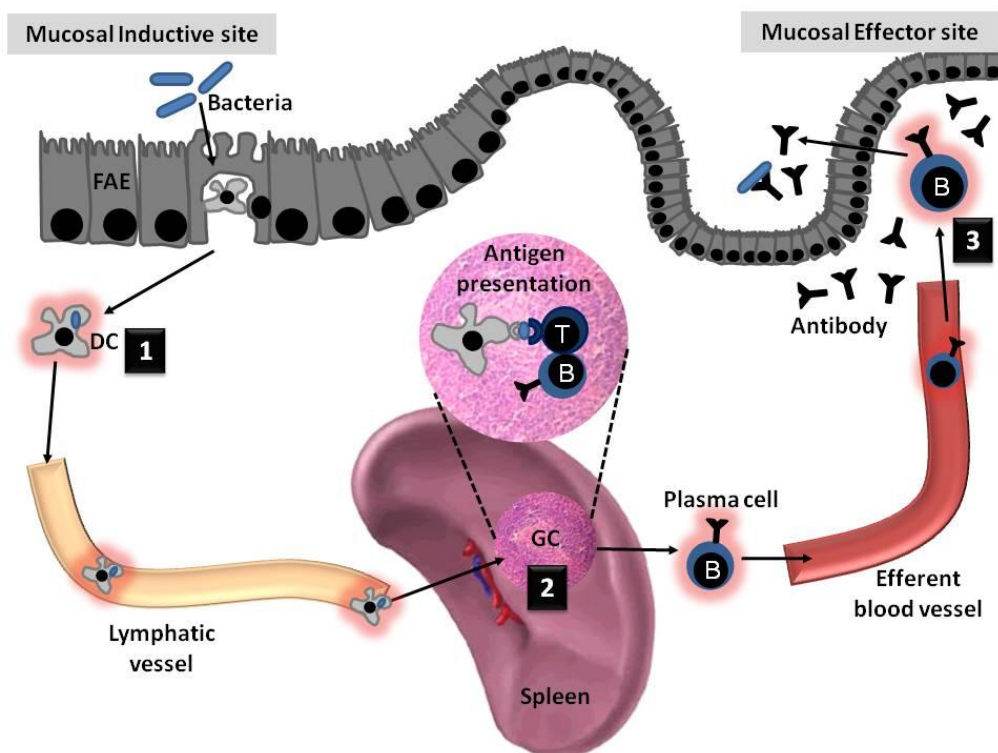
Figure 17. Function of GALT

Schematic representation of the function of GALT. M cells within the FAE sample antigen from the gut lumen and transport it through the epithelium to APCs, such as dendritic cells (DC), in the underlying sub-epithelial dome (SED). Upon binding immunogenic ligands, DCs are activated and begin up-regulating their expression of MHCII and co-stimulatory molecules B7 and CD40. (1) Activated DCs traffic via the lymphatic system to lymphoid follicles within secondary lymphoid organs; Peyer's patches, ILFs, spleen and mesenteric lymph nodes. (2) Once within the secondary lymphoid organs, APCs process the phagocytosed material and present derivative peptides complexed with MHCII to naive CD4 T cells. In turn, activated T cells stimulate differentiation and IgA class-switching in B cells. (3) IgA$^+$ B cells passage into the mucosa via efferent blood vessels and secreted IgA is transported across the epithelium, where it serves as a first line of defence against pathogens and for the maintenance of gut-flora homeostasis.

As discussed previously, the main function of GALT is in the development of IgA, an extremely important antibody that plays a critical role in protecting the mucosal surfaces from infection[124, 152]. IgA$^+$ B cells generated during germinal centre reactions in GALT enter the blood, and preferentially home to the gut lamina propria. Once within the lamina propria, IgA$^+$ B cells undergo terminal differentiation to become plasma cells, capable of secreting large volumes of IgA[124, 153]. Approximately 80% of all plasma cells are estimated to be located within the intestinal lamina propria[124]. Most of the IgA secreted is in the form of dimers, two IgA molecules linked at the constant regions of their heavy chains by a peptide known as the J chain[124, 132]. Mucosal epithelial cells express a polymeric immunoglobulin receptor (pIgR) on their basolateral membranes that recognize and bind dimeric IgA, triggering internalization and transport through the epithelial cells into the lumen[124, 132]. Secretory IgA serves as a first line of defence against mucosal pathogens; binding of IgA to luminal pathogens can prevent their attachment to the epithelium whilst IgA binding to pathogens positioned within the lamina propria is thought to promote their export back out into the lumen[132]. Furthermore, pathogens coated in IgA are either phagocytosed by macrophages or destroyed via antibody-dependent cell –mediated cytotoxicity (ADCC) mechanisms.

1.4 **Citrobacter rodentium**

1.4.1 History

C. rodentium, formerly known as *Citrobacter freundii* biotype 4280 is a non-invasive natural mouse pathogen that infects the distal colon of mice, potentially causing transmissible murine colonic hyperplasia (TMCH)[154]. *C. rodentium* was originally identified in the mid 1900s after a number of spontaneous disease outbreaks occurred in mouse colonies across the USA and Japan. All outbreaks were associated with thickening of the colon (colitis) and the bacteria isolated were either classified as atypical *C. freundii* strains or murine pathogenic *Escherichia coli* (MPEC). Eventually, all the atypical *C. freundii* and MPEC strains isolated during the outbreaks were grouped together under a new species name *C. rodentium*[155].

1.4.2 Attaching-Effacing enteric bacterial pathogens

C. rodentium is genetically related to *E. coli* and is a member of the Enterobacteriacae. *C. rodentium* shares a number of virulence factors and colonisation mechanisms with Enteropathogenic *E. coli* (EPEC) and Enterohaemorrhagic *E. coli* (EHEC). EPEC and EHEC are 'virulent' *E. coli* which, infect the gastrointestinal tract of humans. EPEC is the leading cause of infantile diarrhoea in developing countries whilst EHEC is the primary cause of haemorrhagic colitis and haemolytic uraemic syndrome (HUS), a potentially life threatening illness. *C. rodentium,* EPEC and EHEC all belong to a group of extracellular enteric pathogens which colonise the gastrointestinal mucosa by forming attaching and effacing (A/E) lesions (Figure 18). A/E lesions are characterised by localized destruction of the brush-border microvilli and intimate attachment of the bacteria with host epithelial cell plasma membranes (Figure 18). In addition, bacteria are able to subvert host cell signalling and induce the formation of actin-rich pedestal-like structures (Figure 18)[156-160].
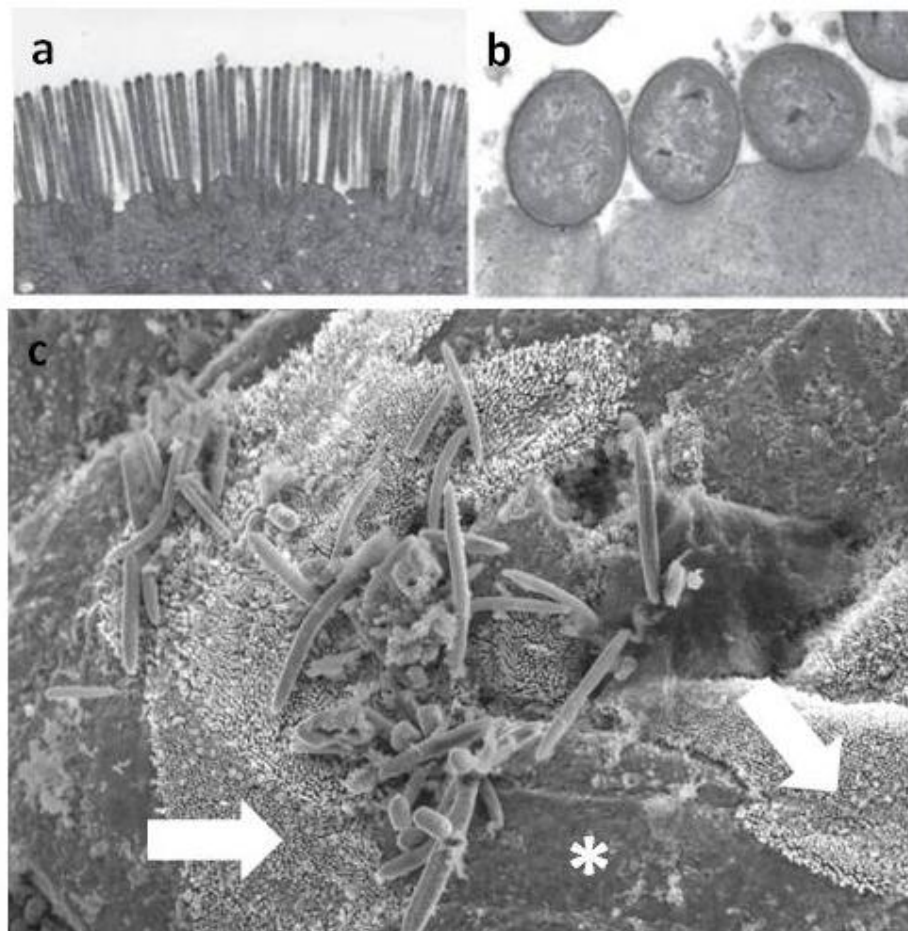
Figure 18. 'Attaching and Effacing' (A/E) lesions

Transmission electron micrographs showing normal brush border microvilli (a) and A/E lesions (b)[161]. Scanning electron micrograph (SEM) of A/E lesions in *C. rodentium* infected colon (c). A/E lesions are characterized by localized destruction (white asterisk) of brush border microvilli (white arrows indicate normal brush border microvilli) and intimate attachment of *C. rodentium* to the underlying apical cell membrane.

1.4.3 Attaching and Effacing (A/E) lesion formation

The genes required for attachment of *C. rodentium*, EPEC and EHEC to host cell plasma membranes and, subversion of host cell signalling during A/E lesion formation are primarily encoded on a horizontally acquired pathogenicity island, known as the locus of enterocyte effacement (LEE). The LEE of *C. rodentium* and those of EPEC and EHEC are not identical but are highly related in terms of overall genetic organization and gene function. The outer membrane adhesion molecule, intimin, and the translocated intimin

receptor (Tir) as well as a type III secretion system (T3SS) and effector proteins have been shown to be important virulence determinants and are encoded on the LEE. Initial attachment of bacteria to host cells requires plasmid encoded bundle forming pili (bfp) and LEE associated EspA filaments (Figure 19). Binding of bfp and EspA to host cell membranes stimulates the secretion of EspB and Tir directly into the host cells (Figure 19). Tir-intimin binding initiates a series of signalling cascades within host cells resulting in actin polymerisation and formation of actin-rich pedestal-like structures beneath the bacteria (Figure 19).
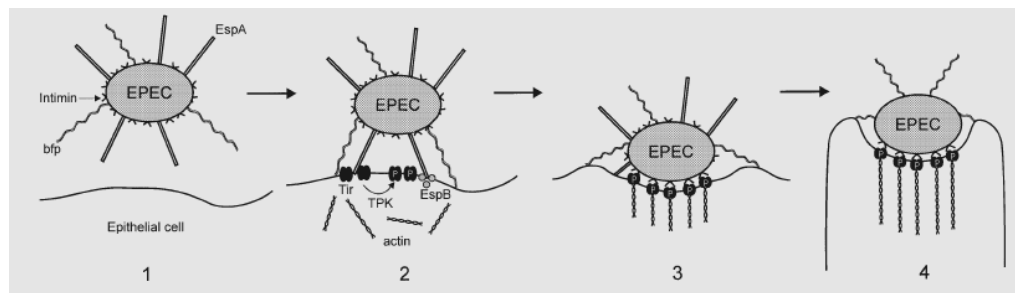
Figure 19. A model of EPEC interaction with epithelial cells

A model of EPEC interaction with epithelial cells. Growth of bacteria in tissue culture media results in expression of adhesins, bundle forming pili (bfp) and intimin and production of EspA filaments (stage 1). Initial attachment of EPEC via bfp and EspA filaments stimulates EspB and Tir translocation, and probably translocation of other, as yet to be identified, effector proteins into the host cell. This in turn leads to tyrosine protein kinase (TPK) activation, formation of the intimin receptor (Tir) and to actin rearrangements (stage 2). Intimin binds to Tir and polymerized actin accumulates beneath intimately attached bacteria; for this to happen, EspA filaments and other surface structures are eliminated from the region of intimate attachment (stage 3). Further actin polymerisation produces the mature A/E lesion in which all EspA filaments and intimin have been eliminated from the bacterial surface (stage 4)[162]

In contrast to our significant knowledge of how attaching-effacing enteric pathogens colonise epithelial cells *in vitro*, we know little about the host immune mechanisms employed to resolve infection. *C. rodentium* provides us with an extremely useful model for studying host-pathogen interactions *in*

vivo and under physiological conditions, with the ability to gain further insights through the manipulation of both host and pathogen[161].

1.4.4 *C. rodentium* infection in mice

The initial site of colonisation after oral gavage with *C. rodentium* is the caecal patch, a specialised lymphoid tissue in the caecum, although the site is actually dependent on how the bacteria are grown Colonisation has been documented to occur within a few hours of the mice receiving oral *C. rodentium*[163]. Within 2-4 days, bacteria spread from the caecal patch to the distal colon. Bacterial levels in the colon peak at around day 4-14 post inoculation (pi) dependent on the mouse strain used, with bacterial numbers reaching approximately 10^9 organisms[161, 164-166]. The infection is mainly restricted to the lumen of the intestine due to the non-invasive nature of the pathogen. Coincident with the peak of infection in the colon can be colonic hyperplasia, characterised by significant proliferation of the colonic epithelia, crypt hyperplasia and dilation and thickening of the colonic mucosa. *C. rodentium* is cleared systematically from the caecal patch first followed by the colon, with complete clearance occurring by days 21-28 pi.

1.4.5 Immune response to *C. rodentium*

Normal immunocompetent mice are able to mount a protective and potentially sterilising primary immune response towards *C. rodentium* with complete clearance of the infection normally occurring within 21-28 days pi. The mice that recover from infection are then highly resistant to further challenges with *C. rodentium*. Infection of the gastrointestinal epithelium elicits a very robust T_h1 biased response, there is a large influx of CD4$^+$ T cells into the colonic lamina propria which secrete copious amounts of the T_h1 cytokine IFN-γ[167, 168]. TNFα and IL-12, two extremely important type 1 cytokines are also upregulated within the colon. The adaptive immune system is critical for clearance. For example, CD4$^+$ T cells are known to be extremely important for the clearance of a *C. rodentium* infection as mice lacking $\alpha\beta$ T cells or CD4 cell subset develop a chronic infection accompanied by a high incidence of

mortality and morbidity (Figure 20)[169-171]. Mice depleted of CD8+ T cells are as competent as control mice in their ability to eradicate a *C. rodentium* infection (Figure 20).
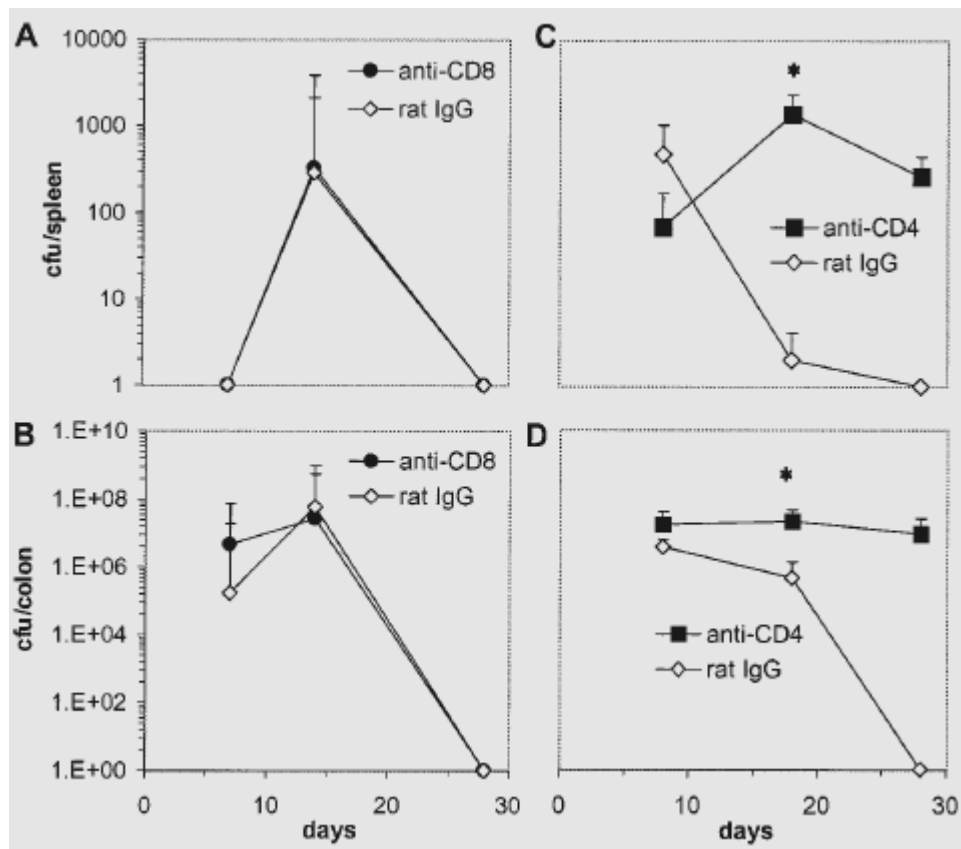
Figure 20. *C. rodentium* counts in mice depleted of CD4+ or CD8+ T cells

Viable counts of *C. rodentium* recovered from colons and spleens of mice depleted of CD4+ or CD8+ T cells. The data depict the mean number of *C. rodentium* CFU recovered from spleens (A) and colons (B) of C57Bl/6 mice (*n* = five per time point) infected orally with 109 CFU of *C. rodentium* and treated with the CD8+-T-cell-depleting MAb YTS169 or the control antibody, rat IgG. Results from a parallel experiment show the number of *C. rodentium* CFU recovered from the spleens (C) and colons (D) of C57Bl/6 mice treated with the CD4+-T-cell-depleting MAb GK1.5 or the control antibody, rat IgG. There were significantly more *C. rodentium* bacteria recovered from the spleen and colons of CD4+-T-cell-depleted mice on day 18 post infection than from rat IgG-treated mice (asterisk, *P* < 0.05). On day 28 post infection, no viable *C. rodentium* bacteria could be recovered from C57Bl/6 mice treated with rat IgG. The data shown are from one of two experiments performed which gave similar results[171]

T cells alone are not able to provide sterilising immunity against *C. rodentium*; µMT mice lacking B cells also fail to clear infection (Figure 21)[171, 172].
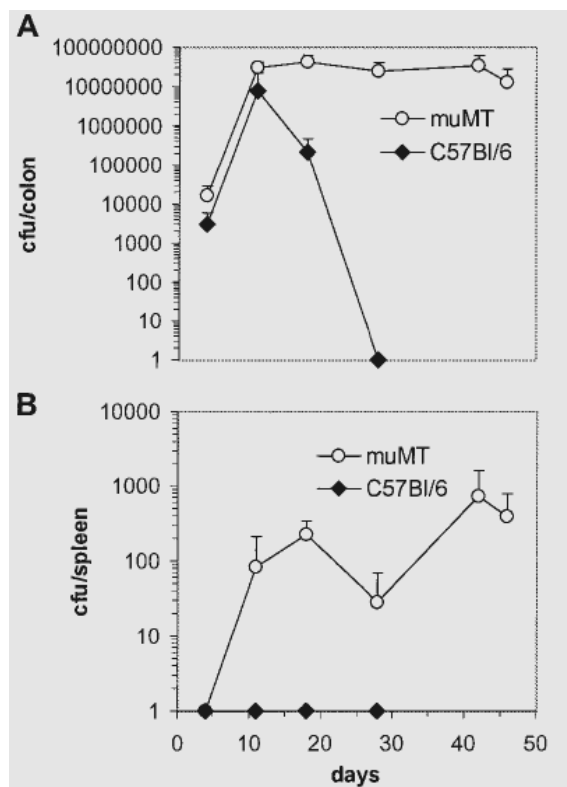
Figure 21. *C. rodentium* counts in µMT and control C57BL/6 mice.

Viable counts of *C. rodentium* recovered from colons and spleens of orally infected _MT and C57Bl/6 control mice. Mice were orally infected with 3×10^9 CFU of *C. rodentium*. The data depict the mean number (± standard deviation) of *C. rodentium* recovered from colons (A) and spleens (B) of muMT and C57Bl/6 mice. There were significantly more *C. rodentium* bacteria recovered from the colons of muMT mice on day 18 post infection than with control C57Bl/6 mice (asterisk, *P*<0.05). *C. rodentium* could not be recovered from C57Bl/6 mice beyond day 28. The data shown are from one of two experiments performed which gave similar results (Simmons et al,. 2003)

Surprisingly, although B cells are essential for clearance, secretory IgA or IgM antibodies are dispensable. Infections in mice lacking IgA or secretory IgM, pIgR or J chain proteins required for antibody secretion into the intestinal lumen showed normal clearance of *C. rodentium*. Transfer of serum

from mice that had cleared a *C. rodentium* infection to naive wild-type mice or pIgR deficient mice receiving oral *C. rodentium* however significantly reduced colonic bacterial numbers[172]. Removing the IgG antibody fraction from the sera before administration completely removed this effect. Thus T helper cell dependent serum antibody responses are required for sterilising immunity against a primary *C. rodentium* infection. Further evidence in support of this is provided by a study of the role of lymphotoxin $\alpha_1\beta_2$/lymphotoxin-β receptor signalling in *C. rodentium*-induced colitis (Figure 22). Inhibition of lymphotoxin $\alpha_1\beta_2$/lymphotoxin-β receptor interactions leads to an increase in *C. rodentium*-induced colitis and bacterial numbers in the colon as well as dissemination of *C. rodentium* to internal organs such as the liver and spleen (Figure 22 and 23)[173].
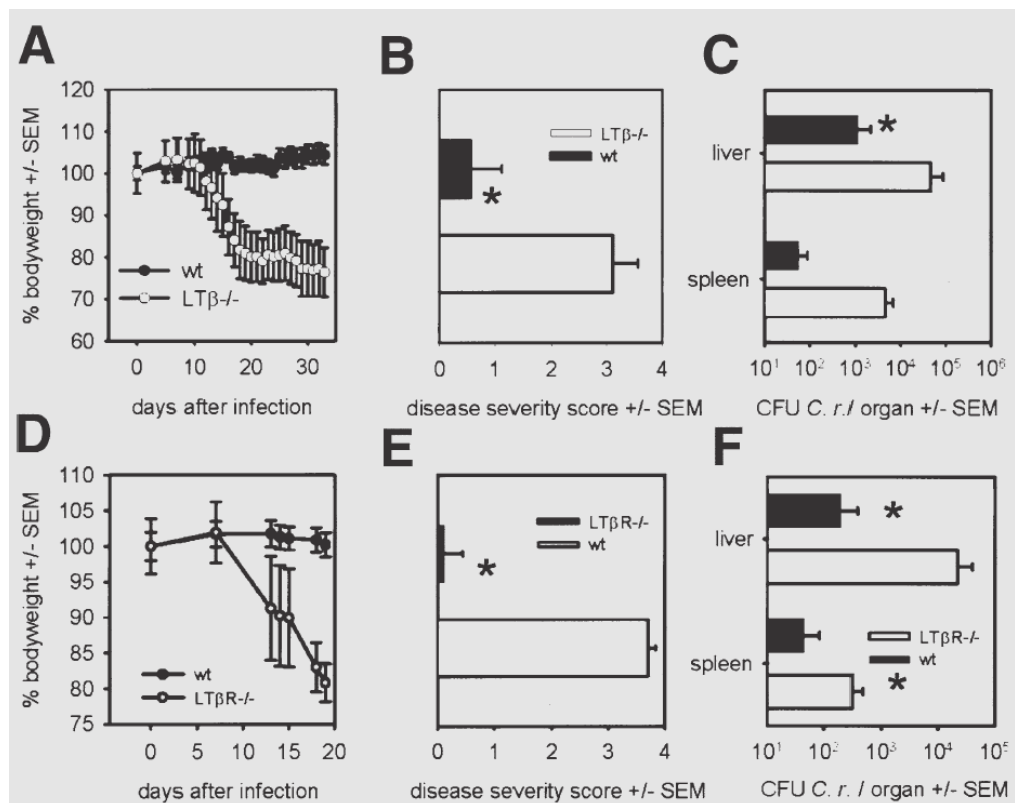
Figure 22. *C. rodentium*-induced colitis in LTβ-/- and LTβR-/- mice

Course of *C rodentium*–induced colitis in LTβ$^{-/-}$ (*A–C*; *open bars* and *open circles*) and LTβR$^{-/-}$ (*D–F*; open bars and open circles) mice and the respective wt mice (filled bars and filled circles). Differences in body weight between LTβ$^{-/-}$ and wt mice (*A*) were statistically

significant (P <.05) from day 17 after infection onward and between LTβR$^{-/-}$ and wt mice (*D*) on days 18–19 after infection. (*A*) Representative experiment out of 2 using 5 (LTβ$^{-/-}$) and 7 (wt) mice per group; (*D*) representative experiment out of 3 using 5–6 mice per group. The average histological disease severity score (*B*) represents pooled data from 2 experiments (wt, n =12; LTβ$^{-/-}$, n =10). (*E*) Pooled data from 2 experiments using 9–10 mice per group. Bacterial growth in liver and spleen organ homogenate cultures from dead LTβ$^{-/-}$ (*C*) and LTβR$^{-/-}$ (*F*) mice and control animals are shown. Bars indicate pooled data from 2 similar experiments: (*C*) wt, n=9; LTβ$^{-/-}$, n =8; (*F*) wt, n =6; LTβR$^{-/-}$, n=5. *P<.05, wt vs. $^{-/-}$. *C. r.*, *C rodentium*. [173]

Mice deficient in CD28 and CD40L develop polymicrobial sepsis, damage to the colon and internal organs and defects in bacterial clearance (Figure 23)[170]. CD28 is critical during a primary *C. rodentium* infection for the survival and proliferation of CD4+ T-helper cells, which not only have effector functions but also aid B cells in the development of protective antibody. CD40L is also involved in providing co-stimulatory effector functions needed to develop protective antibody responses. Summarised in the figure below are the cells, molecules and pathways identified in various studies that are involved in sterilising immunity against *C. rodentium* and have an impact on the pathology seen during infection (Figure 23).

Gene deleted mice who cannot clear infection	Gene deleted mice who clear infection	Gene deleted mice who show reduced pathology	Gene deleted mice who show enhanced pathology
• RAG-/- (lacking T and B cells) • TcRβ-/- (lacking αβ T cells) • CD4-/- mice • μMT (lacking B cells) • Igh-6^{tm1Cgn} (lacking B cells) • LTβR-/- (lacking the lymphotoxin-β receptor)	• TcRδ-/- (lacking γδ T cells) • CD8-/- • β7-/- (largely lacking mucosal lymphocytes) • pIgR-/- (lacking the polymeric immunoglobulin receptor on epithelial cells) • IgA-deficient • IgM-deficient • IgG3-deficient • J chain-deficient (lacking polymeric immunoglobulins) • mCRAMP-/- • MMP3-/-	• PAR2-/- (lacking proteinase activated receptor 2) • iNOS-/-	• TNFα-/- • IL-12 p40-/- • Interferon-γ -/- • LTβR-/- • μMT (lacking B cells) • MMP3-/-

Figure 23. Manipulation of the mouse host effect sterilising immunity, other antibacterial pathways and pathology[161].

1.5 *S*. Typhimurium

Salmonella enterica is a broad enterobacterial species that can cause invasive diseases in a number of animal species. Different members of *S. enterica* can be classified using antisera into serovars that can manifest different disease syndromes and exhibit different patterns of host restriction. For example, *Salmonella enterica* serovar Typhi (*S*. Typhi) is the causative agent of systemic typhoid fever. Although Typhoid fever has been virtually eradicated from the western world it still poses a major health problem in developing countries where water contamination with human faeces and urine is common and antibiotic treatment of infections is becoming increasingly difficult with the increasing emergence of resistant bacteria. In 2004, Crump *et al* estimated that there are more than 21 million cases of typhoid fever each year and approximately 216,510 deaths[174]. *S*. Typhi is human host restricted and consequently is avirulent in animals such as mice; this makes it extremely difficult to study the aetiology of typhoid fever in the laboratory. *Salmonella enterica* serovar Typhimurium (*S*. Typhimurium) causes a typhoid-like enteric fever in susceptible mice with some similarities to that seen in humans infected with *Salmonella* Typhi. As a result *Salmonella* Typhimurium infection in mice is a widely used experimental model for studying typhoid fever in humans.

1.5.1 *S*. Typhimurium infection in mice

Salmonella naturally infects animals and humans via the oral route[175, 176]. Following oral infection of mice with either an attenuated strain or a sub-lethal dose of virulent *S*. Typhimurium, the resulting infection follows a regular time course made up of three relatively distinct phases[177]. During the first phase of infection, *Salmonella* begin colonizing and traversing the intestinal epithelium into the lymphoid follicles beneath (Figure 24)[175]. Experiments using murine intestinal ligated loop models have demonstrated that M cells within the FAE are an important portal of entry for invasive

Salmonella[175, 178]. Following passage through the intestinal epithelium, invading bacteria preferentially infect phagocytes such as dendritic cells and macrophages that inadvertently favour dissemination through the lymphatic system and blood stream to visceral organs such as the mesenteric lymph nodes, spleen and liver (Figure 24)[178].
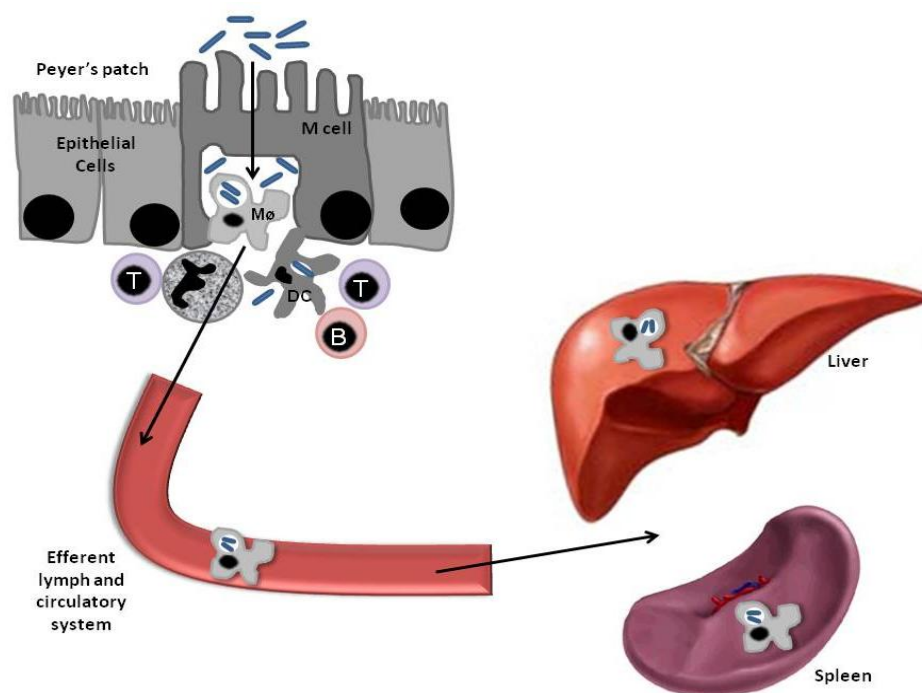
Figure 24. *S*. Typhimurium infection in mice

Schematic representation of *S*. Typhimurium infection in mice. Following oral ingestion of *S*. Typhimurium, bacteria enter the Peyer's patches of the intestinal tract mucosal surface by invading M cells. This is followed by inflammation and phagocytosis of bacteria by neutrophils, dendritic cells (DC) and macrophages (Mø) as well as recruitment of T and B cells. *Salmonella* disseminate through the lymphatics and blood stream to the mesenteric lymph nodes (mLNs) and to deeper tissues. Eventually bacteria are transported to the spleen and liver where they undergo exponential replication, intracellularly.

Bacteria are rapidly cleared from the blood by phagocytes within the liver and spleen, and a large fraction of bacteria are killed by these cells[178]. However, *Salmonella* has evolved a number of mechanisms to force entry into and

survive within the intracellular vacuoles of macrophages by preventing phago-lysosomal fusion and delaying vacuole acidification[179]. Viable and dividing *Salmonella* can be found within the un-fused vacuoles of macrophages[175]. Furthermore, previous experiments have shown that the growth state of *S*. Typhimurium rapidly changes after entry into macrophages[175]. Immediately after entry, bacteria can be killed by treatment with the antibiotics, chloramphenicol and ampicillin. However, if bacteria are allowed to reside within macrophages for greater than two hours prior to antibiotic treatment, some are no longer susceptible, although net growth is inhibited. This suggests that upon entry into macrophages, bacteria undergo a period of rapid growth and require protein synthesis for survival but as infection time increases, the bacteria adapt to their intracellular environment and switch from a rapidly growing state to a survival mode that does not require protein synthesis[175]. Bacteria that circumvent or escape destruction begin a period of intracellular replication, lasting several days[177, 178]. During this time, bacterial titres in the liver and spleen increase (Figure 25). Eventually, bacterial growth is restricted and a phase characterised by splenomegaly, general macrophage-mediated immune suppression and a plateau in bacterial numbers is observed (Figure 25)[178]. Conversely, in lethally infected mice, once bacterial titres reach a critical load threshold of approximately 10^8 bacteria per organ, the animal is no longer able to contain the infection and bacteraemia, endotoxic shock and rapid death ensue (Figure 25)[178]. Bacterial numbers in the liver and spleen begin to fall progressively during the ultimate phase of infection this, coincides with the generation of an acquired immune response capable of eliminating *S*. Typhimurium (Figure 25). Following eradication of bacteria, *Salmonella*-specific lymphocytes generated provide long lasting immunity against re-infection[178].
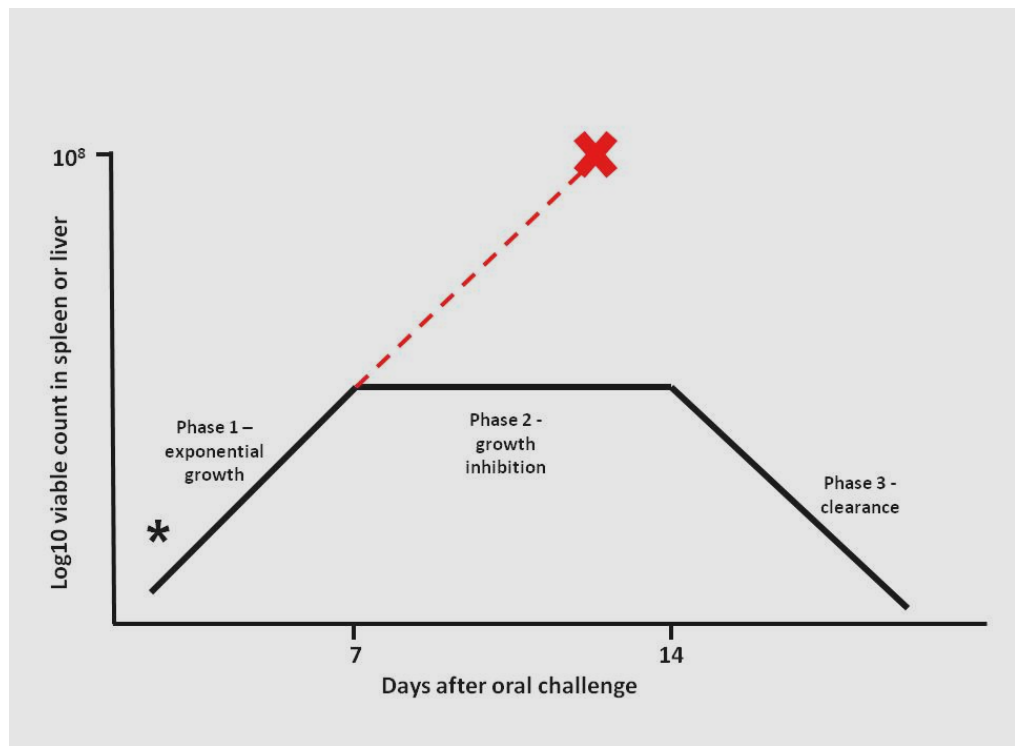
Figure 25. Pathogenesis of *S*. Typhimurium in mice

Schematic representation of the different phases of *S*. Typhimurium infection in mice. During *S*. Typhimurium infection, bacteria ingested orally colonise and breach the intestinal epithelium, and enter the lymphoid follicles beneath. From the follicles *S*. Typhimurium move into the mLNs, and from there bacteria spread via the lymphatic and circulatory systems to the spleen and liver. Bacteria then undergo a phase of intracellular replication lasting several days, during which bacterial titres in the liver and spleen increase. Lethally infected mice (red broken line) are unable to restrict bacterial growth and rapidly succumb to infection once bacterial titres reach a critical load of 10^8 bacteria. However, during non-fatal infection, mice restrict bacterial growth and a subsequent phase of infection characterised by a plateau level of bacterial load ensues. Depending on the mouse strain and the strain of S. Typhimurium used, this phase can last from one to several weeks. The final phase of infection is characterised by a progressive drop in bacterial titres until complete eradication of bacteria is achieved[178]. * A short period of initial kill of approximately a Log can occur following i.v. challenge.

1.5.2 The innate immune response to *S.* Typhimurium

During the early phases of infection, the production of a number of cytokines and soluble factors as well as the recruitment of bone marrow derived macrophages and the development of organized granulomas have been shown to be critical for controlling *Salmonella* spread and growth in the reticuloendothelial system (Figure 26)[180].

Macrophages and neutrophilic granulocytes of the innate immune system are decisive for controlling the net growth of bacteria during the early phase (first week) of infection, with a large fraction of bacteria being killed by these cells[178]. The expression of a functional *Slc11a1* (formerly known as *Nramp1*) gene appears to be a key factor contributing to the efficiency by which macrophages kill *S.* Typhimurium[181]. *Slc11a1* encodes a proton/divalent-cation antiporter which is localised to the vacuolar membrane and controls the intracellular replication of *Salmonella* bacteria by depriving intravascular bacteria of divalent cations. Mice lacking a functional *Slc11a1* gene have a higher susceptibility to *Salmonella* infection[178].

Following infection, components of the bacterial cell wall such as lipopolysaccharide (LPS), DNA, flagella and certain lipoproteins activate Toll like receptors (TLRs) on host cells which in turn induces a robust inflammatory response within tissues, characterised by the production of T_h1-like cytokines IFN-γ, TNF-α and interleukins (IL)-1, 6, 12 and 18 as well as macrophage migration inhibitory factor and inducible nitric oxide synthase (iNOS) (Figure 26)[180]. IFN-γ has been shown to be vital for resistance against infections involving intracellular pathogens, especially *S.* Typhimurium, in part because it stimulates the bactericidal activity of macrophages, including the production of iNOS[180, 182]. Reactive nitrogen intermediates (RNIs) generated by iNOS expression inhibit the growth of phagocytosed *Salmonella*. Mice treated with anti-IFN-γ antibodies are impaired in their ability to clear a sub-lethal dose of virulent *S.* Typhimurium and succumb to infection 7-8 days post-inoculation (pi)[177, 183]. IL-12 and IL-18, secreted by activated macrophages act both independently and synergistically on NK and helper T

cells to induce the production of IFN-γ, which further activates the macrophages through a positive feedback loop. Additionally, IL-12 is important for the polarization of T helper cells toward the T_h1 response[59, 60, 178].

Mastroeni *et al* observed that the suppression of bacterial growth in the reticuloendothelial system coincided with the formation of granulomatous lesions in the liver and spleen and that administration of anti-TNF-α antibodies exacerbated the course of a *Salmonella* infection in both susceptible and resistant mouse strains by inhibiting their formation[184-186]. They also showed that treatment with anti- TNF-α antibodies well after the suppression of bacterial growth and formation of granulomatous lesions, prompted a relapse of the infection and a regression of already established granulomas suggesting that TNF-α is required throughout infection[177, 184-186].

It is important to note that T cells do not play a key role during the early phases of infection, as nude, αβ T cell knockout, and CD4 and CD8 T cell depleted mice are all capable of suppressing the growth of *Salmonella*. However, whilst the innate immune response is highly successful in controlling the initial growth of *S*. Typhimurium, it is insufficient for achieving full protective immunity. Effective control and eventual eradication of bacteria during the late phases of infection (3-4 weeks post-inoculation) and generation of protective immunity against subsequent infections requires the development of a *Salmonella*-specific lymphocyte response (Figure 26)[178].
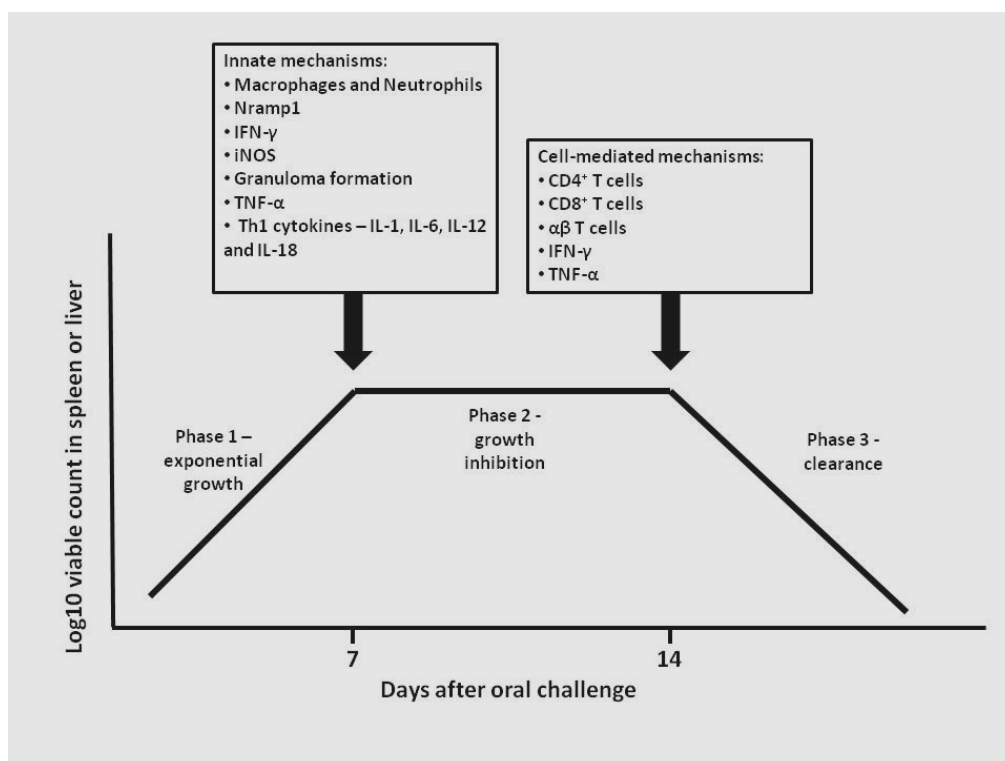
Figure 26. The immune response to *Salmonella*.

Schematic representation of the immune mechanisms required at various stages of *S.* Typhimurium infection in mice.

1.5.3 The adaptive immune response to *S.* Typhimurium

1.5.3.1 Role of T cells during the immune response against *S.* Typhimurium

Following intravenous challenge with *S.* Typhimurium, protective or acquired immunity is mainly T cell mediated, with the participation of both CD4$^+$ and CD8$^+$ subpopulations[182]. However, since a number of studies have shown that the depletion of CD4$^+$ T cells (as opposed to CD8$^+$ T cells) has a more profound effect on the control of primary *Salmonella* infection and on protection induced by vaccination with an attenuated strain of *S.* Typhimurium it would suggest that CD4$^+$ T cells are more important than CD8$^+$ T cells[178]. Additionally, αβ T cells appear to be more important than γδ T cells for protective immunity against *Salmonella* infection since mice on a

susceptible background and deficient in γδ T cells are able to control systemic infection with an attenuated strain of *S*. Typhimurium while mice containing defects in the αβ T cell receptor are not[178].

T cell-mediated protection most likely involves the production of cytokines, in particular IFN-γ, and through IFN-γ-independent mechanisms including the production of other macrophage-activating cytokines, cytotoxicity against infected host cells and provision of help for B cells[178]. For example, Th1 cells are capable of producing large amounts of IFN-γ and TNF-α which, as discussed previously are crucial for macrophage activation and granuloma formation, respectively. During infection with *S*. Typhimurium, CD8$^+$ T cells differentiate into CTLs which, may also play a key role in protection by liberating intracellular *S*. Typhimurium from infected macrophages[178]. Bacteria released during this process are more likely to be killed by activated phagocytes or by granulysin, an antibacterial molecule produced by the CTLs. Arguably, the most important function of T cells during the development of protective immunity is in the regulation of antigen-specific B cell activation and maturation which, will be discussed in greater detail later[178].

Infection of vaccinated mice with virulent *Salmonellae* has led to similar conclusions about the importance of IFN-γ-producing CD4$^+$ T cells. A number of groups have reported that there is a limited protective effect following vaccination with an attenuated strain of *Salmonella* if immunised mice are depleted of CD4$^+$ T cells just prior to challenge with a virulent strain. Additionally, the depletion of Th1-like cytokines such as IFN-γ, TNF-α and IL-12, using neutralising antibodies after vaccination, greatly exacerbates secondary infection. Thus, the activation of T_h1 cells is required not only for the defence against primary infection with *Salmonellae* but also for the vaccine-induced resolution of infection[187].

1.5.3.2 Role of B cells during the immune response against *S*. Typhimurium

Resolution of a primary infection in mice with attenuated *S*. Typhimurium is predominantly T cell mediated but is largely independent of B cells. In contrast, B cells have been shown to be essential for the expression of full protective immunity to virulent oral challenge. Mastroeni *et al* have used gene targeted B cell-deficient, innately susceptible mice on a C57BL/6 background (Igh-6$^{-/-}$) to investigate the role of B cells in protective immunity to *Salmonella* infection. They discovered that Igh-6$^{-/-}$ mice infected with a live, attenuated *aroA S*. Typhimurium vaccine strain were able to control and clear the inoculum from the reticuloendothelial system (Figure 27)[188]. However, unlike control C57BL/6 mice, Igh-6$^{-/-}$ mice challenged orally with virulent *S*. Typhimurium strain C5 four months after vaccination, were unable to control infection, suggesting that B cells are required for acquired resistance (Figure 27)[188]. It appears that the role of B cells in acquired resistance to *Salmonella* involves more than just the production of *Salmonella*-specific antibodies since passive transfer of large amounts of immune serum into immunized Igh-6$^{-/-}$ mice before challenge does not fully restore resistance[188]. Additionally, total splenocytes and purified CD4$^+$ T cells isolated from Igh-6$^{-/-}$ mice 4 months after vaccination showed a reduced ability to release the Th1-type cytokines IL-2 and IFN-γ upon re-stimulation in vitro with *S*. Typhimurium soluble extracts, but not ConA[188]. B cells have been shown to play an essential role *in vivo* to amplify the CD4$^+$ T cell response to antigen by providing co-stimulation[189]. Furthermore, the size of the memory CD4$^+$ T cell pool that develops is determined by the degree of B cell-dependent T cell expansion that occurs in the primary response thus, the absence of B cells results in a significant impairment of Th1-type immunological memory[189]. In fact, a recent study found that the frequency of memory CD4$^+$ T cells generated in μMT mice immunised with NP-KLH was ~ 30-fold lower than that in C57BL/6 mice[189].
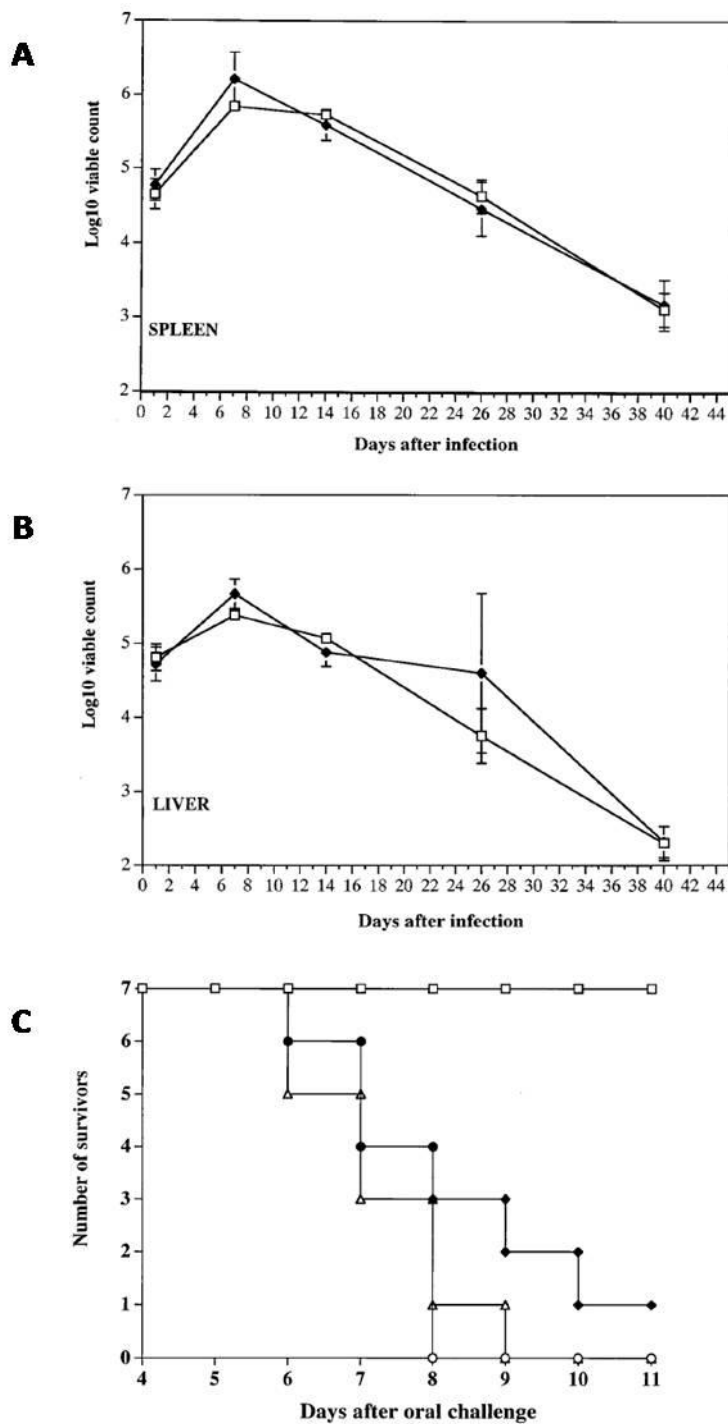
Figure 27. Igh-6$^{-/-}$ (B cell deficient) mice fail to mount solid acquired resistance to oral challenge with virulent *Salmonella* Typhimurium.

Igh-6$^{-/-}$ mice (closed diamonds) and C57BL/6 mice (open squares) were infected i.v. with 5 X 10^5 CFU of *S*. Typhimurium strain SL3261. Spleen (A) and liver (B) counts of viable bacteria were obtained thereafter. Results are means ± standard deviations from groups of four mice. Igh-6$^{-/-}$ mice (closed diamonds) and C57BL/6 mice (open squares) were immunized with *S*. Typhimurium SL3261 as for (A) and (B). Age-matched naive Igh-6$^{-/-}$ mice (closed triangles) and naive C57BL/6 mice (open circles) were used as unimmunized controls. Four months after vaccination, all mice were challenged orally with ca. 2.5 X 10^9 CFU of virulent *S*. Typhimurium strain C5 (C)[188].

1.6 **Hypothesis**

As discussed previously, recent studies have identified miR-155 as an extremely important miRNA of the immune system. To date miR-155 has been shown to be induced in cells of both the innate and adaptive immune system following antigenic stimulation[28, 29, 33, 34]. Furthermore, miR-155-deficient mice exhibit impairments in the ability of miR-155-deficient DCs to activate cognate T cells in addition to defective T and B cell immunity[31]. Therefore, we hypothesize that miR-155 is important for both the development of immunity and infection control.

1.7 **Aims of this thesis**

Relatively little is known about the role of miR-155 in protection against infection or in mucosal associated immunity. The aim of this study was to elucidate the role of miR-155 in controlling a mucosal *C. rodentium* infection and a systemic infection with *S*. Typhimurium, in the context of the overall immune response.

2 Materials and methods

2.1 Materials

2.1.1 Reagents

All chemicals were obtained from Sigma (Poole, Dorset, UK) unless otherwise stated. Reagents were prepared and stored according to the manufacturer's guidelines.

2.1.2 Bacterial strains

Bacterial strain	Characteristics	Reference/source
S. Typhimurium SL3261	*aroA his* deletion harbours pnir15TetC plasmid that drives TetC expression	Supplied by Derek Pickard[32]
S. Typhimurium SL1344	Wild-type of SL3261	Supplied by Derek Pickard[190]
S. Typhimurium C5	Fully virulent strain	Supplied by Simon Clare[180]
C. rodentium DBS100	Wild type naladixic acid resistant	Supplied by Derek Pickard[191]

Table 1. Bacterial strains used during study

2.1.3 Immunofluorescence antibodies

Target Molecule	Host	Isotype	Conjugate	Source
CD45R/B220 clone RA3-6B2	Rat	$IgG_{2a,\kappa}$	FITC	Pharmingen
PNA	*Arachis hypogaea*	N/A	Rhodamine	Pharmingen

Table 2. Antibodies for immunofluorescence staining

2.1.4 ELISA antibodies

Target Molecule	Host	Isotype	Conjugate	Source
Ig	Goat	Ig	Horse Radish Peroxidase (HRP)	BD Pharmingen
IgG	Goat (Rat absorbed)	IgG	HRP	AbD Serotec
IgG_1	Rat	IgG_1,κ	HRP	BD Pharmingen
IgG_{2a}	Rat	IgG_1,κ	HRP	BD Pharmingen
IgA	Goat	IgG	HRP	AbD Serotec
IgM	Goat	IgG	HRP	AbD Serotec

Table 3. Antibodies Used for ELISAs

2.1.5 Mice

Female and male 5-7 week old C57BL/6 and miR155-deficient mice obtained from the Sanger Institute were used in all animal experiments. miR-155-deficient mice (*Bic*[m2] allele) were previously described[31]. All animals were given food and water *ad libitum*. Mice were sacrificed by cervical dislocation. Animal husbandry and experimental procedures were conducted according to the United Kingdom Animals (Scientific Procedures) Act 1986.

2.1.5.1 Chimeric mice

Wild type- and miR-155-deficient, μMT chimeric mice were produced by Dr Elena Vigorito (Babraham Institute, Cambridge) as previously described. Briefly, μMT (B cell-deficient) mice were irradiated (5.0 Gy) and reconstituted with 3×10^6 bone-marrow cells. For the generation of mixed chimeras, irradiated μMT mice received a mixture of 80% bone-marrow cells of μMT origin and 20% wild-type or miR-155-deficient cells.

2.2 Methods

2.2.1 Bacterial growth conditions

All strains were routinely grown at 37°C in Luria Bertani (LB) broth, in air.

Citrobacter Rodentium strain DBS100 was grown at 37°C overnight with shaking (220 rpm) and aeration in LB broth.

S. Typhimurium strains SL1344, SL3261and C5 were grown at 37°C for 16 h as a standing culture without aeration in LB broth.

2.2.2 Animal methods

2.2.2.1 Preparation of inoculum

2.2.2.1.1 Oral *C. rodentium*

C. rodentium cultures were grown overnight as described above. Cultures were harvested by centrifugation at 4000 rpm for 10 minutes at 4°C and resuspended in 1/10 of the original volume in Dulbecco's Phosphate Buffered Saline (D-PBS). Mice were orally inoculated, with anaesthetic, using a gavage needle with 200µl (approximately 1×10^9 CFU of *C. rodentium* organisms) of the bacterial suspension. The viable count of the inocula was determined by plating on LB agar supplemented with nalidixic acid (100µg/mL).

2.2.2.1.2 Intravenous *S.* Typhimurium SL3261

S. Typhimurium SL3261 cultures were grown overnight as described above. Cultures were harvested by centrifugation at 4000 rpm for 10 minutes at 4°C and resuspended in D-PBS. Mice were injected with 200µl (approximately 1×10^5 CFU of SL3261 organisms) of solution into their tail vein. Actual numbers of CFU administered were determined by serial dilutions of the inoculum followed by plating on LB plates prior to animal infection.

2.2.2.1.3 Intravenous *S*. Typhimurium SL1344

S. Typhimurium SL1344 cultures were grown overnight as described above. Cultures were harvested by centrifugation at 4000 rpm for 10 minutes at 4°C and resuspended in D-PBS. Mice were injected with 200µl (approximately1 x 10^2 CFU) of solution into the lateral tail vein. Inocula were cultured on LB agar to determine the administered dose.

2.2.2.1.4 Oral *S*. Typhimurium C5

S. Typhimurium C5 cultures were grown overnight as described above. Cultures were harvested by centrifugation at 4000 rpm for 10 minutes at 4°C and resuspended in D-PBS. Mice were orally inoculated, with anaesthetic, using a blunt-tipped gavage needle with 200µl (approximately 1 x 10^{10} CFU S. Typhimurium C5 organisms). Actual numbers of CFU administered were determined by serial dilutions of the inoculum followed by plating on LB plates prior to animal infection.

2.2.2.2 Determination of number of viable *C. rodentium* in faecal samples

At regular time-points post-infection, mice were placed individually in sterile beakers and faecal samples from individual mice were collected in separate sterile eppendorfs. Faecal samples were weighed and for every 0.01g of faeces 100µL of sterile PBS was added (example – 0.02g faeces add 200µL PBS). Faecal samples were homogenised on a vortex and serially diluted. The number of viable bacteria was determined by viable count on LB agar supplemented with nalidixic acid (100µg/mL). The assay was repeated at least 3 times to ensure reproducibility.

2.2.2.3 Determination of pathogen burden in tissues

At selected time-points post-infection, mice were sacrificed by cervical dislocation and surface sterilized with 70% ethanol. Colons, caecums, caecal patches, livers, spleens and mesenteric lymph nodes (MLNs) were removed aseptically. The terminal 6cm of colon was removed, and the colon weighed after removal of faecal pellets. Caecums were flushed with Phosphate Buffered Saline (PBS) before being processed further, the flow through was collected in a 15mL falcon tube to determine the number of bacteria not intimately attached to the epithelium. Colons, caecums, caecal patches, livers, spleens and mesenteric lymph nodes (MLNs) were placed into individual sterile Seward Stomacher® 400 classic bags and homogenized in 5mL of sterile double distilled water using a Seward Stomacher 80 (Seward, London UK) for 2 minutes at high speed. The number of viable bacteria in tissue homogenates were enumerated by serial dilution and plating in triplicate on LB agar [for C. rodentium LB agar was supplemented with nalidixic acid (100µg/mL)]. Colonies were counted after overnight incubation at 37°C to determine the Log_{10} CFU per gram of tissue. Lower detection limits were approximately 83 CFU/gram of tissue. The assay was repeated twice for each mouse strain to ensure reproducibility.

2.2.3 Molecular methods

2.2.3.1 Total RNA and miRNA extraction

At selected time-points post-infection, mice were sacrificed by cervical dislocation and surface sterilized with 70% ethanol. Caecal patches and colons were removed aseptically and a 2.5mm^2 piece of each placed immediately into 5mL of RNA*later*® solution (Ambion). Samples were incubated at 4°C overnight before either being immediately processed or placed at -70°C for long term storage. Surfaces and equipment were thoroughly cleaned with 70% ethanol followed by RNase*Zap*® and DNase*Zap*® (Ambion) before use. Pieces of tissue were then individually removed from RNA*later*® solution

and placed into a 50mL falcon tube containing double the volume of Qiazol lysis reagent recommended in the Qiagen miRNeasy mini kit (Qiagen) handbook. Caecal patch and colon tissues were homogenized using a tissue homogenizer. Total Caecal patch and colon RNAs and miRNAs were then isolated using the Qiagen miRNeasy mini kit (Qiagen) as per the manufacturer's instructions. Eluted RNAs and miRNAs were stored at -70°C until needed.

2.2.3.2 RNA/miRNA quantification and quality control

All RNA/miRNA samples were quantified using a Thermo Scientific NanoDrop™ 1000 spectrophotometer (Thermo Scientific) as per the manufacturer's instructions. The qualities of the samples were checked using an Agilent 2100 bioanalyser (Agilent Technologies) as per the manufacturer's instructions.

2.2.3.3 Microarray

Gene-expression profiling was performed by the Wellcome Trust Sanger Institute Microarray Facility. Total RNA (500 ng) was amplified using the illumina Total Prep RNA Amplification Kit (Ambion) according to the manufacturer's instructions. Briefly the mRNA is reverse-transcribed with oligo (dT) primers. The oligo (dT) primer incorporates a T7 RNA polymerase (pol) binding site at the 5'-end. After this reaction (2 hours (h) at 42°C) the RNA is digested with RNaseH and the cDNA is converted to double strand cDNA with DNA polymerase (single reaction, 2 h at 16°C). The purified cDNA is then incubated overnight at 37°C with T7 RNA pol and rNTPs (including biotin-tagged rUTP) to produce biotinylated single-stranded anti-sense RNA (often called aRNA or cRNA). Once purified, the cRNA is quantified using a Thermo Scientific NanoDrop™ 1000 spectrophotometer (Thermo Scientific). The biotinylated cRNA (1500ng per sample/array) is then mixed with hybridisation buffer and applied to illumina MouseWG-6 v2 Expression BeadChips and incubated in a humidified atmosphere at 58°C for

16-20 h. Chips were washed according to the standard illumina protocol: 10 min in high temp wash buffer at 55°C (this is the high stringency wash), 5 min in E1BC, 10 min in 100% ethanol (this is to remove any unwanted remnants of the hybridization gasket and to 'clean' the array), 2 min in E1BC (another rinse), 10 min in blocking agent (this is a casein block in PBS to prevent non-specific binding in the next step), 10 min in blocking agent containing 1 ug/ml streptavidin-cy3 (the strp-cy3 will bind to the biotinylated cRNA that has hybridized to the probes on the array) and finally a 5 min rinse in E1BC and a spin-dry (4 min at 275 g). All washes were performed at room temperature except the first high temperature wash. The slides are scanned using a BeadArray reader according to the manufacturer's instructions and the scanner output imported into BeadStudio software (Illumina).

2.2.3.4 Analysis and annotation of microarray data

Analysis and annotation of microarray data was performed by Cei Abreu-Goodger, European Bioinformatics Institute (EBI), Wellcome Trust Genome Campus. Briefly the raw expression values for all samples were exported from Illumina BeadStudio version 3.1.8 as a Sample Gene Profile file. All further data processing was performed using open software packages available through R and Bioconductor[192, 193]. The *lumi* package was used to import the raw expression values, perform a Variance-stabilizing Transformation (VST) and quantile normalisation[194, 195]. In order to discover differentially expressed genes, linear models were fit to each probe and an empirical Bayes approach was used to shrink the estimated variance according to the *limma* package[196]. The resulting P-values for differential expression were adjusted for multiple testing by the Benjamini and Hochberg procedure[197].

Probe annotation was derived from a variety of sources. The Bioconductor packages *lumiMouseAll.db*, *GO.db* and *KEGG.db* were used to retrieve information about Entrez and RefSeq identifiers, gene descriptions, gene Symbols, assignment to GO Biological Process terms and KEGG pathways[198-200]. Information about Ensembl gene and transcript annotation and the 3'UTR

sequences was obtained directly from Ensembl[201]. The 3'UTR sequences were queried for seed matching sites of miR-155 using custom Perl scripts. Predicted targets of miR-155 were also retrieved from TargetScan v4 and PITA[202, 203].

Sylamer was used to test for significant enrichment or depletion of 7-nucleotide words complementary to the seed region of all known mouse microRNAs[204]. Two independent gene lists were derived, one for colon tissue and one for ceacal patch, both containing all genes on the microarrays sorted from the most up- to the most down-regulated in the *bic* mice. The expected result when comparing the expression profile of a microRNA knockout against wild type is a clear enrichment of seed-matching words towards the up-regulated portion of the gene list. The Sylamer plots did not reveal a significant enrichment of miR-155 seed words beyond the expected background distribution. A likely explanation is that miR-155 is expressed exclusively in certain cell types, and that the whole tissue samples being analysed on the microarrays contained a large amount of expression changes coming from other cell types. These changes would not be direct targets of miR-155, and thus the expected enrichment signal might be diluted beyond detection.

2.2.3.5 Quantitative, Real-Time PCR (RT-PCR) for RNA

2.2.3.5.1 Reverse-Transcription of total RNA

Total RNA was reverse transcribed using the Qiagen Quantitect Reverse Transcription Kit (Qiagen) according to the manufacturer's instructions. Briefly the purified RNA sample is briefly incubated in gDNA Wipeout Buffer at 42°C for 2 minutes to effectively remove contaminating genomic DNA (according to table 4).

Component	Volume/reaction	Final concentration
gDNA Wipeout Buffer, 7x	2 μl	1x
Template RNA	Variable (up to 1 μg*)	
RNase-free water	Variable	
Total volume	**14 μl**	–

* This amount corresponds to the entire amount of RNA present, including any rRNA, mRNA, viral RNA, and carrier RNA present, and regardless of the primers used or cDNA analyzed.

Table 4. Genomic DNA (gDNA) elimination reaction components

After genomic DNA elimination, the RNA sample is ready for reverse transcription using a master mix prepared from Quantiscript Reverse Transcriptase, Quantiscript RT Buffer and RT primer mix according to Table 5.

Component	Volume/reaction	Final concentration
Reverse-transcription master mix		
Quantiscript Reverse Transcriptase*	1 μl	
Quantiscript RT Buffer, 5x[†‡]	4 μl	1x
RT Primer Mix[‡]	1 μl	
Template RNA		
Entire genomic DNA elimination reaction (step 3)	14 μl (add at step 5)	
Total volume	**20 μl**	–

* Also contains RNase inhibitor.

[†] Includes Mg^{2+} and dNTPs.

[‡] For convenience, premix RT Primer Mix and 5x Quantiscript RT Buffer in a 1:4 ratio if RT Primer Mix will be used routinely for reverse transcription. This premix is stable when stored at –20°C. Use 5 μl of the premix per 20 μl reaction.

Table 5. Reverse-transcription reaction components

The entire reaction takes place at 42°C for 15 minutes and is then inactivated at 95°C for 3 minutes.

2.2.3.5.2 Real-Time PCR step

Two-Step RT-PCR (standard protocol) was performed with QuantiTect Primer Assays and QuantiTect SYBR Green PCR kit (Qiagen) according to the manufacturer's instructions; using glyceraldehydes 3-phosphate dehydrogenase (GAPDH) for normalisation across samples. Briefly, 2x QuantiTect SYBR Green PCR Master Mix, 10x QuantiTect Primer Assay, template cDNA (50ng/reaction), and RNase-free water were thawed and a reaction mix prepared according to Table 6.

Component	Volume/reaction	Final concentration
2x QuantiTect SYBR Green PCR Master Mix*	25 μl	1x
10x QuantiTect Primer Assay	5 μl	1x
Template cDNA (added at step 4)	Variable	≤100 ng/reaction
Optional: Uracil-N-glycosylase†	0.5 μl	0.5 units/reaction
RNase-free water	Variable	–
Total volume	**50 μl‡**	–

* Provides a final concentration of 2.5 mM MgCl$_2$.

† Supplied with the QuantiTect SYBR Green PCR +UNG Kit.

‡ If using a total volume other than 50 μl, adjust the amounts of the master mix and the primer assay so that their final concentrations remain 1x, but continue to use 0.5 units of UNG and ≤100 ng of template cDNA.

Table 6. Reverse-transcription reaction components

The reaction mix was mixed thoroughly, and 25 μL dispensed into a MicroAmp™ Fast Optical 96-well reaction plate (Applied Biosystems). Template cDNA (50ng/reaction) was added to the individual wells containing the reaction mix. Data acquisition was performed on a StepOnePlus™ Real-Time PCR system (Applied Biosystems) using the cycling conditions recommended in the QuantiTect Primer Assay handbook (see Table 7).

Step	Time	Temperature	Additional comments
UNG (optional) Carryover prevention	2 min	50°C	UNG will eliminate any dUMP-containing PCR products resulting from carryover contamination
PCR **Initial activation step**	**15 min**	**95°C**	This step activates HotStarTaq DNA Polymerase
3-step cycling:			
Denaturation*	15 s	94°C	
Annealing	30 s	55°C	
Extension†	30 s	72°C	Perform fluorescence data collection
Number of cycles	35–40 cycles		The number of cycles depends on the amount of template cDNA and abundance of the target

Table 7. Cycling conditions for two-step RT-PCR

The expression of each target gene was determined by calculating the average of 4 technical replicates for each of 5 biological replicates. The expression of each target gene was determined by the Comparative Ct method ($2^{-[\Delta][\Delta]Ct}$ method), in which Ct is the threshold cycle, ΔCt = [Ct target gene - Ct reference gene (GAPDH)] and the $\Delta\Delta Ct$ = [ΔCt experiment – ΔCt control].

2.2.3.5.2.1 QuantiTect Primers

QuantiTect Primer Assays were shipped lyophilized. To reconstitute a tube of 10x QuantiTect Primer Assay, tubes were briefly centrifuged and 1.1 mL TE, pH 7.0 (Ambion®) was added before mixing the tube by vortexing 4-6 times. Aliquots of the reconstituted primers were stored at -20°C until required.

Gene Name Species mouse (mus musculus)	Entrez Gene ID	Detected transcript	Ensembl Transcript ID	QuantiTect Primer Assay
Matrix metallopeptidase 3 (Mmp3)	17392	NM_010809	ENSMUST00000034497	Mm_Mmp3_1_SG QuantiTect Primer Assay (QT00107751)
B-cell leukaemia/lymphoma 6 (Bcl6)	12053	NM_009744	ENSMUST00000023151	Mm_Bcl6_1_SG QuantiTect Primer Assay (QT01057196)
CD86 antigen (CD86)	12524	NM_019388	ENSMUST00000023618	Mm_Cd86_1_SG QuantiTect Primer Assay (QT01055250)
matrix metallopeptidase 10 (Mmp10)	17384	NM_019471	ENSMUST00000034488	Mm_Mmp10_1_SG QuantiTect Primer Assay (QT00115521)
CD19 antigen (CD19)	12478	NM_009844	ENSMUST00000032968	Mm_Cd19_1_SG QuantiTect Primer Assay (QT00108801)
chemokine (C-X-C motif) receptor 3 (Cxcr3)	12766	NM_009910	Not Applicable (N/A)	Mm_Cxcr3_1_SG QuantiTect Primer Assay (QT00249438)
glyceraldehyde-3-phosphate dehydrogenase (Gapdh)	14433	NM_008084	ENSMUST00000073605	Mm_Gapdh_3_SG QuantiTect Primer Assay (QT01658692)

Table 8. Quantitect Primers

2.2.3.6 Quantitative, RT- PCR for miRNA

miR-155 expression was determined using the miScript System (Qiagen), a three-component system which comprises the miScript Reverse Transcription Kit, miScript SYBR Green PCR Kit, and miScript Primer Assay.

2.2.3.6.1 Reverse-Transcription Step

The miScript Reverse Transcription Kit (Qiagen) includes miScript Reverse Transcriptase mix and miScript RT Buffer. miScript Reverse Transcriptase Mix is an optimized blend of enzymes comprising a poly(A) polymerase and a reverse transcriptase. miScript RT Buffer has been developed specifically for use with the miScript Reverse Transcriptase Mix. This buffer system enables maximum activity of both enzymes as well as containing Mg^{2+}, dNTPs, oligo-dT primers, and random primers. Unlike mRNA, miRNAs are not polyadenylated in nature. During the reverse transcription step, miRNAs are polyadenylated by poly(A) polymerase. Reverse transcriptase converts RNA (including miRNA, other small noncoding RNA, and mRNA) to cDNA using oligo-dT and random primers. Polyadenylation and reverse transcription are performed in parallel in the same tube. The oligo-dT primers have a universal tag sequence on the 5' end. This universal tag allows amplification in the real-time PCR step.

For reverse transcription, template RNA/miRNA was thawed on ice and 5x miScript RT buffer thawed at room temperature. Each solution was mixed by gently flicking the tubes and then centrifuged briefly. The reverse-transcription master mix was prepared on ice according to Table 9.

Component	Volume/reaction	Final concentration
miScript RT Buffer, 5x*	4 μl	1x
miScript Reverse Transcriptase Mix	1 μl	
RNase-free water	Variable	
Template RNA	Variable (up to 1 μg)	
Total volume	**20 μl**	–

* Includes Mg^{2+}, dNTPs, and primers

Table 9. Reverse-transcription reaction components for miRNA or Non-coding RNA

Template RNA (1 μg) was added to each tube containing reverse-transcription master mix and incubated for 60 min at 37°C. tubes were then incubated for 5 min at 95°C to inactivate miScript Reverse Transcriptase Mix and subsequently stored at -20°C prior to real-time PCR.

2.2.3.6.2 Real-Time PCR for Detection of miRNA or Noncoding RNA

2x QuantiTect SYBR Green PCR Master Mix, 10x miScript Universal Primer, 10x miScript Primer Assay, template cDNA, and RNase-free water were thawed and mixed according to Table 10. The miScript Universal Primer allows detection of mature miRNAs in combination with a miRNA-specific primer (miScript Primer assay), an miRNA-specific forward primer which is used for mature miRNA detection. Template cDNA was then dispensed into individual wells of a 96-well plate along with appropriate volumes of the reaction mix, and briefly centrifuged.

Component	Volume/reaction (384-well)	Volume/reaction (96-well)	Final conc.
2x QuantiTect SYBR Green PCR Master Mix*	10 μl	25 μl	1x
10x miScript Universal Primer	2 μl	5 μl	1x
10x miScript Primer Assay	2 μl	5 μl	1x
RNase-free water	Variable	Variable	–
Template cDNA (added at step 4)[†]	≤2 μl	≤5 μl	≤100 ng/ reaction
Total volume	**20 μl**	**50 μl**	–

* Provides a final concentration of 2.5 mM $MgCl_2$.

[†] The volume of cDNA should not exceed 10% of the final reaction volume

Table 10. Reaction setup for RT-PCR detection of miRNA and noncoding RNA

Data acquisition was performed on a Stratagene Mx3000P QPCR System (Agilent Technologies, Inc) according to the cycling conditions provided in the miScript System Handbook (see Table 11).

Step	Time	Temperature	Additional comments
PCR Initial activation step	**15 min**	**95°C**	HotStarTaq DNA Polymerase is activated by this heating step.
3-step cycling:			
Denaturation	15 s	94°C	
Annealing	30 s	55°C	
Extension[†]	30 s	70°C	Perform fluorescence data collection.
Cycle number	35–40 cycles		Cycle number depends on the amount of template cDNA and abundance of the target.

Table 11. Cycling conditions for real-time PCR using block cyclers.

The expression of miR-155 at each time point was determined by calculating the average of 4 technical replicates for each of 2 biological replicates. The

expression of miR-155 was determined by the Comparative Ct method ($2^{-[\Delta][\Delta]Ct}$ method), in which Ct is the threshold cycle, ΔCt = [Ct miR-155 - Ct GAPDH] and the $\Delta\Delta Ct$ = [ΔCt experiment (after infection) – ΔCt control (naive)].

2.2.3.6.2.1 miScript Primer Assay

miScript Primer Assays were shipped lyophilized. To reconstitute a tube of 10x miScript Primer Assay, vials were briefly centrifuged and 550 µL TE, pH 7.0 (Ambion®) was added before mixing the tube by vortexing 4-6 times. Aliquots of the reconstituted primers were stored at -20°C until required.

Gene Name	Entrez Gene ID	Transcripts for this gene	miScript Primer Assay
microRNA-155 (Mir155)	387173	NR_029565	Mm_miR-155_1 miScript Primer Assay (MS00001701)

Table 12. miScript primer Assay

2.2.4 ELISA methods

2.2.4.1 Serum extraction

Mice were placed in a heated box at 37°C for 15 minutes prior to tail bleed. 200µL of whole blood was collected in a sterile eppendorfs and centrifuged at full speed for 15 mins, before serum was collected and stored at 4°C until required.

2.2.4.2 ELISA for total Ig, IgG, IgG1, IgG2a, IgA and IgM in mouse sera (General ELISA protocol)

Flat bottomed Nunc Maxisorp plates were coated overnight at 4°C with 50µL of a solution of relevant antigen (2.5µg/mL ESPA or 5µg/mL TetC) in carbonate buffer (pH 9.6, H$_2$O containing 0.00303% Na$_2$CO$_3$ and 0.006%

$NaHCO_3$). After incubation, antigen/carbonate buffer solution was removed from the plate by inversion and the plate washed once with PBS containing 0.01% Tween-20 (wash buffer). Plates were blocked with 100µL of 3% bovine serum albumin (BSA) in PBS (blocking solution) at room temperature for 1 hour. After blocking solution was removed, plates were washed once with wash buffer, and sera from experimental animal groups was added as follows: 3µL of sera was added to 27µL of PBS + 1% BSA (antibody buffer), 12.5µL of this was added to 112.5µL of antibody buffer placed in the top well of the ELISA plate, which is a 1:100 dilution of serum and then diluted 5 fold down the plate. Each plate contained control wells with pre-immune (naive) serum and PBS alone. Then plates were then left to incubate for 1 hour at 37^oC. After 3 washes with wash buffer, antibodies conjugated to horse radish peroxidise (HRP) diluted 1:1000 in antibody buffer were added at 100µL per well. Conjugate antibodies were either anti-mouse total Ig, anti-mouse IgG, anti-mouse IgG1, anti-mouse IgG2a, anti-mouse IgA or anti-mouse IgM. Plates were incubated at 37^oC for 1 hour, washed 5 times in wash buffer. To develop the plates, 50µL of Sigma fast OPD tablet set dissolved in double distilled water was added to each well and allowed to incubate for 15 minutes at room temperature. The reaction was stopped by adding 25µL 3M sulphuric acid to each of the wells. Absorbances were read at OD490nm and titres were determined arbitrarily as the reciprocal of the serum dilution giving an absorbance of 0.3, using a computer based program called Endpoint. Where possible, a minimum of 5 mice of each mouse strain from at least 2 independent experiments were analyzed.

2.2.4.3 ELISA for IgA in faecal samples

Flat bottomed Nunc maxisorp plates were coated overnight at 4^oC with 50µL faecal homogenate. After incubation faecal homogenate solution was removed by inverting the plate and washing 3 times in PBS containing 0.01% Tween-20 (wash buffer). Plates were blocked with 100µL of 3% bovine serum albumin (BSA) in PBS (blocking solution) at 25^oC for 1 hour. Blocking solution was removed, plates were washed once with wash buffer, and sera

from experimental animal groups was added as follows: 3μL of sera was added to 27μL of PBS + 1% BSA (antibody buffer), 12.5μL of this was added to 112.5μL of antibody buffer placed in the first well of the ELISA plate, which is a 1:100 dilution of serum and then diluted 5 fold down the plate. Each plate contained control wells with naive serum and PBS alone. The plates were then left to incubate for 1 hour at 37°C. After 3 washes with wash buffer, antibodies conjugated to horse radish peroxidise (HRP) diluted 1:1000 in antibody buffer were added at 100μL per well. Conjugate antibodies were anti-mouse IgA. Plates were incubated at 37°C for 1 hour, washed 5 times in wash buffer. To develop the plates, 50μL of Sigma fast OPD tablet set dissolved in double distilled water were added to each well and allowed to incubate for 15 minutes at 25°C. The reaction was stopped by adding 25μL 3M sulphuric acid to wells. Absorbances were read at 490nm and titres calculated based on the reciprocal dilution giving an absorbance of 0.3, using a computer based program called Endpoint. Where possible, a minimum of 5 mice of each mouse strain from at least 2 independent experiments were analyzed.

2.2.5 Tissue staining methods

2.2.5.1 Paraffin embedding tissue and sectioning

Mice were sacrificed by cervical dislocation and surface sterilized with 70% ethanol. Spleens, livers, mesenteric lymph nodes (MLNs), colons and caecal patches were removed and immediately placed in 4% formaldehyde and incubated overnight at room temperature. Tissues were processed in a Shandon Excelsior Tissue Processor (Thermo Fisher Scientific) and then embedded in paraffin wax. 5μm sections were cut using a Leica RM2125 microtome (Leica) and transferred to superfrost plus slides (VWR international).

2.2.5.1.1 Histology

Paraffin sections were deparaffinised and rehydrated by passing slides through Histoclear for 2 minutes, 100% ethanol for 2 minutes, fresh 100% ethanol for

a further 2 minutes, 90% ethanol for 2 minutes, 70% ethanol for 2 minutes and finally washed with water for 5 minutes. Sections were then placed in Mayer's haematoxylin for 2 minutes and washed with running water for 5 minutes. After washing, sections were placed in 1% ethanol for a few seconds to remove excess haematoxylin dye. Sections were washed with water, incubated in eosin for 5 minutes and washed again with water. Sections were dehydrated; 70% ethanol for 2 minutes, 90% ethanol for 2 minutes, 100% ethanol for 2 minutes, fresh 100% ethanol for 2 minutes and finally 2 minutes in Histoclear. Slides were subsequently mounted with DPX and allowed to air-dry overnight before visualization using a Zeiss LSM510 Meta Confocal Microscope and/or Zeiss Axiovision Wide Field Microscope (Zeiss). Crypt depths in colon were determined microscopically, from at least 5 mice per group. Multiple sites were measured throughout each organ, and used to calculate the average crypt depth for each sample.

2.2.5.2 General Chemical Fixation and fine preservation for Transmission Electron Microscopy (TEM)

Mice were sacrificed by cervical dislocation and surface sterilized with 70% ethanol. Colon, caecum and caecal patch tissue were removed and 1mm x 1mm pieces were placed immediately in primary fixative (2% paraformaldehyde (PFA) with 2.5% glutaraldehyde (GA) in 0.1M sodium cacodylate buffer at pH7.42 with added 0.1% and 0.05% magnesium and calcium chloride, respectively) and subsequently incubated at 20°C for 15 minutes, then on ice for remainder of 1 hour. Specimens were rinsed three times for 10 minutes each, in sodium cacodylate buffer with added chlorides, as above. Specimens were then placed into 1% osmium tetroxide in sodium cacodylate buffer only, at room temperature for 1 hour. All the following steps were performed at room temperature. Specimens were rinsed 3 times in cacodylate buffer over 30 minutes and mordanted with 1% tannic acid for 30 minutes to 1 hr and rinsed with 1% sodium sulfate for 10 minutes. Samples were dehydrated by passage through an ethanol series: 20%, 30%, 50%, 70%, 90% and 95% ethanol for 20 minutes each, then 100% ethanol for 3 x 20

minutes. A rotator was used throughout the following steps to aid infiltration. Specimens were incubated twice for 15 minutes in propylene oxide (PO) and then for at least 1 hour in 1:1 PO to Epoxy embedding resin kit (TAAB Epon:812 (48g), DDSA (19g), MNA (33g) and DMP30 (2g) weighed out and mixed in a 50ml falcon) mixture. Specimens were then placed over night in neat Epon (with a few drops of PO). Specimens were embedded in fresh Epon, in a flat moulded tray and cured in an oven at 65°C. Subsequently, 500nm semithin sections were cut on a UCT ultramicrotome and stained with toluidine blue on a microscope slide. Images were recorded on a Zeiss Axiovert CCD camera and areas for ultrathin 50nm sectioning were selected. Thin 50nm sections were collected onto copper grids and contrast stained with uranyl acetate and lead citrate before viewing on an FEI 120kV Spirit Biotwin TEM and recording CCD images on an F4.15 Tietz camera. Images are representative of 3 mice per group.

2.2.5.3 Scanning Electron Microscopy

Colon and caecum samples were fixed with 2.5% glutaraldehyde and 4% paraformaldehyde in 0.01M PBS at 4°C for 1 hour, rinsed thoroughly in 0.1M sodium cacodylate buffer 3 times and fixed again in 1% buffered osmium tetroxide for 3 hours at room temperature. For better conductivity the samples were then further impregnated with 1% aqueous thiocarbohydrazide and osmium tetroxide layers separated by sodium cacodylate washes following the protocol for OTOTO[205]. The samples were dehydrated in an ethanol series 30%, 50%, 70%, 90% and then 3 x 100% for 20 minutes each before critical point drying in a Bal-Tec CPD030 and mounted onto aluminium stubs with silver dag. Finally each sample was sputter coated on the luminal surface with a 2nm gold layer in a Bal-Tec SCD050 and examined on a Hitachi S-4800 SEM. Images are representative of 3 mice per group.

2.2.5.4 Frozen sectioning

Mice were sacrificed by cervical dislocation and surface sterilized with 70% ethanol. Spleens, livers, mesenteric lymph nodes (MLNs), and colons were

removed into separate Corning® External Thread Cryogenic vials tubes (Corning) and immediately snap-frozen in liquid nitrogen. 5µm sections were cut using a Shanndon cryostat. Sections were transferred to HistoBond® slides, allowed to air-dry for 1 hour at room temperature and subsequently fixed in 100% acetone for 10 minutes before use.

2.2.5.4.1. Immunofluorescent staining of frozen tissue sections

Fixed frozen tissue sections were washed 3 times, 5 minute per wash in PBS, sections were subsequently blocked with PBS supplemented with 10% normal goat serum, 5% fish gelatin, 0.01% sodium azide, 0.1% BSA and 0.01% Tween-20 (IHC blocking solution) for 45 minutes at room temperature. Blocking buffer was tapped off, and relevant antibodies added (see Table for antibodies used). For directly conjugated fluorochrome primaries, all antibodies were diluted 1:100 with IHC blocking solution. Control sections for each group did not have any antibody added; only PBS was added to these sections. Slides were incubated for 1 hour at 37°C in darkness. After incubation sections were washed in PBS at room temperature for 15 minutes, in total darkness. Finally slides were mounted with ProLong Gold (Invitrogen) and coverslips, before being left to air-dry in the dark overnight before visualization using a Zeiss LSM510 Meta Confocal Microscope and/or Zeiss Axiovision Wide Field Microscope (Zeiss). The numbers and size of germinal centres within mesenteric lymph nodes were determined microscopically, from at least 4 mice per group. Multiple sites were measured throughout each organ, and used to calculate the average germinal centre size and number.

2.3 Statistical analysis

Statistical analysis was performed with two-tailed Student's unpaired t-test unless otherwise stated with the graphing and statistical software, GraphPad Prism 5 (GraphPad Software, Inc, USA).

3 Immune response to *C. rodentium* in miR-155-deficient mice

3.1 Introduction

Infection of C57BL/6 mice with the bacterial pathogen *C. rodentium* can result in colonic mucosal hyperplasia and a local T_h1 inflammatory response characterised by increased transcription of type 1 cytokines such as IL-12, TNF-α, and IFN-γ. Bacterial colonisation is associated with the colonic mucosa, and normal wild-type adult mice clear the infection spontaneously within ~21-28 days pi. Studies in mice with targeted deletions of the immune system have helped to identify a number of immune factors involved in control of *C. rodentium* infection. In particular, the adaptive immune system, including T and B cells, has been shown to play an essential role in containing and eradicating the infection.

miR-155 has recently been implicated as an important player in both the innate and adaptive immune systems. Previous studies have shown that miR-155 is expressed in a variety of activated immune cells. Specifically, miR-155 is rapidly expressed in $CD4^+$ T cells and macrophages following activation with bacterially and virally relevant stimuli and consequently enhances the production of TNF-α. Furthermore, miR-155-deficient mice show reduced B cell-associated humoral responses. However, most studies have focused on the critical role of miR-155 in isolated immune cells, and thus the role of miR-155 in the context of the overall immune response during active infection still remains to be elucidated.

3.2 Results

3.2.1 miR-155 expression in C57BL/6 mice following infection with *C. rodentium*

To identify whether miR-155 is induced during a mucosal infection, we orally infected wild-type C57BL/6 mice with 10^9 organisms of *C. rodentium* and the

expression of miR-155 in colonic tissue was monitored at various time-points pi, using RT-PCR. The colonisation and clearance of *C. rodentium* was simultaneously measured throughout infection by assessing viable counts recovered from stools. Shedding of *C. rodentium* during this period followed the classical growth curve reported previously[171]. Briefly, *C. rodentium* levels in the colon peaked on day 4 after infection and remained high (~10^7 CFU/g faeces) for approximately a week. Following day 12 pi, bacterial levels began to decline until complete clearance had been achieved by day 23 pi. Time course studies demonstrated that transcription of miR-155 is significantly induced in colonic tissue by *C. rodentium* infection (Figure 28). Additionally, we observed that miR-155 expression is closely associated with the burden of colonic *C. rodentium*. In mice orally infected with *C. rodentium*, miR-155 transcripts rapidly increased following infection, peaked on day 4 pi when colonisation in the colon is at its highest and subsequently fell as bacterial numbers decayed. Upon clearance of *C. rodentium*, the expression of miR-155 returned to pre-infection levels.

However, it should be noted that the single biggest limitation of this study is that, expression data at each of the time points assayed is based on sampling from two mice. Consequently, such a sample size may be too small to provide robust results and additionally could be a major contributing factor to the variation observed in miR-155 expression, particularly as miR-155 expression declines. Such experiments are expensive and labour intensive so to date we have been unable to repeat this experiment.
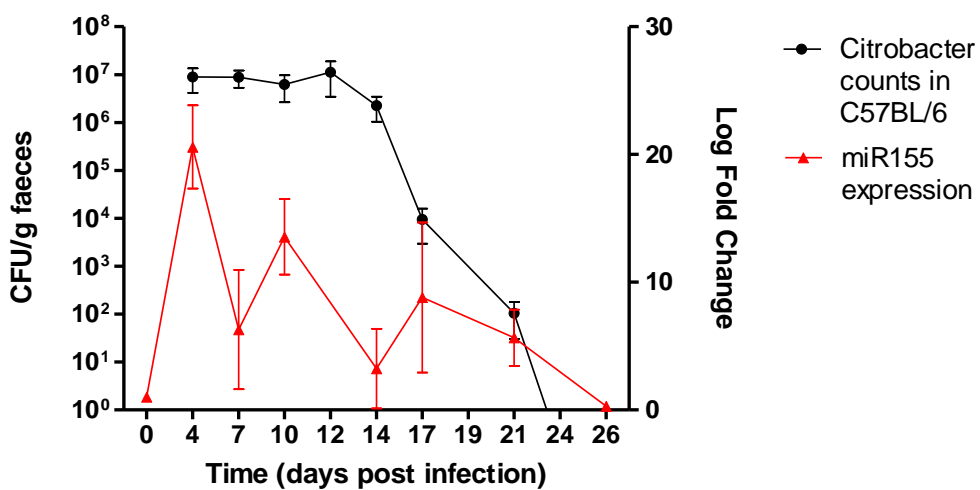
Figure 28. Expression of *miR-155* gene in C57BL/6 mice infected with *C. rodentium*.

C57BL/6 mice were orally infected with 10^9 organisms of *C. rodentium*. The colonisation and clearance of *C. rodentium* was measured throughout infection by assessing viable counts recovered from faecal samples at 4, 7, 10, 12, 14, 17, 19, 21 and 23 days after inoculation (black line), (±SEM), n=7 mice. Total miRNAs were extracted from colonic tissues of mice orally infected with *C. rodentium*. The expression of miR-155 at various time-points pi was monitored by RT-PCR (red line). Data depicts the mean Log fold change (± SEM) of miR-155 transcripts, n=2 mice per time point.

3.2.2 Prolonged clearance of *C. rodentium* infection in miR-155-deficient mice

Given that miR-155 is significantly induced by *C. rodentium* infection we wished to ascertain the impact of the loss of miR-155 on pathogenesis. To this end, we used a genetic approach to determine if miR-155 contributes to immunity to *C. rodentium* by employing mice with targeted deletions of the miR-155 gene[31]. miR-155-deficient and control C57BL/6 mice were orally infected with *C. rodentium* and the numbers of CFUs in faecal samples were determined as an indication of the extent of colonisation. We found that during the early to middle phases of infection, days 4-14 after challenge, there were no obviously significant differences in faecal CFU between miR-155-deficient and control mice (Figure 29a). However, after day 14, whilst control mice began to clear infection, miR-155-deficient mice remained chronically infected and displayed significantly greater bacterial loads (Figure 29a). By day 20, all C57BL/6 mice had resolved infection. This was in stark contrast to miR-155-deficient mice which took on average 20 additional days to achieve complete clearance, P value < 0.0001 (Figure 29b). It is worth noting that during infection there were no obvious disease related mortalities amongst either group and, all miR-155-deficient mice eventually successfully resolved infection.
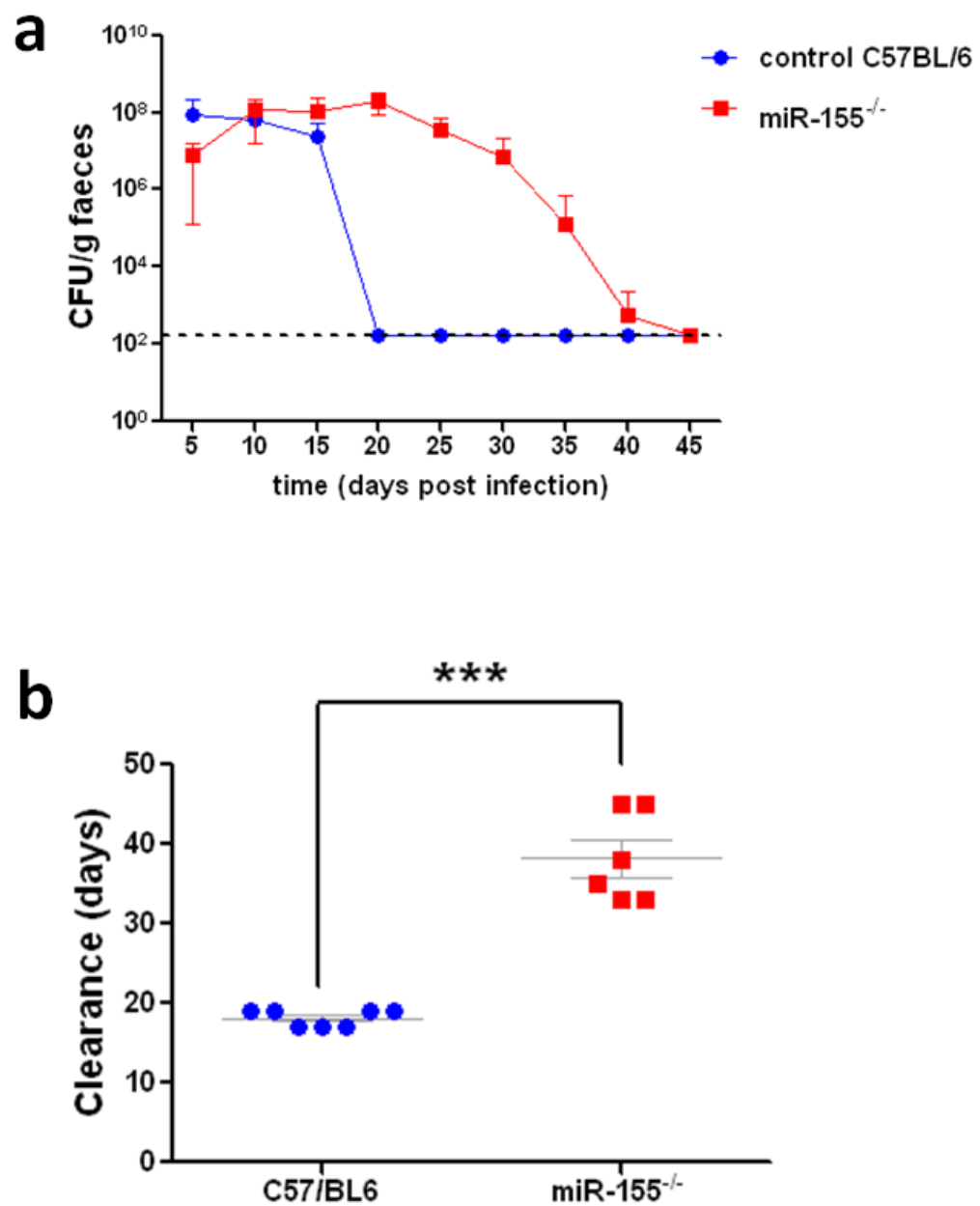
Figure 29. Colonisation and clearance of *C. rodentium* in miR-155-deficient and C57BL/6 mice

Susceptibility to *C. rodentium* infection in miR-155-deficient (miR-155^{-/-}) mice. miR-155-deficient and control C57BL/6 mice were orally gavaged with approximately 1×10^9 CFU of *C. rodentium*. (a) Viable *C. rodentium* were enumerated from faecal samples by plating on LB agar supplemented with naladixic acid, n=7 C57BL/6 and n=6 miR-155-deficient mice. (b) Time (days) taken to resolve infection (± SEM), *** indicates P value <0.0001 by Student's t-test.

3.2.3 Increased *C. rodentium* pathogen burden in gastrointestinal tissues of miR-155-deficient mice

To establish whether the prolonged clearance time observed in miR-155-deificent mice was associated with increased pathogen burden within infected tissues, miR-155-deficient and control C57BL/6 mice were orally infected with 10^9 CFU of *C. rodentium* and the numbers of CFUs in gastrointestinal tissues were determined at various time points pi.

miR-155-deficient mice demonstrated gastrointestinal burdens of *C. rodentium* similar to those seen in control mice during the initial stages of infection. At days 4 and 14 pi, bacterial burden in the colon, caecal patch and caecal contents of miR-155-deficient mice were not significantly different from those observed in controls (Figure 30). However, whilst pathogen burdens in C57BL/6 had fallen considerably by day 20 pi, the burden in miR-155-deficient mice was persistent (Figure 31). Additionally, on day 20 pi, miR-155-deficient mice had significantly greater numbers of bacteria in the caecum than in similarly infected C57BL/6 mice (Figure 31b). Furthermore, 26 days after infection, we were still able to isolate viable *C. rodentium* from the gastrointestinal tissues taken from miR-155-deficient mice, but not those from C57BL/6 mice (Figure 31c).
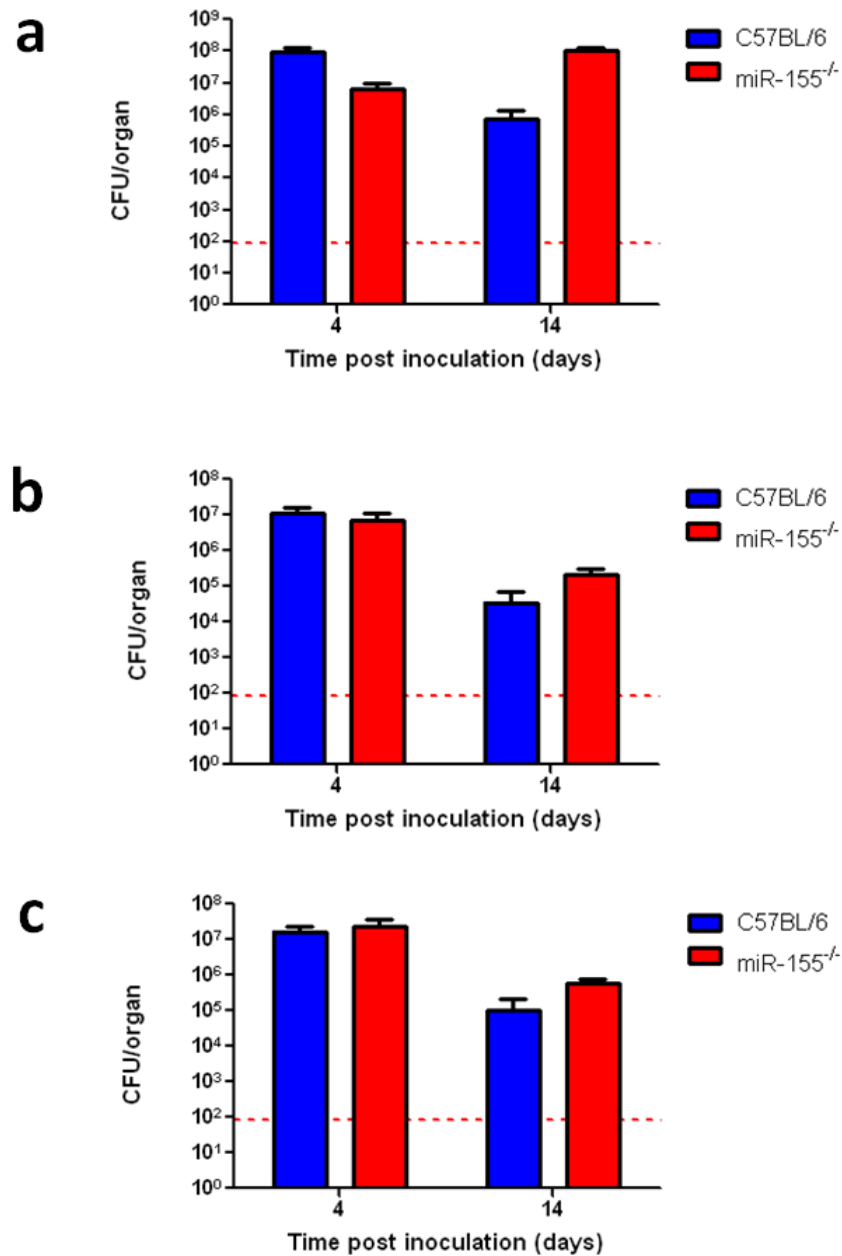
Figure 30. *C. rodentium* burden in gastrointestinal tissues of C57BL/6 and miR-155-deficient mice on day 4 and 14 pi.

Control C57BL/6 (blue bars) and miR-155-deficient (red bars) mice were orally infected with 10^9 organisms of *C. rodentium.* On days 4 and 14 pi, mice were sacrificed and numbers of *C. rodentium* (±SEM) in gastrointestinal tissue; (a) colon, (b) caecum and (c) caecal patch were enumerated, n=5 mice per group. Red broken lines indicate the detection level of the assay.
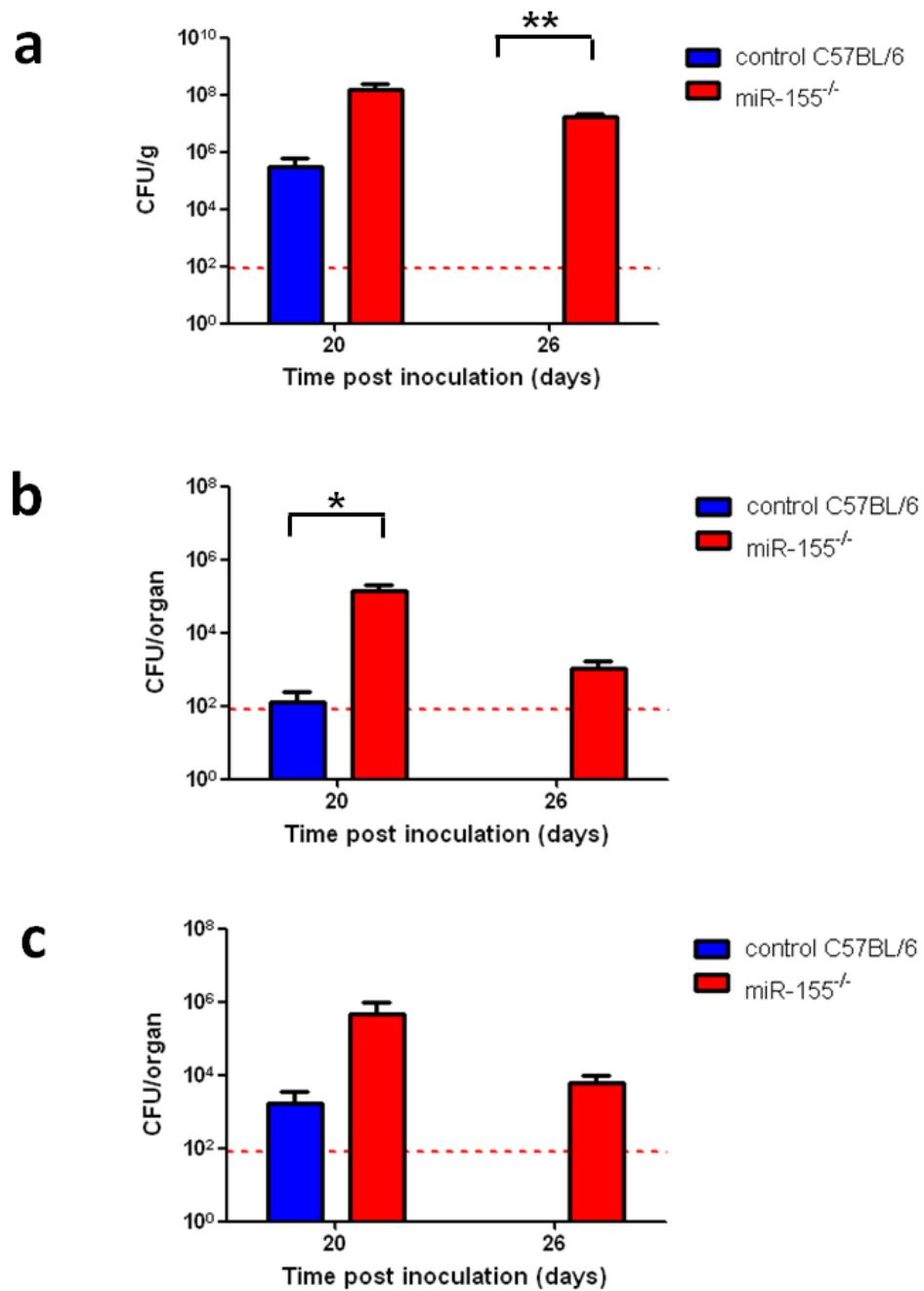
Figure 31. *C. rodentium* burden in gastrointestinal tissues of C57BL/6 and miR-155-deficient mice on day 20 and 26 pi

Control C57BL/6 (blue bars) and miR-155-deficient (red bars) mice were orally infected with 10^9 organisms of *C. rodentium.* On days 20 and 26 pi, mice were sacrificed and numbers of *C. rodentium* (±SEM) in gastrointestinal tissue; (a) colon, (b) caecum and (c) ceacal patch were enumerated, n=5 mice per group, ** indicates P value <0.0027 and * indicates P value <0.0353 by students t test. Red broken lines indicate the detection level of the assay.

3.2.4 miR-155-deficient mice develop more severe pathological changes in the colonic mucosa

C57BL/6 mice infected with *C. rodentium* characteristically develop colonic hyperplasia concurrently with peak pathogen burden in the colon, as indicated by significant proliferation of the colonic epithelia, crypt hyperplasia and dilation and thickening of the colonic mucosa. Analysis of distal colons from infected mice revealed that miR-155-deficient mice develop more severe *C. rodentium*-induced colonic hyperplasia than control C57BL/6 mice. From 14 days after infection the distal colons of infected miR-155-deficient mice were visibly thickened and weighed significantly more than colons of infected C57BL/6 mice (Figure 32a, b and c). Histological analysis of colonic tissue from infected miR-155-deficient mice revealed grossly elongated colonic crypts and polymorphonuclear infiltrate in the lamina propria and submucosa (Figure 32d, e and f).
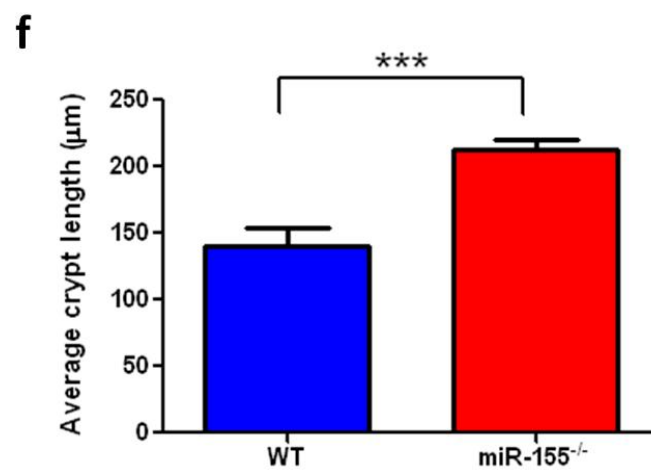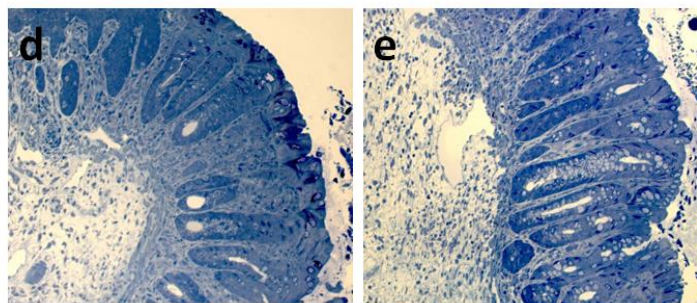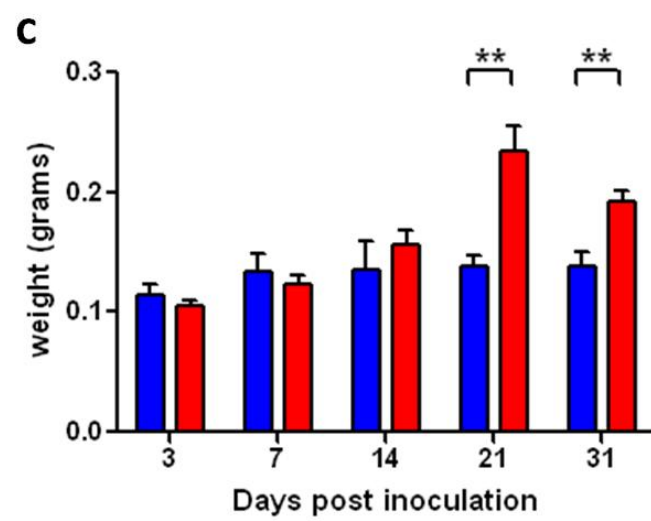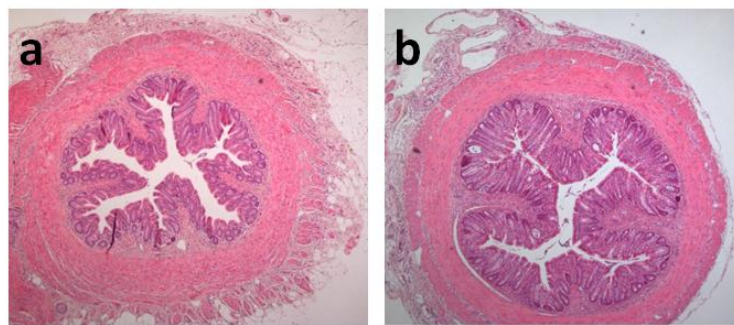
Figure 32. Histopathological analysis of infected colons from miR-155-deficient and control C57BL/6 mice

Histopathological analyses (haematoxylin and eosin-stained sections; original magnification, x5) of colon sections from control C57BL/6 (a) and miR-155-deficient mice (b) on day 14 pi, images are representative of 5 mice per group. The distal colon of infected miR-155-deficient mice weighed significantly more than the colons of infected C57BL/6 mice at 21 and 31 days pi, n=4 mice per group, ** indicates P value <0.0052 and <0.0091 respectively (c). The panels (toluidine blue-stained sections; original magnification x40) show representative stained colonic sections from infected C57BL/6 (d) and miR-155-deficient mice (e) on day 14 pi. Colonic crypts in infected miR-155-deficient mice were significantly elongated (f) Average crypt length (±SEM) was determined from colon sections, n=5 mice per group, *** indicates P value <0.0001 by students t test.

3.2.5 Deficiency of miR-155 leads to the development of polymicrobial infections and severe damage to the colonic mucosa

Closer examination of colons from infected mice using histochemistry and electron microscopy revealed that while the colonic epithelium remained grossly intact in wild-type, knockout mice demonstrated more severe destruction of the epithelium of the distal colon. On day 14 pi, whilst control C57BL/6 mice showed relatively few remaining bacteria present on the epithelial surface and only minor damage to the colonic epithelium, miR-155-deficient mice displayed areas still heavily colonised by bacteria and considerable damage to luminal colonocytes (Figure 33a, c, d and f). Additionally, in miR-155-deficient mice, we observed frequent breaks in the epithelium integrity through which neutrophils and other polymorphonuclear cells had leaked into the lumen (Figure 33b and e).

Unusually, in amongst the areas that remained densely colonised, we noted the presence of microcolonies of cocci intimately adhered to the epithelial surface in miR-155-deficient mice but not controls (Figure 34). This is suggestive that infection with *C. rodentium* in miR-155-deficient mice may lead to a polymicrobial infection, perhaps involving association with components of the microbial flora with the epithelial surface. 16S ribosomal DNA sequence analysis would allow us to accurately identify spatial and temporal changes in the gut microbiome of miR-155-deficient and control mice during infection with *C. rodentium* and we are currently undertaking this analysis[206, 207].
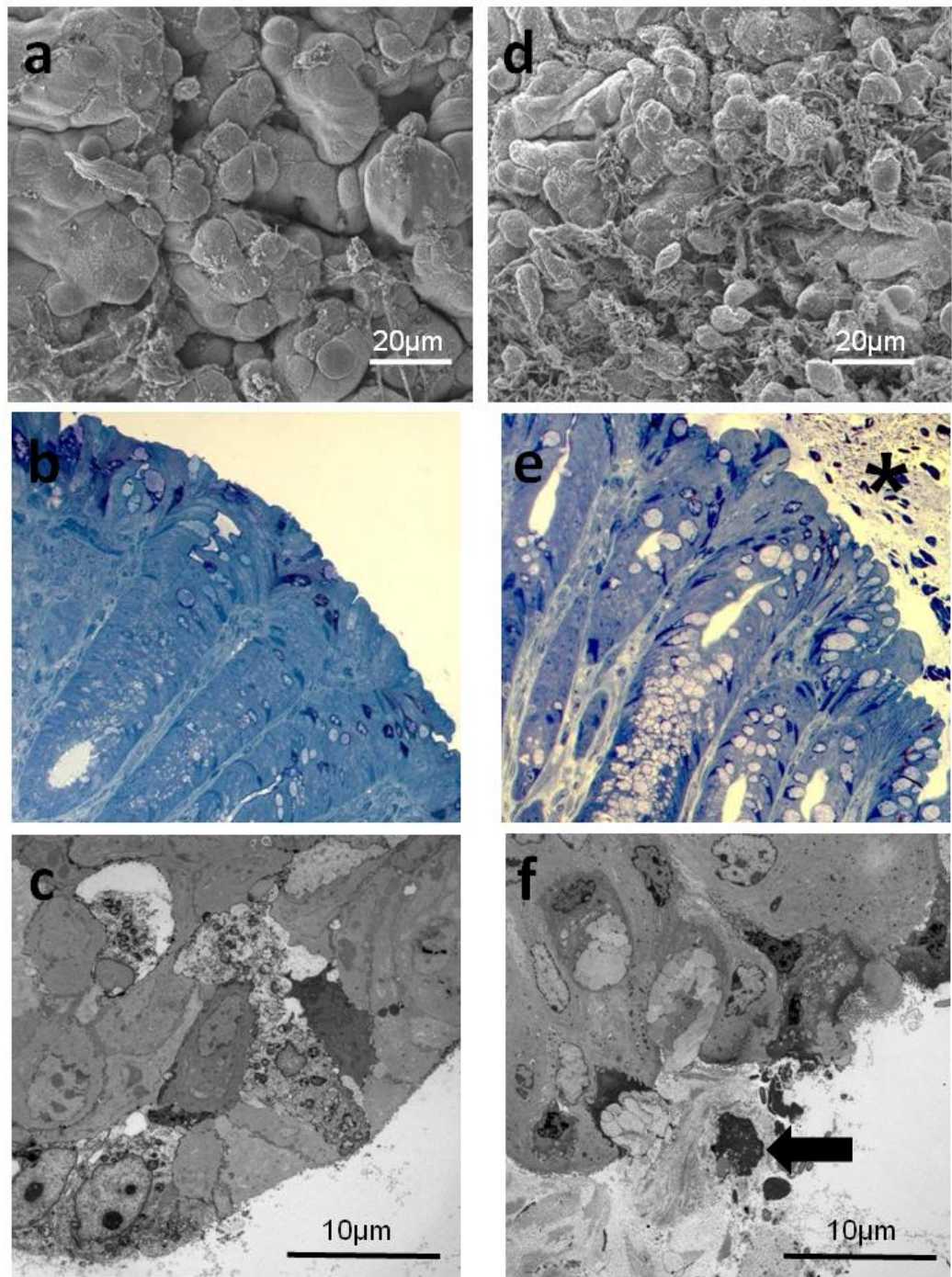
Figure 33. Histopathology in the distal colon of infected C57BL/6 and miR-155$^{-/-}$ mice

Colonic pathology observed at day 14 pi with *C. rodentium*. Colonic epithelium from
C57BL/6 (a) and miR-155-deficient mice (d) was examined by scanning electron microscopy
(SEM). Micrograph from a C57BL/6 mouse showing relatively few remaining bacteria
present on the epithelial surface and only minor damage (a) whilst miR-155-deficient
demonstrate heavy bacterial colonisation and considerable damage to luminal colonocytes.

Toluidine blue staining, magnification x200 (b and e) and transmission electron microscopy (c and f) of colonic mucosa from C57BL/6 and miR-155-deficient mice, respectively, at 14 days pi. C57BL/6 mouse, demonstrating a grossly intact colonic epithelium (b and c). miR-155-deficient mouse showing considerably more severe destruction of the epithelium and breaks through which neutrophils have entered the lumen (asterisk and arrow) (e and f).
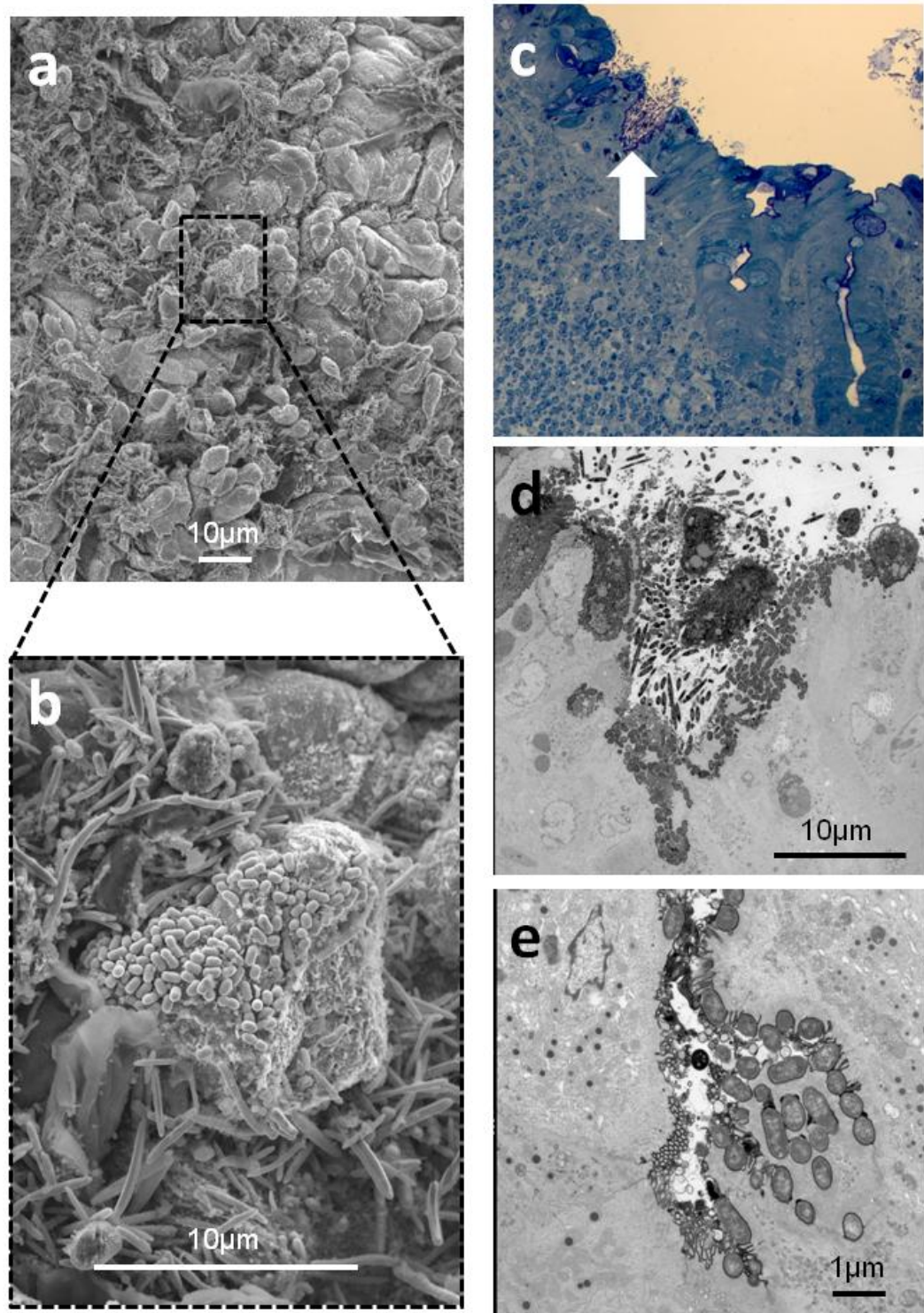
Figure 34. Polymicrobial infection in miR-155-deficient mice infected with *C. rodentium*.

Scanning electron microscopy (a and b), toluidine blue staining, magnification x40 (c), and

transmission electron microscopy (d and e) of polymicrobial colonies observed in colonic

epithelium from miR-155-deficient mice 14 days after infection with *C. rodentium*. Amongst the areas heavily colonised by *C. rodentium* we observed numerous isolated dense microcolonies of cocci intimately attached to the epithelial surface (a and b). Arrow points to a crypt heavily colonised with *C. rodentium* and unidentified cocci (c). Dead and/ or severely damaged infected colonocytes are exfoliated into the lumen (d). Cocci intimately attached to luminal colonocytes, causing localized destruction of the brush-border microvilli and beginning to penetrate through the epithelial barrier into the lamina propria beneath (e).

3.2.6 Systemic spread of *C. rodentium* in miR-155-deficient mice

During the peak of infection, bacterial numbers in the colon can exceed 10^9 organisms per gram of tissue, a significant pathogen burden[161, 164-166]. However, despite the extremely high levels of colonisation the colonic epithelium remains grossly intact, with rare breaks occurring only occasionally as a result of abscess formation and subsequent efflux of neutrophils into the lumen[170]. Such breaks provide portals through which *C. rodentium* and resident gut flora may disseminate to systemic sites[170, 208]. Given that miR-155-deficient mice display more severe colonic damage and frequent epithelial breaks during infection with *C. rodentium*, we wished to investigate if bacteria are able to traverse the damaged epithelia and disseminate to distant sites resulting in a systemic infection.

miR-155-deficient and C57BL/6 mice were infected with *C. rodentium* and systemic tissues were collected on days 20 and 26 pi, and the pathogen burden was determined by viable count. No CFU were cultured from internal organs of C57BL/6 mice at either time point assayed (Figure 35). Unlike C57BL/6 mice, several miR-155-deficient mice exhibited considerable numbers (~10^3 CFU/organ) of *C. rodentium* in the spleen, liver and mLNs on day 20 pi, thus providing evidence of systemic infection (Figure 35). Additionally, 26 days after infection, 25% of miR-155-deficient mice still had significantly greater pathogen burdens in the spleen (Figure 35b).
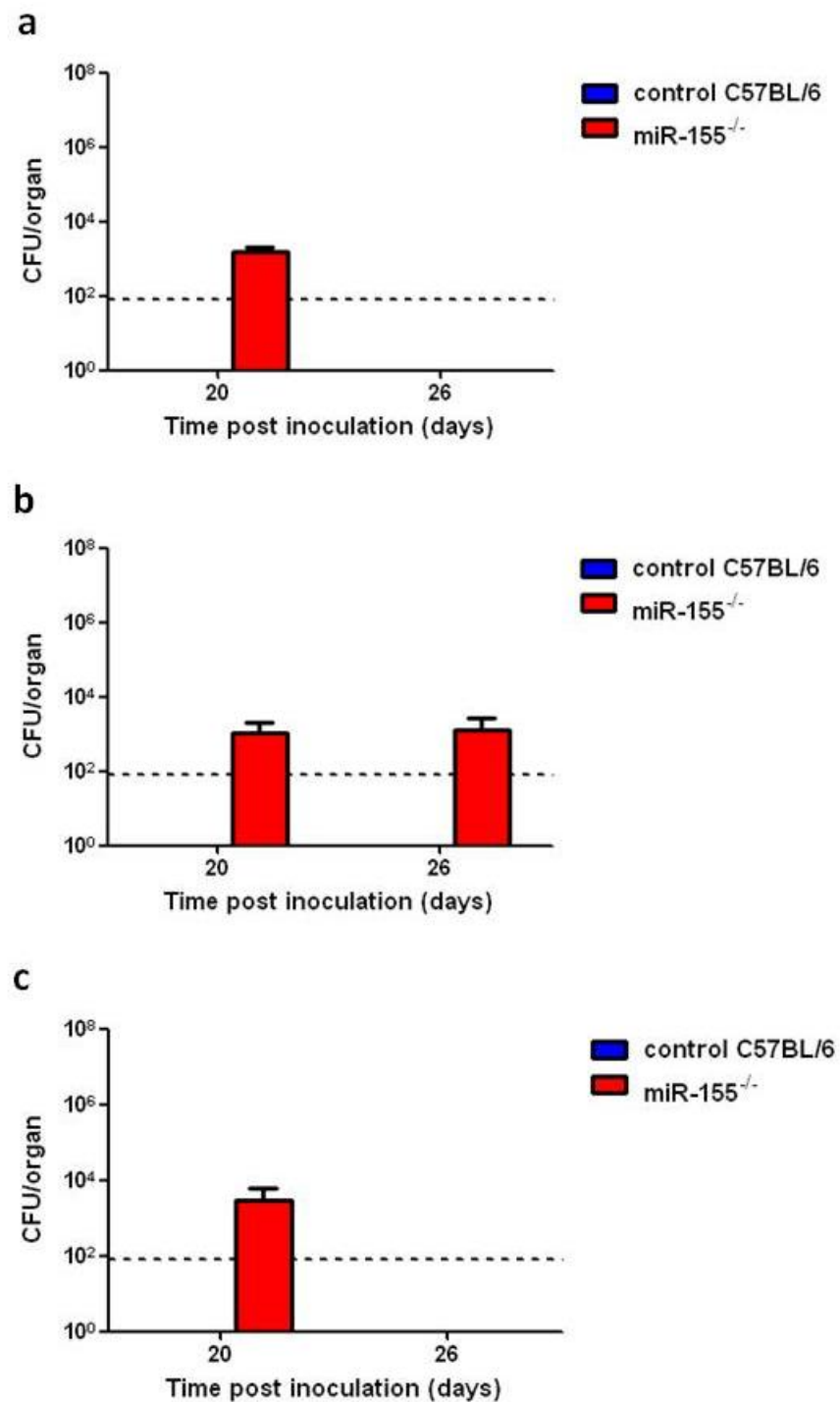
Figure 35. miR-155-deficient mice exhibit systemic spread of *C. rodentium*.

miR-155-deficient (red bars) and control C57BL/6 (blue bars) mice were orally infected with
C. rodentium. On days 20 and 26 pi, mice were sacrificed and numbers of *C. rodentium*
(±SEM) in systemic tissues; mesenteric lymph nodes(a), spleen (b)and liver (c) were
enumerated, n=5 mice per group. Broken lines indicate the detection level of the assay.

3.2.7 miR-155-deficient mice mount a blunted humoral immune responses to *C. rodentium*

The previous data suggests that miR-155 is important for the development of full protective immunity to *C. rodentium* as miR-155-deficient mice are hyper-susceptible to infection. However, a more defined role for this microRNA still remained to be elucidated. Given that the phenotype we observed in *C. rodentium* infected miR-155-deficient mice closely resembled that observed in μMT (B-cell deficient) and RAG2-deficient (lacking B and T cells) mice, we speculated that the susceptibility of miR-155-deficient mice might be due to impaired antibody responses. Thus, we assessed serum antibody responses against the *C. rodentium* surface-associated protein EspA in miR-155-deficient and C57BL/6 mice at 14 and 45 days after infection. EspA filaments are essential for mediating A/E lesion formation and are normally targeted by host antibody responses[171]. We found that while infected wild-type mice developed a robust antibody response to *C. rodentium* by day 14 pi, miR-155-deficient mice produced significantly reduced levels of EspA-specific Ig, IgG and IgA (Figure 36a, b and e). Furthermore, when antibody responses were examined 45 days pi, miR-155-deficient mice demonstrated significantly diminished anti-*Citrobacter* serum IgG responses compared to C57BL/6 mice (Figure 36f and g). Recent reports have demonstrated that while the production and transport of secretory antibodies is not detectably required for clearance of *C. rodentium*, non-secretory IgG antibodies are extremely important for passive immune protection[172].

In addition, C57BL/6 mice infected with *C. rodentium* also mounted EspA-specific IgA responses in supernatants of faecal homogenates. Whilst faecal homogenate EspA-specific IgA titres were highly variable in C57BL/6 mice we observed that miR-155-deficient mice had dramatically diminished titres at all time points assayed (Figure 37).

Figure 36. Humoral immune responses to *C. rodentium* surface protein EspA

Serum antibody responses against the *C. rodentium* surface-associated protein EspA in
C57BL/6 (blue circles) and miR-155-deficient (red squares) mice at 14 and 45 days pi with *C.
rodentium*. Relative titres (± SEM) of anti-EspA serum Ig (a), IgG (b), IgG1 (c), IgG2 (d),
and IgA (e) at day 14 pi were calculated. Relative titres of anti-EspA serum Ig (f) and IgG (g)
at 45 days after infection. The outlying data point observed in the anti-EspA serum Ig titres of
miR-155-deficient mice at 45 days after infection could have arisen either as a result of
human or instrument error or could simply be due to natural deviation within the population
of mice. As we could not be ascertained that this deviation was not significant we did not
exclude this outlier from our analysis.
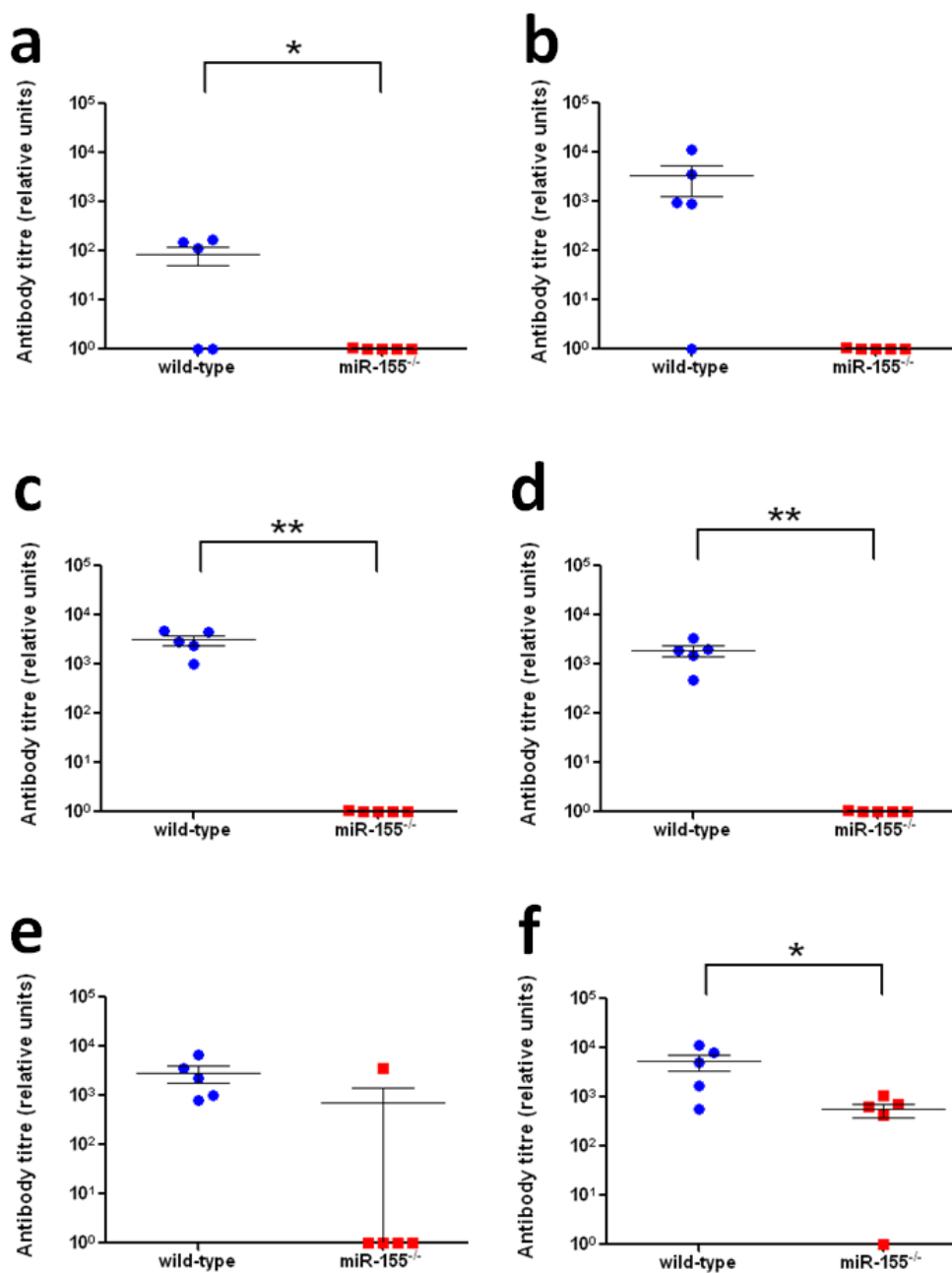
Figure 37. Faecal IgA responses to *C. rodentium* surface protein EspA

Relative titres of faecal IgA (± SEM) responses against the *C. rodentium* surface-associated protein EspA in C57BL/6 (blue circles) and miR-155-deficient (red squares) mice at 8 (a), 11 (b), 14 (c), 18 (d), 21 (e) and 30 (f) days pi with *C. rodentium*. The outlying data point observed in faecal IgA titres from miR-155-deficient mice at 21 days after infection could have arisen either as a result of human or instrument error or could simply be due to natural deviation within the population of mice. As we could not be ascertained that this deviation was not significant we did not exclude this outlier from our analysis.

3.2.8 Germinal centre formation is adversely affected in infected miR-155-deficient mice

Germinal centres develop in the primary B cell follicles of secondary lymphoid organs and support the generation of memory B cells and plasma cells capable of producing high affinity pathogen-specific class-switched antibodies[73, 74, 77, 94, 96, 97, 101, 209]. During infection with *C. rodentium* germinal centres rapidly develop in GALT, especially the mLNs. Previous studies have reported a requirement of miR-155 during regulation of the germinal centre response and generation of class-switched plasma cells[33, 34]. Accordingly, we wanted to study germinal centre formation in the mLNs of miR-155-deficient following infection with *C. rodentium*.

Examination of mLNs from naive miR-155-deficient mice revealed that there were no obvious abnormalities in the development of primary B cell follicles (Figure 38a and b). However, we observed that there were significantly fewer germinal centres in the mLNs of miR-155-deficient mice 14 days after infection compared to control C57BL/6 mice (Figure 38c, d and e). Moreover, the germinal centres formed in miR-155-deficient mice were noticeably smaller in size (Figure 38c, d and f).
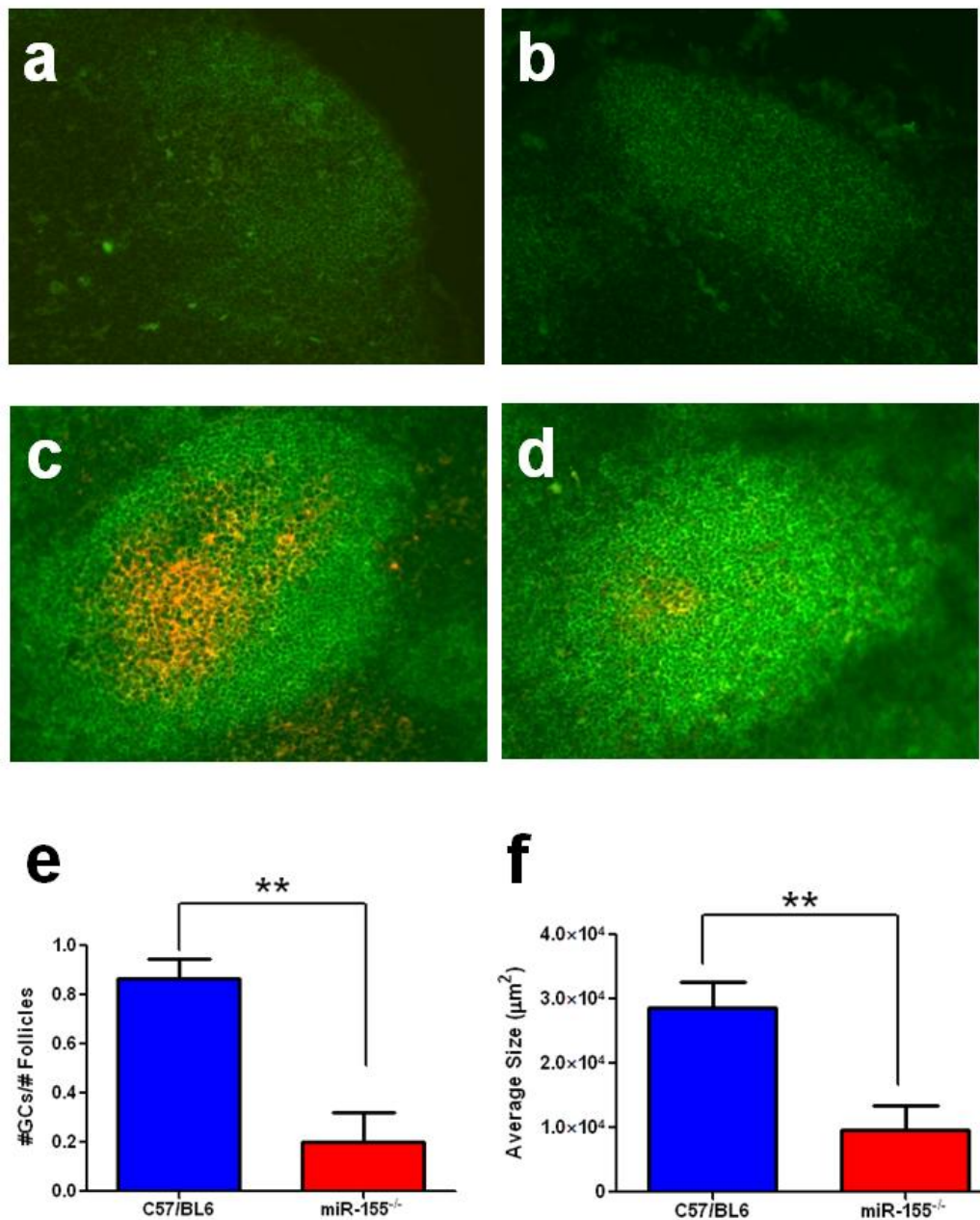
Figure 38. Germinal centre formation in C57BL/6 and miR-155-deficient mice following infection with *C. rodentium*.

C57BL/6 and miR-155-deficient mice were infected orally with *C. rodentium* and germinal centre formation was analyzed 14 days pi. Immunohistochemistry was performed on mLNs from naive C57BL/6 (a), naive miR-155-deficient (b), infected C57BL/6 (c) and infected miR-155-deficient (d) mice 14 days pi to detect germinal centres, magnification x40 (Green, B220[+]; Red/Orange, PNA[+]). Number (e) and size (f) of GCs (±SEM) was determined from sections; n = 4 mice per group.

Additionally, we wanted to look at germinal centre formation in the caecal patch, a specialised lymphoid tissue in the caecum and initial site of colonisation during *C. rodentium* infection. However, due to technical difficulties we were unable to use conventional immunofluorescent staining to follow the development of germinal centres. Upon analysis of toluidine blue – stained caecal patch sections from C57BL/6 and miR-155-deficient mice 14 days after infection, we observed that the latter contained markedly fewer tingible body macrophages (TBMs), a characteristic feature of germinal centres (Figure 39). TBMs are unique, large [20 to 30 microns (μ)] phagocytic cells that reside in close proximity to antigen-retaining FDCs in germinal centres of secondary lymphoid organs. These cells were first identified because they appeared in lymphoid organs following antigenic stimulation and contained many phagocytised, chromatin-condensed apoptotic cells (called tingible bodies) in varying stages of lysis. Recent studies have shown that centrocytes that have undergone somatic hypermutation leading to the expression of low affinity antigen receptors do not receive essential survival signals and are thus condemned to apoptose. The apoptotic centrocytes are rapidly and efficiently removed by TBMs[102, 210]. We tentatively speculate that the decreased numbers of TBMs observed in caecal patch sections from miR-155-deficient mice may indicate that germinal centre formation is diminished not only in mLNs but also in the lymphoid tissue of the caecum. But perhaps most importantly the lack of TBMs in miR-155-deficient mice indicates that there may not be as high a death rate among miR-155-deficient plasmablasts as has been suggested previously[34]. Consequently, it is possible that the lack of miR-155 prevents the majority of B cells from differentiating into plasmablasts.
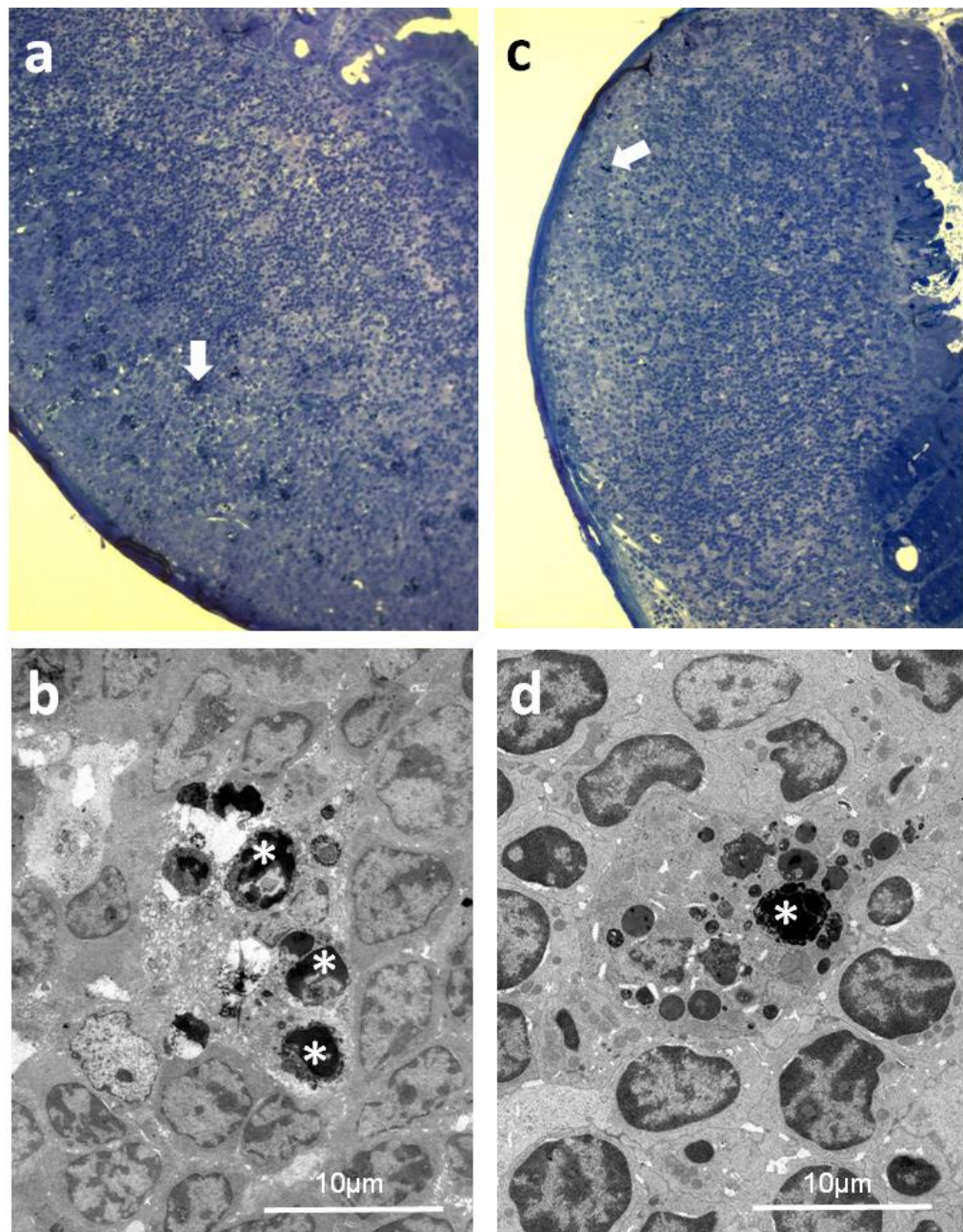
Figure 39. Presence of tingible body macrophages in the caecal patches of C57BL/6 and miR-155-deficient mice 14 days after infection with *C. rodentium*

Toluidine blue staining and transmission electron microscopy of caecal patch sections from infected C57BL/6 and miR-155-deficient mice, 14 days pi. Sections stained with toluidine blue demonstrate that there is an abundance of TBMs (arrow) in control C57BL/6 mice (a), whereas miR-155-deficient mice contain considerably fewer TBMs (c), magnification x20. A transmission electron micrograph showing of a tingible body macrophage from germinal centre of C57BL/6 (b) and miR-155-deficient (d) mice, containing a variable number of tingible bodies (asterisk) in varying stages of degradation.

3.2.9 Genome-wide analysis of gene expression in *C. rodentium* infected tissues

The primary mode of action of miR-155 is through specific mRNA targeting. In view of the fact that animal miRNAs have been shown to regulate large numbers of target mRNAs and the finding that miR-155 is expressed in numerous different cell types following activation, we conducted microarray analysis on infected tissues from C57BL/6 and miR-155-deficient mice, with the aim identifying key components of the immune system which dysfunction in the absence of miR-155, *in vivo*.

Mice were orally infected with *C. rodentium* and total RNA was extracted from the caecal patch and colon at 4 and 14 days pi. Gene expression levels in miR-155-deficient mice were then related to a parallel cohort of infected control C57BL/6 mice. We initially chose to examine the gene expression profiles in these specific tissues, at these particular time points for two reasons. Firstly, we know from previous studies looking at the colonisation dynamics of *C. rodentium* that, the caecal patch and colon are the main sites of infection[161]. Primary colonization of the mouse by *C. rodentium* occurs within the caecal patch, just hours after receiving 10^9 organisms of *C. rodentium* orally. Within 2-4 days, the infection becomes established in the distal colon. In C57BL/6 mice the peak of infection in the colon occurs at around days 5-14, and is accompanied by colonic crypt hyperplasia. Normal immunocompetent mice are capable of mounting a protective sterilising immune response and consequently completely clear infection by day 21 pi. Secondly, from our research we find that from 4-14 days pi the numbers of *C. rodentium* within the caecal patch and colon of miR-155-deficient mice are comparable with control C57BL/6 mice. However, after day 14 pi whilst control mice begin clearing infection, miR-155-deficient mice remain heavily infected in addition to developing grossly exaggerated colonic hyperplasia.

To gain an even greater insight into how the absence of miR-155 affects global gene-expression, gene expression data was further analysed using Innate DB (www.innatedb.ca), a comprehensive database and analysis

platform that enables testing for over-representation of differentially expressed genes in greater than 2,500 known innate immune response pathways, sourced from several of the publicly available pathway databases[211]. Additionally, it provides us with a useful tool for conducting comprehensive network analysis, for the identification of signalling cascades and functionally relevant sub-networks involving molecular interactions between differentially expressed genes and their non-differentially expressed interacting partners. Using network analysis it is possible to identify key regulators of gene expression, which exert their effects through protein modification or other non-transcriptional mechanisms.

Differentially expressed mRNAs were only considered significant if they were altered by at least 1.5 fold and had an adjusted P-value of less than 0.05. Using these strict criteria, we found that 314 genes (229 up- and 85 down-regulated) on day 4 and 8 genes (7 up- and 1 down-regulated) on day 14 pi were differentially expressed in miR-155-deficient caecal patches, compared with infected controls (Table S1-4 and S10-13). Perhaps surprisingly, in colon samples taken from infected miR-155-deficient mice we found that only 3 genes (1 up-and 2 down-regulated) on day 4 pi and 7 genes (7 up-regulated) on day 14 pi were reproducibly significantly differentially expressed, far less than might be expected given the gross changes in pathology, increased pathogen burden and prolonged clearance time (Table S19-22 and S28-31). This lack of reproducible differential regulation in the colon could be due in part to the significant pathological changes occurring in these tissues, perhaps causing significant variations in cell populations.

However, whilst transcriptional profiling allows the analysis of a large number of genes simultaneously, due to the statistical issue of multiple testing it can be susceptible to producing false-positive results. To overcome this problem we selected 6 genes of interest that were differentially expressed in miR-155-deficient mice and reanalyzed them using Real-Time PCR (or reverse transcriptase real-time PCR) with SYBR green. Real-Time PCR (RT-PCR) was performed on cDNA synthesized from the same total RNA used as templates for the cDNA probes hybridised to the arrays. All genes tested

changed in the same direction as they had on the arrays thus, the RT-PCR results agreed well with the microarray results (Figure 40c and d).

3.2.9.1 Transcriptional profiling of *C. rodentium*-infected ceacal patches reveals that B cell function is affected in the absence of miR-155, on day 4 pi

Global gene expression analysis revealed that 314 genes were significantly differentially expressed in the caecal patch of miR-155-deficient mice, 4 days after *C. rodentium* infection. A total of 229 genes were up-regulated while 85 genes were decreased in expression. Because we were concerned with genes that are important for host defence during *C. rodentium* infection, we focused primarily on genes that have an immunomodulatory role. Of the 85 genes down-regulated in miR-155-deficient caecal patches on day 4 pi, we observed that a considerable number, approximately 17 percent, have a reported immune function. Furthermore, we noted that many of the genes are involved, at some stage, in the differentiation and/or function of B cells (Figure 40a). For example CD19 has a role in germinal center formation, B cell homing and apoptosis. Similar to miR-155-deficient mice, CD19 null mice have decreased mitogenic responses, low germinal center formation and decreased humoral immune responses to T cell-independent type 1- and T cell-dependent antigens. In addition, Bcl6 is essential for the differentiation of germinal center B cells since Bcl6 null mice have severely impaired germinal center formation. When we further analysed the expression data using KEGG pathway analysis, and the data analysis and pathway over-representation analysis tools in InnateDB, the B cell receptor (BCR) signalling pathway was identified as being significantly associated with down-regulated genes (Table S6, S8 and S9 and Figure S1). These data together with our results thus far suggest that BCR signalling and consequently B cell function is adversely affected in miR-155-deficient mice. This finding is consistent with previously published reports which have shown that miR-155 is expressed upon BCR cross-linking and CD40 stimulation[23, 34].

It is also worth noting that the most significantly down-regulated gene in the caecal patch on day 4 pi was matrix metalloproteinase-3 (or stomelysin-1) (Table S3 and S4). Matrix metalloproteinase-3 (MMP3) is a member of the matrix metalloproteinase family, a group of molecules which are involved in mediating matrix remodelling and cell migration during tissue injury and repair. A recent study has found that MMPs are strongly induced in epithelial cells during bacterial infections. MMP3, in particular, was shown to be extremely important during infection with *C. rodentium*[212]. MMP3-deficient mice infected with *C. rodentium* exhibited delayed clearance of bacteria from the colon as a result of delayed migration of $CD4^+$ T lymphocytes into the intestinal lamina propria and reduced transcription of TNF-α. MMP3 is thought to function by opening up tight junctions between endothelial cells subsequently enabling lymphocytes to migrate through. In support of this hypothesis, it has been shown that treatment of mice with MMP inhibitors results in an accumulation of lymphocytes on the lymph node endothelium and reduced diapedesis. Accordingly, KEGG testing for overrepresentation amongst the down-regulated genes showed that there was an overrepresentation of genes involved in leukocyte transendothelial migration (Table S6). Thus, it is possible that lymphocyte migration may be affected in miR-155-deficient mice and analysis of their movements during infection will be an important topic for future studies.

Lastly, we sought to identify whether differentially expressed mRNAs represent direct miR-155 targets. To this end, we analysed the 3'UTRs of mRNAs for the presence of miR-155 seed matches using a target prediction algorithm, called Sylamer[213]. We found that there was no significant enrichment or depletion of miR-155 seed sequences amongst the differentially expressed genes (Figure S2). There are two possible explanations for this, firstly the differentially expressed genes may represent indirect miR-155 targets or alternatively, secondary effects such as differential recruitment and activation of cells may be occurring above the direct effects of miR-155.

a

Target Identification	Symbol	Fold Change	Adjusted P-Value	GO Biological Process
scl37307.8.1_29-S	Mmp3	-3.79	0.00669	peptidoglycan metabolic process (GO:0000270) | proteolysis (GO:0006508) | collagen catabolic process (GO:0030574)
scl48501.9_645-S	Cd86	-1.68	0.0127	defense response (GO:0006952)
scl38155.8_378-S	Tnfaip3	-1.99	0.0136	ubiquitin cycle (GO:0006512) | apoptosis (GO:0006915)
scl25940.13_350-S	Lat2	-1.92	0.0144	immune response (GO:0006955) | B cell activation(GO:0042113) | mast cell degranulation (GO:0043303) | B cell receptor signaling pathway (GO:0050853)
scl0003597.1_94-S	Mmp3	-2.45	0.0152	peptidoglycan metabolic process (GO:0000270) | proteolysis (GO:0006508) | collagen catabolic process (GO:0030574)
scl37305.10.1_6-S	Mmp10	-2.02	0.0187	peptidoglycan metabolic process (GO:0000270) | proteolysis (GO:0006508) | collagen catabolic process (GO:0030574)
scl48625.8_280-S	Bcl6	-1.93	0.0341	negative regulation of transcription from R- polymerase II promoter (GO:0000122) | cell morphogenesis (GO:0000902) | negative regulation of cell-matrix adhesion (GO:0001953) | germinal center formation (GO:0002467) | negative regulation of T-helper 2 type immune response (GO:0002829) | transcription (GO:0006350) | regulation of transcription, D--dependent (GO:0006355) | Rho protein signal transduction (GO:0007266) | spermatogenesis (GO:0007283) | protein localization (GO:0008104) | negative regulation of cell proliferation (GO:0008285) | actin cytoskeleton organization and biogenesis (GO:0030036) | B cell differentiation (GO:0030183) | positive regulation of B cell proliferation (GO:0030890) | regulation of Rho GTPase activity (GO:0032319) | negative regulation of mast cell cytokine production (GO:0032764) | negative regulation of Rho protein signal transduction (GO:0035024) | T-helper 2 type immune response (GO:0042092) | regulation of cell proliferation (GO:0042127) | negative regulation of apoptosis (GO:0043066) | regulation of memory T cell differentiation (GO:0043380) | negative regulation of cell differentiation (GO:0045596) | negative regulation of T-helper 2 cell differentiation (GO:0045629) | negative regulation of isotype switching to IgE isotypes (GO:0048294) | erythrocyte development (GO:0048821) | regulation of inflammatory response (GO:0050727) | positive regulation of cell motility (GO:0051272)
scl30689.14.1_1-S	Cd19	-1.98	0.0377	-
scl0012514.2_91-S	Cd68	-1.56	0.038	-
scl41469.8_427-S	Tnfrsf13b	-2.18	0.0401	B cell homeostasis (GO:0001782) | immune response (GO:0006955) | negative regulation of B cell proliferation (GO:0030889)
scl38756.3.1_44-S	Vpreb3	-2.27	0.0404	-
scl21758.4.1_5-S	Cd2	-1.67	0.0404	protein amino acid phosphorylation (GO:0006468) | defense response (GO:0006952) | cell adhesion (GO:0007155)
scl44840.4_185-S	Cd83	-2.26	0.0449	-
scl44948.10_526-S	Irf4	-1.6	0.0458	transcription (GO:0006350) | regulation of transcription, D–dependent (GO:0006355) | myeloid dendritic cell differentiation (GO:0043011)

b

Target Identification	Symbol	Fold Change	Adjusted P-Value	GO Biological Process
scl53984.2_610-S	Cxcr3	-1.52	0.0361	chemotaxis (GO:0006935) | defense response (GO:0006952) | signal transduction (GO:0007165) | G-protein coupled receptor protein signaling pathway (GO:0007186)

Figure 40. Genome-wide analysis of gene expression in *C. rodentium* infected tissues

Gene expression profiling in *C. rodentium*-infected tissues. miR-155-deficient and control C57BL/6 mice were infected orally with *C. rodentium* and transcriptional responses in infected caecal patches and colon sections were analysed 4 and 14 days pi. Immunomodulatory genes and genes involved in B cell differentiation and/or function (grey) that were significantly down-regulated in miR-155-deficient caecal patches on days 4 (a) and 14 (b) after infection, compared with control mice. We selected six genes of interest that were differentially expressed in miR-155-deficient mice and reanalyzed them using RT-PCR, all genes tested changed in the same direction as they had on the arrays (c and d).

3.2.9.2 Loss of miR-155 results in the up-regulation of genes involved in metabolism, catabolism and biosynthesis

Analysis of genes up-regulated in miR-155-deficient caecal patches 4 days after infection showed that there was no enrichment for genes involved in the immune response. However perhaps interestingly, Gene Ontology (GO) and KEGG Pathway analysis revealed that there was an over-representation of genes involved in a number of different metabolic, biosynthetic and catabolic processes as well as ion transport (Table 13, S5 and S7).

The intestine is a complex ecosystem involving the interactions of a diverse microbial community with the physiology, genetics and behaviour of the animal host. Bacterial colonisation in the intestine is essential for many normal physiological processes, such as enhancing intestinal development and contributing to the host's nutrition but also for immune system development and defence against pathogens. The microbiota is known to play an essential role in 'colonization resistance' whereby resident commensal bacteria prevent the growth of many pathogenic bacteria by competing with them for space, nutrients and host-receptors in addition to producing metabolic bi-products with anti-microbial properties. We are only just beginning to understand the complex, mutually beneficial, symbiotic relationship that exists between the host and the intestinal microbiota but prior experiments have shown that certain nutritional factors can modify the composition of flora residing in the gut. Bärbel Stecher and Wolf-Dietrich Hardt have recently reviewed 'The food hypothesis' which speculates that increased nutrient availability and fewer inhibitory substances in the gut provide ideal conditions for growth of pathogenic organisms[38]. They suggest that in the normal gut, high energy nutrients are scarce and any available nutrients are used up efficiently by the microbiota. Consequently, the severe nutrient limitations inhibit the growth of incoming pathogens. However, whilst steady growth conditions and a limited nutrient supply help to stabilize the resident microbiota population structure, considerable shifts in nutrient range and availability (such as those seen

during infection and inflammation) allow the outgrowth of bacterial species that grow at high rates on these substrates. For example, enteropathogens such as *Salmonella* spp., pathogenic *E. coli* spp., *Shigella* spp., *Citrobacter* spp., and *Vibrio cholerae* exhibit rapid growth on nutrient rich media, in the laboratory. In 1977, Barthold *et al* suggested a role for gut flora in transmissible murine colonic hyperplasia (TMCH) after it was found that the severity of hyperplasia during infection with *C. rodentium* could be modified not only by host strain and species but also by the diets fed to inoculated mice. It is thus possible that the up-regulation of metabolism, catabolism, biosynthesis and ion transport in miR-155-deficient mice might perturb the composition of intestinal flora and contribute to the increased severity of infection. However, the relative availability of nutrients in the infected gut and their subsequent utilisation by *C. rodentium* and commensal microbiota has yet to be analyzed quantitatively.

GOBPID	Pvalue	OddsRatio	ExpCount	Count	Size	Term
GO:0006631	9.7e-07	5.3	3.30	15	133	fatty acid metabolic process
GO:0019752	3.8e-05	2.9	8.45	22	342	carboxylic acid metabolic process
GO:0044255	6.1e-05	3.2	6.31	18	270	cellular lipid metabolic process
GO:0006816	2.5e-04	4.8	2.11	9	85	calcium ion transport
GO:0006812	3.1e-04	2.5	9.10	21	367	cation transport
GO:0050801	5.9e-04	3.3	3.94	12	159	ion homeostasis
GO:0055082	1.2e-03	3.2	3.70	11	149	cellular chemical homeostasis
GO:0008272	1.6e-03	17.0	0.25	3	10	sulfate transport
GO:0001523	2.1e-03	14.9	0.27	3	11	retinoid metabolic process
GO:0006694	2.5e-03	4.8	1.38	6	56	steroid biosynthetic process
GO:0030003	3.6e-03	3.8	1.98	7	80	cellular cation homeostasis
GO:0042445	4.2e-03	4.3	1.54	6	62	hormone metabolic process
GO:0006766	7.1e-03	4.5	1.22	5	49	vitamin metabolic process
GO:0051234	8.9e-03	1.4	47.55	63	1917	establishment of localization
GO:0006829	1.3e-02	7.0	0.50	3	20	zinc ion transport
GO:0042493	1.3e-02	7.0	0.50	3	20	response to drug
GO:0055066	1.3e-02	3.3	1.93	6	78	di-, tri-valent inorganic cation homeostasis
GO:0030155	1.3e-02	4.8	0.92	4	37	regulation of cell adhesion
GO:0006732	1.7e-02	2.8	2.65	7	107	coenzyme metabolic process
GO:0006639	1.9e-02	6.0	0.57	3	23	acylglycerol metabolic process
GO:0006814	1.9e-02	3.0	2.11	6	85	sodium ion transport
GO:0008366	2.1e-02	5.7	0.60	3	24	axon ensheathment
GO:0008015	2.1e-02	3.0	2.16	6	87	blood circulation
GO:0006790	2.3e-02	4.0	1.09	4	44	sulfur metabolic process
GO:0006941	2.3e-02	5.4	0.62	3	25	striated muscle contraction
GO:0019228	2.3e-02	5.4	0.62	3	25	regulation of action potential in neuron
GO:0006721	2.4e-02	9.9	0.25	2	10	terpenoid metabolic process
GO:0007431	2.4e-02	9.9	0.25	2	10	salivary gland development
GO:0030865	2.4e-02	9.9	0.25	2	10	cortical cytoskeleton organization and biogenesis
GO:0006811	2.6e-02	2.2	4.22	9	179	ion transport
GO:0042592	3.1e-02	1.8	8.04	14	324	homeostatic process
GO:0002009	3.3e-02	2.6	2.41	6	97	morphogenesis of an epithelium
GO:0002026	3.4e-02	7.9	0.30	2	12	regulation of the force of heart contraction
GO:0009069	3.4e-02	7.9	0.30	2	12	serine family amino acid metabolic process
GO:0042364	3.4e-02	7.9	0.30	2	12	water-soluble vitamin biosynthetic process
GO:0006081	4.0e-02	7.2	0.32	2	13	aldehyde metabolic process
GO:0008152	4.1e-02	1.3	133.96	148	5400	metabolic process
GO:0001501	4.3e-02	2.1	3.92	8	158	skeletal development
GO:0044242	4.3e-02	4.1	0.79	3	32	cellular lipid catabolic process
GO:0006776	4.6e-02	6.6	0.35	2	14	vitamin A metabolic process
GO:0007339	4.6e-02	6.6	0.35	2	14	binding of sperm to zona pellucida
GO:0043506	4.6e-02	6.6	0.35	2	14	regulation of JNK activity

Table 13. GO conditional test for over-representation of genes up-regulated in miR-155-deficient caecal patches, 4 days after infection.

3.2.9.3 Chemokine (C-X-C motif) receptor 3 (CXCR3) is down-regulated in miR-155-deficient caecal patches 14 days after infection with *C. rodentium*

On day 14 pi, there appeared to be little detectable transcriptional difference between the caecal patches from miR-155-deficient mice and those from controls (Table S10, S11, S12 and S13). In fact, CXCR3 was the only gene identified as being significantly down-regulated at this time point (Figure 40b and Table S12 and S13). CXC chemokines are rapidly induced in the colons of mice infected with *C. rodentium*, and are critical chemoattractants and activators of leukocyte subsets[214]. CXCR3 is one of a number of CXC chemokine receptors which bind CXC chemokines. A recently published report has shown that CXCR3 and its cognate ligands have a physiological function in mucosal defence against *C. rodentium*[214]. *C. rodentium*-infected CXCR3-deficient mice display significantly increased faecal CFU at 14 and 17 days after infection as well as higher pathogen burdens in the liver and spleen. Analysis of antibody titres against *C. rodentium* showed that deficiency of CXCR3 results in significantly delayed induction of specific IgG responses, but not IgM[214]. CXCR3 is predominantly expressed on activated T cells, particularly T_h1 cells[214]. As discussed previously, T_h1 cells are extremely important for the clearance of a *C. rodentium* infection because they produce large amounts of IFN-γ which stimulates the bacterial killing capacity of phagocytic cells and they additionally provide essential help to B cells for the generation of specific IgG responses[167-171]. In mice, IFN-γ induces the expression of CXCR3 on memory B cells and plasma cell precursors, which is likely to further aid in the generation of *C. rodentium* specific antibody.

Given these data it is possible that the decreased expression of CXCR3 observed in miR-155-deficient mice could affect leukocyte migration and/or activation. In support of this, GO conditional testing for overrepresentation amongst the genes down-regulated in miR-155-deficient caecal patches on day 14 pi, showed that there was a significant overrepresentation of genes

involved in chemotaxis, locomotory behaviour and leukocyte migration (Table S17). In addition, the positive regulation of adaptive immune response based on somatic recombination of immune receptors built from immunoglobulin superfamily domains pathway was also significantly associated with down-regulated genes (Figure S17). This is consistent with previous results suggesting that germinal centre formation and antibody responses are impaired in miR-155-deficient mice following infection with *C. rodentium*.

3.2.9.4 Global gene expression analysis of the colonic response to *C. rodentium* in miR-155-deficient mice reveals only minor differences, despite gross pathological changes

We observed that very few genes were significantly reproducibly differentially expressed in the colons of miR-155-deficient on either day 4 or day 14 after infection (Table S19-22 and S28-31). This was perhaps unexpected given that miR-155-deficient mice develop more severe pathology as well as increased pathogen burdens in the colon after infection (Figure 31, 32 and 33). There are several possible explanations for this; first, unlike the caecal patch which has a significant percentage of B and T cells, the colon consists of more complex populations of cells which change rapidly during the course of infection. Given the considerable changes in cell populations that take place in infected animals it is possible that the background noise in these samples may have masked any underlying trends within specific cells. Secondly, this type of analysis can only identify miRNA targets that have altered mRNA levels. In animals, because there is only partial miRNA pairing to target mRNAs, regulation is thought to act mainly through translational repression rather than mRNA cleavage. Thus it is possible that by using this method we may miss some miR-155 targets that are regulated at the protein level.

Despite the apparent lack of significantly differentially expressed genes, we analysed all the differentially expressed (up- and down-regulated) genes using the analysis tools in InnateDB, GO and KEGG. As observed in the caecal patch samples, GO conditional testing showed that there was a significant overrepresentation of genes involved in numerous different metabolic, catabolic and biosynthesis pathways amongst the up- and down-regulated genes in miR-155-deficient colons, 4 days after infection (Table S25 and S26). In addition, while the immune response-activating cell surface receptor signalling pathway and I-κβ Kinase/NF-κβ cascade were found to be

significantly associated with down-regulated genes, a number of immune response pathways were conversely associated with up-regulated genes, these included the inflammatory response, acute-phase response, leukocyte migration and phosphoinositide-mediated signalling pathways (Table S25 and S26).

On day 14 after infection, we found that an overwhelming number of diverse immune response pathways ranging from leukocyte migration, chemotaxis and activation to antigen processing and presentation were significantly overrepresented amongst the down-regulated genes, according to GO conditional analysis (Table S35). This finding was further supported by InnateDB analysis which additionally identified several immune response pathways highly associated with down-regulated genes (Table S36). These included, the IL-7 signalling (JAK1 JAK3 STAT5) pathway, phosphorylation of CD3 and TCR zeta chains pathway, T cell receptor signalling pathway as well as CD4 T cell receptor signalling (through Vav, Rac and JNK cascade) pathway, immunoregulatory interactions between a Lymphoid and a non-Lymphoid cell pathway, Natural killer (NK) cell mediated cytotoxicity pathway and Translocation of ZAP-70 to Immunological synapse pathway (Table S36). Both these analyses highlight the global disruption caused by the loss of miR-155; it suggests that multiple different cell types and signalling pathways may be affected in colons of miR-155-deficient mice. However, many of the pathways identified as being greatly associated with differentially expressed genes were not significant after correction for multiple testing and thus should be interpreted with extreme caution.

3.3 Phenotype is recapitulated in miR-155-deficient, μMT-deficient chimeric mice

Our data strongly suggests that BCR signalling and B cell function is overwhelmingly disrupted in miR-155-deficient mice, we therefore wished to ascertain whether the defect was intrinsic to B cells. Accordingly we created mixed chimeras by transferring 20% of either wild-type or miR-155-deficient bone-marrow cells with 80% of μMT-deficient bone-marrow cells into sub-lethally irradiated μMT mice, as previously described[34]. Since μMT have a deletion of the Ig H chain that halts B cell development (although adult μMT-deficient mice may possess IgA$^+$ B cells in systemic and mucosal compartments), animals receiving miR-155-deficient bone-marrow will have only miR-155-deficient B cells whilst animals receiving wild-type bone-marrow will have wild-type B cells. The 20/80 ratio favours reconstitution of all other hematopoietic lineages from wild-type precursors. Both groups of chimeras had similar proportions and numbers of B, CD4$^+$, and CD8$^+$ T cells, data not shown.

3.3.1 miR-155-deficient, μMT-deficient chimeras take significantly longer to resolve infection with *C. rodentium*

miR-155-deficient, μMT-deficient and control wild-type, μMT-deficient mice were orally infected with *C. rodentium*. During infection, there were no obvious disease related mortalities amongst either group of chimeric mice. Similar to that observed in miR-155-deficient germ line mice, all miR-155-deficient, μMT-deficient chimeras successfully eradicated infection but remained chronically infected for an additional 11 days, compared with controls, P value < 0.01 (Figure 41).
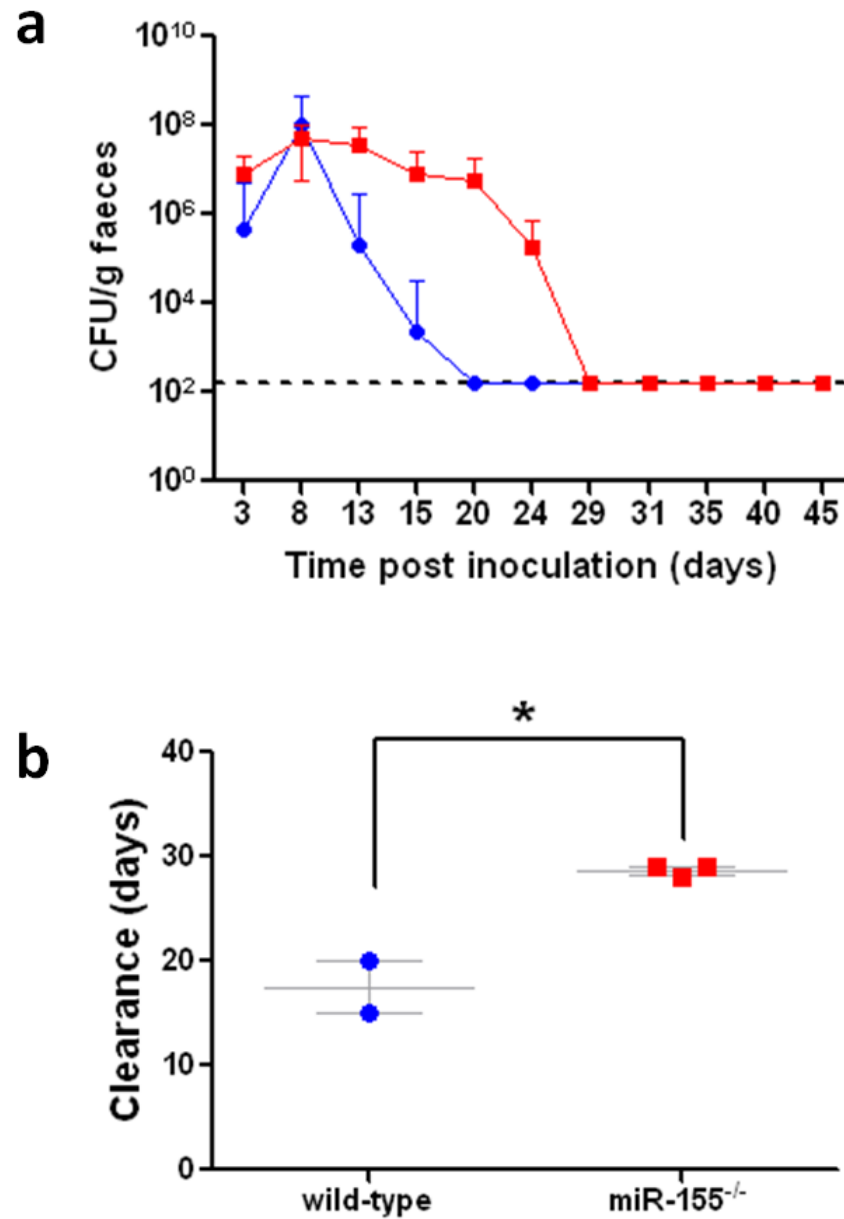
Figure 41. Colonisation and clearance of *C. rodentium* in miR-155-deficient, µMT-deficient and wild-type, µMT-deficient chimeric mice

Susceptibility to *C. rodentium* infection in miR-155-deficient, µMT-deficient chimeric mice. miR-155-deficient, µMT-deficient (Red squares) and wild-type, µMT-deficient (Blue circles) chimeric mice were orally gavaged with approximately $1x10^9$ CFU of *C. rodentium*. (a) Viable *C. rodentium* were enumerated from faecal samples by plating on LB agar supplemented with naladixic acid, n=2 wild-type, µMT-deficient and n=3 miR-155-deficient,

µMT-deficient mice. (b) Time (days) taken to resolve infection (± SEM), * indicates P value <0.01 by Student's t-test.

3.3.2 miR-155-deficient, µMT-deficient chimeras are highly susceptible to *C. rodentium* infection

In an independent experiment, gastrointestinal and systemic tissues were collected from infected mice at various time points pi, and the size of pathogen burden was determined by viable count. On day 14 pi, the pathogen burden in gastrointestinal tissues of miR-155-deficient, µMT-deficient mice were not significantly different than those observed in wild-type, µMT-deficient chimeras (Figure 42). Although unusually, we did observe considerably greater bacterial counts in the colons of wild-type, µMT-deficient chimeras at this time point. Despite there being merely negligible differences between the gastrointestinal burdens of miR-155-deficient, µMT-deficient and wild-type, µMT-deficient mice 14 days after infection, we observed that several miR-155-deficient, µMT-deficient chimeras had a considerably greater burden of *C. rodentium* in liver, spleen and mLN cultures (Figure 43). Thus, providing evidence that miR-155-deficient, µMT-deficient chimeras are less capable in their ability to control a primary mucosal infection and consequently this has lead to systemic spread of *C. rodentium*.

Whilst all wild-type, µMT-deficient chimeras had cleared infection by day 21 after infection, miR-155-deficient, µMT-deficient chimeras remained heavily infected and demonstrated a sizeable burden of *C. rodentium* in the colon, caecum and caecal contents (Figure 42).
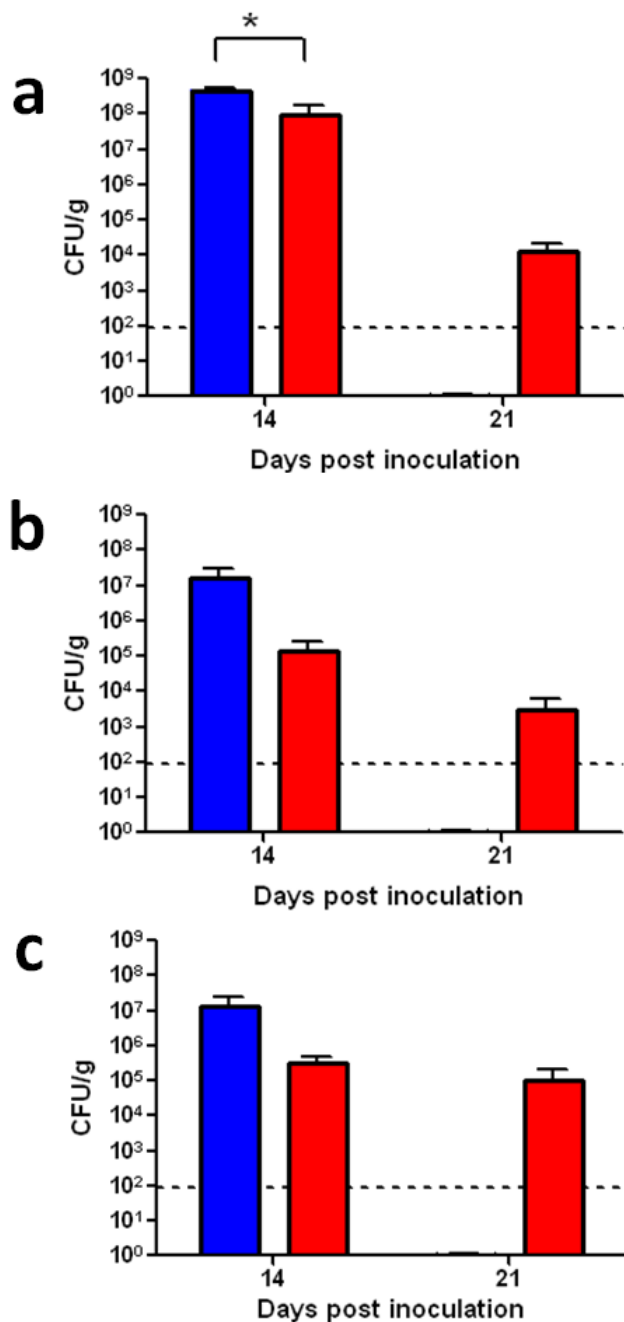
Figure 42. CFU of *C. rodentium* in gastrointestinal tissues of miR-155-deficient, μMT-deficient and control wild-type, μMT-deficient chimeras

Control wild-type, μMT-deficient (blue bars) and miR-155-deficient, μMT-deficient (red bars) mice were orally infected with 10^9 organisms of *C. rodentium.* On days 14 and 21 pi, mice were sacrificed and numbers of *C. rodentium* (±SEM) in gastrointestinal tissue; colon(a), caecum (b) and ceacal patch (c)were enumerated, n=2 and n=5 mice per group respectively, * indicates P value <0.0355 by students t test. Black broken lines indicate the detection level of the assay.
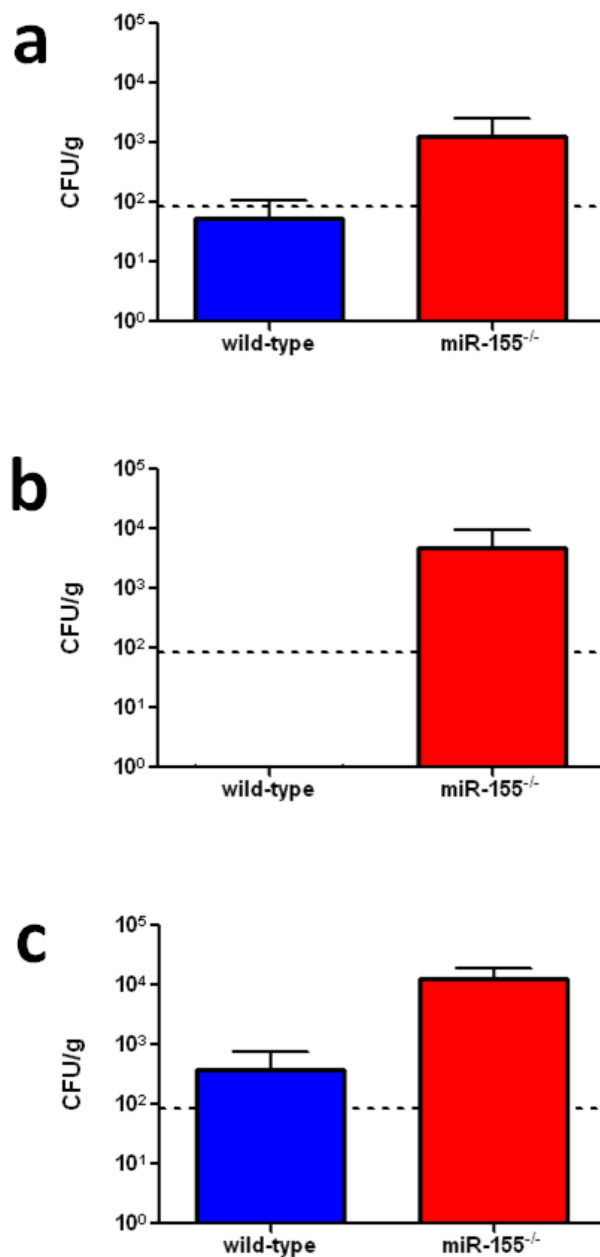
Figure 43. CFU of *C. rodentium* in systemic tissues of miR-155-deficient, µMT-deficient and control wild-type, µMT-deficient chimeras

Control wild-type, µMT-deficient (blue bars) and miR-155-deficient, µMT-deficient (red bars) mice were orally infected with 10^9 organisms of *C. rodentium*. On days 14, mice were sacrificed and numbers of *C. rodentium* (±SEM) in systemic tissues; spleen(a), liver (b) and mLNs (c)were enumerated, n=2 and n=5 mice per group respectively. Black broken lines indicate the detection level of the assay.

3.3.3 Absence of miR-155 leads to impaired production of *C. rodentium*-specific antibody

We also examined serum antibody responses against the *C. rodentium* surface-associated protein EspA in chimeric mice 14 days after challenge. Similar to the phenotype observed in miR-155-deficient mice, we found that there was a general trend towards reduced serum EspA-specific Ig and IgG production in chimeras with miR-155-deficient B cells compared to controls, although this was not statistically significant (Figure 44). It is worth noting that consistent with previously published work, we detected considerable amounts of EspA-specific Ig in one miR-155-deficient, μMT-deficient chimeric mouse perhaps, suggesting that some degree of antibody production is occurring[34]. However, this outlier could also have arisen either as a result of human or instrument error.

We were unable to detect EspA-specific IgG1 and IgG2a subclasses in either group of mice possibly because the levels are too small for our analysis.
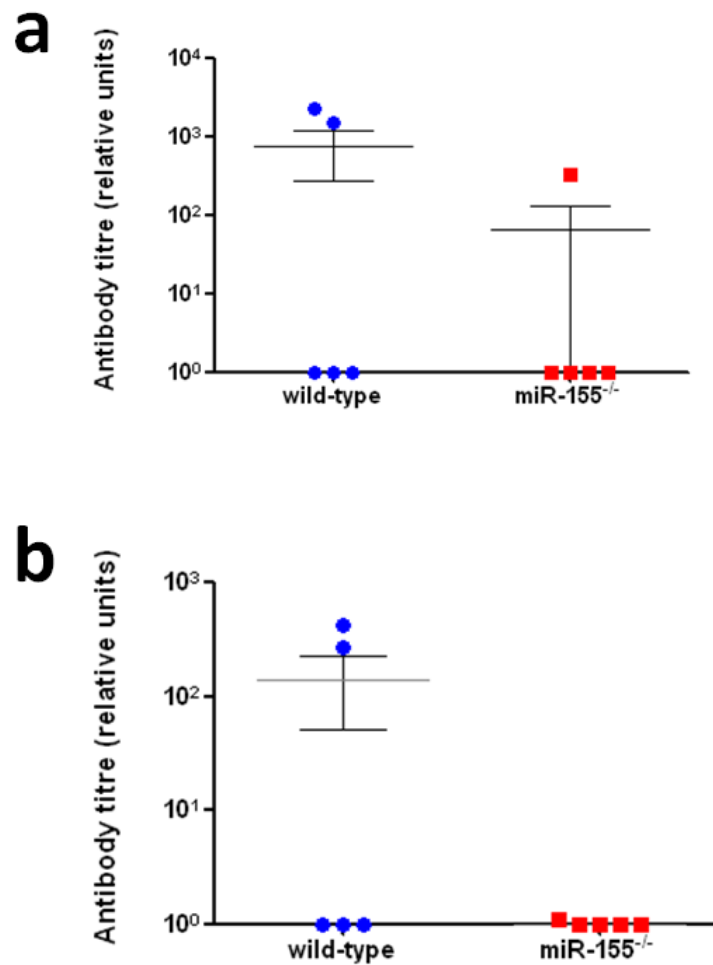
Figure 44. Humoral immune responses to *C. rodentium* surface protein EspA in miR-155-deficient, μMT-deficient and wild-type, μMT-deficient mice

Serum Ig (a) and IgG (b) antibody responses (± SEM) against the *C. rodentium* surface-associated protein EspA were determined in wild-type, μMT-deficient (blue circles) and miR-155-deficient, μMT-deficient (red squares) mice at 14 days pi with *C. rodentium*.

3.3.4 Impaired germinal centre formation is B cell intrinsic

Having found that miR-155-deficient, μMT-deficient chimeras produce very much reduced levels of EspA-specific antibody following challenge with *C. rodentium*, we further wished to determine whether this defect was accompanied by impaired germinal centre formation. We observed that miR-155-deficient, μMT-deficient chimeras displayed significantly fewer numbers of germinal centres in mLNs 21 days pi (Figure 45a, b and c). Additionally, the germinal centres produced were noticeably smaller than those of controls (Figure 45d). Together these results suggest that miR-155 plays an essential role in germinal centre formation and production of antigen-specific antibody in a B cell-autonomous manner.
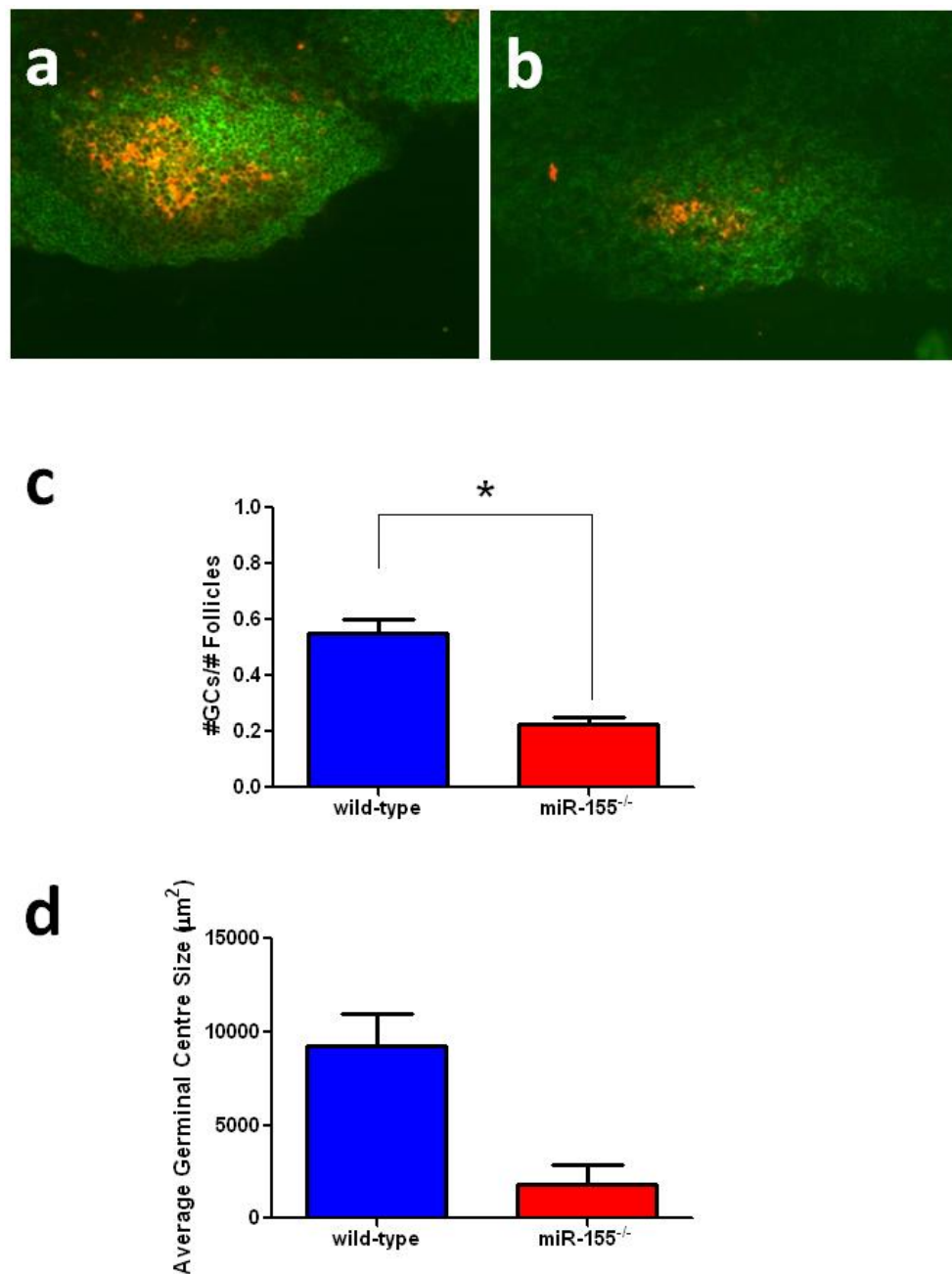
Figure 45. Germinal centre formation in miR-155-deficient, μMT-deficient and control wild-type, μMT-deficient mice, following infection with *C. rodentium*.

miR-155-deficient, μMT-deficient and control wild-type, μMT-deficient mice were infected orally with *C. rodentium* and germinal centre formation was analyzed 21 days pi. Immunohistochemistry was performed on mLNs from infected control wild-type, μMT-deficient (a), and infected miR-155-deficient, μMT-deficient (b) mice 21 days pi to detect germinal centres (Green, B220[+]; Red/Orange, PNA[+]), magnification x40. Number (c) and size (d) of GCs (±SEM) were determined from sections; n = 4 mice per group.

3.4 Discussion

The results of the current study provide valuable evidence for the importance of miR-155 in controlling infection with the mucosal pathogen, *C. rodentium*. We demonstrate that miR-155-deficient mice are highly susceptible to mucosal and even systemic infection with *C. rodentium*. We found that whilst colonisation in miR-155-deficient mice remained comparable with that observed in control mice throughout the early to middle phases of infection (4-14 days pi), during the later stages miR-155-deficient mice exhibited significantly greater pathogen burdens in all gastrointestinal tissues assayed. Furthermore, there was on average, a mean 20-day lag in resolution time of infection in miR-155-deficient mice. These data suggest that miR-155 is not obviously essential for the early innate control of bacteria but is critically important for acquired immune responses during the late bacterial clearance phase of infection.

The high and sustained pathogen load in the colons of *C. rodentium* infected miR-155-deficient mice was associated with the development of severe colonic pathology, in particular gross elongation of colonic crypts, polymorphonuclear infiltrate in the lamina propria and submucosa and frequent breaks in the epithelium integrity. We provide evidence that bacteria resident in the colon are able to translocate across the damaged epithelium and disseminate to internal tissues as indicated by the presence of significant numbers of *C. rodentium* in the spleens and livers of miR-155-deficient mice. Since it is known that systemic T cell-dependent antibody responses are critical for preventing bacteria spreading through the damaged mucosa, we hypothesised that the production of *C. rodentium*-specific antibody may be impaired in the absence of miR-155[170, 171, 208]. Subsequently, serum EspA-specific antibody responses were found to be significantly reduced in miR-155-deficient mice 14 and 45 days after infection. Furthermore, analysis of germinal centre formation in the mLNs and caecal patches of infected mice revealed that miR-155-deficient mice produce significantly fewer germinal centres than C57BL/6 mice. Genome-wide analysis of gene expression in *C.*

rodentium infected caecal patches provided indirect evidence that BCR signalling is significantly down-regulated in the absence of miR-155. This is consistent with a recently published report showing that miR-155 is rapidly expressed following cross-linking of the BCR and might explain why germinal centre development and the generation of plasma cells is severely impaired in mice lacking miR-155[23]. In addition, we found that the expression of chemokine receptor, CXCR3, was reduced in infected miR-155-deficient caecal patches. CXCR3 is known to be involved in the activation and chemotaxis of leukocytes as well as homing of murine-IgG-secreting plasma cells. Thus, it is likely that the down-regulation of CXCR3 is additionally likely to contribute to the defective germinal centre response observed in miR-155-deficient mice.

Having established that mice lacking miR-155 develop greatly increased tissue pathology following infection, we were somewhat surprised to find that there was very little difference in the overall colonic mRNA response to *C. rodentium* between infected miR-155-deficient and C57BL/6 mice. However, results from GO and KEGG conditional testing for overrepresentation and InnateDB analysis suggest that in the absence of miR-155 there is large scale dysregulation of numerous different immune response pathways, in addition to B cell mediated immunity, although the data did not reach significance. Specifically, all analyses identified that the T cell receptor signalling pathway was significantly associated with down-regulated genes. It is therefore likely that T cell function is also affected. Such a view is consistent with previously published reports that have shown that miR-155 is expressed in various different immune cells, including T and B lymphocytes, macrophages and dendritic cells following activation and plays an active role in their function[28, 29, 31, 33, 34].

It is worth noting that amongst the down-regulated genes in miR-155-deficient caecal patches and colons at both day 4 and 14 pi, there was an over-representation of genes involved in leukocyte migration and chemotaxis. For example, MMP3 was notably down-regulated in miR-155-deficient caecal patches, 4 days after infection. MMP3 is known to be involved in mediating

cell migration during tissue injury and is crucially important for the migration of CD4$^+$ T lymphocytes into the intestinal lamina propria during infection with *C. rodentium*. Based on these findings, we speculate that leukocyte trafficking may also be affected by the loss of miR-155 and may contribute to the susceptibility of miR-155-deficient mice. Though, further investigation would be needed to test this hypothesis, and this will be the next challenge.

It is apparent that B cell-mediated immune responses are central to the resolution of a *C. rodentium* infection and whilst ultimate eradication of infection depends on the production of pathogen-specific antibodies, it has been suggested that resistance to *C. rodentium* at the epithelium may additionally depend upon a population of CD4$^+$ T cells that produce proinflammatory cytokines which activate effector mechanisms at the epithelium[171]. Considering this and the fact that T cell-dependent B cell responses require reciprocal interactions between both B and T cells it was important for us to ascertain the relative contributions of miR-155-deficient T and B cells in pathogen-specific antibody responses. To address this, miR-155-deficient, μMT-deficient and wild-type, μMT-deficient chimeric mice were orally infected with 10^9 CFU of *C. rodentium*. Similar to that observed in miR-155-deficient germline mice, miR-155-deficient, μMT-deficient mice were highly susceptible to mucosal and systemic infection with *C. rodentium*. Chimeras with miR-155-deficient B cells took significantly longer to resolve infection than control chimeras and exhibited dramatically higher pathogen burdens in systemic and gastrointestinal tissues on days 14 and 21 after infection, respectively. Furthermore, miR-155-deficient, μMT-deficient mice had reduced serum EspA-specific Ig and IgG levels as a result of defective germinal centre formation. Collectively, these data imply that the susceptibility of miR-155-deficient mice and defective antibody responses is intrinsic to miR-155-deficient B cells. We observed that there was a slight amelioration in disease severity in chimeras possessing only miR-155-deficient B cells, compared with miR-155-deficient germline mice. miR-155-deficient, μMT-deficient chimeric mice infected with *C. rodentium* resolved infection within 4 weeks whereas germline mice took up to 6 weeks to

achieve complete clearance. The heightened susceptibility of miR-155-deficient germline mice could suggest that multiple different cells and signalling pathways are affected by the loss of miR-155. This corroborates our previous findings that B and T cell receptor signalling, chemotactic and leukocyte migration pathways are all significantly down-regulated in *C. rodentium* infected miR-155-deficient germline mice. Additionally, previous studies have also shown that miR-155-deficient mice exhibit defective B and T cell immunity as well as abnormal function of antigen-presenting cells[31, 33, 34].

4 Immune response to *S.* Typhimurium in miR-155-deficient mice

4.1 General introduction

Unlike *C. rodentium* which causes a mucosal infection restricted to the intestinal tract, *S.* Typhimurium can establish a systemic infection in mice, which has superficial similarities to typhoid fever in humans.

Components of the immune mechanisms contributing to the control and clearance of *S.* Typhimurium infection in mice have previously been elucidated[175, 176]. For example, it is known that during the early phase of infection, cells of the innate immune system such as macrophages and neutrophilic granulocytes can be decisive for controlling the net growth, with a large fraction of *Salmonella* being killed by these cells, perhaps in association with complement and other serum factors[178]. The innate immune response, whilst successful in controlling initial growth of *S.* Typhimurium, is normally inadequate for achieving full protective immunity, particularly if higher doses of *Salmonella* or innately susceptible *Nramp1* defective mice are used[176]. Eventual eradication of bacteria during the late phases of infection (3-4 weeks post-inoculation) requires the development of a *Salmonella*-specific lymphocyte-associated response[178]. In particular, the induction of IFN-γ-producing CD4$^+$ T cells are critical for the resolution of infection[182, 187]. In contrast, B cell-mediated immune responses are generally regarded as having a less important role during the primary immune response but have been shown to contribute to the development and expression of full protective immunity[181, 187, 188].

4.2 Results

4.2.1 Infection with virulent *S*. Typhimurium strain SL1344

Full vaccine-induced resistance to infection with virulent *Salmonella* in mice is dependent on a combination of B and T cell responses, including the presence of specific antibody[187]. Virulent *Salmonellae* can replicate extremely rapidly in vivo and consequently bacterial numbers can reach a critical load threshold ($>10^8$ CFU per gram tissue) before an effective CD4$^+$ T cell or B cell response can be generated in unimmunised animals. *Salmonella*-specific CD4$^+$ T cell responses generally begin to be detectable by ~7 days post infection. Thus, vaccine induced antibody is thought to delay the growth of bacteria or facilitate clearance, allowing time for CD4$^+$ T cells and macrophages to become activated[179, 187].

We wished to ascertain the impact of the lack of miR-155 production during infection with *Salmonella* infection. To this end, naive miR-155-deficient and innately susceptible C57BL/6 mice were infected intravenously with 1 x 10^2 CFU of virulent *S*. Typhimurium SL1344. Spleens and livers were collected from infected mice at different time points after infection, and the size of pathogen burden was determined by viable count. Throughout infection the pathogen burden of *S*. Typhimurium SL1344 in systemic tissues of miR-155-deficient mice did not differ significantly from controls (Figure 46). From day 2 to day 4 pi, bacterial numbers in the liver and spleen increased by 2-3 logs and were beginning to near the critical load threshold (Figure 46). By 5 day pi, all remaining miR-155-deficient and C57BL/6 mice succumbed to infection (data not shown), thus demonstrating that both miR-155-deficient and control mice are similarly susceptible to infection with virulent *Salmonella.* This is consistent with previously published reports showing that unvaccinated miR-155-deficient and wild-type control mice infected orally with 1 x 10^8 CFU of SL1344, died within 7 days after infection[31]. Furthermore, this study subsequently went on to show that following *S*. Typhimurium *aroA* vaccination, miR-155-deficient mice were

less readily protected than controls when challenged with virulent *S.* Typhimurium.
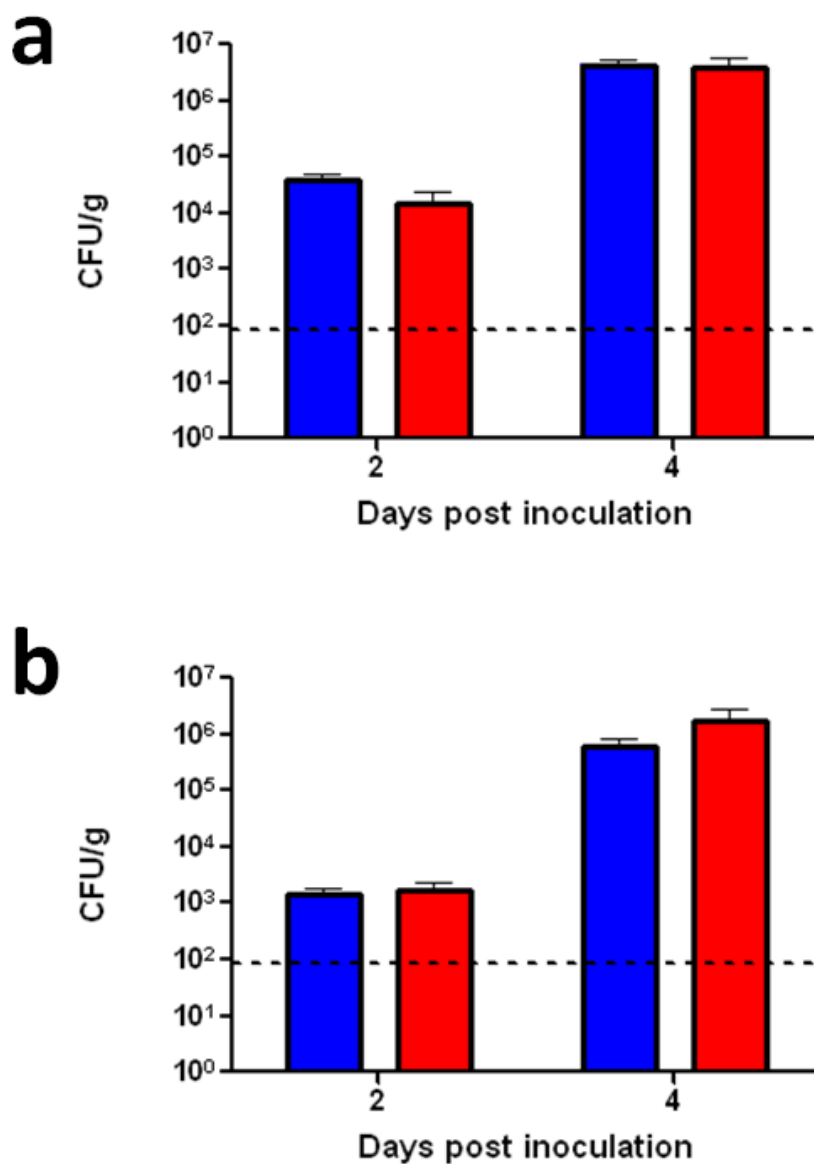
Figure 46. CFU of *S*. Typhimurium SL1344 in systemic tissues of miR-155-deficient and C57BL/6 mice

Control C57BL/6 (blue bars) and miR-155-deficient (red bars) mice were infected intravenously with 1 x 10^2 CFU of virulent *S*. Typhimurium SL1344. On days 2 and 4 pi, mice were sacrificed and numbers of *S*. Typhimurium (±SEM) in systemic tissue; (a) spleen, and (b) liver were enumerated, n=3 mice per group. Black broken lines indicate the detection level of the assay.

4.2.2 miR-155 is not required for the formation of pathological lesions at infection foci during infection with virulent *S.* Typhimurium

Following passage through the FAE and colonisation of the Peyer's patches, bacteria are believed to subsequently move predominantly into the mLNs via the lymphatic system. From there bacteria are able to disseminate to other tissues of the reticuloendothelial system, such as the liver and spleen. During the early stages of infection, control of bacterial growth in the reticuloendothelial system depends on a number of innate immune factors including the gene *Nramp1* (expressed by cells of the monocytes/macrophage lineage) and the production of IFN-γ, IL-12, IL-18, TNF-α and nitric oxide[187]. Suppression of bacterial growth also coincides with the formation of granulomatous lesions within the liver and spleen. Such pathological lesions consist of infected macrophages organised into discrete foci, surrounded by normal tissue. Mastroeni *et al* have suggested that the formation of these lesions confine bacteria to localised foci and in doing so prevent uncontrolled spread of bacteria throughout the body[176]. In fact, failure to form granulomas can result in abnormal growth and dissemination of the bacteria within infected tissues[176]. Lesion formation has been shown to be a highly dynamic process involving cell adhesion molecules such as ICAM1 and the balanced action of TNF-α, IFN-γ, IL-4, IL-12, IL-15 and IL-18[176, 180].

Whilst previous studies have focused on the ability of miR-155-deficient mice to resist oral challenge with virulent *S.* Typhimurium, none have looked at the distribution of *Salmonella* within infected tissues. Therefore, we next examined the formation of granulomatous lesions in miR-155-deficient and C57BL/6 mice following infection with SL1344. No obvious overt abnormalities were observed in the appearance or structure of granulomas in infected miR-155-deficient mice (Figure 47). By day 2 pi, organised granulomas had begun forming in the liver of miR-155-deficient and control mice (Figure 47b and e). We observed that as bacterial numbers in the liver increased from day 2 to day 4 after infection, there was a corresponding

increase in the size and number of pathological lesions (Figure 46 and 47). This is consistent with recently published data showing that the number of infected lesions increases in parallel with net bacterial growth rate, with a small increase in the size of the lesion and in the numbers of infected cells per lesion[176]. On day 4 pi, miR-155-deficient and C57BL/6 mice demonstrated widespread granulomatous lesions as well as areas of necrosis (Figure 47c and f). These data thus suggest that there is no failure to form pathological lesions in the absence of miR-155. Additionally, it indicates that macrophage function is not adversely affected by the loss of miR-155.
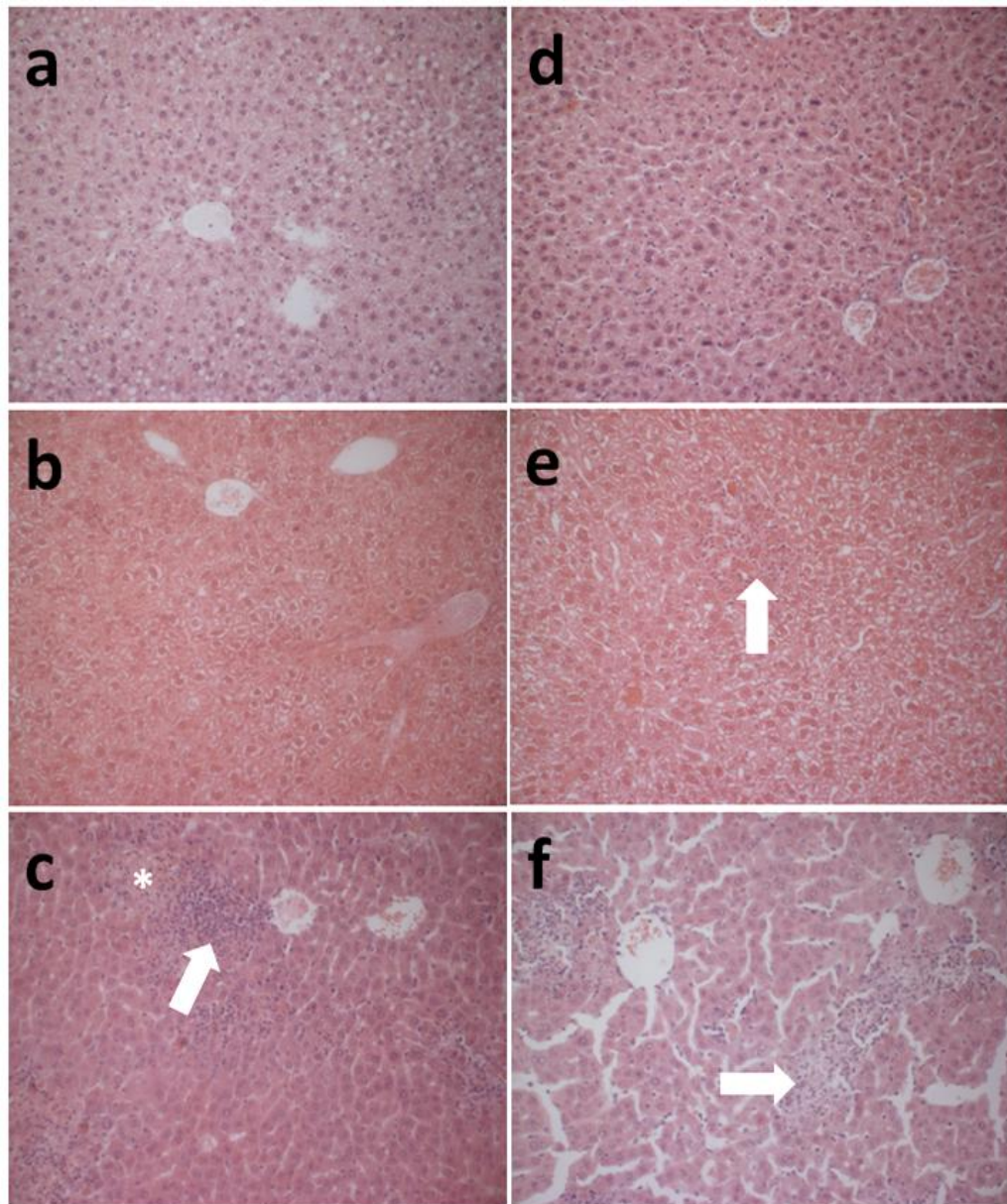
Figure 47. Granuloma formation in miR-155-deficient and C57BL/6 mice following infection with *S*. Typhimurium SL1344

Histopathological analyses (haematoxylin and eosin-stained sections; original magnification, x20) of liver sections from naive C57BL/6 (a) and naive miR-155-deficient mice (d), infected C57BL/6 (b) and infected miR-155-deficient mice (e) on day 2 pi and infected C57BL/6 (c) and infected miR-155-deficient mice (f) 4 days after infection, images are representative of 3 mice per group. By day 2 pi, granulomas (arrow) had begun forming in miR-155-deficient and control livers. 4 days after infection we observed numerous large granulomatous lesions in the liver sections as well as signs of necrosis (asterisk).

4.2.3 miR-155 not essential to resolve infection with attenuated *S*. Typhimurium

Effective clearance of a primary infection with attenuated *S*. Typhimurium is critically dependent on T cells. In contrast, B cells are not so important for the resolution of primary or secondary infection with attenuated *Salmonella*. This may be explained by the fact that attenuated *Salmonellae*, while able to replicate in vivo, do so at a much reduced rate than virulent strains thus, allowing a CD4$^+$ T cell response to develop before excessive bacterial growth can occur[187].

Whilst we know that miR-155-deficient mice are capable of effectively clearing an infection with attenuated *S*. Typhimurium, we do not know if they exhibit differences in the bacterial load within infected tissues. For that reason, we infected miR-155-deficient and C57BL/6 mice intravenously with 1 x 10^5 CFU of a live, attenuated *aroA S*. Typhimurium vaccine strain and spleen and liver counts of viable bacteria were assayed thereafter. There were no obvious disease related mortalities amongst either group of mice and all miR-155-deficient and C57BL/6 mice effectively eliminated the bacteria from the reticuloendothelial system[31]. Throughout infection there were no significant differences in bacterial counts in either the spleen or liver between miR-155-deficient and control mice (Figure 48). On day 14 pi, both groups of mice had efficiently controlled the initial growth of bacteria and had begun clearing the inoculum, as indicated by a log decrease in bacterial numbers between days 14 and 21 (Figure 48). By 6 weeks after infection, all mice sampled were found to be clear of this strain (data not shown). These results indicate that miR-155-deficient mice show no defects in the rate of clearance of bacteria from the reticuloendothelial system and that miR-155 is not essential for the effective resolution of infection with attenuated *S*. Typhimurium.
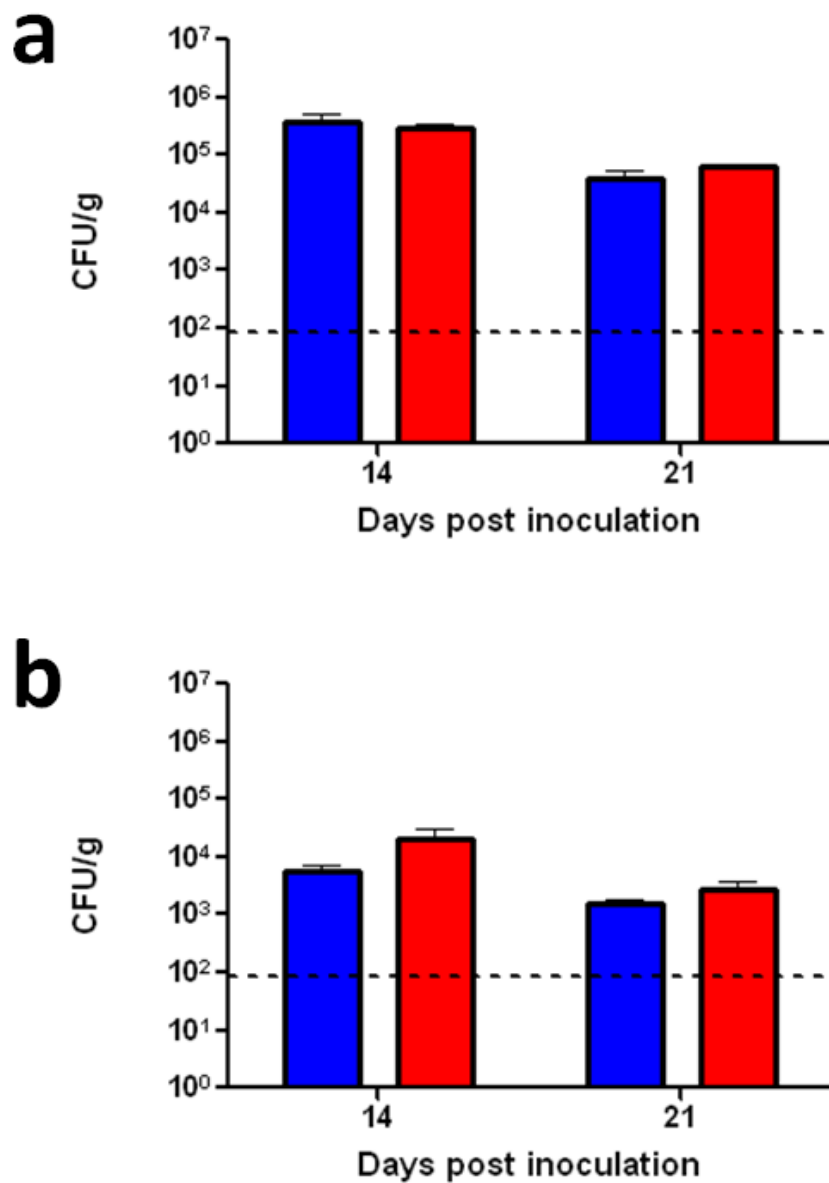
Figure 48. CFU of *S*. Typhimurium SL3261 in systemic tissue from miR-155-deficient and C57BL/6 mice

Control C57BL/6 (blue bars) and miR-155-deficient (red bars) mice were infected intravenously with 1 x 10^5 CFU of a live, attenuated aroA *S*. Typhimurium vaccine strain, SL3261. On days 14 and 21 pi, mice were sacrificed and numbers of *S*. Typhimurium (±SEM) in systemic tissue; (a) spleen, and (b) liver were enumerated, n=3 mice per group. Black broken lines indicate the detection level of the assay.

4.3 Chimeras with miR-155-deficient B cells have impaired humoral immune responses following vaccination

Previous studies have shown that miR-155-deficient mice produce significantly reduced amounts of IgM and switched antigen-specific antibodies after *aroA* vaccination and are consequently less readily protected when challenged with virulent *Salmonella*[31]. Development of pathogen-specific humoral immune responses requires cross-talk between T cells and B cells. Since the original study used miR-155-deficient germ-line mice we could not decipher whether the defect in humoral immunity was intrinsic to miR-155-deficient B or T cells. To this end, we utilised miR-155-deficient, µMT-deficient and wild-type, µMT-deficient chimeric mice possessing either miR-155-deficient or wild-type B cells, respectively. We first immunised mice intravenously with *S*. Typhimurium SL3261 (pnir15TetC) expressing TetC, the non-toxic protective C-terminal domain of tetanus toxin. TetC is a good model antigen through which to study antigen-specific responses, in vivo[180]. On day 20 pi, spleens and livers were collected from infected mice and the size of pathogen burden was determined by viable count. There were no significant differences in bacterial counts in either the spleen or liver of miR-155-deficient, µMT-deficient and wild-type, µMT-deficient mice (Figure 49). However, when serum TetC-specific antibody titres in infected mice were assessed on days 21 and 56 post immunization we found that immunisation of chimeric mice with miR-155-deficient B cells yielded significantly reduced production of TetC-specific Ig, IgG and IgM compared to immunized controls (Figure 50 and 51). In addition, we observed a general trend toward reduced production of TetC-specific IgG1 and IgG2a subclasses in miR-155-deficient, µMT-deficient chimeras (Figure 50 and 51). Thus it would appear that the impaired humoral immune response observed in miR-155-deficient mice is B cell autonomous.
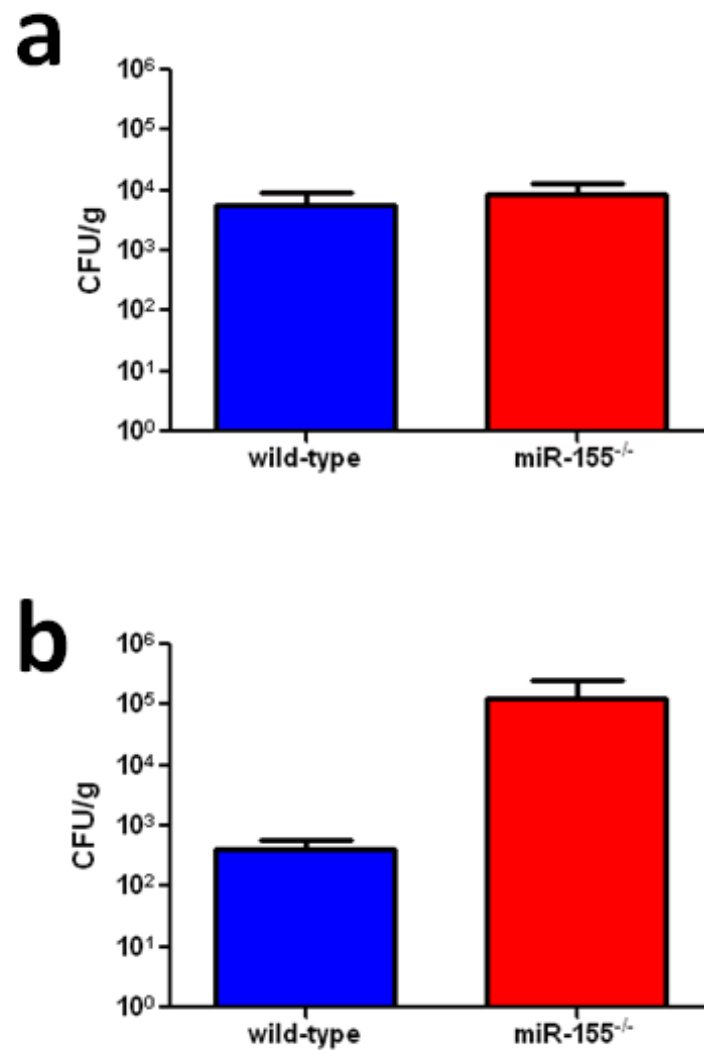
Figure 49. CFU of *S*. Typhimurium SL3261 in systemic tissue from miR-155-deficient, μMT-deficient and wild-type, μMT-deficient mice at day 20 pi

Control wild-type, μMT-deficient (blue bars) and miR-155-deficient, μMT-deficient (red bars) mice were infected intravenously with 1 x 10^5 CFU of a live, attenuated aroA *S*. Typhimurium vaccine strain, SL3261. On day 20 pi, mice were sacrificed and numbers of *S*. Typhimurium (±SEM) in systemic tissue; (a) spleen, and (b) liver were enumerated, n=6 mice per group.
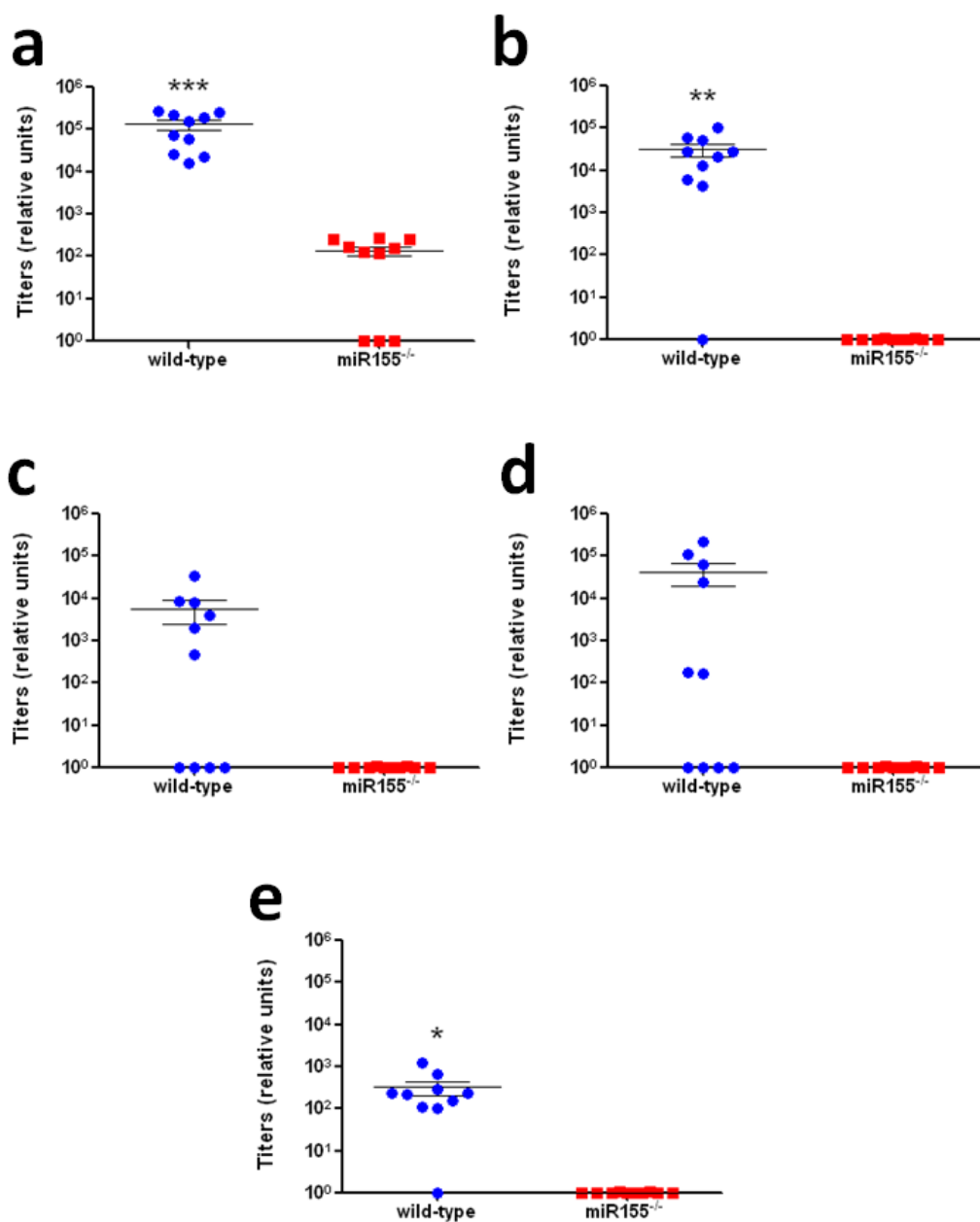
Figure 50. TetC-specific Ig levels from miR-155-deficient, μMT-deficient and wild-type, μMT-deficient chimeras infected with attenuated *Salmonella*, 21 days after infection

Serum antibody responses against TetC in wild-type, μMT-deficient (blue circles) and miR-155-deficient, μMT-deficient (red squares) mice at 21 days pi with attenuated *Salmonella*. Relative titres of anti-TetC serum Ig (± SEM) (a), IgG (b), IgG1 (c), IgG2 (d), and IgM (e) at day 21 pi were calculated.
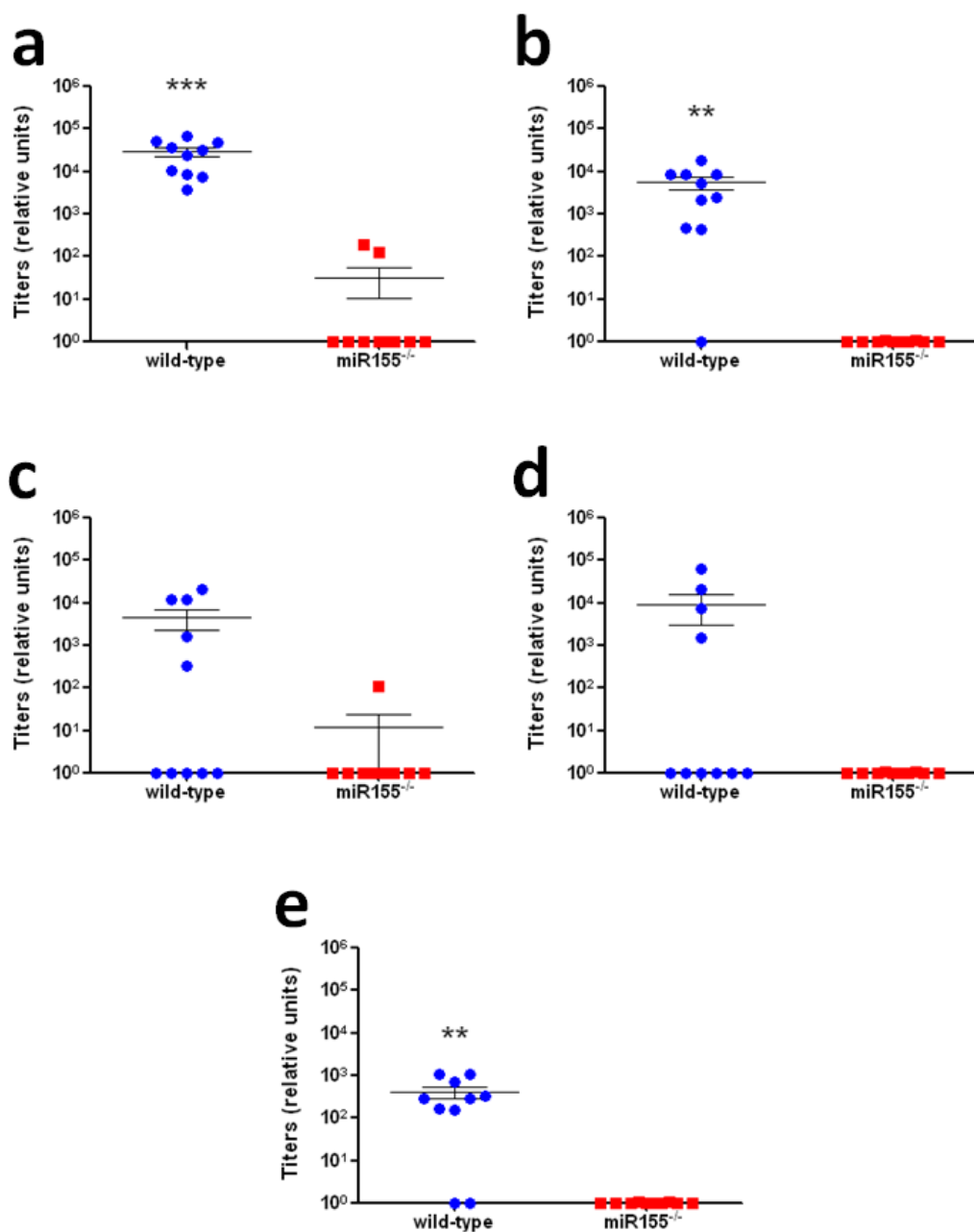
Figure 51. TetC-specific Ig levels from miR-155-deficient, µMT-deficient and wild-type, µMT-deficient chimeras infected with attenuated *Salmonella*, 56 days after infection

Serum antibody responses against TetC in wild-type, µMT-deficient (blue circles) and miR-155-deficient, µMT-deficient (red squares) mice at 56 days pi with attenuated *Salmonella*. Relative titres of anti-TetC serum Ig (± SEM) (a), IgG (b), IgG1 (c), IgG2 (d), and IgM (e) at day 21 pi were calculated.

4.3.1 Immunised miR-155-deficient, µMT-deficient mice are less readily protected when challenged with virulent *Salmonella*

Specific antibody can play a critical role in vaccine-induced protection against virulent bacteria thus we hypothesised that chimeric mice with miR-155-deficient B cells would be less readily protected after immunisation with a *Salmonella*-based vaccine. miR-155-deficient, µMT-deficient and wild-type, µMT-deficient chimeric mice together with miR-155-deficient germline mice were infected intravenously with 1×10^5 CFU of *S*. Typhimurium SL3261 live vaccine. After 3 months, livers and spleens from a sample of mice from each group were checked for the presence of the inoculating strain and found to be completely clear (data not shown). Subsequently, all remaining immunised mice were challenged with virulent *S*. Typhimurium C5. Naive unimmunised C57BL/6 mice were simultaneously similarly challenged. 100 % of naive C57BL/6 mice succumbed to infection by day 7 pi and in agreement with previously published reports immunised miR-155-deficient germline mice exhibited reduced protection against challenge with the majority of mice (5 out of 7; n = 7) succumbing to challenge by 21 days after infection[31] (Figure 52). We found that 8 out of 12 (n = 12) miR-155-deficient, µMT-deficient mice were unable to control a virulent challenge following immunisation (Figure 52). However, unexpectedly the majority of chimeric mice with only wild-type B cells also succumbed to challenge, despite their robust production of *Salmonella*-specific antibody (Figure 52). Because it was not possible to include a control group of immunised C57BL/6 mice we were unable to determine whether this is a problem with the vaccination or whether another cell type was inadvertently affected during the generation of chimeras. Such experiments are long term, labour intensive and expensive so to date we have been unable to repeat this experiment. Consequently we have planned a related experiment involving the passive transfer of antibody raised in these mice to naive germline miR-155-deficient mice. This will involve administering immune antibody and appropriate controls to mice and then

challenging them intraperitoneally with small doses of virulent *S*.

Typhimurium to carefully monitor any passive protective effect.
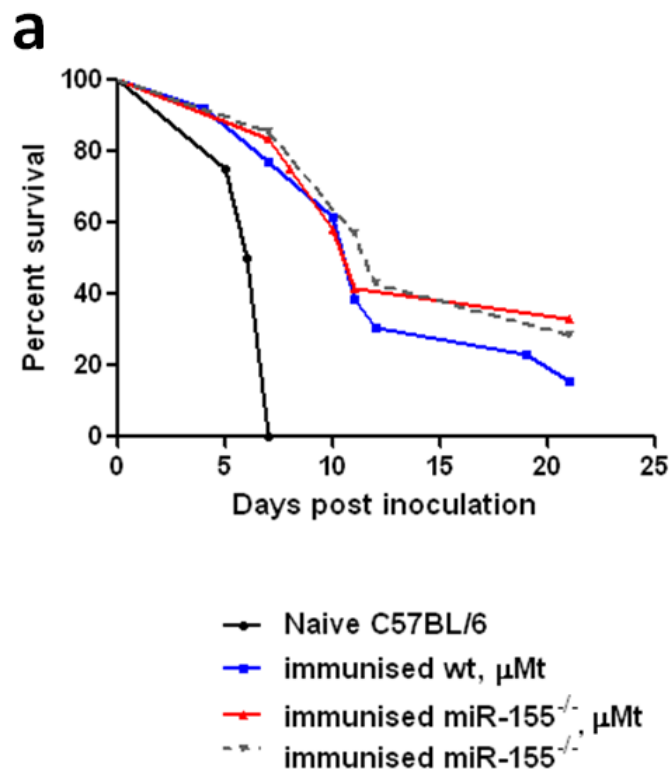
Figure 52. Survival of immunised mice challenged with virulent *S*. Typhimurium

miR-155-deficient, μMT-deficient and wild-type, μMT-deficient and miR-155-deficient
germ-line mice were infected intravenously with 1 x 10^5 CFU of *S*. Typhimurium SL3261.
After 3 months, remaining immunised mice were challenged orally with 1 x 10^{10} CFU of
virulent *S*. Typhimurium C5. Naive unimmunised C57BL/6 mice were simultaneously
challenged. Immunised miR-155-deficient, μMT-deficient mice n = 12, immunised wild-type,
μMT-deficient mice n = 13, immunised germline miR-155-deficient mice n = 7 and naive
unimmunised C57BL/6 mice n = 4.

4.4 Discussion

The results presented here highlight the importance of miR-155 during the development and generation of protective immunity against murine Salmonellosis. We provide further evidence that the susceptibility of miR-155-deficient mice and defective antibody responses is intrinsic to miR-155-deficient B cells.

Like C57BL/6 mice, unimmunised naive miR-155-deficient mice are highly susceptible to infection with virulent *Salmonella* and rapidly succumb to infection. During the early stages of infection, control of bacterial growth depends on the formation of pathological lesions (known as granulomas) within the liver and spleen which prevent the uncontrolled spread of bacteria throughout the body. Lesion formation depends on a variety of factors including the production of numerous cytokines and the expression of a variety of cell adhesion molecules such as ICAM-1[180]. The liver granulomas formed in miR-155-deficient mice were histologically indistinguishable from those in control mice. Additionally, we were unable to detect any obvious differences in bacterial counts or the rate of clearance between naive miR-155-deficient and C57BL/6 mice challenged with attenuated aroA *S.* Typhimurium. The innate immune system is essential for suppressing initial growth of *Salmonella* until an effective T and B cell response can be generated. During the late phases of infection, effective control and eventual eradication of bacteria critically depends on the presence of *salmonella*-specific CD4$^+$ T cells. Thus the results of our study indicate that both the innate immune and T cell responses function in the absence of miR-155, although we do not know if other defects are present that were not detected in these challenges.

However, previous studies have shown that germline miR-155-deficient mice whilst able to control infection with an attenuated strain of *Salmonella* are less readily protected following immunisation due to severely diminished pathogen-specific antibody production. Serum antibody produced by B cells during the initial infection is critical for protection from virulent *Salmonellae*

in immune hosts and requires the participation of B and T cells. Thus we wanted to ascertain whether the impaired antibody production in the absence of miR-155 is B or T cell autonomous, complementing our related studies with *C. rodentium* described previously. To this end we exploited chimeras possessing either miR-155-deficient or wild-type B cells. Key phenotypic alterations observed in germline miR-155-deficient mice were recapitulated in chimeric mice with only miR-155-deficient B cells. miR-155-deficient, μMT-deficient chimeras immunised with attenuated *S*. Typhimurium produced dramatically less *Salmonella*-specific Ig, IgG and IgM as well as IgG1 and IgG2a compared to control mice. This suggests that B cells require miR-155 for the production of pathogen-specific antibody and that the impaired humoral immune response observed in miR-155-deficient mice is B cell autonomous. However, for unknown reasons we found that following immunisation miR-155-deficient, μMT-deficient and wild-type, μMT-deficient mice alike were unable to control challenge with virulent *Salmonella* and due to time and practical constraints we have been unable to repeat this demanding experiment. Consequently, we will determine the protective capacity of serum antibody produced during immunisation, independently. This can be performed by injecting fractionated serum antibody intraperitoneally into naive mice and monitoring their survival following an intraperitoneal injection with exponentially growing *Salmonella,* as previously described[215].

5 Final discussion

The data obtained in the present study have demonstrated that miR-155 is important for controlling a mucosal *C. rodentium* infection and for the development of full vaccine-induced resistance to infection with virulent *Salmonella.* Furthermore, we have shown that miR-155 is intrinsically required by B cells for the production of pathogen-specific antibody following both mucosal and systemic infections.

   In recent years, miR-155 has been highlighted as an important miRNA after it was shown to be expressed in a number of different innate and adaptive immune cells following their activation. Furthermore, mice lacking miR-155 are immunodeficient and display defective T and B cell responses in addition to impaired DC-mediated T cell activation. However, the role of miR-155 in control of infection, in the context of the overall immune response, still remained to be elucidated. Thus, in this present body of work we have utilised mice with a targeted deletion of the miR-155 gene and miR-155-deficient, μMT-deficient chimeras to examine what effect the loss of miR-155 would have on disease progression, immunity and pathogenesis.

   The innate immune system is responsible for providing an immediate response against invading organisms before the generation of pathogen-specific lymphocytes. While a number of previous studies have speculated that miR-155 may participate in the function of various innate immune cells including macrophages and dendritic cells, the data obtained from the above study suggests that miR-155 is not obviously essential for the early innate control of bacteria. Following infection with *C. rodentium,* we observed that miR-155-deficient germline mice and control C57BL/6 mice exhibited comparable numbers of bacteria in gastrointestinal tissues during the early and middle phases of infection, which are highly dependent upon innate immune mechanisms. Similarly, a number of innate immune factors play a vital role in controlling bacterial growth during the early stages of infection with *S.* Typhimurium. We established that the pathogen burden in systemic tissues

from unimmunised miR-155-deficient mice infected with virulent and attenuated *S*. Typhimurium did not differ significantly from controls throughout infection. Previous analyses have shown that macrophage activation and recruitment plays a decisive role in controlling the net growth of *Salmonella* within the reticuloendothelial system of infected mice. Histologically, we observed no overt abnormalities in the appearance or structure of granulomatous lesions in infected miR-155-deficient mice thus implying that macrophage function is not visibly affected in the absence of miR-155. Given that granuloma formation is a highly dynamic process that depends upon the balanced action of a number of cytokines including TNF-α, IFN-γ, IL-4, IL-12, IL-15 and IL-18, we further speculate that early cytokine production is not significantly affected in miR-155-deficient mice, such a view is contradictory to what has previously been suggested[28, 31, 33, 176, 180].

Additionally, we provide evidence that during infection with *C. rodentium* the deficiency in miR-155 results in severe damage to the colonic epithelium and may lead to the development of a polymicrobial infection. We found that coincident with the peak of infection, miR-155-deficient mice developed grossly exaggerated *C. rodentium*-induced colonic hyperplasia. Colons from miR-155-deficient mice weighed significantly more than colons from similarly infected C57BL/6 mice and were visibly thickened as a result of increased proliferation of the colonic epithelia, dilation and thickening of the colonic mucosa and considerable polymorphonuclear infiltrate. Furthermore, closer examination of colons from infected mice revealed that whilst the colonic epithelium remained grossly intact in C57BL/6 mice, miR-155 knockout mice exhibited considerable damage to luminal colonocytes and developed frequent breaks in the epithelial integrity. We subsequently isolated considerable numbers of *C. rodentium* in the livers, spleens and mLNs of several miR-155-deficient mice indicating that bacteria are able to disseminate through the damaged epithelia. In addition, the spread of bacteria to systemic sites implies that T cell-dependent antibody responses may be impaired in the absence of miR-155. The increased severity of hyperplasia observed in miR-155-deficient mice could be as a result of significant changes in metabolic,

catabolic, biosynthetic and ion transport pathways. Considerable shifts in nutrient range and availability in the gut can allow the outgrowth of bacterial species such as *C. rodentium,* which grow at high rates on these substrates. A role for diet and gut flora in transmissible murine colonic hyperplasia has previously been suggested but to the best of my knowledge has not been analyzed quantitatively and this may be something that can be performed.

During histopathological analysis we additionally noted the presence of microcolonies of coccus-shaped bacteria intimately attached to the epithelial surface of miR-155-deficient mice. Thus we tentatively suggest that infection with *C. rodentium* in miR-155-deficient mice may lead to a polymicrobial infection. Nevertheless, we have yet to identify the spatial and temporal changes in the gut microbiome of miR-155-deficient and control mice during infection with *C. rodentium* and thus we cannot speculate further. However, we are currently performing 16S ribosomal RNA (16S rRNA) sequence analysis. The 16S rRNA is a component of the 30S subunit of prokaryotic ribosomes which is highly conserved between different bacterial species and is highly species-specific. Therefore, 16S rRNA gene sequencing provides us with a rapid and accurate method for bacterial identification[206, 207].

Whilst the innate immune response is highly successful in controlling the initial growth of bacteria, the adaptive immune system, including T and B cells, plays an essential role in the eventual eradication of infection. This study highlights the importance of miR-155 for the development of acquired immune responses, in particular for the production of pathogen-specific antibody. Following infection with *C. rodentium,* we observed that miR-155-deficient mice displayed significantly greater pathogen loads in gastrointestinal tissues during the later stages of infection and remained chronically infected for a significant period of time after control animals had achieved complete clearance. These data suggest that miR-155 is important for the development of full protective immunity. When we studied serum antibody responses in mice infected with *C. rodentium* it became apparent that miR-155-deficient mice mount a blunted humoral immune response and produce significantly reduced levels of pathogen-specific Ig, IgG and IgA. We

were subsequently able to show that the impaired antibody responses observed in knockout mice was accompanied by defective germinal centre formation in mLNs. Additionally, we found preliminary evidence that germinal centre responses may also be affected in the caecal patch. This assumption was based on the presence of markedly fewer tingible body macrophages, a characteristic feature of germinal centres within the lymphoid tissue of the caecal patch. TBMs are thought to be responsible for removing apoptotic centrocytes thus their absence may possibly indicate that there is not a high death rate among miR-155-deficient plasmablasts as has been previously suggested[102, 210]. More likely the loss of miR-155 prevents the majority of B cells from differentiating into plasmablasts. In support of this, mir-155 has been shown to be expressed following BCR cross-linking and our microarray analysis identified that BCR signalling was significantly associated with down-regulated genes in miR-155-deficient mice. Furthermore, we noted that amongst the genes significantly down-regulated in miR-155-deficient caecal patches on day 4 pi, there was an over-representation of genes involved, at some stage, in the differentiation and function of B cells.

Microarray analysis additionally revealed that the expression of MMP3 and CXCR3 was significantly reduced in the caecal patches of knockout mice on day 4 and 14 pi, respectively. Both these genes are known to be involved in leukocyte trafficking and accordingly, KEGG testing for overrepresentation showed that the leukocyte transendothelial migration pathway was significantly associated with down-regulated genes. Therefore, we cautiously hypothesize that lymphocyte migration may possibly be affected in miR-155-deficient mice. Nevertheless, we have not studied the movement of different cell populations within *C. rodentium*-infected tissues and further investigation would be required to establish if lymphocyte migration is perturbed. This will be the next challenge.

Our studies have shown that miR-155-deficient germline mice are hyper-susceptible to infection due to impaired humoral immune responses and our data strongly points towards the defect being predominately within miR-155-

deficient B cells. However, the development of pathogen-specific humoral immune responses requires cross-talk between T cells and B cells. To assess the intrinsic requirement of miR-155 for B cell function we utilised mixed chimeras reconstituted with either wild-type or miR-155-deficient B cells. miR-155-deficient, μMT-deficient mice orally infected with *C. rodentium* successfully resolved infection but did so in a significantly delayed fashion compared to control chimeras. Similar to that observed in miR-155-deficient germline mice, chimeric mice with miR-155-deficient B cells remained heavily infected for an extended period of time after wild-type, μMT-deficient mice had cleared infection. Additionally, we observed that several miR-155-deficient, μMT-deficient mice demonstrated considerable levels of *C. rodentium* in systemic tissues such as the liver, spleen and mLNs indicating that they are highly susceptible to systemic infection. Examination of serum antibody responses in chimeric mice infected with *C. rodentium* showed that there was a general trend towards the reduced production of EspA-specific Ig and IgG in miR-155-deficient, μMT-deficient mice as a result of impaired germinal centre formation. However, it should be noted that in chimeras possessing only miR-155-deficient B cells, we observed a slight improvement in disease severity compared with miR-155-deficient germline mice. The increased susceptibility of miR-155-deficient germline mice could suggest that not only B cells are affected by the loss of miR-155. In support of this, previous studies have shown that miR-155-deficient mice exhibit defective B and T cell immunity as well as abnormal function of antigen-presenting cells and correspondingly, our microarray analysis identified that a number of diverse immune response pathways are under-represented in miR-155-deficient mice during infection with *C. rodentium* but, these were not significant after correction for multiple testing[31, 33, 34].

As discussed previously, miR-155-deficient mice infected intravenously with a live, attenuated *aroA S.* Typhimurium displayed no obvious differences in the rate or time of clearance compared to C57BL/6 mice. Eventual eradication of attenuated *Salmonella* from the reticuloendothelial system critically depends on the presence of *Salmonella*-specific CD4^{+} T cells. Thus

these results imply that T cell function is not obviously affected in the absence of miR-155. Rodriguez *et al* showed however that miR-155-deficient mice whilst able to clear infection with attenuated *S*. Typhimurium produce significantly reduced amounts of IgM and switched antigen-specific antibodies following vaccination and are consequently less readily protected when challenged with a virulent *Salmonella* strain[31]. Consequently we wished to study humoral immune responses and the level of protection in miR-155-deficient, μMT-deficient mice following immunisation. We first immunised chimeras with *S*. Typhimurium SL3261 expressing TetC and serum TetC-specific antibody titres were subsequently measured. Despite exhibiting similar bacterial counts throughout infection, chimeric mice with miR-155-deficient B cells were found to produce significantly less Salmonella-specific Ig, IgG and IgM as well as considerably lower levels of IgG1 and IgG2a subclasses thus indicating that humoral immune responses are impaired. However, following challenge with virulent *S*. Typhimurium C5 even though there is some level of protection compared to naive C57BL/6 mice, both miR-155-deficient, μMT-deficient and wild-type, μMT-deficient mice were not fully protected with the majority of mice rapidly succumbing to infection. Although it is not entirely apparent at this time why wild-type, μMT-deficient chimeras are susceptible to challenge regardless of their robust production of *Salmonella*-specific antibodies, we next intend to determine whether serum antibody produced during immunisation can protect experimentally injected animals, independently.

Because the majority of phenotypic alterations observed in germline mice were recapitulated in chimeric mice with miR-155-deficient B cells we propose that miR-155 is required intrinsically by B cells for the production of pathogen-specific antibody and that the impaired humoral immune response observed in miR-155-deficient mice is B cell autonomous.

References

1. Ambros, V. microRNAs: tiny regulators with great potential. Cell 107, 823-6 (2001).

2. Ambros, V., Lee, R. C., Lavanway, A., Williams, P. T. & Jewell, D. MicroRNAs and other tiny endogenous RNAs in C. elegans. Curr Biol 13, 807-18 (2003).

3. Reinhart, B. J. et al. The 21-nucleotide let-7 RNA regulates developmental timing in Caenorhabditis elegans. Nature 403, 901-6 (2000).

4. Bagga, S. et al. Regulation by let-7 and lin-4 miRNAs results in target mRNA degradation. Cell 122, 553-63 (2005).

5. Lee, R. C., Feinbaum, R. L. & Ambros, V. The C. elegans heterochronic gene lin-4 encodes small RNAs with antisense complementarity to lin-14. Cell 75, 843-54 (1993).

6. Lai, E. C. Micro RNAs are complementary to 3' UTR sequence motifs that mediate negative post-transcriptional regulation. Nat Genet 30, 363-4 (2002).

7. Brennecke, J., Stark, A., Russell, R. B. & Cohen, S. M. Principles of microRNA-target recognition. PLoS Biol 3, e85 (2005).

8. Jackson, R. J. & Standart, N. How do microRNAs regulate gene expression? Sci STKE 2007, re1 (2007).

9. Preall, J. B. & Sontheimer, E. J. RNAi: RISC gets loaded. Cell 123, 543-5 (2005).

10. Filipowicz, W. RNAi: the nuts and bolts of the RISC machine. Cell 122, 17-20 (2005).

11. Gregory, R. I., Chendrimada, T. P., Cooch, N. & Shiekhattar, R. Human RISC couples microRNA biogenesis and posttranscriptional gene silencing. Cell 123, 631-40 (2005).

12. Liu, J., Valencia-Sanchez, M. A., Hannon, G. J. & Parker, R. MicroRNA-dependent localization of targeted mRNAs to mammalian P-bodies. Nat Cell Biol 7, 719-23 (2005).

13. Jabri, E. P-bodies take a RISC. Nat Struct Mol Biol 12, 564 (2005).

14. Rossi, J. J. RNAi and the P-body connection. Nat Cell Biol 7, 643-4 (2005).

15.   Clurman, B. E. & Hayward, W. S. Multiple proto-oncogene activations in avian leukosis virus-induced lymphomas: evidence for stage-specific events. Mol Cell Biol 9, 2657-64 (1989).

16.   Tam, W., Hughes, S. H., Hayward, W. S. & Besmer, P. Avian bic, a gene isolated from a common retroviral site in avian leukosis virus-induced lymphomas that encodes a noncoding RNA, cooperates with c-myc in lymphomagenesis and erythroleukemogenesis. J Virol 76, 4275-86 (2002).

17.   Tam, W. Identification and characterization of human BIC, a gene on chromosome 21 that encodes a noncoding RNA. Gene 274, 157-67 (2001).

18.   Tam, W., Ben-Yehuda, D. & Hayward, W. S. bic, a novel gene activated by proviral insertions in avian leukosis virus-induced lymphomas, is likely to function through its noncoding RNA. Mol Cell Biol 17, 1490-502 (1997).

19.   Lagos-Quintana, M. et al. Identification of tissue-specific microRNAs from mouse. Curr Biol 12, 735-9 (2002).

20.   Kluiver, J. et al. Lack of BIC and microRNA miR-155 expression in primary cases of Burkitt lymphoma. Genes Chromosomes Cancer 45, 147-53 (2006).

21.   Kluiver, J. et al. BIC and miR-155 are highly expressed in Hodgkin, primary mediastinal and diffuse large B cell lymphomas. J Pathol 207, 243-9 (2005).

22.   Metzler, M., Wilda, M., Busch, K., Viehmann, S. & Borkhardt, A. High expression of precursor microRNA-155/BIC RNA in children with Burkitt lymphoma. Genes Chromosomes Cancer 39, 167-9 (2004).

23.   van den Berg, A. et al. High expression of B-cell receptor inducible gene BIC in all subtypes of Hodgkin lymphoma. Genes Chromosomes Cancer 37, 20-8 (2003).

24.   Kluiver, J. et al. Regulation of pri-microRNA BIC transcription and processing in Burkitt lymphoma. Oncogene 26, 3769-76 (2007).

25.   Tam, W. & Dahlberg, J. E. miR-155/BIC as an oncogenic microRNA. Genes Chromosomes Cancer 45, 211-2 (2006).

26.   Eis, P. S. et al. Accumulation of miR-155 and BIC RNA in human B cell lymphomas. Proc Natl Acad Sci U S A 102, 3627-32 (2005).

27.   Costinean, S. et al. Pre-B cell proliferation and lymphoblastic leukemia/high-grade lymphoma in E(mu)-miR155 transgenic mice. Proc Natl Acad Sci U S A 103, 7024-9 (2006).

28.   Tili, E. et al. Modulation of miR-155 and miR-125b levels following lipopolysaccharide/TNF-alpha stimulation and their possible roles in regulating the response to endotoxin shock. J Immunol 179, 5082-9 (2007).

29.   O'Connell, R. M., Taganov, K. D., Boldin, M. P., Cheng, G. & Baltimore, D. MicroRNA-155 is induced during the macrophage inflammatory response. Proc Natl Acad Sci U S A 104, 1604-9 (2007).

30.   Haasch, D. et al. T cell activation induces a noncoding RNA transcript sensitive to inhibition by immunosuppressant drugs and encoded by the proto-oncogene, BIC. Cell Immunol 217, 78-86 (2002).

31.   Rodriguez, A. et al. Requirement of bic/microRNA-155 for Normal Immune Function. Science 316, 608-11 (2007).

32.   Marshall, D. G. et al. Use of the stationary phase inducible promoters, spv and dps, to drive heterologous antigen expression in Salmonella vaccine strains. Vaccine 18, 1298-306 (2000).

33.   Thai, T. H. et al. Regulation of the germinal center response by microRNA-155. Science 316, 604-8 (2007).

34.   Vigorito, E. et al. microRNA-155 Regulates the Generation of Immunoglobulin Class-Switched Plasma Cells. Immunity 27, 847-59 (2007).

35.   Teng, G. et al. MicroRNA-155 is a negative regulator of activation-induced cytidine deaminase. Immunity 28, 621-9 (2008).

36.   Dorsett, Y. et al. MicroRNA-155 suppresses activation-induced cytidine deaminase-mediated Myc-Igh translocation. Immunity 28, 630-8 (2008).

37.   Desiderio, S. Along came a spider: AID escapes a microRNA web. Immunity 28, 596-8 (2008).

38.   Stecher, B. & Hardt, W. D. The role of microbiota in infectious disease. Trends Microbiol 16, 107-14 (2008).

39.   Muller, U., Vogel, P., Alber, G. & Schaub, G. A. The innate immune system of mammals and insects. Contrib Microbiol 15, 21-44 (2008).

40. Zhong, B., Tien, P. & Shu, H. B. Innate immune responses: crosstalk of signaling and regulation of gene transcription. Virology 352, 14-21 (2006).

41. Bauer, M. et al. Bacterial CpG-DNA triggers activation and maturation of human CD11c-, CD123+ dendritic cells. J Immunol 166, 5000-7 (2001).

42. Bourhis, L. L. & Werts, C. Role of Nods in bacterial infection. Microbes Infect 9, 629-36 (2007).

43. Cario, E., Gerken, G. & Podolsky, D. K. "For whom the bell tolls!" -- innate defense mechanisms and survival strategies of the intestinal epithelium against lumenal pathogens. Z Gastroenterol 40, 983-90 (2002).

44. Dalpke, A. H., Frey, M., Morath, S., Hartung, T. & Heeg, K. Interaction of lipoteichoic acid and CpG-DNA during activation of innate immune cells. Immunobiology 206, 392-407 (2002).

45. Elson, G., Dunn-Siegrist, I., Daubeuf, B. & Pugin, J. Contribution of Toll-like receptors to the innate immune response to Gram-negative and Gram-positive bacteria. Blood 109, 1574-83 (2007).

46. Farhat, K. et al. Heterodimerization of TLR2 with TLR1 or TLR6 expands the ligand spectrum but does not lead to differential signaling. J Leukoc Biol 83, 692-701 (2008).

47. Gibson, D. L. et al. Toll-like receptor 2 plays a critical role in maintaining mucosal integrity during Citrobacter rodentium-induced colitis. Cell Microbiol 10, 388-403 (2008).

48. Heine, H. & Ulmer, A. J. Recognition of bacterial products by toll-like receptors. Chem Immunol Allergy 86, 99-119 (2005).

49. Janssens, S. & Beyaert, R. Role of Toll-like receptors in pathogen recognition. Clin Microbiol Rev 16, 637-46 (2003).

50. Kirschning, C. J. & Schumann, R. R. TLR2: cellular sensor for microbial and endogenous molecular patterns. Curr Top Microbiol Immunol 270, 121-44 (2002).

51. Kufer, T. A., Fritz, J. H. & Philpott, D. J. NACHT-LRR proteins (NLRs) in bacterial infection and immunity. Trends Microbiol 13, 381-8 (2005).

52. Netea, M. G., Van der Graaf, C., Van der Meer, J. W. & Kullberg, B. J. Recognition of fungal pathogens by Toll-like receptors. Eur J Clin Microbiol Infect Dis 23, 672-6 (2004).

53.   Netea, M. G., Van der Meer, J. W. & Kullberg, B. J. Recognition of pathogenic microorganisms by Toll-like receptors. Drugs Today (Barc) 42 Suppl A, 99-105 (2006).

54.   Philpott, D. J. & Girardin, S. E. The role of Toll-like receptors and Nod proteins in bacterial infection. Mol Immunol 41, 1099-108 (2004).

55.   Tietze, K. et al. Differences in innate immune responses upon stimulation with gram-positive and gram-negative bacteria. J Periodontal Res 41, 447-54 (2006).

56.   Wagner, H. Interactions between bacterial CpG-DNA and TLR9 bridge innate and adaptive immunity. Curr Opin Microbiol 5, 62-9 (2002).

57.   Areschoug, T. & Gordon, S. Pattern recognition receptors and their role in innate immunity: focus on microbial protein ligands. Contrib Microbiol 15, 45-60 (2008).

58.   Arancibia, S. A. et al. Toll-like receptors are key participants in innate immune responses. Biol Res 40, 97-112 (2007).

59.   Glimcher, L. H. & Murphy, K. M. Lineage commitment in the immune system: the T helper lymphocyte grows up. Genes Dev 14, 1693-711 (2000).

60.   Murphy, K. M. et al. Signaling and transcription in T helper development. Annu Rev Immunol 18, 451-94 (2000).

61.   Afkarian, M. et al. T-bet is a STAT1-induced regulator of IL-12R expression in naive CD4+ T cells. Nat Immunol 3, 549-57 (2002).

62.   Muraille, E. & Leo, O. Revisiting the Th1/Th2 paradigm. Scand J Immunol 47, 1-9 (1998).

63.   Mosmann, T. R. & Sad, S. The expanding universe of T-cell subsets: Th1, Th2 and more. Immunol Today 17, 138-46 (1996).

64.   Abbas, A. K., Murphy, K. M. & Sher, A. Functional diversity of helper T lymphocytes. Nature 383, 787-93 (1996).

65.   Coffman, R. L., Lebman, D. A. & Rothman, P. Mechanism and regulation of immunoglobulin isotype switching. Adv Immunol 54, 229-70 (1993).

66.   Ouyang, W. et al. Inhibition of Th1 development mediated by GATA-3 through an IL-4-independent mechanism. Immunity 9, 745-55 (1998).

67.   Zheng, W. & Flavell, R. A. The transcription factor GATA-3 is necessary and sufficient for Th2 cytokine gene expression in CD4 T cells. Cell 89, 587-96 (1997).

68.   Gellert, M. V(D)J recombination: RAG proteins, repair factors, and regulation. Annu Rev Biochem 71, 101-32 (2002).

69.   Fanning, L. J., Connor, A. M. & Wu, G. E. Development of the immunoglobulin repertoire. Clin Immunol Immunopathol 79, 1-14 (1996).

70.   Kondo, M., Weissman, I. L. & Akashi, K. Identification of clonogenic common lymphoid progenitors in mouse bone marrow. Cell 91, 661-72 (1997).

71.   Dal Porto, J. M. et al. B cell antigen receptor signaling 101. Mol Immunol 41, 599-613 (2004).

72.   Bishop, G. A. & Hostager, B. S. B lymphocyte activation by contact-mediated interactions with T lymphocytes. Curr Opin Immunol 13, 278-85 (2001).

73.   MacLennan, I. C. Germinal centers still hold secrets. Immunity 22, 656-7 (2005).

74.   Liu, Y. J., Johnson, G. D., Gordon, J. & MacLennan, I. C. Germinal centres in T-cell-dependent antibody responses. Immunol Today 13, 17-21 (1992).

75.   MacLennan, I. C., Liu, Y. J. & Johnson, G. D. Maturation and dispersal of B-cell clones during T cell-dependent antibody responses. Immunol Rev 126, 143-61 (1992).

76.   MacLennan, I. C. Somatic mutation. From the dark zone to the light. Curr Biol 4, 70-2 (1994).

77.   MacLennan, I. C. Germinal centers. Annu Rev Immunol 12, 117-39 (1994).

78.   McHeyzer-Williams, L. J. & McHeyzer-Williams, M. G. Antigen-specific memory B cell development. Annu Rev Immunol 23, 487-513 (2005).

79.   Banchereau, J. et al. The CD40 antigen and its ligand. Annu Rev Immunol 12, 881-922 (1994).

80.   Quezada, S. A., Jarvinen, L. Z., Lind, E. F. & Noelle, R. J. CD40/CD154 interactions at the interface of tolerance and immunity. Annu Rev Immunol 22, 307-28 (2004).

81.   Xiao, Y., Hendriks, J., Langerak, P., Jacobs, H. & Borst, J. CD27 is acquired by primed B cells at the centroblast stage and promotes germinal center formation. J Immunol 172, 7432-41 (2004).

82.   Kraal, G., Weissman, I. L. & Butcher, E. C. Germinal centre B cells: antigen specificity and changes in heavy chain class expression. Nature 298, 377-9 (1982).

83.   Klein, U. & Dalla-Favera, R. Germinal centres: role in B-cell physiology and malignancy. Nat Rev Immunol 8, 22-33 (2008).

84.   Liu, M. et al. Two levels of protection for the B cell genome during somatic hypermutation. Nature 451, 841-5 (2008).

85.   Phan, T. G. et al. High affinity germinal center B cells are actively selected into the plasma cell compartment. J Exp Med 203, 2419-24 (2006).

86.   Meyer-Hermann, M. E., Maini, P. K. & Iber, D. An analysis of B cell selection mechanisms in germinal centers. Math Med Biol 23, 255-77 (2006).

87.   Park, C. S. & Choi, Y. S. How do follicular dendritic cells interact intimately with B cells in the germinal centre? Immunology 114, 2-10 (2005).

88.   Iber, D. & Maini, P. K. A mathematical model for germinal centre kinetics and affinity maturation. J Theor Biol 219, 153-75 (2002).

89.   Lindhout, E., Koopman, G., Pals, S. T. & de Groot, C. Triple check for antigen specificity of B cells during germinal centre reactions. Immunol Today 18, 573-7 (1997).

90.   Matsumoto, M. et al. Affinity maturation without germinal centres in lymphotoxin-alpha-deficient mice. Nature 382, 462-6 (1996).

91.   Apel, M. & Berek, C. Somatic mutations in antibodies expressed by germinal centre B cells early after primary immunization. Int Immunol 2, 813-9 (1990).

92.   Berek, C. & Ziegner, M. The maturation of the immune response. Immunol Today 14, 400-4 (1993).

93.   Liu, Y. J. et al. Mechanism of antigen-driven selection in germinal centres. Nature 342, 929-31 (1989).

94.   Klaus, G. G. & Kunkl, A. The role of germinal centres in the generation of immunological memory. Ciba Found Symp 84, 265-80 (1981).

95.   Coico, R. F., Bhogal, B. S. & Thorbecke, G. J. Relationship of germinal centers in lymphoid tissue to immunologic memory. VI. Transfer of B cell memory with lymph node cells fractionated according to their receptors for peanut agglutinin. J Immunol 131, 2254-7 (1983).

96.   Tsiagbe, V. K., Inghirami, G. & Thorbecke, G. J. The physiology of germinal centers. Crit Rev Immunol 16, 381-421 (1996).

97.   Thorbecke, G. J., Amin, A. R. & Tsiagbe, V. K. Biology of germinal centers in lymphoid tissue. Faseb J 8, 832-40 (1994).

98.   Tsiagbe, V. K., Linton, P. J. & Thorbecke, G. J. The path of memory B-cell development. Immunol Rev 126, 113-41 (1992).

99.   Caron, G., Le Gallou, S., Lamy, T., Tarte, K. & Fest, T. CXCR4 expression functionally discriminates centroblasts versus centrocytes within human germinal center B cells. J Immunol 182, 7595-602 (2009).

100.   Allen, C. D. et al. Germinal center dark and light zone organization is mediated by CXCR4 and CXCR5. Nat Immunol 5, 943-52 (2004).

101.   Allen, C. D., Okada, T. & Cyster, J. G. Germinal-center organization and cellular dynamics. Immunity 27, 190-202 (2007).

102.   Smith, J. P., Burton, G. F., Tew, J. G. & Szakal, A. K. Tingible body macrophages in regulation of germinal center reactions. Dev Immunol 6, 285-94 (1998).

103.   Bransteitter, R., Sneeden, J. L., Allen, S., Pham, P. & Goodman, M. F. First AID (activation-induced cytidine deaminase) is needed to produce high affinity isotype-switched antibodies. J Biol Chem 281, 16833-6 (2006).

104.   Peled, J. U. et al. The biochemistry of somatic hypermutation. Annu Rev Immunol 26, 481-511 (2008).

105.   Xu, Z. et al. Regulation of aicda expression and AID activity: relevance to somatic hypermutation and class switch DNA recombination. Crit Rev Immunol 27, 367-97 (2007).

106.   de Yebenes, V. G. & Ramiro, A. R. Activation-induced deaminase: light and dark sides. Trends Mol Med 12, 432-9 (2006).

107.   Cattoretti, G. et al. Nuclear and cytoplasmic AID in extrafollicular and germinal center B cells. Blood 107, 3967-75 (2006).

108. Pasqualucci, L., Kitaura, Y., Gu, H. & Dalla-Favera, R. PKA-mediated phosphorylation regulates the function of activation-induced deaminase (AID) in B cells. Proc Natl Acad Sci U S A 103, 395-400 (2006).

109. Muramatsu, M. et al. Class switch recombination and hypermutation require activation-induced cytidine deaminase (AID), a potential RNA editing enzyme. Cell 102, 553-63 (2000).

110. Muramatsu, M. et al. Specific expression of activation-induced cytidine deaminase (AID), a novel member of the RNA-editing deaminase family in germinal center B cells. J Biol Chem 274, 18470-6 (1999).

111. Halle, S. et al. Solitary intestinal lymphoid tissue provides a productive port of entry for Salmonella enterica serovar Typhimurium. Infect Immun 75, 1577-85 (2007).

112. Cesta, M. F. Normal structure, function, and histology of mucosa-associated lymphoid tissue. Toxicol Pathol 34, 599-608 (2006).

113. Elmore, S. A. Enhanced histopathology of mucosa-associated lymphoid tissue. Toxicol Pathol 34, 687-96 (2006).

114. Kraehenbuhl, J. P., Hopkins, S. A., Kerneis, S. & Pringault, E. Antigen sampling by epithelial tissues: implication for vaccine design. Behring Inst Mitt, 24-32 (1997).

115. Michetti, P. et al. Monoclonal immunoglobulin A prevents adherence and invasion of polarized epithelial cell monolayers by Salmonella typhimurium. Gastroenterology 107, 915-23 (1994).

116. Haneberg, B. et al. Induction of specific immunoglobulin A in the small intestine, colon-rectum, and vagina measured by a new method for collection of secretions from local mucosal surfaces. Infect Immun 62, 15-23 (1994).

117. Neutra, M. R. & Kraehenbuhl, J. P. Mucosal immunization via M cells for production of protective secretory IgA antibodies. Am J Trop Med Hyg 50, 10-3 (1994).

118. Monath, T. P. & Neutra, M. R. Special symposium on mucosal immunity: protection against pathogens. Introduction. Am J Trop Med Hyg 50, 1-2 (1994).

119. Cebra, J. J., Griffin, P. M., Lebman, D. A. & London, S. D. Perturbations in Peyer's patch B cell populations indicative of priming for a secretory IgA response. Adv Exp Med Biol 216A, 3-14 (1987).

120. Crabbe, P. A., Nash, D. R., Bazin, H., Eyssen, H. & Heremans, J. F. Immunohistochemical observations on lymphoid tissues from conventional and germ-free mice. Lab Invest 22, 448-57 (1970).

121. Hamada, H. et al. Identification of multiple isolated lymphoid follicles on the antimesenteric wall of the mouse small intestine. J Immunol 168, 57-64 (2002).

122. Lorenz, R. G., Chaplin, D. D., McDonald, K. G., McDonough, J. S. & Newberry, R. D. Isolated lymphoid follicle formation is inducible and dependent upon lymphotoxin-sufficient B lymphocytes, lymphotoxin beta receptor, and TNF receptor I function. J Immunol 170, 5475-82 (2003).

123. Wang, C., McDonald, K. G., McDonough, J. S. & Newberry, R. D. Murine isolated lymphoid follicles contain follicular B lymphocytes with a mucosal phenotype. Am J Physiol Gastrointest Liver Physiol 291, G595-604 (2006).

124. Fagarasan, S. & Honjo, T. Intestinal IgA synthesis: regulation of front-line body defences. Nat Rev Immunol 3, 63-72 (2003).

125. Farquhar, M. G. & Palade, G. E. Junctional complexes in various epithelia. J Cell Biol 17, 375-412 (1963).

126. Jang, M. H. et al. Intestinal villous M cells: an antigen entry site in the mucosal epithelium. Proc Natl Acad Sci U S A 101, 6110-5 (2004).

127. Kucharzik, T. et al. Role of M cells in intestinal barrier function. Ann N Y Acad Sci 915, 171-83 (2000).

128. Miller, H., Zhang, J., Kuolee, R., Patel, G. B. & Chen, W. Intestinal M cells: the fallible sentinels? World J Gastroenterol 13, 1477-86 (2007).

129. Mach, J., Hshieh, T., Hsieh, D., Grubbs, N. & Chervonsky, A. Development of intestinal M cells. Immunol Rev 206, 177-89 (2005).

130. Kraehenbuhl, J. P. & Neutra, M. R. Epithelial M cells: differentiation and function. Annu Rev Cell Dev Biol 16, 301-32 (2000).

131. Sierro, F., Pringault, E., Assman, P. S., Kraehenbuhl, J. P. & Debard, N. Transient expression of M-cell phenotype by enterocyte-like cells of the follicle-associated epithelium of mouse Peyer's patches. Gastroenterology 119, 734-43 (2000).

132. Hathaway, L. J. & Kraehenbuhl, J. P. The role of M cells in mucosal immunity. Cell Mol Life Sci 57, 323-32 (2000).

133. Borghesi, C., Taussig, M. J. & Nicoletti, C. Rapid appearance of M cells after microbial challenge is restricted at the periphery of the follicle-associated epithelium of Peyer's patch. Lab Invest 79, 1393-401 (1999).

134. Sansonetti, P. J. & Phalipon, A. M cells as ports of entry for enteroinvasive pathogens: mechanisms of interaction, consequences for the disease process. Semin Immunol 11, 193-203 (1999).

135. Debard, N., Sierro, F. & Kraehenbuhl, J. P. Development of Peyer's patches, follicle-associated epithelium and M cell: lessons from immunodeficient and knockout mice. Semin Immunol 11, 183-91 (1999).

136. Owen, R. L. Mid-life crisis for M cells. Gut 42, 11-2 (1998).

137. Jepson, M. A. et al. Targeting to intestinal M cells. J Anat 189 (Pt 3), 507-16 (1996).

138. Smith, M. W. et al. Selective transport of microparticles across Peyer's patch follicle-associated M cells from mice and rats. Exp Physiol 80, 735-43 (1995).

139. Pappo, J. & Mahlman, R. T. Follicle epithelial M cells are a source of interleukin-1 in Peyer's patches. Immunology 78, 505-7 (1993).

140. Nagura, H., Ohtani, H., Masuda, T., Kimura, M. & Nakamura, S. HLA-DR expression on M cells overlying Peyer's patches is a common feature of human small intestine. Acta Pathol Jpn 41, 818-23 (1991).

141. Fujimura, Y. et al. Distribution of microfold cells (M cells) in human follicle-associated epithelium. Gastroenterol Jpn 25, 130 (1990).

142. Pabst, R. The anatomical basis for the immune function of the gut. Anat Embryol (Berl) 176, 135-44 (1987).

143. Rosner, A. J. & Keren, D. F. Demonstration of M cells in the specialized follicle-associated epithelium overlying isolated lymphoid follicles in the gut. J Leukoc Biol 35, 397-404 (1984).

144. Bhalla, D. K. & Owen, R. L. Migration of B and T lymphocytes to M cells in Peyer's patch follicle epithelium: an autoradiographic and immunocytochemical study in mice. Cell Immunol 81, 105-17 (1983).

145. Kraehenbuhl, J. P. & Neutra, M. R. Molecular and cellular basis of immune protection of mucosal surfaces. Physiol Rev 72, 853-79 (1992).

146. Neutra, M. R. & Kraehenbuhl, J. P. Transepithelial transport and mucosal defence I: the role of M cells. Trends Cell Biol 2, 134-8 (1992).

147. Tyrer, P. C., Ruth Foxwell, A., Kyd, J. M., Otczyk, D. C. & Cripps, A. W. Receptor mediated targeting of M-cells. Vaccine 25, 3204-9 (2007).

148. Jensen, V. B., Harty, J. T. & Jones, B. D. Interactions of the invasive pathogens Salmonella typhimurium, Listeria monocytogenes, and Shigella flexneri with M cells and murine Peyer's patches. Infect Immun 66, 3758-66 (1998).

149. Rescigno, M. & Borrow, P. The host-pathogen interaction: new themes from dendritic cell biology. Cell 106, 267-70 (2001).

150. Rescigno, M., Rotta, G., Valzasina, B. & Ricciardi-Castagnoli, P. Dendritic cells shuttle microbes across gut epithelial monolayers. Immunobiology 204, 572-81 (2001).

151. Rescigno, M. et al. Dendritic cells express tight junction proteins and penetrate gut epithelial monolayers to sample bacteria. Nat Immunol 2, 361-7 (2001).

152. Craig, S. W. & Cebra, J. J. Peyer's patches: an enriched source of precursors for IgA-producing immunocytes in the rabbit. J Exp Med 134, 188-200 (1971).

153. Kraehenbuhl, J. P. & Neutra, M. R. Transepithelial transport and mucosal defence II: secretion of IgA. Trends Cell Biol 2, 170-4 (1992).

154. Schauer, D. B. & Falkow, S. The eae gene of Citrobacter freundii biotype 4280 is necessary for colonization in transmissible murine colonic hyperplasia. Infect Immun 61, 4654-61 (1993).

155. Schauer, D. B. et al. Genetic and biochemical characterization of Citrobacter rodentium sp. nov. J Clin Microbiol 33, 2064-8 (1995).

156. Lebeis, S. L., Sherman, M. A. & Kalman, D. Protective and destructive innate immune responses to enteropathogenic Escherichia coli and related A/E pathogens. Future Microbiol 3, 315-28 (2008).

157. Bergstrom, K. S. et al. Modulation of intestinal goblet cell function during infection by an attaching and effacing bacterial pathogen. Infect Immun 76, 796-811 (2008).

158. Bishop, A. L., Wiles, S., Dougan, G. & Frankel, G. Cell attachment properties and infectivity of host-adapted and environmentally adapted Citrobacter rodentium. Microbes Infect 9, 1316-24 (2007).

159. Guttman, J. A., Samji, F. N., Li, Y., Vogl, A. W. & Finlay, B. B. Evidence that tight junctions are disrupted due to intimate bacterial contact and not inflammation during attaching and effacing pathogen infection in vivo. Infect Immun 74, 6075-84 (2006).

160. Guttman, J. A. et al. Attaching and effacing pathogen-induced tight junction disruption in vivo. Cell Microbiol 8, 634-45 (2006).

161. Mundy, R., MacDonald, T. T., Dougan, G., Frankel, G. & Wiles, S. Citrobacter rodentium of mice and man. Cell Microbiol 7, 1697-706 (2005).

162. Knutton, S. et al. A novel EspA-associated surface organelle of enteropathogenic Escherichia coli involved in protein translocation into epithelial cells. Embo J 17, 2166-76 (1998).

163. Wiles, S. et al. Organ specificity, colonization and clearance dynamics in vivo following oral challenges with the murine pathogen Citrobacter rodentium. Cell Microbiol 6, 963-72 (2004).

164. Luperchio, S. A. et al. Citrobacter rodentium, the causative agent of transmissible murine colonic hyperplasia, exhibits clonality: synonymy of C. rodentium and mouse-pathogenic Escherichia coli. J Clin Microbiol 38, 4343-50 (2000).

165. Wiles, S., Pickard, K. M., Peng, K., MacDonald, T. T. & Frankel, G. In vivo bioluminescence imaging of the murine pathogen Citrobacter rodentium. Infect Immun 74, 5391-6 (2006).

166. Barthold, S. W., Coleman, G. L., Bhatt, P. N., Osbaldiston, G. W. & Jonas, A. M. The etiology of transmissible murine colonic hyperplasia. Lab Anim Sci 26, 889-94 (1976).

167. Higgins, L. M., Frankel, G., Douce, G., Dougan, G. & MacDonald, T. T. Citrobacter rodentium infection in mice elicits a mucosal Th1 cytokine response and lesions similar to those in murine inflammatory bowel disease. Infect Immun 67, 3031-9 (1999).

168. MacDonald, T. T., Frankel, G., Dougan, G., Goncalves, N. S. & Simmons, C. Host defences to Citrobacter rodentium. Int J Med Microbiol 293, 87-93 (2003).

169. Spahn, T. W. et al. CD4+ T cells transfer resistance against Citrobacter rodentium-induced infectious colitis by induction of Th 1 immunity. Scand J Immunol 67, 238-44 (2008).

170.   Bry, L., Brigl, M. & Brenner, M. B. CD4+-T-cell effector functions
        and costimulatory requirements essential for surviving mucosal
        infection with Citrobacter rodentium. Infect Immun 74, 673-81 (2006).

171.   Simmons, C. P. et al. Central role for B lymphocytes and CD4+ T cells
        in immunity to infection by the attaching and effacing pathogen
        Citrobacter rodentium. Infect Immun 71, 5077-86 (2003).

172.   Maaser, C. et al. Clearance of Citrobacter rodentium requires B cells
        but not secretory immunoglobulin A (IgA) or IgM antibodies. Infect
        Immun 72, 3315-24 (2004).

173.   Spahn, T. W. et al. The lymphotoxin-beta receptor is critical for
        control of murine Citrobacter rodentium-induced colitis.
        Gastroenterology 127, 1463-73 (2004).

174.   Crump, J. A., Luby, S. P. & Mintz, E. D. The global burden of typhoid
        fever. Bull World Health Organ 82, 346-53 (2004).

175.   Jones, B. D. Host responses to pathogenic Salmonella infection. Genes
        Dev 11, 679-87 (1997).

176.   Mastroeni, P. & Sheppard, M. Salmonella infections in the mouse
        model: host resistance factors and in vivo dynamics of bacterial spread
        and distribution in the tissues. Microbes Infect 6, 398-405 (2004).

177.   Nauciel, C. & Espinasse-Maes, F. Role of gamma interferon and
        tumor necrosis factor alpha in resistance to Salmonella typhimurium
        infection. Infect Immun 60, 450-4 (1992).

178.   Mittrucker, H. W. & Kaufmann, S. H. Immune response to infection
        with Salmonella typhimurium in mice. J Leukoc Biol 67, 457-63
        (2000).

179.   McSorley, S. J., Cookson, B. T. & Jenkins, M. K. Characterization of
        CD4+ T cell responses during natural infection with Salmonella
        typhimurium. J Immunol 164, 986-93 (2000).

180.   Clare, S. et al. Intracellular adhesion molecule 1 plays a key role in
        acquired immunity to salmonellosis. Infect Immun 71, 5881-91
        (2003).

181.   Mittrucker, H. W., Raupach, B., Kohler, A. & Kaufmann, S. H.
        Cutting edge: role of B lymphocytes in protective immunity against
        Salmonella typhimurium infection. J Immunol 164, 1648-52 (2000).

182.   Pie, S., Matsiota-Bernard, P., Truffa-Bachi, P. & Nauciel, C. Gamma
        interferon and interleukin-10 gene expression in innately susceptible

and resistant mice during the early phase of Salmonella typhimurium infection. Infect Immun 64, 849-54 (1996).

183. Muotiala, A. & Makela, P. H. The role of IFN-gamma in murine Salmonella typhimurium infection. Microb Pathog 8, 135-41 (1990).

184. Mastroeni, P., Villarreal, B., Demarco de Hormaeche, R. & Hormaeche, C. E. Serum TNF alpha inhibitor in mouse typhoid. Microb Pathog 12, 343-9 (1992).

185. Mastroeni, P., Villarreal-Ramos, B. & Hormaeche, C. E. Role of T cells, TNF alpha and IFN gamma in recall of immunity to oral challenge with virulent salmonellae in mice vaccinated with live attenuated aro- Salmonella vaccines. Microb Pathog 13, 477-91 (1992).

186. Mastroeni, P., Villarreal-Ramos, B. & Hormaeche, C. E. Effect of late administration of anti-TNF alpha antibodies on a Salmonella infection in the mouse model. Microb Pathog 14, 473-80 (1993).

187. McSorley, S. J. & Jenkins, M. K. Antibody is required for protection against virulent but not attenuated Salmonella enterica serovar typhimurium. Infect Immun 68, 3344-8 (2000).

188. Mastroeni, P., Simmons, C., Fowler, R., Hormaeche, C. E. & Dougan, G. Igh-6(-/-) (B-cell-deficient) mice fail to mount solid acquired resistance to oral challenge with virulent Salmonella enterica serovar typhimurium and show impaired Th1 T-cell responses to Salmonella antigens. Infect Immun 68, 46-53 (2000).

189. Linton, P. J., Harbertson, J. & Bradley, L. M. A critical role for B cells in the development of memory CD4 cells. J Immunol 165, 5558-65 (2000).

190. Hoiseth, S. K. & Stocker, B. A. D. Aromatic-dependent Salmonella typhimurium are non-virulent and effective as live vaccines. Nature 291, 238-239 (1981).

191. Schauer, D. B. & Falkow, S. Attaching and effacing locus of a Citrobacter freundii biotype that causes transmissible murine colonic hyperplasia. Infect Immun 61, 2486-92 (1993).

192. R Development Core Team, R: A language and environment for statistical computing. R Foundation for Statistical Computing, Vienna, Austria. ISBN 3-900051-07-0, URL http://www.R-project.org..

193. Gentleman, R. C. et al. Bioconductor: open software development for computational biology and bioinformatics. Genome Biol 5, R80 (2004).

194. Du, P., Kibbe, W. A. and Lin, S. M. lumi: a pipeline for processing Illumina microarray. Bioinformatics 24(13), 1547-8 (2008).

195. Lin, S. M., Du, P., Huber, W. and Kibbe, W. A. Model-based variance-stabilizing transformation for Illumina microarray data. Nucleic Acids Res. 36, e11 (2008).

196. Smyth, G. K. Limma: linear models for microarray data. In: Bioinformatics and Computational Biology Solutions using R and Bioconductor, R. Gentleman, V. Carey, S. Dudoit, R. Irizarry, W. Huber (eds.), Springer, New York, pages 397-420.

197. Benjamini, Y. and Hochberg, Y. Controlling the False Discovery Rate: A Practical and Powerful Approach to Multiple Testing. J. R. Stat. Soc. Ser. B Methodol. 57, 289-300 (1995)

198. Marc Carlson, Seth Falcon, Herve Pages and Nianhua Li.GO.db: A set of annotation maps describing the entire Gene Ontology.

199. Gang Feng, Pan Du, Warren Kibbe and Simon Lin. LumiMouseAll.db: Illumina Mouse Expression BeadChips (include all versions: version 1 to 2) annotation data (chip lumiMouseAll)

200. Marc Carlson, Seth Falcon, Herve Pages and Nianhua Li. KEGG.db: A set of annotation maps for KEGG.

201. Hubbard, T. J. et al. Ensembl 2009. Nucleic Acids Res 37, D690-7 (2009).

202. Grimson, A. et al. MicroRNA targeting specificity in mammals: determinants beyond seed pairing. Mol Cell 27, 91-105 (2007).

203. Kertesz, M., Iovino, N., Unnerstall, U., Gaul, U. & Segal, E. The role of site accessibility in microRNA target recognition. Nat Genet 39, 1278-84 (2007).

204. van Dongen, S., Abreu-Goodger, C. & Enright, A. J. Detecting microRNA binding and siRNA off-target effects from expression data. Nat Methods 5, 1023-5 (2008).

205. Malick, L. E. & Wilson, R. B. Modified thiocarbohydrazide procedure for scanning electron microscopy: routine use for normal, pathological, or experimental tissues. Stain Technol 50, 265-9 (1975).

206. Mignard, S. & Flandrois, J. P. 16S rRNA sequencing in routine bacterial identification: a 30-month experiment. J Microbiol Methods 67, 574-81 (2006).

207.   Hoffmann, C. et al. Community-wide response of the gut microbiota to enteropathogenic Citrobacter rodentium infection revealed by deep sequencing. Infect Immun 77, 4668-78 (2009).

208.   Bry, L. & Brenner, M. B. Critical role of T cell-dependent serum antibody, but not the gut-associated lymphoid tissue, for surviving acute mucosal infection with Citrobacter rodentium, an attaching and effacing pathogen. J Immunol 172, 433-41 (2004).

209.   Wolniak, K. L., Shinall, S. M. & Waldschmidt, T. J. The germinal center response. Crit Rev Immunol 24, 39-65 (2004).

210.   Saitoh, H. A., Maeda, K. & Yamakawa, M. In situ observation of germinal center cell apoptosis during a secondary immune response. J Clin Exp Hematop 46, 73-82 (2006).

211.   Lynn, D. J. et al. InnateDB: facilitating systems-level analyses of the mammalian innate immune response. Mol Syst Biol 4 (2008).

212.   Li, C. K. et al. Impaired immunity to intestinal bacterial infection in stromelysin-1 (matrix metalloproteinase-3)-deficient mice. J Immunol 173, 5171-9 (2004).

213.   Enright, A. J. et al. MicroRNA targets in Drosophila. Genome Biol 5, R1 (2003).

214.   Spehlmann, M. E. et al. CXCR2-dependent mucosal neutrophil influx protects against colitis-associated diarrhea caused by an attaching/effacing lesion-forming bacterial pathogen. J Immunol 183, 3332-43 (2009).

215.   Saxen, H. & Makela, O. The protective capacity of immune sera in experimental mouse salmonellosis is mainly due to IgM antibodies. Immunol Lett 5, 267-72 (1982).

Supplementary Figures and Tables
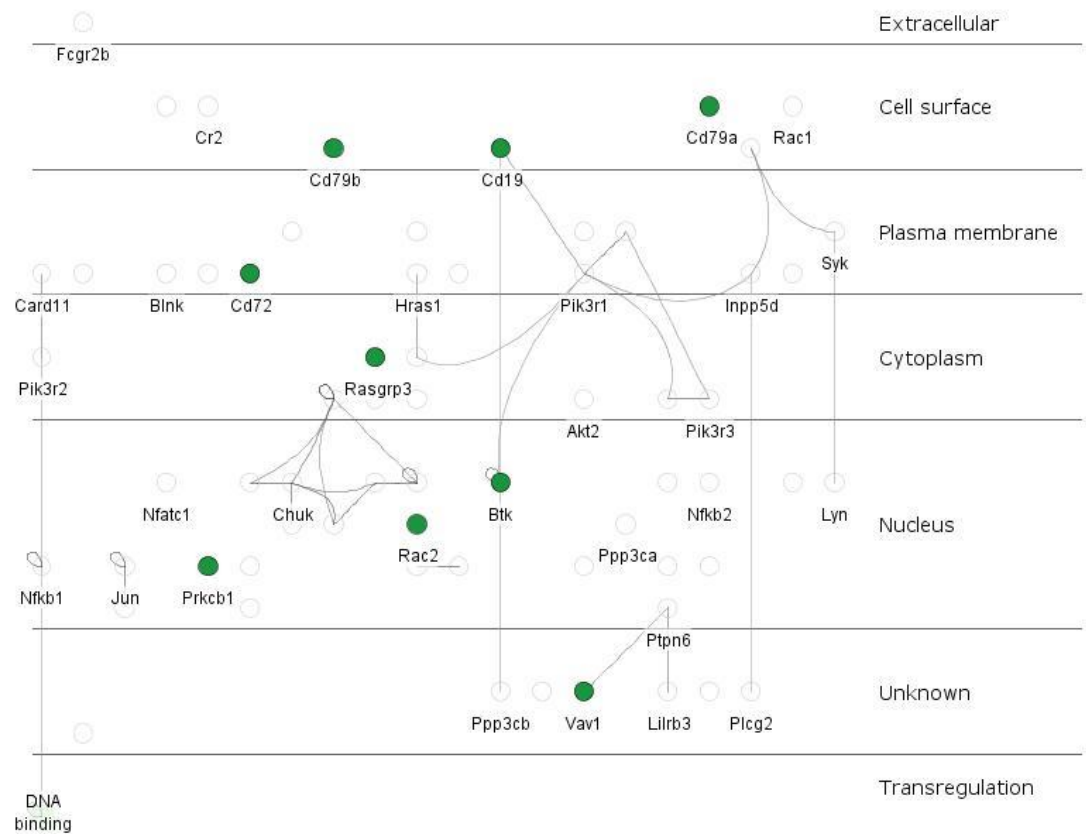
Figure S 1. The B cell Receptor signalling pathway is downregulated in the caecal patch of miR-155-deficient mice on day 4 pi

InnateDB analysis of mRNAs down-regulated in miR-155-deficient vs wild-type caecal patch 4 days pi identified that there was an over-representation of genes involved in the B cell receptor signalling pathway. Figure shows genes involved in B cell receptor signalling and those identified as being significantly down-regulated (green nodes).

Colon bic vs wt
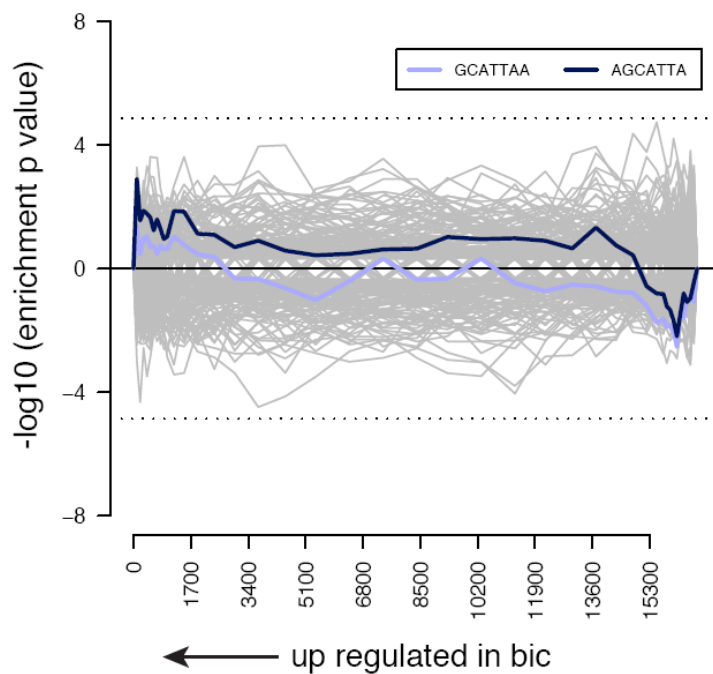
Cecal patch bic vs wt

Figure S 2. Sylamer analysis

Sylamer analysis of mRNAs extracted from colon (colon, bic (miR-155-deficient) vs wt (wild-type)) and caecal patch (caecal patch, bic (miR-155-deficient) vs wt (wild-type)). The x-axis represents all the genes with an annotated 3'UTR sequence, sorted starting from the most up-regulated in the miR-155-deficient samples. The y-axis represents the -log10transformed hyper-geometric P-values, with positive values denoting enrichment and negative values depletion. Each gray line represents a single 7-nucleotide seed-matching word and those corresponding to miR-155 are highlighted. Dotted lines represent Bonferroni-corrected P-value significance thresholds of 0.01.

KEGG ID	Pvalue	OddsRatio	ExpCount	Count	Size	Term	Description
00980	8.5e-08	9.4	1.75	12	57	Metabolism of xenobiotics by cytochrome P450	Metabolism of xenobiotics by cytochrome P450
00071	1.4e-06	10.6	1.17	9	38	Fatty acid metabolism	Fatty acid metabolism
00150	1.5e-04	7.3	1.20	7	39	Androgen and estrogen metabolism	Androgen and estrogen metabolism
00280	9.1e-04	6.2	1.17	6	38	Valine, leucine and isoleucine degradation	Valine, leucine and isoleucine degradation
00040	1.5e-03	10.0	0.52	4	17	Pentose and glucuronate interconversions	Pentose and glucuronate interconversions
00010	2.5e-03	5.0	1.42	6	46	Glycolysis / Gluconeogenesis	Glycolysis / Gluconeogenesis
00410	2.8e-03	8.2	0.62	4	20	beta-Alanine metabolism	beta-Alanine metabolism
00360	3.4e-03	7.7	0.65	4	21	Phenylalanine metabolism	Phenylalanine metabolism
00220	4.8e-03	6.9	0.71	4	23	Urea cycle and metabolism of amino groups	Urea cycle and metabolism of amino groups
00640	6.5e-03	6.2	0.77	4	25	Propanoate metabolism	Propanoate metabolism
00350	8.6e-03	4.4	1.29	5	42	Tyrosine metabolism	Tyrosine metabolism
00650	9.5e-03	4.3	1.32	5	43	Butanoate metabolism	Butanoate metabolism
00120	1.3e-02	5.0	0.92	4	30	Bile acid biosynthesis	Bile acid biosynthesis
00860	1.4e-02	4.8	0.95	4	31	Porphyrin and chlorophyll metabolism	Porphyrin and chlorophyll metabolism
00340	1.7e-02	4.5	1.02	4	33	Histidine metabolism	Histidine metabolism
00680	1.8e-02	12.8	0.22	2	7	Methane metabolism	Methane metabolism
00590	1.9e-02	3.5	1.57	5	51	Arachidonic acid metabolism	Arachidonic acid metabolism
00480	2.1e-02	4.2	1.08	4	35	Glutathione metabolism	Glutathione metabolism
00140	2.3e-02	10.7	0.25	2	8	C21-Steroid hormone metabolism	C21-Steroid hormone metabolism
00920	2.3e-02	10.7	0.25	2	8	Sulfur metabolism	Sulfur metabolism
00641	2.9e-02	9.2	0.28	2	9	3-Chloroacrylic acid degradation	3-Chloroacrylic acid degradation
03320	3.4e-02	3.0	1.82	5	59	PPAR signaling pathway	PPAR signaling pathway
00720	4.3e-02	7.1	0.34	2	11	Reductive carboxylate cycle (CO2 fixation)	Reductive carboxylate cycle (CO2 fixation)

Table S 5. Gene to KEGG test for over-representation within upregulated mRNAs in miR-155-deficient caecal patch on day 4 pi

Gene to KEGG test for over-representation within up-regulated mRNAs in miR-155-deficient vs wild-type caecal patch 4 days pi.

KEGGID	Pvalue	OddsRatio	ExpCount	Count	Size	Term	Description
04662	1.0e-06	8.0	1.81	11	57	B cell receptor signaling pathway	B cell receptor signaling pathway
04514	1.6e-05	4.5	3.77	14	119	Cell adhesion molecules (CAMs)	Cell adhesion molecules (CAMs)
04940	5.8e-04	5.7	1.49	7	47	Type I diabetes mellitus	Type I diabetes mellitus
04650	7.7e-04	3.8	3.04	10	96	Natural killer cell mediated cytotoxicity	Natural killer cell mediated cytotoxicity
04670	2.6e-03	3.4	2.98	9	94	Leukocyte transendothelial migration	Leukocyte transendothelial migration
04612	6.6e-03	3.5	2.25	7	71	Antigen processing and presentation	Antigen processing and presentation
04060	7.8e-03	2.3	6.18	13	195	Cytokine-cytokine receptor interaction	Cytokine-cytokine receptor interaction
04640	1.7e-02	3.2	2.09	6	66	Hematopoietic cell lineage	Hematopoietic cell lineage
00601	2.5e-02	10.4	0.25	2	8	Glycosphingolipid biosynthesis - lactoseries	Glycosphingolipid biosynthesis - lactoseries
00240	2.8e-02	2.8	2.35	6	74	Pyrimidine metabolism	Pyrimidine metabolism
04664	4.5e-02	2.8	1.96	5	62	Fc epsilon RI signaling pathway	Fc epsilon RI signaling pathway

Table S 6. Gene to KEGG test for over-representation within downregulated mRNAs in miR-155-deficient caecal patch on day 4 pi

Gene to KEGG test for over-representation within down-regulated mRNAs in miR-155-deficient vs wild-type caecal patch 4 days pi.

GOBPID	Pvalue	OddsRatio	ExpCount	Count	Size	Term
GO:0006631	9.7e-07	5.3	3.30	15	133	fatty acid metabolic process
GO:0019752	3.8e-05	2.9	8.45	22	342	carboxylic acid metabolic process
GO:0044255	6.1e-05	3.2	6.31	18	270	cellular lipid metabolic process
GO:0006816	2.5e-04	4.8	2.11	9	85	calcium ion transport
GO:0006812	3.1e-04	2.5	9.10	21	367	cation transport
GO:0050801	5.9e-04	3.3	3.94	12	159	ion homeostasis
GO:0055082	1.2e-03	3.2	3.70	11	149	cellular chemical homeostasis
GO:0008272	1.6e-03	17.0	0.25	3	10	sulfate transport
GO:0001523	2.1e-03	14.9	0.27	3	11	retinoid metabolic process
GO:0006694	2.5e-03	4.8	1.38	6	56	steroid biosynthetic process
GO:0030003	3.6e-03	3.8	1.98	7	80	cellular cation homeostasis
GO:0042445	4.2e-03	4.3	1.54	6	62	hormone metabolic process
GO:0006766	7.1e-03	4.5	1.22	5	49	vitamin metabolic process
GO:0051234	8.9e-03	1.4	47.55	63	1917	establishment of localization
GO:0006829	1.3e-02	7.0	0.50	3	20	zinc ion transport
GO:0042493	1.3e-02	7.0	0.50	3	20	response to drug
GO:0055066	1.3e-02	3.3	1.93	6	78	di-, tri-valent inorganic cation homeostasis
GO:0030155	1.3e-02	4.8	0.92	4	37	regulation of cell adhesion
GO:0006732	1.7e-02	2.8	2.65	7	107	coenzyme metabolic process
GO:0006639	1.9e-02	6.0	0.57	3	23	acylglycerol metabolic process
GO:0006814	1.9e-02	3.0	2.11	6	85	sodium ion transport
GO:0008366	2.1e-02	5.7	0.60	3	24	axon ensheathment
GO:0008015	2.1e-02	3.0	2.16	6	87	blood circulation
GO:0006790	2.3e-02	4.0	1.09	4	44	sulfur metabolic process
GO:0006941	2.3e-02	5.4	0.62	3	25	striated muscle contraction
GO:0019228	2.3e-02	5.4	0.62	3	25	regulation of action potential in neuron
GO:0006721	2.4e-02	9.9	0.25	2	10	terpenoid metabolic process
GO:0007431	2.4e-02	9.9	0.25	2	10	salivary gland development
GO:0030865	2.4e-02	9.9	0.25	2	10	cortical cytoskeleton organization and biogenesis
GO:0006811	2.6e-02	2.2	4.22	9	179	ion transport
GO:0042592	3.1e-02	1.8	8.04	14	324	homeostatic process
GO:0002009	3.3e-02	2.6	2.41	6	97	morphogenesis of an epithelium
GO:0002026	3.4e-02	7.9	0.30	2	12	regulation of the force of heart contraction
GO:0009069	3.4e-02	7.9	0.30	2	12	serine family amino acid metabolic process
GO:0042364	3.4e-02	7.9	0.30	2	12	water-soluble vitamin biosynthetic process
GO:0006081	4.0e-02	7.2	0.32	2	13	aldehyde metabolic process
GO:0008152	4.1e-02	1.3	133.96	148	5400	metabolic process
GO:0001501	4.3e-02	2.1	3.92	8	158	skeletal development
GO:0044242	4.3e-02	4.1	0.79	3	32	cellular lipid catabolic process
GO:0006776	4.6e-02	6.6	0.35	2	14	vitamin A metabolic process
GO:0007339	4.6e-02	6.6	0.35	2	14	binding of sperm to zona pellucida
GO:0043506	4.6e-02	6.6	0.35	2	14	regulation of JNK activity

Table S 7. Gene to GO-BP conditional test for over-representation within mRNAs upregulated in miR-155-deficient caecal patch on day 4 pi

Gene to GO-biological process terms test for over-representation within up-regulated mRNAs in miR-155-deficient vs wild-type caecal patch 4 days pi.

GOBPID	Pvalue	OddsRatio	ExpCount	Count	Size	Term
GO:0006334	2.3e-19	15.8	2.37	25	85	nucleosome assembly
GO:0006323	2.0e-17	11.0	3.37	27	121	DNA packaging
GO:0006333	5.7e-17	11.1	3.21	26	115	chromatin assembly or disassembly
GO:0065003	3.8e-11	4.8	7.78	31	279	macromolecular complex assembly
GO:0051276	7.6e-10	4.4	7.75	29	278	chromosome organization and biogenesis
GO:0006955	3.0e-08	4.3	6.49	24	239	immune response
GO:0002504	1.8e-06	23.7	0.42	6	15	antigen processing and presentation of peptide or polysaccharide antigen via MHC class II
GO:0048534	7.6e-06	3.6	5.94	19	213	hemopoietic or lymphoid organ development
GO:0019886	2.6e-05	19.7	0.39	5	14	antigen processing and presentation of exogenous peptide antigen via MHC class II
GO:0046649	6.0e-05	3.6	4.63	15	166	lymphocyte activation
GO:0001775	1.2e-04	3.2	5.49	16	197	cell activation
GO:0019884	2.3e-04	11.1	0.59	5	21	antigen processing and presentation of exogenous antigen
GO:0030217	2.7e-04	5.4	1.70	8	61	T cell differentiation
GO:0050863	3.0e-04	5.3	1.73	8	62	regulation of T cell activation
GO:0007067	4.4e-04	3.5	3.82	12	137	mitosis
GO:0042100	5.5e-04	8.9	0.70	5	25	B cell proliferation
GO:0002521	5.5e-04	3.6	3.37	11	121	leukocyte differentiation
GO:0032943	5.7e-04	4.8	1.90	8	68	mononuclear cell proliferation
GO:0048002	6.6e-04	8.4	0.72	5	26	antigen processing and presentation of peptide antigen
GO:0051301	6.8e-04	2.8	5.77	15	207	cell division
GO:0002684	7.7e-04	3.4	3.51	11	126	positive regulation of immune system process
GO:0002694	1.3e-03	4.7	1.66	7	60	regulation of leukocyte activation
GO:0002429	1.3e-03	7.1	0.84	5	30	immune response-activating cell surface receptor signaling pathway
GO:0045619	1.5e-03	6.8	0.86	5	31	regulation of lymphocyte differentiation
GO:0051251	1.6e-03	4.5	1.73	7	62	positive regulation of lymphocyte activation
GO:0050670	1.8e-03	5.2	1.31	6	47	regulation of lymphocyte proliferation
GO:0050867	1.9e-03	4.4	1.78	7	64	positive regulation of cell activation
GO:0006954	2.0e-03	2.8	4.54	12	163	inflammatory response
GO:0002376	2.3e-03	2.8	4.61	12	183	immune system process
GO:0000278	2.3e-03	2.7	5.24	13	188	mitotic cell cycle
GO:0050776	2.6e-03	3.7	2.38	8	86	regulation of immune response
GO:0006935	3.1e-03	3.6	2.45	8	88	chemotaxis
GO:0030574	5.0e-03	10.6	0.36	3	13	collagen catabolic process
GO:0044243	5.0e-03	10.6	0.36	3	13	multicellular organismal catabolic process
GO:0044256	5.0e-03	10.6	0.36	3	13	protein digestion
GO:0044266	5.0e-03	10.6	0.36	3	13	multicellular organismal macromolecule catabolic process
GO:0044268	5.0e-03	10.6	0.36	3	13	multicellular organismal protein metabolic process

GO:0009605	5.6e-03	2.0	10.01	19	359	response to external stimulus
GO:0000279	5.9e-03	2.5	5.19	12	186	M phase
GO:0030890	6.2e-03	9.6	0.39	3	14	positive regulation of B cell proliferation
GO:0006260	6.3e-03	2.9	3.35	9	120	DNA replication
GO:0022402	6.4e-03	2.2	7.28	15	261	cell cycle process
GO:0006220	1.3e-02	7.0	0.50	3	18	pyrimidine nucleotide metabolic process
GO:0032946	1.4e-02	4.7	0.95	4	34	positive regulation of mononuclear cell proliferation
GO:0045582	1.5e-02	6.6	0.53	3	19	positive regulation of T cell differentiation
GO:0051239	1.9e-02	2.0	6.78	13	245	regulation of multicellular organismal process
GO:0048584	2.0e-02	2.7	2.76	7	99	positive regulation of response to stimulus
GO:0007265	2.6e-02	2.2	4.24	9	152	Ras protein signal transduction
GO:0051130	2.7e-02	3.8	1.14	4	41	positive regulation of cellular component organization and biogenesis
GO:0030155	2.8e-02	5.1	0.67	3	24	regulation of cell adhesion
GO:0002253	2.9e-02	3.1	1.73	5	62	activation of immune response
GO:0019882	2.9e-02	8.9	0.27	2	10	antigen processing and presentation
GO:0009220	3.0e-02	8.8	0.28	2	10	pyrimidine ribonucleotide biosynthetic process
GO:0051056	3.1e-02	2.3	3.68	8	132	regulation of small GTPase mediated signal transduction
GO:0002695	3.1e-02	4.8	0.70	3	25	negative regulation of leukocyte activation
GO:0030099	3.6e-02	2.6	2.45	6	88	myeloid cell differentiation
GO:0006911	3.6e-02	7.8	0.31	2	11	phagocytosis, engulfment
GO:0007051	3.6e-02	7.8	0.31	2	11	spindle organization and biogenesis
GO:0007159	3.6e-02	7.8	0.31	2	11	leukocyte adhesion
GO:0043331	3.6e-02	7.8	0.31	2	11	response to dsRNA
GO:0045191	3.6e-02	7.8	0.31	2	11	regulation of isotype switching
GO:0050869	3.6e-02	7.8	0.31	2	11	negative regulation of B cell activation
GO:0001776	3.8e-02	4.4	0.75	3	27	leukocyte homeostasis
GO:0006270	4.3e-02	7.0	0.33	2	12	DNA replication initiation
GO:0006541	4.3e-02	7.0	0.33	2	12	glutamine metabolic process
GO:0050766	4.3e-02	7.0	0.33	2	12	positive regulation of phagocytosis
GO:0050798	4.3e-02	7.0	0.33	2	12	activated T cell proliferation
GO:0051085	4.3e-02	7.0	0.33	2	12	chaperone cofactor-dependent protein folding
GO:0009617	4.3e-02	2.8	1.92	5	69	response to bacterium
GO:0022610	4.4e-02	1.6	12.44	19	446	biological adhesion
GO:0001817	4.6e-02	4.1	0.81	3	29	regulation of cytokine production
GO:0032615	4.9e-02	6.4	0.36	2	13	interleukin-12 production
GO:0045785	4.9e-02	6.4	0.36	2	13	positive regulation of cell adhesion
GO:0050777	4.9e-02	6.4	0.36	2	13	negative regulation of immune response
GO:0009607	5.0e-02	2.1	4.04	8	145	response to biotic stimulus

Table S 8. Gene to GO-BP conditional test for over-representation within mRNAs downregulated in miR-155-deficient caecal patch on day 4 pi

Gene to GO-biological process terms test for over-representation within down-regulated mRNAs in miR-155-deficient vs wild-type caecal patch 4 days pi.

KEGGID	Pvalue	OddsRatio	ExpCount	Count	Size	Term	Description
00150	0.025	9.3	0.247	2	39	Androgen and estrogen metabolism	Androgen and estrogen metabolism
04115	0.048	6.3	0.355	2	56	p53 signaling pathway	p53 signaling pathway
00140	0.050	23.5	0.051	1	8	C21-Steroid hormone metabolism	C21-Steroid hormone metabolism
00920	0.050	23.5	0.051	1	8	Sulfur metabolism	Sulfur metabolism

Table S 14. Gene to KEGG test for over-representation within mRNAs upregulated in miR-155-deficient caecal patch on day 14 pi

Gene to KEGG test for over-representation within up-regulated mRNAs in miR-155-deficient vs wild-type caecal patch 14 days pi.

KEGGID	Pvalue	OddsRatio	ExpCount	Count	Size	Term	Description
00601	0.036	34	0.036	1	8	Glycosphingolipid biosynthesis - lactoseries	Glycosphingolipid biosynthesis - lactoseries

Table S 15. Gene to KEGG test for over-representation within mRNAs downregulated in miR-155-deficient caecal patch on day14 pi

Gene to KEGG test for over-representation within down-regulated mRNAs in miR-155-deficient vs wild-type caecal patch 14 days pi

GOBPID	Pvalue	OddsRatio	ExpCount	Count	Size	Term
GO:0006953	0.00026	28.9	0.13	3	20	acute-phase response
GO:0007050	0.00204	13.3	0.25	3	40	cell cycle arrest
GO:0008202	0.00604	5.9	0.73	4	115	steroid metabolic process
GO:0045859	0.00642	5.8	0.74	4	117	regulation of protein kinase activity
GO:0051338	0.00808	5.5	0.79	4	125	regulation of transferase activity
GO:0006986	0.01258	12.9	0.17	2	27	response to unfolded protein
GO:0033673	0.01955	10.1	0.22	2	34	negative regulation of kinase activity
GO:0043086	0.04001	6.7	0.32	2	50	negative regulation of catalytic activity
GO:0006066	0.04479	3.2	1.34	4	211	alcohol metabolic process
GO:0051726	0.04544	3.1	1.35	4	212	regulation of cell cycle
GO:0008643	0.04754	6.1	0.35	2	55	carbohydrate transport

Table S 16. Gene to GO-BP conditional test for over-representation within mRNAs upregulated in miR-155-deficient caecal patch on day14 pi

Gene to GO-biological process terms test for over-representation within up-regulated mRNAs in miR-155-deficient vs wild-type caecal patch 14 days pi

GOBPID	Pvalue	OddsRatio	ExpCount	Count	Size	Term
GO:0006935	0.00005	23.7	0.210	4	88	chemotaxis
GO:0002437	0.00030	101.5	0.026	2	11	inflammatory response to antigenic stimulus
GO:0050766	0.00035	91.3	0.029	2	12	positive regulation of phagocytosis
GO:0007626	0.00047	12.9	0.374	4	157	locomotory behavior
GO:0002824	0.00064	65.2	0.038	2	16	positive regulation of adaptive immune response based on somatic recombination of immune receptors built from immunoglobulin superfamily domains
GO:0002708	0.00101	50.7	0.048	2	20	positive regulation of lymphocyte mediated immunity
GO:0002819	0.00101	50.7	0.048	2	20	regulation of adaptive immune response
GO:0032103	0.00101	50.7	0.048	2	20	positive regulation of response to external stimulus
GO:0006690	0.00111	48.0	0.050	2	21	icosanoid metabolic process
GO:0002703	0.00145	41.5	0.057	2	24	regulation of leukocyte mediated immunity
GO:0050727	0.00158	39.6	0.060	2	25	regulation of inflammatory response
GO:0031349	0.00171	38.0	0.062	2	26	positive regulation of defense response
GO:0030100	0.00184	36.5	0.064	2	27	regulation of endocytosis
GO:0050900	0.00198	35.1	0.067	2	28	leukocyte migration
GO:0002768	0.00242	31.4	0.074	2	31	immune response-regulating cell surface receptor signaling pathway
GO:0001525	0.00265	12.3	0.281	3	118	angiogenesis
GO:0002757	0.00291	28.5	0.081	2	34	immune response-activating signal transduction
GO:0048583	0.00387	10.7	0.321	3	135	regulation of response to stimulus
GO:0051130	0.00421	23.3	0.098	2	41	positive regulation of cellular component organization and biogenesis
GO:0007599	0.00442	22.8	0.100	2	42	hemostasis
GO:0050817	0.00462	22.2	0.102	2	43	coagulation
GO:0009611	0.00520	9.7	0.358	3	163	response to wounding
GO:0051240	0.00530	9.6	0.360	3	151	positive regulation of multicellular organismal process
GO:0006952	0.00541	6.5	0.726	4	305	defense response
GO:0002526	0.00801	16.5	0.136	2	57	acute inflammatory response
GO:0001568	0.00887	7.9	0.433	3	182	blood vessel development
GO:0042060	0.01094	14.0	0.160	2	67	wound healing
GO:0002449	0.01357	12.4	0.179	2	75	lymphocyte mediated immunity
GO:0002460	0.01357	12.4	0.179	2	75	adaptive immune response based on somatic recombination of immune receptors built from immunoglobulin superfamily domains
GO:0051239	0.01941	10.3	0.216	2	102	regulation of multicellular organismal process
GO:0007155	0.01990	4.3	1.062	4	446	cell adhesion
GO:0000272	0.02357	48.5	0.024	1	10	polysaccharide catabolic process
GO:0019370	0.02357	48.5	0.024	1	10	leukotriene biosynthetic process
GO:0050854	0.02357	48.5	0.024	1	10	regulation of antigen receptor-mediated signaling pathway
GO:0006928	0.02491	5.3	0.638	3	268	cell motility
GO:0009605	0.02517	9.0	0.249	2	129	response to external stimulus
GO:0006693	0.02590	43.7	0.026	1	11	prostaglandin metabolic process
GO:0006911	0.02590	43.7	0.026	1	11	phagocytosis, engulfment
GO:0043449	0.02590	43.7	0.026	1	11	alkene metabolic process
GO:0045055	0.02590	43.7	0.026	1	11	regulated secretory pathway
GO:0048286	0.02590	43.7	0.026	1	11	alveolus development
GO:0002252	0.02740	8.5	0.260	2	109	immune effector process
GO:0030199	0.03054	36.4	0.031	1	13	collagen fibril organization
GO:0042461	0.03054	36.4	0.031	1	13	photoreceptor cell development
GO:0006044	0.03285	33.6	0.033	1	14	N-acetylglucosamine metabolic process
GO:0019886	0.03285	33.6	0.033	1	14	antigen processing and presentation of exogenous peptide antigen via MHC class II
GO:0030335	0.03285	33.6	0.033	1	14	positive regulation of cell migration
GO:0032635	0.03285	33.6	0.033	1	14	interleukin-6 production
GO:0002504	0.03516	31.2	0.036	1	15	antigen processing and presentation of peptide or polysaccharide antigen via MHC class II
GO:0032640	0.03516	31.2	0.036	1	15	tumor necrosis factor production
GO:0048519	0.03660	3.1	1.896	5	796	negative regulation of biological process
GO:0000902	0.03738	4.5	0.748	3	314	cell morphogenesis
GO:0040017	0.03746	29.1	0.038	1	16	positive regulation of locomotion
GO:0002682	0.03911	6.9	0.315	2	138	regulation of immune system process
GO:0050852	0.03975	27.3	0.040	1	17	T cell receptor signaling pathway
GO:0006040	0.04433	24.2	0.045	1	19	amino sugar metabolic process
GO:0048593	0.04433	24.2	0.045	1	19	camera-type eye morphogenesis
GO:0002699	0.04472	24.0	0.046	1	20	positive regulation of immune effector process
GO:0006958	0.04661	23.0	0.048	1	20	complement activation, classical pathway
GO:0019884	0.04888	21.8	0.050	1	21	antigen processing and presentation of exogenous antigen
GO:0006909	0.04913	21.7	0.050	1	22	phagocytosis

Table S 17. Gene to GO-BP conditional test for over-representation within downregulated mRNAs in miR-155-deficient caecal patch on day 14 pi

Gene to GO-biological process terms test for over-representation within down-regulated mRNAs in miR-155-deficient vs wild-type caecal patch 14 days pi.

KEGGID	Pvalue	OddsRatio	ExpCount	Count	Size	Term	Description
04620	0.012	16	0.177	2	84	Toll-like receptor signaling pathway	Toll-like receptor signaling pathway
00100	0.046	26	0.046	1	22	Biosynthesis of steroids	Biosynthesis of steroids

Table S 23. Gene to KEGG test for over-representation within mRNAs upregulated in miR-155-deficient colon on day4 pi

Gene to KEGG test for over-representation within up-regulated mRNAs in miR-155-deficient vs wild-type colon 4 days pi.

KEGGID	Pvalue	OddsRatio	ExpCount	Count	Size	Term	Description
00910	0.043	28	0.043	1	18	Nitrogen metabolism	Nitrogen metabolism

Table S 24. Gene to KEGG test for over-representation within mRNAs downregulated in miR-155-deficient colon on day4 pi

Gene to KEGG test for over-representation within down-regulated mRNAs in miR-155-deficient vs wild-type colon 4 days pi.

GOBPID	Pvalue	OddsRatio	ExpCount	Count	Size	Term
GO:0006954	0.00082	20.6	0.194	3	163	inflammatory response
GO:0009605	0.00776	9.1	0.427	3	359	response to external stimulus
GO:0009607	0.01235	13.9	0.173	2	145	response to biotic stimulus
GO:0051704	0.01368	13.1	0.182	2	153	multi-organism process
GO:0009161	0.01420	83.1	0.014	1	12	ribonucleoside monophosphate metabolic process
GO:0009124	0.01538	76.2	0.015	1	13	nucleoside monophosphate biosynthetic process
GO:0006629	0.01809	6.6	0.583	3	490	lipid metabolic process
GO:0006749	0.02124	53.7	0.021	1	18	glutathione metabolic process
GO:0007157	0.02124	53.7	0.021	1	18	heterophilic cell adhesion
GO:0006953	0.02357	48.1	0.024	1	20	acute-phase response
GO:0030258	0.02357	48.1	0.024	1	20	lipid modification
GO:0009615	0.02912	38.6	0.029	1	27	response to virus
GO:0016126	0.03170	35.1	0.032	1	27	sterol biosynthetic process
GO:0006950	0.03234	5.2	0.728	3	611	response to stress
GO:0050900	0.03285	33.8	0.033	1	28	leukocyte migration
GO:0048015	0.03976	27.6	0.040	1	34	phosphoinositide-mediated signaling

Table S 25. Gene to GO-BP conditional test for over-representation within mRNAs upregulated in miR-155-deficient colon on day4 pi

Gene to GO-biological process terms test for over-representation within up-regulated mRNAs in miR-155-deficient vs wild-type colon 4 days pi.

GOBPID	Pvalue	OddsRatio	ExpCount	Count	Size	Term
GO:0006631	0.018	10.8	0.211	2	133	fatty acid metabolic process
GO:0006635	0.020	55.8	0.021	1	13	fatty acid beta-oxidation
GO:0016525	0.020	55.8	0.021	1	13	negative regulation of angiogenesis
GO:0030574	0.020	55.8	0.021	1	13	collagen catabolic process
GO:0044243	0.020	55.8	0.021	1	13	multicellular organismal catabolic process
GO:0044256	0.020	55.8	0.021	1	13	protein digestion
GO:0044266	0.020	55.8	0.021	1	13	multicellular organismal macromolecule catabolic process
GO:0044268	0.020	55.8	0.021	1	13	multicellular organismal protein metabolic process
GO:0006094	0.022	51.5	0.022	1	14	gluconeogenesis
GO:0046395	0.030	37.2	0.030	1	19	carboxylic acid catabolic process
GO:0051260	0.030	37.2	0.030	1	19	protein homooligomerization
GO:0019216	0.031	35.2	0.032	1	20	regulation of lipid metabolic process
GO:0046364	0.033	33.5	0.033	1	21	monosaccharide biosynthetic process
GO:0001944	0.034	7.7	0.294	2	185	vasculature development
GO:0010033	0.041	26.8	0.041	1	26	response to organic substance
GO:0032502	0.042	2.8	3.502	7	2206	developmental process
GO:0008645	0.042	25.7	0.043	1	27	hexose transport
GO:0042593	0.042	25.7	0.043	1	27	glucose homeostasis
GO:0050770	0.042	25.7	0.043	1	27	regulation of axonogenesis
GO:0000187	0.045	23.9	0.046	1	29	activation of MAPK activity
GO:0002429	0.047	23.1	0.048	1	30	immune response-activating cell surface receptor signaling pathway
GO:0048731	0.047	3.0	2.086	5	1314	system development
GO:0007249	0.050	21.6	0.051	1	32	I-kappaB kinase/NF-kappaB cascade

Table S 26. Gene to GO-BP conditional test for over-representation within mRNAs downregulated in miR-155-deficient colon on day 4 pi

Gene to GO-biological process terms test for over-representation within down-regulated mRNAs in miR-155-deficient vs wild-type colon 4 days pi.

KEGGID	Pvalue	OddsRatio	ExpCount	Count	Size	Term	Description
00150	0.0036	11.3	0.32	3	39	Androgen and estrogen metabolism	Androgen and estrogen metabolism
00361	0.0081	17.4	0.14	2	17	gamma-Hexachlorocyclohexane degradation	gamma-Hexachlorocyclohexane degradation
00910	0.0090	16.4	0.15	2	18	Nitrogen metabolism	Nitrogen metabolism
00980	0.0105	7.5	0.46	3	57	Metabolism of xenobiotics by cytochrome P450	Metabolism of xenobiotics by cytochrome P450
00340	0.0289	8.4	0.27	2	33	Histidine metabolism	Histidine metabolism
00480	0.0323	7.9	0.29	2	35	Glutathione metabolism	Glutathione metabolism

Table S 32. Gene to KEGG test for over-representation within mR NAs upregulated in miR-155-deficient colon on day14 pi

Gene to KEGG test for over-representation within up-regulated mRNAs in miR-155-deficient vs wild-type colon 14 days pi.

KEGGID	Pvalue	OddsRatio	ExpCount	Count	Size	Term	Description
04514	0.0085	4.5	1.29	5	119	Cell adhesion molecules (CAMs)	Cell adhesion molecules (CAMs)
04660	0.0099	5.3	0.86	4	79	T cell receptor signaling pathway	T cell receptor signaling pathway
04650	0.0192	4.3	1.04	4	96	Natural killer cell mediated cytotoxicity	Natural killer cell mediated cytotoxicity
04640	0.0338	4.6	0.72	3	66	Hematopoietic cell lineage	Hematopoietic cell lineage
04512	0.0392	4.4	0.76	3	70	ECM-receptor interaction	ECM-receptor interaction

Table S 33. Gene to KEGG test for over-representation within mRNAs downregulated in miR-155-deficient colon on day14 pi

Gene to KEGG test for over-representation within down-regulated mRNAs in miR-155-deficient vs wild-type colon 4 days pi.

GOBPID	Pvalue	OddsRatio	ExpCount	Count	Size	Term
GO:0006508	0.0020	3.1	3.98	11	472	proteolysis
GO:0006629	0.0026	3.0	4.13	11	490	lipid metabolic process
GO:0008202	0.0028	5.6	0.97	5	115	steroid metabolic process
GO:0006953	0.0121	13.4	0.17	2	20	acute-phase response
GO:0006323	0.0190	4.2	1.02	4	121	DNA packaging
GO:0003012	0.0262	5.0	0.64	3	76	muscle system process
GO:0006937	0.0262	8.6	0.25	2	30	regulation of muscle contraction
GO:0006334	0.0349	4.4	0.72	3	85	nucleosome assembly

Table S 34. Gene to GO-BP conditional test for over-representation within mRNAs upregulated in miR-155-deficient colon on day14 pi

Gene to GO-biological process terms test for over-representation within up-regulated mRNAs in miR-155-deficient vs wild-type colon 14 days pi.

GOBPID	Pvalue	OddsRatio	ExpCount	Count	Size	Term
GO:0050900	1.3e-06	32.9	0.197	5	28	leukocyte migration
GO:0006935	3.4e-05	11.2	0.620	6	88	chemotaxis
GO:0007155	5.8e-05	4.5	3.142	12	446	cell adhesion
GO:0009605	5.9e-05	5.3	2.193	10	319	response to external stimulus
GO:0050766	7.0e-05	49.0	0.085	3	12	positive regulation of phagocytosis
GO:0002696	8.3e-05	12.8	0.451	5	64	positive regulation of leukocyte activation
GO:0006954	1.2e-04	7.1	1.125	7	162	inflammatory response
GO:0050865	3.2e-04	9.4	0.599	5	85	regulation of cell activation
GO:0019884	4.1e-04	24.5	0.148	3	21	antigen processing and presentation of exogenous antigen
GO:0051240	6.6e-04	6.3	1.064	6	151	positive regulation of multicellular organismal process
GO:0048002	7.8e-04	19.2	0.183	3	26	antigen processing and presentation of peptide antigen
GO:0007626	8.1e-04	6.0	1.106	6	157	locomotory behavior
GO:0030100	8.7e-04	18.4	0.190	3	27	regulation of endocytosis
GO:0045321	1.8e-03	5.1	1.296	6	184	leukocyte activation
GO:0002764	1.9e-03	13.8	0.247	3	35	immune response-regulating signal transduction
GO:0000272	2.1e-03	36.2	0.070	2	10	polysaccharide catabolic process
GO:0002861	2.6e-03	32.2	0.077	2	11	regulation of inflammatory response to antigenic stimulus
GO:0006911	2.6e-03	32.2	0.077	2	11	phagocytosis, engulfment
GO:0050729	2.6e-03	32.2	0.077	2	11	positive regulation of inflammatory response
GO:0051249	2.6e-03	7.6	0.578	4	82	regulation of lymphocyte activation
GO:0006955	2.7e-03	4.7	1.406	6	212	immune response
GO:0051130	2.9e-03	11.6	0.289	3	41	positive regulation of cellular component organization and biogenesis
GO:0006950	3.4e-03	2.9	4.305	11	611	response to stress
GO:0006044	4.2e-03	24.1	0.099	2	14	N-acetylglucosamine metabolic process
GO:0019886	4.2e-03	24.1	0.099	2	14	antigen processing and presentation of exogenous peptide antigen via MHC class II
GO:0032635	4.2e-03	24.1	0.099	2	14	interleukin-6 production
GO:0050870	4.4e-03	10.0	0.331	3	47	positive regulation of T cell activation
GO:0002504	4.8e-03	22.3	0.106	2	15	antigen processing and presentation of peptide or polysaccharide antigen via MHC class II
GO:0048584	5.1e-03	6.2	0.697	4	99	positive regulation of response to stimulus
GO:0002821	5.5e-03	20.7	0.113	2	16	positive regulation of adaptive immune response
GO:0050852	6.2e-03	19.3	0.120	2	17	T cell receptor signaling pathway
GO:0006040	7.7e-03	17.0	0.134	2	19	amino sugar metabolic process
GO:0016054	7.7e-03	17.0	0.134	2	19	organic acid catabolic process
GO:0019724	7.8e-03	8.0	0.409	3	58	B cell mediated immunity
GO:0002705	8.6e-03	16.1	0.141	2	20	positive regulation of leukocyte mediated immunity
GO:0002822	8.6e-03	16.1	0.141	2	20	regulation of adaptive immune response based on somatic recombination of immune receptors built from immunoglobulin superfamily domains
GO:0046634	8.6e-03	16.1	0.141	2	20	regulation of alpha-beta T cell activation
GO:0002253	9.4e-03	7.4	0.437	3	62	activation of immune response
GO:0006690	9.4e-03	15.2	0.148	2	21	icosanoid metabolic process
GO:0042398	9.4e-03	15.2	0.148	2	21	amino acid derivative biosynthetic process
GO:0045621	9.4e-03	15.2	0.148	2	21	positive regulation of lymphocyte differentiation
GO:0048872	1.0e-02	7.2	0.451	3	64	homeostasis of number of cells
GO:0006928	1.1e-02	3.4	1.888	6	268	cell motility
GO:0002706	1.2e-02	13.2	0.169	2	24	regulation of lymphocyte mediated immunity
GO:0032270	1.5e-02	6.3	0.514	3	73	positive regulation of cellular protein metabolic process

GO:0001558	1.6e-02	6.1	0.528	3	75	regulation of cell growth
GO:0002250	1.6e-02	6.1	0.528	3	75	adaptive immune response
GO:0051050	1.6e-02	11.3	0.195	2	28	positive regulation of transport
GO:0002429	1.7e-02	10.9	0.201	2	29	immune response-activating cell surface receptor signaling pathway
GO:0002443	1.9e-02	5.7	0.564	3	80	leukocyte mediated immunity
GO:0050776	2.2e-02	5.3	0.603	3	88	regulation of immune response
GO:0002520	2.2e-02	3.3	1.613	5	229	immune system development
GO:0030098	2.3e-02	5.3	0.606	3	86	lymphocyte differentiation
GO:0051094	2.6e-02	3.2	1.684	5	239	positive regulation of developmental process
GO:0002440	2.6e-02	8.5	0.254	2	36	production of molecular mediator of immune response
GO:0051258	2.9e-02	8.0	0.268	2	38	protein polymerization
GO:0044264	3.1e-02	7.8	0.275	2	39	cellular polysaccharide metabolic process
GO:0032101	3.2e-02	7.6	0.282	2	40	regulation of response to external stimulus
GO:0008361	3.3e-02	4.6	0.697	3	99	regulation of cell size
GO:0042742	3.4e-02	7.4	0.289	2	41	defense response to bacterium
GO:0031347	3.7e-02	7.0	0.303	2	43	regulation of defense response
GO:0032787	3.9e-02	3.3	1.282	4	182	monocarboxylic acid metabolic process
GO:0042035	4.0e-02	6.7	0.317	2	45	regulation of cytokine biosynthetic process
GO:0051707	4.0e-02	4.2	0.761	3	108	response to other organism
GO:0031328	4.3e-02	6.4	0.331	2	47	positive regulation of cellular biosynthetic process
GO:0042110	4.3e-02	4.0	0.782	3	111	T cell activation
GO:0009309	4.7e-02	6.1	0.345	2	49	amine biosynthetic process
GO:0030097	4.7e-02	3.1	1.360	4	193	hemopoiesis
GO:0018108	4.8e-02	6.0	0.352	2	50	peptidyl-tyrosine phosphorylation

Table S 35. Gene to GO-BP conditional test for over-representation within mRNAs downregulated in miR-155-deficient colon on day14 pi

Gene to GO-biological process terms test for over-representation within down-regulated mRNAs in miR-155-deficient vs wild-type colon 14 days pi.

List of Supplementary Figures and Tables

Figure S1. B cell Receptor signalling pathway downregulated Caecal patch Day 4

InnateDB analysis of mRNAs down-regulated in miR-155-deficient vs wild-type caecal patch 4 days pi identified that there was an over-representation of genes involved in the B cell receptor signalling pathway. Figure shows genes involved in B cell receptor signalling identified as being down-regulated (green nodes).

Figure S2. Sylamer analysis

Sylamer analysis of mRNAs extracted from colon (colon, bic (miR-155-deficient) vs wt (wild-type)) and caecal patch (caecal patch, bic (miR-155-deficient) vs wt (wild-type)). The x-axis represents all the genes with an annotated 3'UTR sequence, sorted starting from the most up-regulated in the miR-155-deficient samples. The y-axis represents the -log10transformed hyper-geometric P-values, with positive values denoting enrichment and negative values depletion. Each gray line represents a single 7-nucleotide seed-matching word and those corresponding to miR-155 are highlighted. Dotted lines represent Bonferroni-corrected P-value significance thresholds of 0.01.

Table S1. Upregulated mRNAs in caecal patch Day 4

Up-regulated mRNAs in miR-155-deficient vs wild-type caecal patch 4 days pi. Differentially expressed genes were only considered significant if they altered by at least 1.5 fold and had adjusted P-value of less than 0.05.

Table S2. Upregulated mRNAs in miR-155-deficient vs wild-type Caecal patch Day 4

 Up-regulated mRNAs in miR-155-deficient vs wild-type caecal patch 4 days pi. Differentially expressed genes were only considered significant if they altered by at least 1.5 fold and had adjusted P-value of less than 0.05.

Table S3. Downregulated mRNAs in Caecal patch Day 4

Down-regulated mRNAs in miR-155-deficient vs wild-type caecal patch 4 days pi. Differentially expressed genes were only considered significant if they altered by at least 1.5 fold and had adjusted P-value of less than 0.05.

Table S4. Downregulated mRNAs in miR-155-deficient vs wild-type Caecal patch Day 4

Down-regulated mRNAs in miR-155-deficient vs wild-type caecal patch 4 days pi. Differentially expressed genes were only considered significant if they altered by at least 1.5 fold and had adjusted P-value of less than 0.05.

Table S5. Gene to KEGG test over-representation Upregulated Caecal patch Day 4

Gene to KEGG test for over-representation within up-regulated mRNAs in miR-155-deficient vs wild-type caecal patch 4 days pi.

Table S6. Gene to KEGG test over-representation Downregulated Caecal patch Day 4

Gene to KEGG test for over-representation within down-regulated mRNAs in miR-155-deficient vs wild-type caecal patch 4 days pi.

Table S7. Gene to GO-BP conditional test over-representation Upreg Caecal patch Day 4

Gene to GO-biological process terms test for over-representation within up-regulated mRNAs in miR-155-deficient vs wild-type caecal patch 4 days pi.

Table S8. Gene to GO-BP conditional test over-representation Downreg Caecal patch Day 4

Gene to GO-biological process terms test for over-representation within down-regulated mRNAs in miR-155-deficient vs wild-type caecal patch 4 days pi.

Table S9. InnateDB Pathways Caecal patch Day 4

InnateDB analysis of mRNAs up- and down-regulated in miR-155-deficient vs wild-type caecal patch 4 days pi.

Table S10. Upregulated mRNAs in Caecal patch Day 14

Up-regulated mRNAs in miR-155-deficient vs wild-type caecal patch 14 days pi. Differentially expressed genes were only considered significant if they altered by at least 1.5 fold and had adjusted P-value of less than 0.05.

Table S11. Upregulated mRNAs in miR-155-deficient vs wild-type Caecal patch Day 14

Up-regulated mRNAs in miR-155-deficient vs wild-type caecal patch 14 days pi. Differentially expressed genes were only considered significant if they altered by at least 1.5 fold and had adjusted P-value of less than 0.05.

Table S12. Downreg mRNAs in Caecal patch Day 14

Down-regulated mRNAs in miR-155-deficient vs wild-type caecal patch 14 days pi. Differentially expressed genes were only considered significant if they altered by at least 1.5 fold and had adjusted P-value of less than 0.05.

Table S13. Downregulated mRNAs in miR-155-deficient vs wild-type Caecal patch Day 14

Down-regulated mRNAs in miR-155-deficient vs wild-type caecal patch 14 days pi. Differentially expressed genes were only considered significant if they altered by at least 1.5 fold and had adjusted P-value of less than 0.05.

Table S14. Gene to KEGG test over-representation Upregulated Caecal patch Day 14

Gene to KEGG test for over-representation within up-regulated mRNAs in miR-155-deficient vs wild-type caecal patch 14 days pi.

Table S15. Gene to KEGG test over-representation Downregulated Caecal patch Day 14

Gene to KEGG test for over-representation within down-regulated mRNAs in miR-155-deficient vs wild-type caecal patch 14 days pi.

Table S16. Gene to GO-BP conditional test over-representation Upreg Caecal patch Day 14

Gene to GO-biological process terms test for over-representation within up-regulated mRNAs in miR-155-deficient vs wild-type caecal patch 14 days pi.

Table S17. Gene to GO-BP conditional test over-representation Downreg Caecal patch Day 14

Gene to GO-biological process terms test for over-representation within down-regulated mRNAs in miR-155-deficient vs wild-type caecal patch 14 days pi.

Table S18. InnateDB Pathways Caecal patch Day 14

InnateDB analysis of mRNAs up- and down-regulated in miR-155-deficient vs wild-type caecal patch 4 days pi.

Table S19. Upregulated mRNAs in Colon Day 4

Up-regulated mRNAs in miR-155-deficient vs wild-type colon 4 days pi. Differentially expressed genes were only considered significant if they altered by at least 1.5 fold and had adjusted P-value of less than 0.05.

Table S20. Upregulated mRNAs in miR-155-deficient vs wild-type Colon Day 4

Up-regulated mRNAs in miR-155-deficient vs wild-type colon 4 days pi. Differentially expressed genes were only considered significant if they altered by at least 1.5 fold and had adjusted P-value of less than 0.05.

Table S21. Downregulated mRNAs in Colon Day 4

Down-regulated mRNAs in miR-155-deficient vs wild-type colon 4 days pi. Differentially expressed genes were only considered significant if they altered by at least 1.5 fold and had adjusted P-value of less than 0.05.

Table S22. Downregulated mRNAs in miR-155-deficient vs wild-type Colon Day 4

Down-regulated mRNAs in miR-155-deficient vs wild-type colon 4 days pi. Differentially expressed genes were only considered significant if they altered by at least 1.5 fold and had adjusted P-value of less than 0.05.

Table S23. Gene to KEGG test over-representation Upregulated Colon Day 4

Gene to KEGG test for over-representation within up-regulated mRNAs in miR-155-deficient vs wild-type colon 4 days pi.

Table S24. Gene to KEGG test over-representation Downregulated Colon Day 4

Gene to KEGG test for over-representation within down-regulated mRNAs in miR-155-deficient vs wild-type colon 4 days pi.

Table S25. Gene to GO-BP conditional test over-representation Upreg mRNAs Colon Day 4

 Gene to GO-biological process terms test for over-representation within up-regulated mRNAs in miR-155-deficient vs wild-type colon 4 days pi.

Table S26. Gene to GO-BP conditional test over-representation Downreg mRNAs Colon Day 4

Gene to GO-biological process terms test for over-representation within down-regulated mRNAs in miR-155-deficient vs wild-type colon 4 days pi.

Table S27. InnateDB Pathways Colon Day 4

 InnateDB analysis of mRNAs up- and down-regulated in miR-155-deficient vs wild-type colon 4 days pi.

Table S28. Upregulated mRNAs in Colon Day 14

Up-regulated mRNAs in miR-155-deficient vs wild-type colon 14 days pi. Differentially expressed genes were only considered significant if they altered by at least 1.5 fold and had adjusted P-value of less than 0.05.

Table S29. Upregulated mRNAs in miR-155-deficient vs wild-type Colon Day 14

Up-regulated mRNAs in miR-155-deficient vs wild-type colon 14 days pi. Differentially expressed genes were only considered significant if they altered by at least 1.5 fold and had adjusted P-value of less than 0.05.

Table S30. Downregulated mRNAs in Colon Day 14

Down-regulated mRNAs in miR-155-deficient vs wild-type colon 14 days pi. Differentially expressed genes were only considered significant if they altered by at least 1.5 fold and had adjusted P-value of less than 0.05.

Table S31. Downregulated mRNAs in miR-155-deficient vs wild-type Colon Day 14

Down-regulated mRNAs in miR-155-deficient vs wild-type colon 14 days pi. Differentially expressed genes were only considered significant if they altered by at least 1.5 fold and had adjusted P-value of less than 0.05.

Table S32. Gene to KEGG test over-representation Upregulated Colon Day 14

Gene to KEGG test for over-representation within up-regulated mRNAs in miR-155-deficient vs wild-type colon 14 days pi.

Table S33. Gene to KEGG test over-representation Downregulated Colon Day 14

Gene to KEGG test for over-representation within down-regulated mRNAs in miR-155-deficient vs wild-type colon 4 days pi.

Table S34. Gene to GO-BP conditional test over-representation Upreg Colon Day 14

Gene to GO-biological process terms test for over-representation within up-regulated mRNAs in miR-155-deficient vs wild-type colon 14 days pi.

Table S35. Gene to GO-BP conditional test over-representation Downreg Colon Day 14

Gene to GO-biological process terms test for over-representation within down-regulated mRNAs in miR-155-deficient vs wild-type colon 14 days pi.

Table S36. InnateDB Pathways Colon Day 14

InnateDB analysis of mRNAs up- and down-regulated in miR-155-deficient vs wild-type colon 14 days pi.